School of Biomedical Sciences

The Molecular mechanism of solvent cryoprotection

Jestin Baby Mandumpal

This thesis is presented for the degree of
Doctor of philosophy
Curtin University of Technology

April 2011

Declaration

To the best of my knowledge and belief this thesis contains no material previously published by any other person except where due to acknowledgement has been made.

This thesis contains no material which has been accepted for the award of any other degree or diploma in any university.

Signature……..

Date…14-04-2011……..

I dedicate this thesis to my father who had been a constant source of inspiration throughout my life.

ACKNOWLEDGEMENTS

First of all, I express my sincere gratitude and appreciation to my supervisor Assoc. Prof. Ricardo L. Mancera who invited me to School of Biomedical Sciences to work on a wonderful project with a Curtin International Research Tuition Scholarship (**CIRTS**), and has been very supportive in planning and execution of the work. I am greatly indebted to Prof. Erik Helmerhorst for his timely advice related to my doctoral work at the school. I also thank Dr. Zhili Zuo and Dr. Zak Hughes for serving on thesis supervisory committee and for helping me in various stages of my work. I extend my gratitude to all staff in Curtin University, School of Biomedical Sciences in particular, who have assisted me one way or another.

I am particularly grateful to **iVEC** staff, **GROMACS**, **NAMD** and **PACKMOL** crew and users for offering their assistance to software related work, without which the completion of the thesis would have been impossible. It is an honour for me to acknowledge Professors Eugene Stanley and William Jorgenson for extending their support in methodology related problems.

I owe my deepest gratitude to Ms. Neha Gandhi, who has been a true companion during my stay at Curtin, Miguel Renteria, Fransisca Lee, Wade Lee, Benjamin Roberts, Caroline Snowball, Cara Kreck and Dr. Thilagavathi Ramasami for sharing their valuable time with me.

And the last but not the least, I would like to thank my mother, who is still encouraging me, and other family members (my wife, brother and others) who have fuelled motivation in me during my endeavour.

TABLE OF CONTENTS

Page

ABBREVIATIONS

High Density Amorphous	HDA
Low Density Amorphous	LDA
Cubic ice	Ic
Hexagonal ice	Ih
Temperature of Maximum Density	TMD
Extra cellular Ice Formation	EIF
Intra cellular Ice Formation	IIF
Hydroxy Ethyl Starch	HES
Di Methyl Sulfoxide	DMSO
Cryo Protective Agents	CPAs
N-methyl formamide	NMF
Plant Vitrification Solution 1	PVS1
Quasi-Elastic Neutron Scattering	QENS
Neutron Spin Echo	NSE
Small Angle Neutron Scattering	SANS
Fourier Transform Infra Red	FTIR
Differential Scanning Calorimetry	DSC
DiOleoyl-PhosphatidylCholine	DOPC
1-Oleoyl-2-Palmitoyl-PhosphatidylCholine	OPPC
1-Steroyl-2-Oleoyl-PhosphatidylCholine	SOPC
1,2-DiMyristoyl-PhosphatidylCholine	DMPC
1,2 – DiPlamitoyl –PhosphatidylCholine	DPPC
Glass Transition	T_g
Melting Temperature	T_m
Vogel- Fulcher- Tamman	VLF
Low Density Liquid	LDL
Fourier Transform Infrared Attenuated Total Reflectance Spectroscopy	FTIATRS
Bernal Fowler	BF
Ben Naim Stillinger	BNS
STillinger 2	ST2
Matsuoka Clementi Yoshimine	MCY

Simple Point Charge	SPC
Transferable Intermolecular Potential Four Point charges	TIP4P
Watanabe Klein	WK
New Simple Point Charge Extended	NSPCE
Transferable Intermolecular Potential five Point charges	TIP5P
Simple Point Charge/Heavy Water	SPC/HW
Central Force	CF
Bopp Jancso Heinzinger	BJH
Simple Point Charge/Fluctuating	SPC/F
Matsuoka Clementi Yoshimine Lie	MCYL
Cieplak Kollman Lybrand	CKL
Simple Point Charge/ Flexible Polarisation	SPC/FP
Niesar Corongiu Clementi	NCC
Polarisable Transferable Intermolecular Potential Four Point charges	PTIP4P
Kozack Jordan	KJ
Revised POLarisable	RPOL
Polarisable Point Charge	PPC
Semiempirical Quantum Polarisable Model	SQPM
Self Consistent Point Dipole Polarizability	SCPDP
Truncated Adiabatic Basis	TAB
Transferable Intermolecular Potential 4 Point/ice	TIP4P/ice
Transferable Intermolecular Potential 4 Point/2005	TIP4P/2005
Transferable Intermolecular Potential 5 Point	TIP5P
Transferable Intermolecular Potential 5 Point – Ewald	TIP5P-Ewald
Nuclear Magnetic Resonance	NMR
Radial Distribution Function	RDF
Fast Fourier Transformation	FFT
Particle Mesh Ewald	PME
Empirical Potential Structure Refinement	EPSR
Small Angle X-ray Scattering	SAXS
Optimised Potential for Liquid Simulations	OPLS

LIST OF FIGURES

LIST OF TABLES

SUMMARY

The cryopreservation of animal and human cells, tissues and organs as well as germplasm of endangered plant species is a key area in contemporary biotechnology. In this thesis, certain classes of chemicals known as cryoprotective agents (CPA) are investigated in detail. The structural, dynamic and vitrification properties of representative CPAs are studied using the state-of-the art molecular dynamics simulation techniques. The simulations provide a rationale at the molecular level of the cryoprotective properties of aqueous solutions of compounds such as DMSO, methanol and ethanol.

This is a brief synopsis of the thesis:

CHAPTER 1. This chapter provides a general introduction of various aspects of cryoprotection. A brief overview of the challenges that are encountered in the cryopreservation protocol is given, followed by a list of known cryoprotectants. Next various mechanisms to account for cryopreservation have been explained in detail. This section is followed by one of the important theme of this thesis, vitrification, and finally water and its properties.

CHAPTER 2. This chapter discusses the theoretical background of molecular dynamics simulations and various analyses, and a brief overview of water forcefields.

CHAPTER 3. Molecular dynamics simulations of DMSO in water elucidating its structural, dynamic and hydrogen bonding properties are described in this chapter. Comparison with its chemical analogue, Acetone, is made in an attempt to rationalise DMSO‟s exceptional properties in a wide range of temperatures.

CHAPTER 4. Structural and hydrogen bonding properties of aqueous ethanol and methanol solutions have been described in this chapter.

CHAPTER 5. Estimation of glass transition temperatures of aqueous mixtures of DMSO, acetone, ethanol, methanol and water using simulated annealing molecular dynamics techniques has been described in this chapter.

CHAPTER 6. Important conclusions arising from this study and scope of the work have been summarised in this chapter.

Chapter 1

LITERATURE REVIEW

INTRODUCTION

Cryopreservation of biological organs and seeds of endangered plants is considered to be thrust areas of research in contemporary biology. Over the years many solvents that confer cryoprotection have been identified and are widely used. However, complex mechanisms of their action have not been completely understood. This literature review provides a concise yet expansive background that is required for a detail understanding of various aspects of cryopreservation: challenges in cryopreservation, various mechanisms that have been suggested for cryoprotective action, a comprehensive list of known cryoprotective agents and their physicochemical properties, phenomenon of glass transition, and the theories developed in order to account for the properties of water that play a pivotal role in ensuring successful cryopreservation. Several experimental techniques have been developed and in use which aid researchers to investigate the properties of various systems at molecular level. Molecular dynamics simulations have been proved to be a robust complimentary tool to these techniques and will be extensively employed in this study. The focus of this thesis is two fold - the investigations of structural, dynamic and solution properties from equilibrium molecular dynamics simulations in order to characterise interactions of cryoprotectant solvents with water, and determination of glass transition temperatures of aqueous cryoprotective solutions to examine vitrification hypothesis which is one of the suggested mechanisms for cryopreservation.

1.1. CRYOPRESERVATION

Long term preservation of biological materials, seeds and food items at sub zero temperature is known as cryopreservation[1-4]. The biological materials that can be cryopreserved include mammalian embryos, oocytes, ovarian and mammalian tissues, organs,[5, 6] and plant germplasms[7]. Preservation of these biological materials is essential

for organ transplantation, sustaining genetic diversity and in vitro fertilisation in humans[6]. Efficient cryopreservation methods are indispensable for restoring several species that are likely to be endangered during processes such as mining[8]. On the other hand, drought and other natural calamities result in rapid erosion in the availability of seeds. In order to make seeds available for cultivation, their germplasms are preserved in gene banks for ensuring bio diversity. Cryopreservation is a current effective method to achieve this aim[4]. In food industry as well, preservation at low temperature is considered to be a successful method that guarantees retaining flavour, colour, texture and nutritive values[3].

Since chemical reactions seldom occur, and most of the biological activities are retarded, preservation of biological organs becomes very feasible at sub zero temperatures[9]. Although cryopreservation is useful for protection of various materials, it encounters several problems such as crystallisation at sub zero temperatures, dehydration as a result of the prolonged storage of the materials in freezing temperatures and ensuing cell death. The key question remaining is how to minimise these issues related to low temperatures including damages that can be occurred to cells and cell membranes during freezing, and to surmount these problems for retaining cell architecture[10].

1.2 STRUCTURE OF CELL MEMBRANE

Cell membranes function as an interface between cells and extra cellular fluid in which cells are immersed. Cells are bounded by outer limiting membrane called plasma membranes which are built up from lipids and proteins. The lipids in the plasma membranes are chiefly made up of cholesterol and phospholipids such as phosphatidyl ethanolamine. Phospholipids are amphiphiles comprised of two regions - hydrophilic (polar region) and hydrophobic (non polar region), as shown in Figure 1-1.

Phospholipids normally exist as bilayer, accommodating their hydrophobic tails face to face, with their hydrophilic parts facing surrounding water solution. A cartoon depicting various component proteins of the phospholipids has been shown in Figure 1-2. In addition, there are three major proteins that make up of plasma membranes-integral membrane proteins, peripheral membrane proteins and trans-membrane

proteins. Integral membrane protein membranes are restricted in their movements, whereas the other two are capable of moving across the lipid bilayer, regulating the molecular movements through the membranes. These membranes, thus, not only act as a wall through cell boundary, but also act as a threshold which selects molecules that enter and leave the cell. Hence, cell membranes retain shape and structure of the cells and keep components separately from outer cellular components.

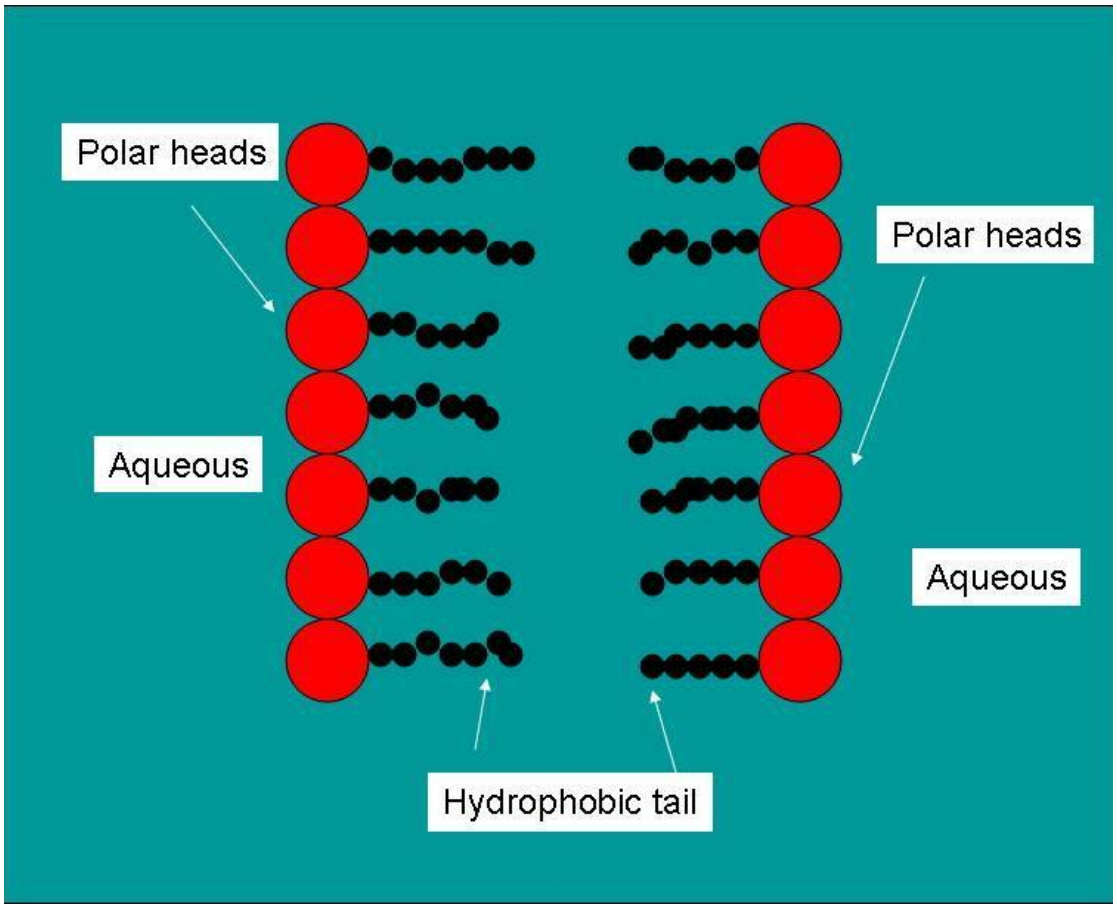

Figure 1-1 *Phospholipid bilayer composed of polar and non polar (hydrocarbon tails) parts and surround by watery regions shown in teal blue. The red spheres indicate polar hydrophilic tails, and the hydrophobic tails have been indicated by the arrows.*

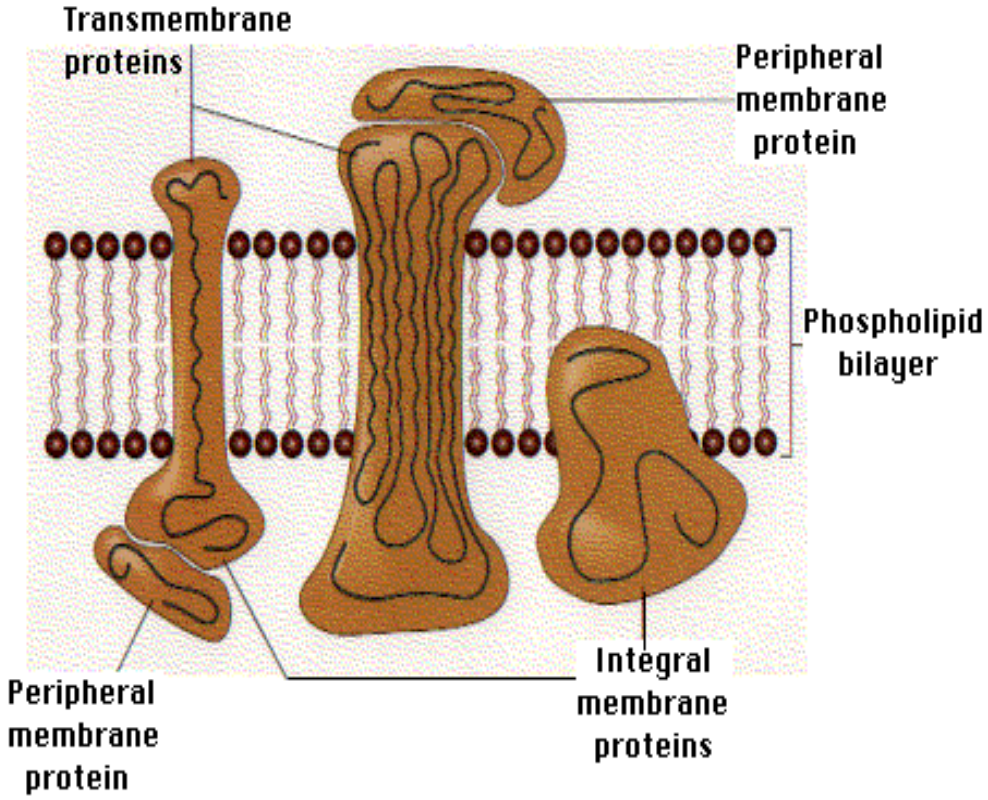

Figure 1-2 *Proteins associated with phospholipids. Integral membrane proteins are restricted in their movements, whereas peripheral and trans membrane proteins are capable of moving across the lipid bilayer. The figure is adapted from* http://users.rcn.com/jkimball.ma.ultranet/BiologyPages/C/CellMembranes.html

1.3. ISSUES RELATED TO CRYOPRESERVATION

Extreme circumstances such as freezing pose several problems to a cell under cryopreservation[10-13]. The temperature at which the organs are kept is achieved by either cooling the organs very slow or fast[14]. But, at temperature below 273K under normal conditions, nucleation of water molecules occurs in the cell[15], which leads into crystallisation (forming ice crystals) both inside (intra cellular ice) and outside (extra cellular ice) the cells[16]. These ice crystals can potentially damage the cell- extra cellular ice formation dehydrates the cells, resulting in cellular shrinkage[10], where as intracellular ice directly leads into the cell death[11]. In any of the artificial cryopreservation methods cells or organs are cooled at optimum rate from room temperature to the freezing temperatures with appropriate additives.

1.3.1 Nucleation

Nucleation is a process initiated due to organisation of water molecules to an ice like structure[15]. Originated from a nucleus, water molecules can organise themselves into an ice like form as temperature drops down from zero Kelvin (0 K), and this tendency becomes more pronounced at lower temperatures. Abrupt aggregation of water molecules is followed by the formation of ice crystals. Number of water molecules required to initiate a nucleation process strongly depends upon the temperature: around 45000 water molecules are required at -5^{o}C, whereas only 234 molecules are required at -40^{o}C, suggesting that crystallisation can happen readily at very low temperature[15, 17]. Number of the aggregated water molecules and their temperature dependence influence the feasibility of the nucleation process. After nuclei attain considerable size, nucleation will be continued until large crystals are formed. This can be explained by the fact that the clusters are energetically favourable for the further water molecules to aggregate on it. The driving force towards nucleation and subsequent crystal growth are dependent upon the size of the crystal. Table 1-1 illustrates the dependency of the number of water molecules and critical radii prologue to crystallisation on the temperatures.

Table 1-1 *Number of water molecules required to form critical nuclei at subzero temperature*

Temperature (K)	Number of water molecules needed for nucleation	Critical radius at the nucleation (nm)
263	15943	4.20
253	1944	2.08
243	566	1.38
233	234	1.03
223	122	0.83

1.3.2 Types of Nucleation

Nucleation is generally classified into two: homogenous nucleation, and heterogeneous nucleation[18, 19]. The nucleation process can be driven by water itself, called as homogenous nucleation, or by the impurities with which water molecules coexist within the cell, called as heterogeneous nucleation[18]. In both these processes the time required for complete nucleation in a container or a cell depends upon the amount of water inside, following the famous Biggs rule[20], which states that the nucleation temperature increases with the amount of water inside the container. Nucleation is inevitably followed by crystallisation under normal conditions of temperature and pressure, when cells are cooled below sub zero temperature[21]. Every crystallisable materials have their own characteristic homogenous nucleation temperatures[22].

1.3.3. Freezing and crystallisation

When materials undergo freezing, two kinds of ice formation (crystallisation) may occur: extra cellular ice and intra cellular ice[11, 14]. The type of ice crystals formed is determined by the rate of cooling with which the cell is subjected to: rapid cooling results in intracellular ice formation, whereas slow cooling results in extra cellular ice formation[23]. The different crystallisation mechanisms as a result of difference in cooling rates have been depicted in Figure 1-3 and Figure 1-4.

As extra cellular ice is formed due to slow cooling[24], the amount of water molecules outside gradually decreases as more water molecules are converted into ice, which concentrates solutes outside the cell that causes solvent (water) leaving the cell osmotically. The net diffusion of water across the cell membrane, from an area with high water concentration to an area with low water concentration, is called as Osmosis.

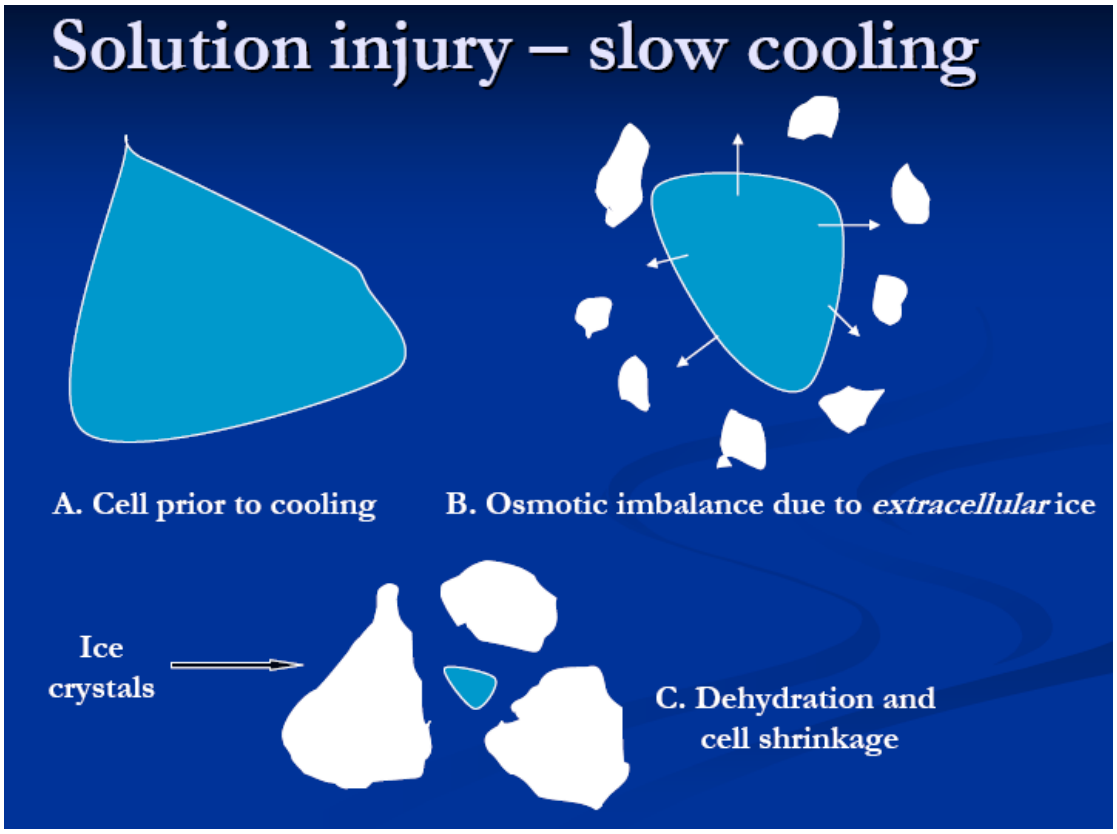

Figure 1-3 *Cell injury due to slow cooling (A) Cell contents remain intact prior to slow cooling, (B) As temperature decreases, solutes are concentrated outside the cells, and more water flows out from the cells due to osmosis resulting in the formation of small ice crystals (shown in white). (C) As cooling proceeds, ice crystals grow bigger drawing out more water from the cells (dehydration), resulting in cell shrinkage.*

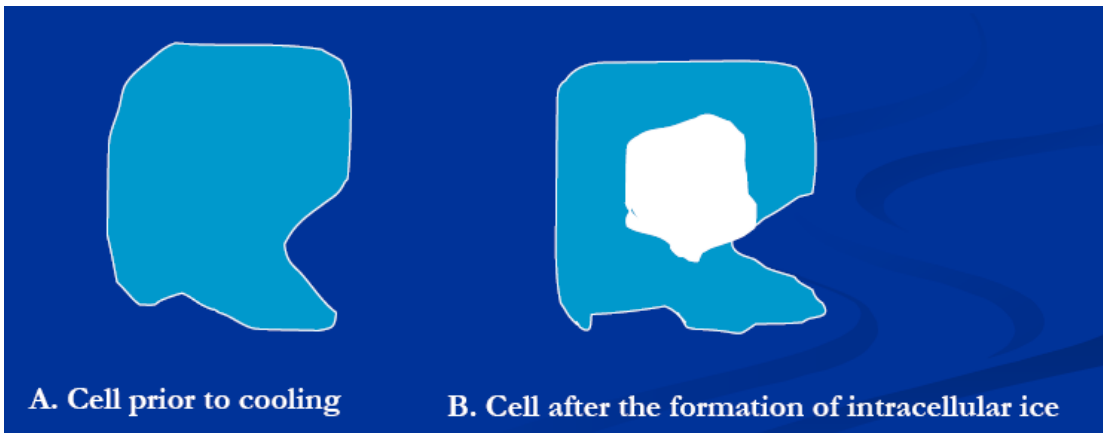

Figure 1-4 *Cell death due to fast cooling rate (A) Cell prior to cooling, (B) as a result of fast cooling, initiation of ice formation occurs within the cell till available water is consumed. Intra cellular ice thus formed pushes the membranes apart in order to make space for the growing ice crystals.*

Cells can become either plasmolysed or turgid during osmosis. As a result of pressure exerted by the protoplasm against the cell wall, it becomes turgid. On the other hand, if the cell is placed in a more concentrated solution (hypertonic), water will flow from the cell, resulting in its shrinkage leading to the collapse of the cell: the system is termed to be plasmolysed[10]. As a result of EIF (Extra cellular Ice Formation), the concentration of water molecules decreases which instigates their flow from the cells, in order to maintain osmotic equilibrium across the cells membrane[23]. Removal of water spurs shrinking the cells, known as granulation which ultimately causes solution injury[25]. Shrinking of cells due to osmotic imbalance is thus a manifestation of extra cellular ice formation. The combined effect of increasing extra cellular solute concentration and cell shrinkage has been proposed by Lovelock and Merryman respectively[12, 26-28]. In Figure 1-5, the effect of extra cellular ice formation on the cells is depicted.

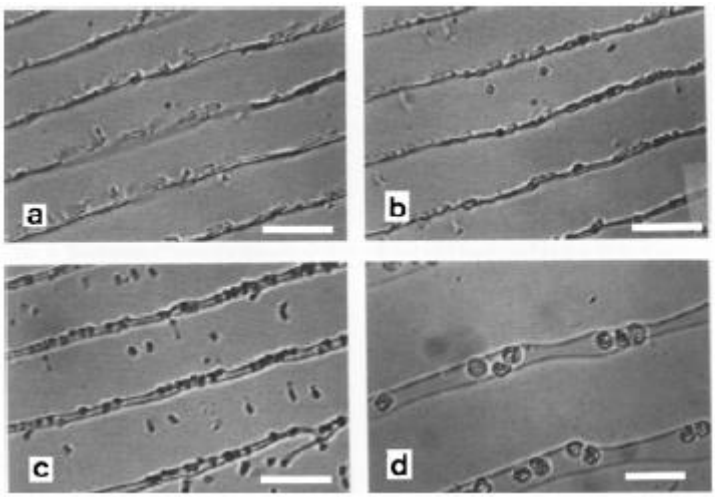

Figure 1-5 *Effect of extra cellular ice formation on the cells. Temperature increases as seen from panels a-d, shrinkage of cells is clearly visible in panels a and b, and at ambient temperature, as is shown in panel d, cells recover their original shape and size. The figure is taken from Rubinsky et al*[9]

The osmotic imbalance resulting from the extra cellular ice formation may lead to an electrical potential difference, due to various ions present in the protoplasm, across the cell membrane as well[29]. A potential range of 150 to 200 mV can be formed as a result of the electrical gradient that can be developed across the membrane. Inevitable effect of this dangerous electrical perturbations is breakage of the membrane, leading to cell fusion[30], as illustrated by the diagram below, Figure 1-6.

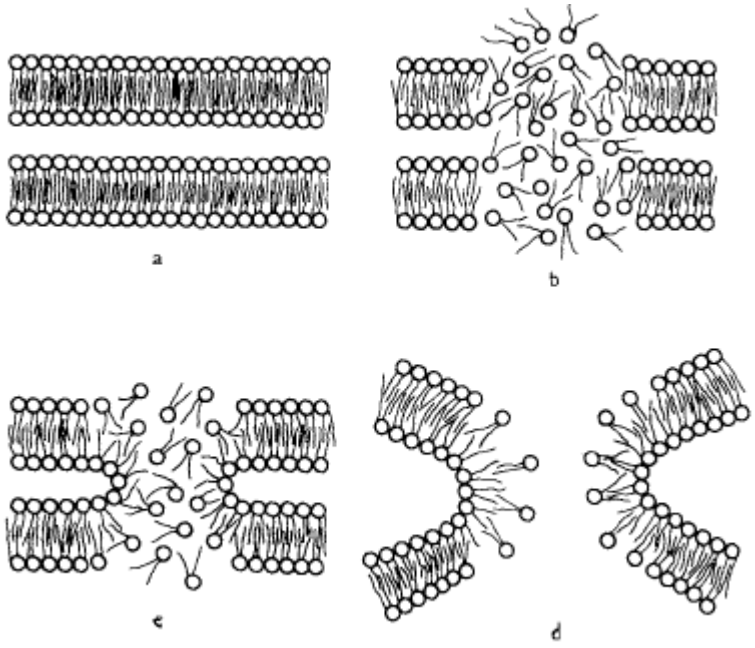

Figure 1-6 *Membrane disruptions due to electrical perturbations. (From top left to bottom right) An undamaged lipid bilayer is shown in the panel a; due to large electrical fluctuations membrane structure is disrupted (panel b), which leads into reorganisation of lipid molecules as shown in the panel c, and two spherical shaped membranes are formed in place of linear membranes, which are energetically favourable due to smaller radius of curvature of the pores (shown in d). This ultimately deforms the membrane system. The figure has been adapted from Zimmerman et al[30] with the permission from the publishers.*

1.3.4. Seeding mechanism and intracellular ice formation

It has been shown that extra cellular ice can act as a precursor of intra cellular ice formation by a process called seeding, sowing of ice crystals[29]. There are two ways by which seeding can occur: propagation of ice crystals through membrane from outside and direct crossing of external ice crystals through the ruptured membranes[31, 32]. This indicates that though it may seem that extra nuclear ice may not be as harmful as other defects such as membrane rupture and intra cellular ice formation, it can nevertheless act as an initiator of the processes that can eventually kill a cell.

Once intracellular ice formation is initiated, the process is continued till all the available water molecules are consumed for producing ice[33]. Intra cellular ice pushes the membranes apart in order to make space for the growing ice crystals. The immediate effect of intra cellular ice formation are membrane disruption, thereby

breaking down cellular compartments and subsequent cell death[34]. Numerous examples related to intracellular freezing injury can be seen in nature: ever green foliage which could resist chilling temperature (-87^{o}C) cannot even withstand at a relatively higher temperature, -10^{o}C, when intra cellular ice formed in it[25]. On the other hand, intra cellular ice are also formed as a result of very rapid cooling[35]. When the system is cooled rapidly, cells are primarily subjected to two negative effects: formation of extra cellular ice and increased concentration of solutes in and out of cells[36], which occur more rapidly than expulsion of water molecules (osmosis) from the cells. This contribute to a situation in which cytoplasm becomes increasingly supercooled, which in turn leads to the formation of intracellular ice[36]. The inevitable damage that can occur on membranes due to the intra cellular ice formation, known as intra cellular ice injury[11], is evidenced from cryo microscopic experiments[37].

1.3.5 Detection of IIF

Prevention of cellular ice formation, in particular IIF, guarantees successful cryopreservation[14]. Hence its detection is very crucial in order to avoid further damage that may occur in the cells. Detection of IIF is possible by experimental techniques, for example, Cryostage microscope[14]. Intra cellular ice is characterised by „flashing" (darkening) of the sample under investigation. Figure 1-7 depicted below elucidates how the formation of intracellular ice is detected using a Cryostage microscope.

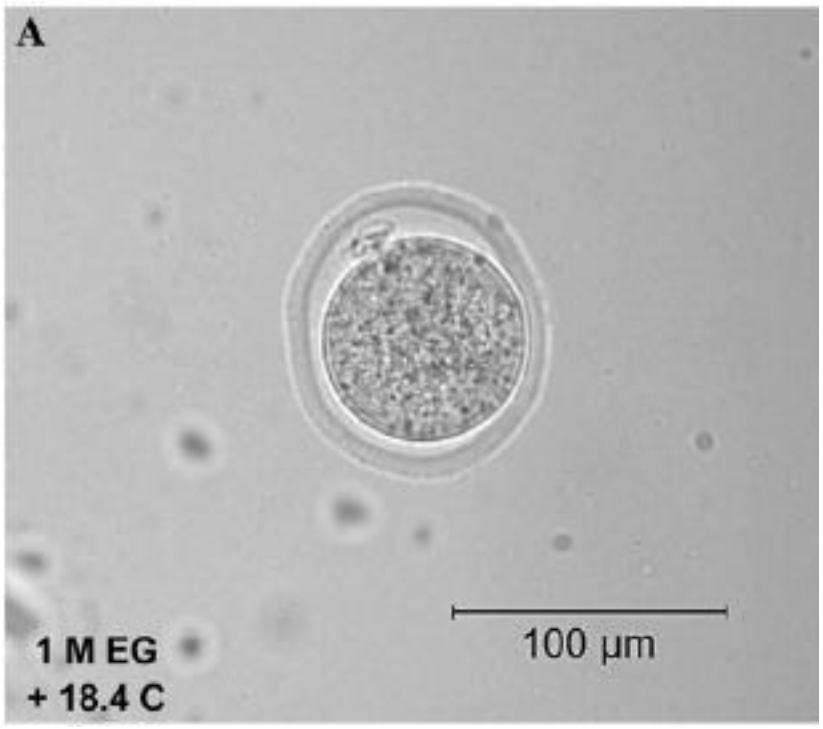

A

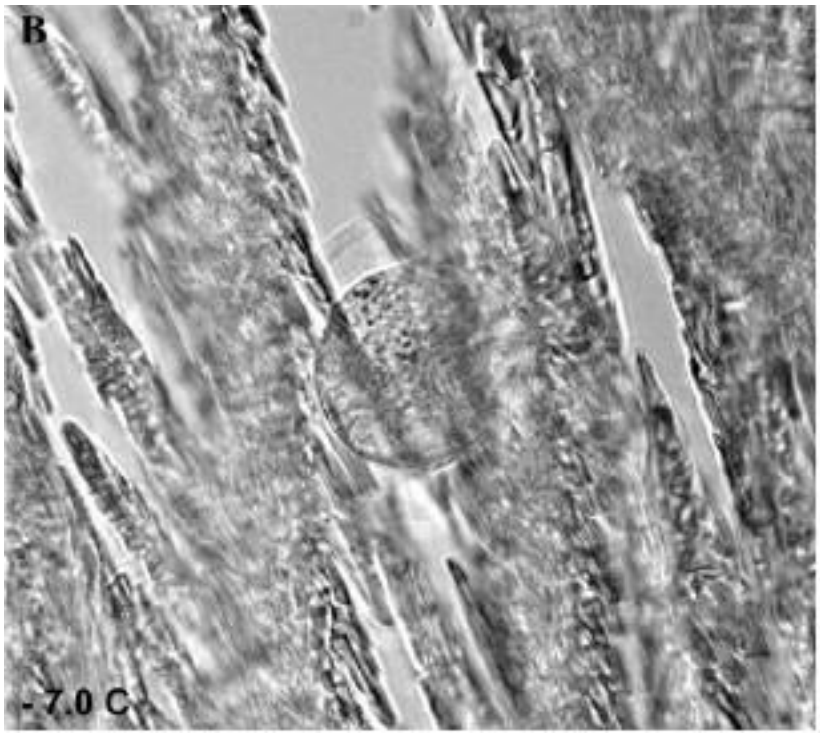

B

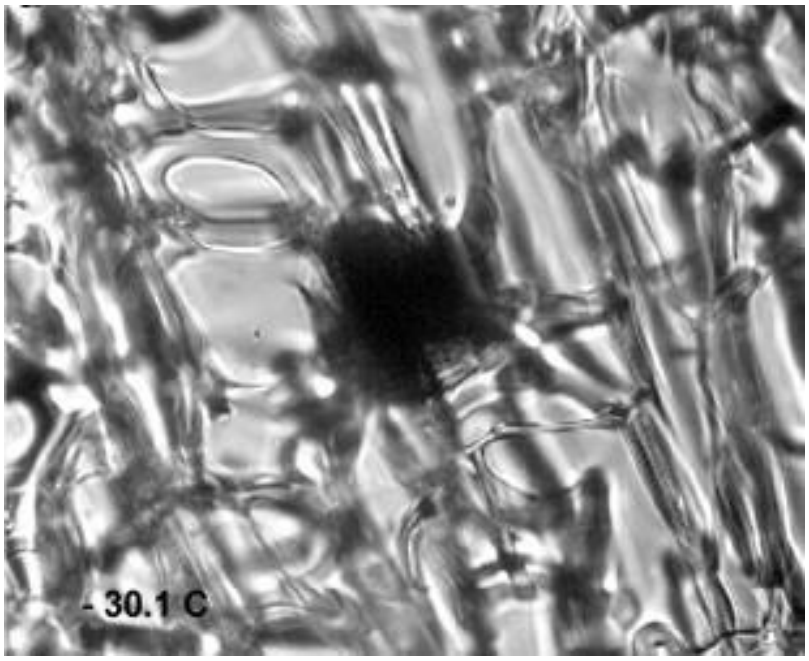

C

Figure 1-7 *Detection of intracellular ice formation. The upper panel A shows the cell before cooling; the middle panel indicates formation of ice crystals growing in and around the cell, at around 267 K- the cells are sequestered by the growing ice crystals (B), the lower panel shows the darkening of the sample, known as flashing, as a result of intracellular ice at temperature near 243K (C). The figures have been taken from Edashige et al*[14].

Membrane cell disruption, as a result of intra cellular ice formation (IIF), can also be detected by more sophisticated equipments; for example an extended cryoscopy technique called Fluorescent Stain SYTO is used to detect the disrupted membranes[38]. Initially the specimen is stained by a special dye that will emit fluorescence that is uniform across the sample. IIF formed in the sample can be detected from a distinctive change in the fluorescence pattern. Figure 1-8 given below demonstrates the difference between the sample before and after intracellular ice formation.

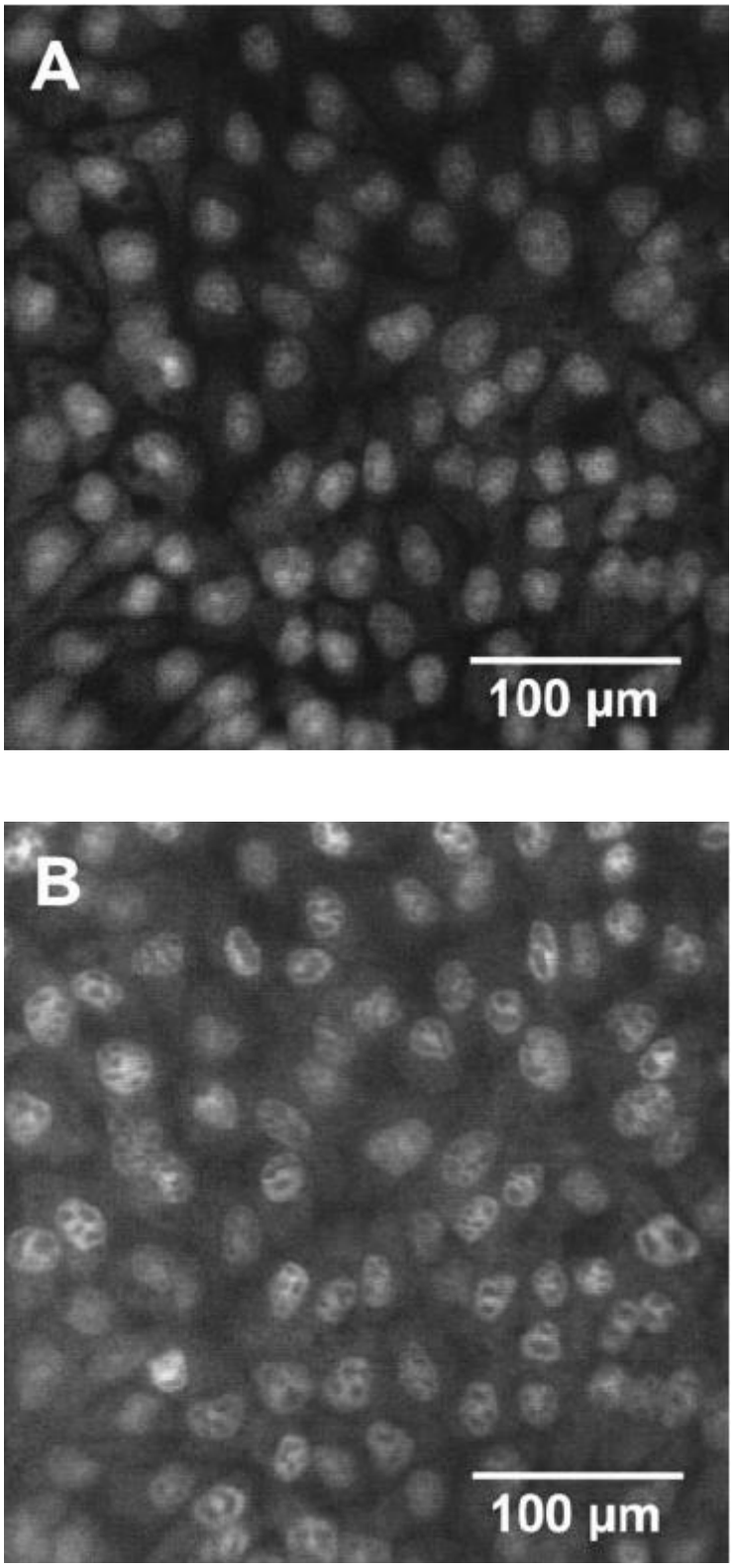

Figure 1-8 *Panel A shows the sample prior to the formation of intracellular ice formation. The sample after cooling to 248K is shown in panel B. Difference in the fluorescence indicates the formation of intracellular ice formation. The figure has been adapted from Acker et al*[38].

1.3.6. Rate of cooling and its implications in cryobiology

The rationale for choosing an optimal cooling rate is to minimise the amount of water that can be crystallised and to maintain the osmotic equilibrium of intra cellular water with external ice and solution[14, 23]. The physical implication of rapid cooling is that cellular water crystallised due to very fast cooling leads to sudden cell death - experimental investigation on endoplasmic reticulum suggests that the rate of freezing determines the extent of cryo injury occurs at low temperature[39]. As a result of different rates of cooling, ice crystals of different magnitudes can be formed - fast cooling results in small ice particles, whereas slow cooling results in larger particles. It has been found out that large ice crystals reduce the survival rates in cherry plants[34]. However, this does not suggest that fast cooling is preferable over slow cooling as fast cooling rate often culminates in intra cellular ice formation.

1.3.7. Alleviation of cellular damage during crystallisation

Even though crystallisation occurs readily in sub zero temperatures, its detrimental effects on the cells and other biological components can be alleviated on certain occasions. Survival of cells, during the crystallisation, is determined by whether the cells are trapped by the advancing ice front or rejected by it. Complete destruction of cells occurs only if the cells are trapped by the ice front; the rate of the advancing ice front (shown in the Figure 1-9) is determined by the medium in which the cells are suspended: if the rate of movement of the ice being formed is less than a critical rate as a result of a repulsive force between cells and the advancing ice crystals, cells are rejected by the growing ice front, limiting the risk of cellular destruction[40, 41].

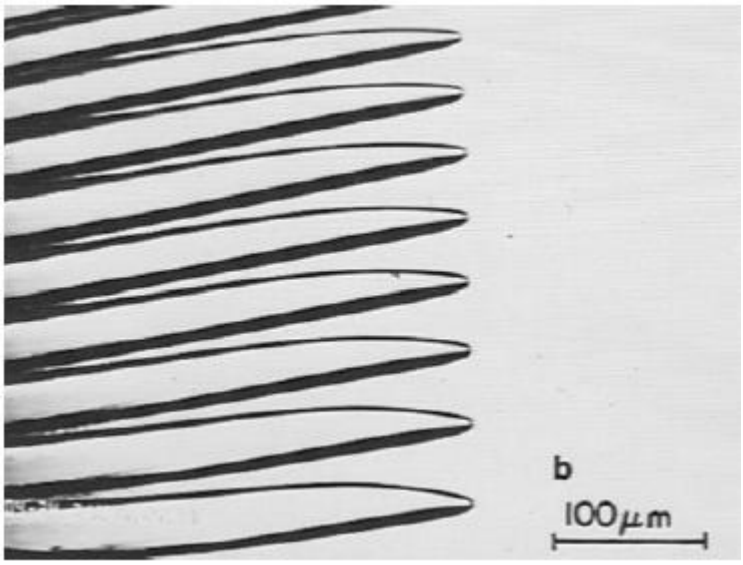

Figure 1-9 *Advancing ice front during freezing. The figure has been adapted from Rubinsky et al*[9].

Velocity of freezing is another factor which determines the survival of cells at subzero temperature. The freezing velocity can be influenced by several factors such as diffusion coefficient of the medium and availability of surface of ice-liquid interface - high diffusivity of the medium that contains ice promotes crystallisation, and larger the liquid-ice interface, the faster the water turns into the ice. Solidification stage microscope experiments on red blood cells indicate that cells are trapped inside and are mechanically deformed to the direction normal to the advancing ice front[42, 43].

Even though freezing and subsequent crystallisation pose a threat to cell architecture, cell membrane can, to some extent, alleviate the problems caused by them, primarily through two mechanisms - balancing water inside and outside the cells[34], and freezing point depression . Membranes, the sieve across the cell border, can balance water in the cell to reduce intracellular ice formation, there by preventing freezing injury that may occur at very low temperature. Expulsion of sufficient amount of water, which is required in some cases to prevent cells from formation of ice crystals inside the cell, can be achieved in cryopreservation experiments either by drying tissues or by osmotic removal of water. Some membranes are capable of interfering with the freezing process and determining the shape of ice crystals. This has an important consequence in the survival of organs as ice crystals with sharp edges can damage them. Nevertheless, these interactions have very little effect compared to the rate at which the organs are

cooled. What is more, certain membranes can interact with ice, which can lead into ice modification. Modified ice thus formed is less injurious to cell structure[34].

1.3.8. Theories on cell death

Several theories have been reported in the literature to account for the cell death due to freezing. It is suggested that prior to cooling, the cells are surrounded by unfrozen water; as temperature drops by unfrozen water will be converted to ice crystals, and the remaining unfrozen water is confined between the ice plates. The cells are also flanked by the growing ice crystals - the forces ice exerts on the cells, called rheological forces, often results in cell deformation[44]. A cell can be exposed to above mentioned injuries depending upon rate of cooling (slow or fast), which is known in cryobiology as two-factor hypothesis of freezing injury[45].

Two other theories related to the cell death are second supercooling-point hypothesis and vital water exotherm hypothesis[25]. Second super cooling point explains that free movement of water molecules are inhibited, and water molecules are trapped in the protoplasm, leading to intracellular nucleation and subsequent cell death. On the other hand, vital water hypothesis posits cell death due to formation of extra cellular ice- during freezing, a point is reached where all readily available water has been frozen and only vital water, that is concentrated with intracellular contents, remains in the protoplasm; upon decreasing the temperature, more water are pulled away from the cell resulting in the extra nuclear ice formation, drawing the protein molecules that are part of membranes together[33]. Some of the theories mentioned in this section draw similarities between various mechanisms of ice formation and their impacts on survival of the cell mentioned in the previous sections.

1.3.9 Dehydration and related issues

Freezing induced dehydration results in membrane stacking[10]. Specific chemical groups of protein structure are too inert to take part in any chemical bond formation if they are hydrated. During dehydration, the membranes tend to stack together, as a result of sulphur- hydrogen bonds transforming into intermolecular sulphur- sulphur bonds[33]. These sulphur-sulphur (S-S) bonds may result in protein denaturation at very low temperature. Further more, these bonds (bond energy = -48.5 kcal/mole) are very

stable than hydrogen bonds (-2 to-9 kcal/mol) in the solution, which means that hydrogen bonds through which water is bound to the protein molecules that are integral part of membranes, can be replaced by the stronger sulphide – sulphide bonds. Dehydration adversely affects the synthesis of Adenosine Tri Phosphate (ATP) that is required for the proper functioning of the cells and membranes. Many process such as synthesis of protein and DNA, active transport of nutrients and ions and maintenance of osmosis across the cells requires a source of ATP. Disruption of synthesis of ATP, the source of energy in an organism, naturally results in cell death[33].

1.3.9.1 Strain during dehydration

In addition to the chemical aspects of membrane stacking explained in the previous section, this section describes the physical aspects of membrane stacking. In a healthy biological tissue, cell membranes normally exist in the liquid crystal fluid phase. In this phase, the chains of the membrane lipids are fluid, and the lipids are free to diffuse in the plane of the membrane. When a cell is fully hydrated, the polar part of its lipid portions is surrounded by approximately as many as ten water molecules. As water surrounding the lipid head groups are removed during dehydration, stress is developed in the membranes which can lead to lipid phase transitions from the normal fluid phase to the deleterious gel phase[19].

When the dehydration is severe, there may be phase separation of membrane components and the membranes may even suffer a transition to non-lamellar phases such as the inverse hexagonal phase. Due to the close proximity of lipids groups owing to dehydration, attractive Van der Waals forces are likely to be developed among them, which contribute to an increase in transition temperature from fluid to gel state. As a result the membrane becomes more rigid and permeable to extra cellular components at very low temperature, which eventually harms the cell[10].

Geometrical strain occurs when a fully hydrated membrane is dehydrated, leading into a reduction in molecule per area in the membrane. The strain is capable of overcoming the hydration forces, which are highly repulsive that keep the lipid layers apart[46]. Although hydration forces are so strong such that they dominate other inter-membrane

interactions at moderate hydration, removal of water during freezing prompted by a much stronger inter membrane stress suppress these repulsive forces[47].

In order to retain cell contents during rehydration, the transition temperature between gel and fluid phases must be suppressed considerably[48]. The relationship between the elevation of transition temperature and bilayer thickness can be mathematically represented in the form of famous Clausius- Clapeyron equation:

$$\Delta T = To\,(a_l - a_g)\Pi/2L$$

ΔT denotes the elevation in the transition temperature from gel to fluid state., To is the transition temperature at fully hydration, L is the latent heat of the transition, Π is the lateral stress due to the gel phase, $\mathbf{a_l}$ and $\mathbf{a_g}$ are the area per lipid in the liquid and gel phase respectively[49]. Figure 1-10 shows how a membrane is stacked during dehydration.

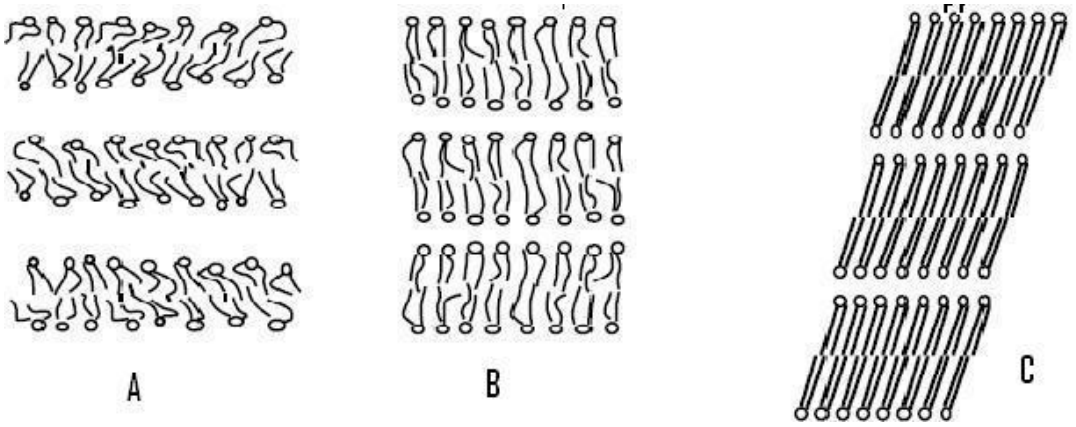

Figure 1-10 *Effect of dehydration on membranes: panel A shows a fully hydrated lipid bilayer; panel B indicates lipid bilayer at low hydration level: area per lipid and inter membrane space decrease at this stage, where as inter lamellar thickness increases; panel C depicts a gel- area per lipid and inter membrane space are further decreased. The figure has been adapted from Wolff et al[10].*

Increase in melting point temperature from fluid state to gel state during dehydration normally occurs in membranes[50]. As indicated by Clausius- Clapeyron equation, the transition is accompanied by liberation of heat and reduction in cross section area of lipid head group, thereby inter membrane space, as shown in Figure 1-10. The

transition drives dramatic changes in entropy as well since high mobility of membrane changes in the hydrated state is restricted in the gel phase where chains are frozen[51]. Removal of bulk water as a result of dehydration instigates the osmotic contraction which brings the membranes into close contact, leading into topological transformations, commonly occurring at low hydration, from inverse cubic phase to inverse hexagonal phase, as shown in the Figure 1-11[46].

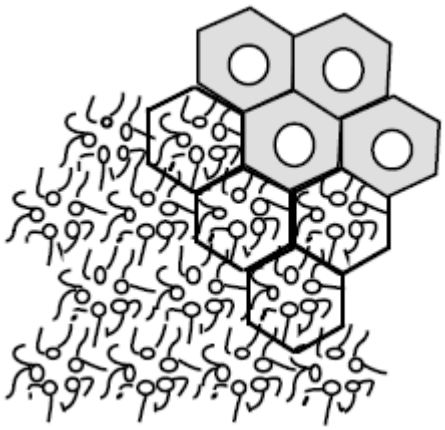

Figure 1-11 *Inverse hexagonal phase- topological response to stress in membranes. Water is surrounded by thick layers of lipid in cylindrical shape, reminiscent of benzene structure. The shaded region in top right of the figure represents lipids, while the unshaded denotes water. The figure has been adapted from Wolfe et al[10].*

Hydration forces exist within membranes in order to keep whole membrane structure intact. This helps them act as an efficient barrier that maintains optimum concentration of various ingredients inside and outside the cells. When these repulsive forces are weakened as a result of excessive dehydration, fusion of individual components (membrane stacking) occurs[10].

1.4. CRYOPROTECTANTS

Membranes or other cell components cannot alone withstand under prolonged cooling. Problems related to freezing, and subsequent dehydration can significantly be reduced with the aid of cryoprotectants – a class of chemicals that has excellent physicochemical properties that help cells retain their architecture under extreme conditions[5, 10]. On the basis of applications, cryo protective agents are divided into two: natural cryoprotectants and artificial (solvent) cryoprotectants. Sugars are widely known natural cryoprotectants[52], whereas organic solvents like DMSO and smaller

alcohols such as methanol and ethanol belong to the second category. Naturally occurring compounds such as disaccharides including trehalose and sucrose have been experimentally found to have excellent cryoprotective activities in animal and plant cells[53-55].

Depending upon permeability through membranes cryoprotectants have been divided into two: permeating (for example, glycerol) and non permeating (for example, hydroxyl ethyl starch)[56, 57]. Permeating cryoprotectants can occupy inside and outside of the membranes simultaneously, whereas non penetrating cryoprotectants can only act from outside[58]. Based on relative size, cryoprotectants fall into three categories- small and medium size molecules, and large macromolecules. Common organic solvents like DMSO and ethyl alcohol belong to the first category-solutes of this class can permeate through the membranes and usually occupy inter membrane space even at low hydration; whereas sugars, belonging to the medium size category, can effectively bind to lipid layers. Dextran and Hydroxy Ethyl Starch (HES) are examples for large macromolecules, which cannot occupy inter membrane space.

1.4.1. CPAs and their applications

There are numerous number of other chemical compounds that are widely used as Cryoprotective agents (CPAs) for successful cryopreservation of biological, agricultural and food materials[5]. Use of CPAs in cryobiology is so common such that they are being used for preservation of all kinds of biological materials at low temperatures - viruses, bacteria, fungi, algae and so forth[5]. Sugars and polyols are naturally synthesised in species living in extreme conditions[59], and are also widely used in artificial cryopreservation[2]. Chemically the CPAs used for various applications chiefly are of five classes: sulfoxides, alcohol and its derivatives, saccharides, amides and large molecules like proteins[2,3,5]. Molecules belonging to sulfoxides, sugars and polyalcohols are the most widely used cryoprotectant agents.

1.4.1.1. Sugars and polyalcohols

Sugars and certain polyols like Mannitol are excellent natural cryoprotectants[60], which are found to be very effective under cold as well as hot (dry) conditions. Thermal

fluctuation analysis and vesicle micromanipulation studies suggest that sugars have strong effect on elastic properties of lipids, which helps them have mutual interaction[61]. The most important disaccharide CPA is trehalose shown in Figure 1-12 along with other members of CPAs in sugar family, since it is found naturally in certain organisms in order to assist them to overcome extreme hot and cold conditions. Trehalose is widely found in variety of organisms- yeast, scorpions and fungi- that are capable of surviving extreme dehydration. It has also been found to be an effective cryoprotectant and a stabilizer during dehydration[62]. Sugars, trehalose in particular, have been found out to reduce membrane transition temperature from fluid to gel states during hydration[51, 63]. On the other hand trehalose shows the least structural fluctuations at low temperatures among disaccharides indicating its bio protective ability[64]. Hence trehalose is used as a potential cryoprotectant in preserving viruses[65], yeasts[66] and fungus[67].

Mannitol is the most abundant polyol in nature and found in many natural organisms[68]. Unlike trehalose, use of poly alcohol like glycerol is not found to be so successful in preventing membrane damage during dehydration; however it acts as a good cryoprotectant in some other way such as retaining water molecules due to osmotic imbalance at very low temperatures[68]. In an comparative study of sugars and poly alcohols, it has been found that compounds containing more number of hydroxyl groups along one side are found to be better cryoprotectants[69]. This alignment of hydroxyl group on one side of the molecule could help themselves establish hydrogen bonding with membranes.

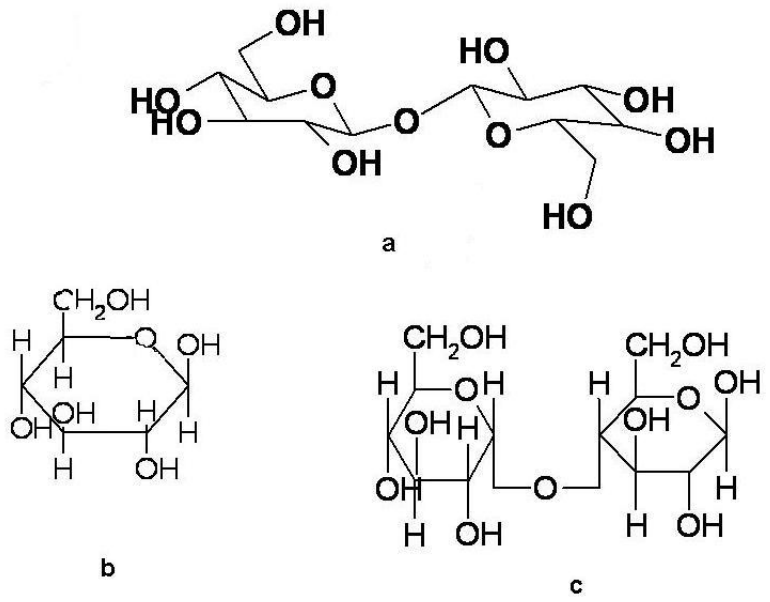

Figure 1-12 *CPAs from sugar family. a. Trehalose, b. Glucose, c. Maltose*

Glucose, a mono saccharide, is used in mild concentrations, in the range between 1 to 18%, to protect bacteria[70] and yeasts[71]. Some bacteria are cryopreserved in aqueous lactose solution[72]. Sucrose is used for preserving certain viruses and bacteria at a higher concentrations, 1-68%[73, 74]. Maltose is not generally a good cryoprotectant; but with mild concentration of glycerol, it is found as a potential cryoprotective agent for certain algae[75].

Various alcohols have also been used in cryobiology as cryoprotectants. Monohydric alcohol like methanol has been found as an effective CPA to protect certain bacteria and algae[76]. Ethanol is another monohydric alcohol which exhibits excellent cryoprotective ability[77]. Other alcohols that are used as cryoprotectants are poly vinyl alcohol[78], ethylene glycol[79], propylene glycol[80] and diethylene glycol[70]. In certain cases, propane diol is found to be more effective than conventional cryoprotectants[81, 82]. Glycerol, a trihydric alcohol, is one of the most common used CPAs. Like DMSO, it is widely used in cryobiology to preserve various kinds of micro organisms: viruses[83], bacteria[84], yeasts[75], algae[75] and protozoa[78]. Its polymeric form poly glycerol, on the other hand, is considered to be potential anti ice nucleators[85]. Poly alcohols such as sorbitol[86] and cholesterol are also effective in certain cases[87]. Important CPAs belonging to alcohol family have been shown in Figure 1-13 and Figure 1-14.

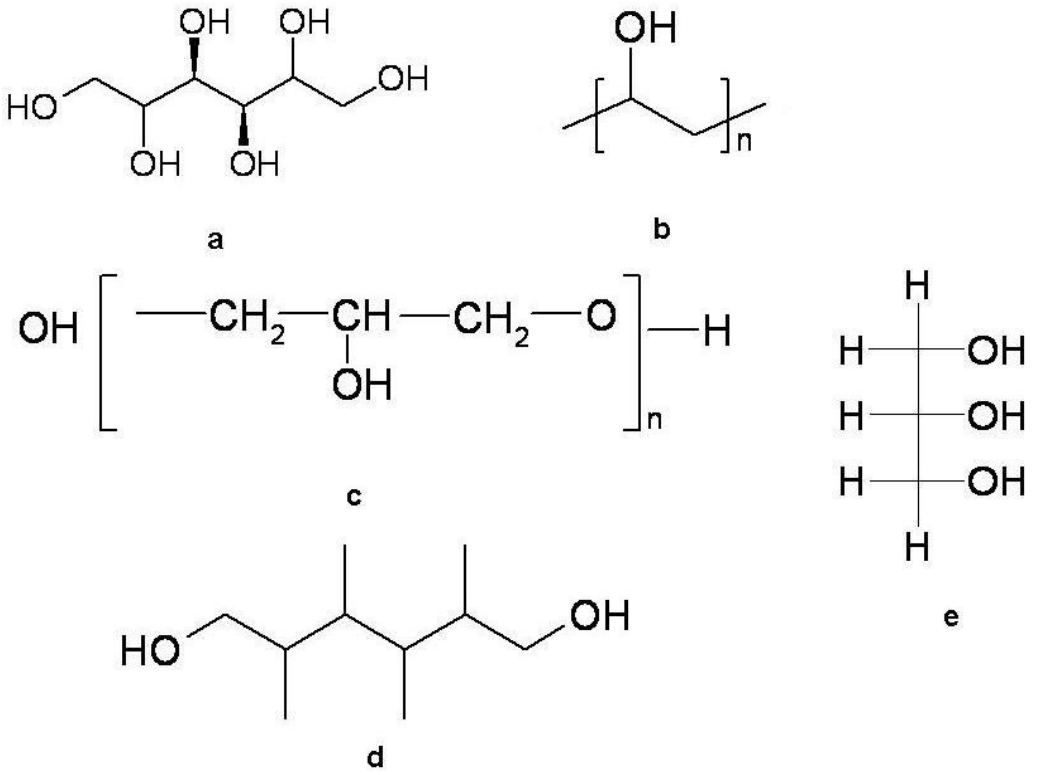

Figure 1-13 *CPAs in alcohol family. 1. Mannitol, 2. Poly vinyl alcohol, 3. Poly glycerol, d. Sorbitol, e. Glycerol*

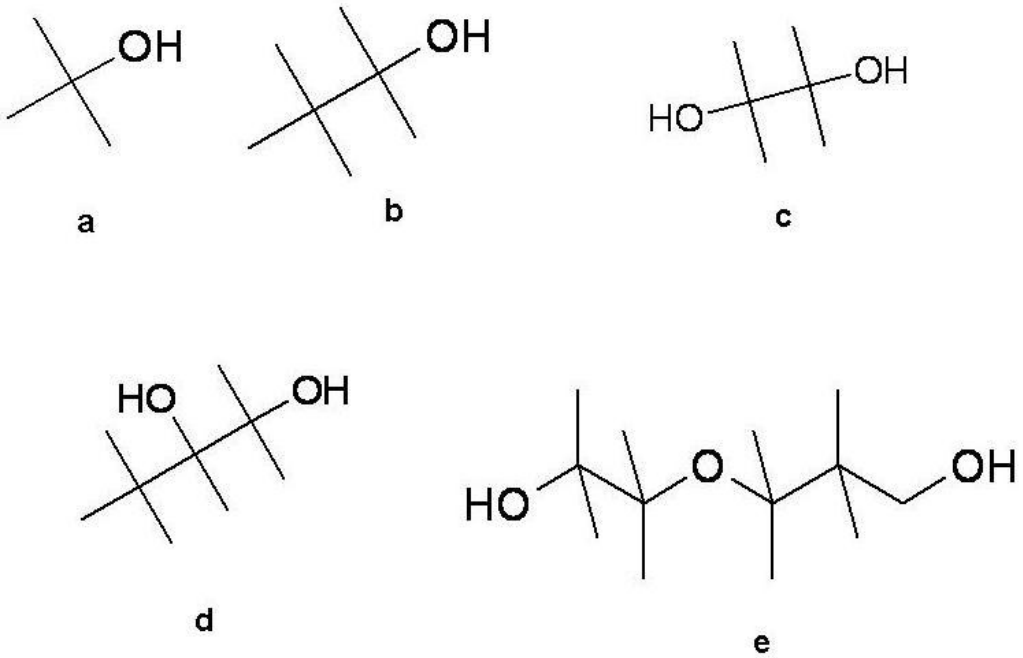

Figure 1-14 *Mono and dihydric alcohol CPAs a. Methanol, b. Ethanol, c. Ethylene glycol, d. Propylene glycol, e. Diethylene glycol*

1.4.1.2. DMSO-most used artificial cryoprotectant

Di methyl sulfoxide (DMSO) belongs to the sulfoxide family, and it is one among the most used CPA"s in contemporary cryobiology[5]. DMSO is also known as universal CPA as it can be applied with most of biological materials : viruses[88, 89], bacteria[90, 91], fungi[75], algae[75] and protozoa[92]. Compared to other class of cryoprotectants like sugars, DMSO differs in many physical and chemical properties: it has got ambivalent character - hydrophobic (due to methyl group) and hydrophilic (due to sulfoxides group), and high diffusivity through the membranes. Due to these properties the presence of di methyl sulfoxide marks a difference in action compared to sugars on various membranes and cells. A recent study suggests that di methyl sulfoxide exhibits three different modes of action depending upon the concentration: at lower concentration DMSO induces membrane thinning; transient water pores are induced at a moderate concentration; and at very high concentration, destruction of bilayer structure is occurred[93]. The effect of dimethyl sulfoxide in destructuring the hydrogen bonding network in water has also been reported in the literature- as the concentration of DMSO increases, more water-water hydrogen bonds are broken[94]. Interestingly at low concentration DMSO carries more water molecules along with them than ions[95].

1.4.1.3. Amides, imides and other Nitrogen compounds

Nitrogen containing compounds such as amides and amides are also used for cryopreservation, albeit at a lower concentration. Acetamide is used for preserving streptococci, a kind of bacteria[96]. Dimethyl formamide is found to be very effective in protecting stallion semen[97]. Recently a solution known as MM2 containing N-methyl formamide (NMF) is found to promote organ vitrification[98]. Succinimide is the sole member of Imide family being used as CPA[99]. Other Nitrogen containing compounds that are used in cryopreservation are N-methyl pyrrolidone[91] and polyvinyl pyrrolidone, the most used heterocyclic CPA[91, 100]. Poly vinyl Pyrrolidone has also been used for preserving certain algae[101]. DMSO and important Nitrogen containing CPAs have been shown in the following figure.

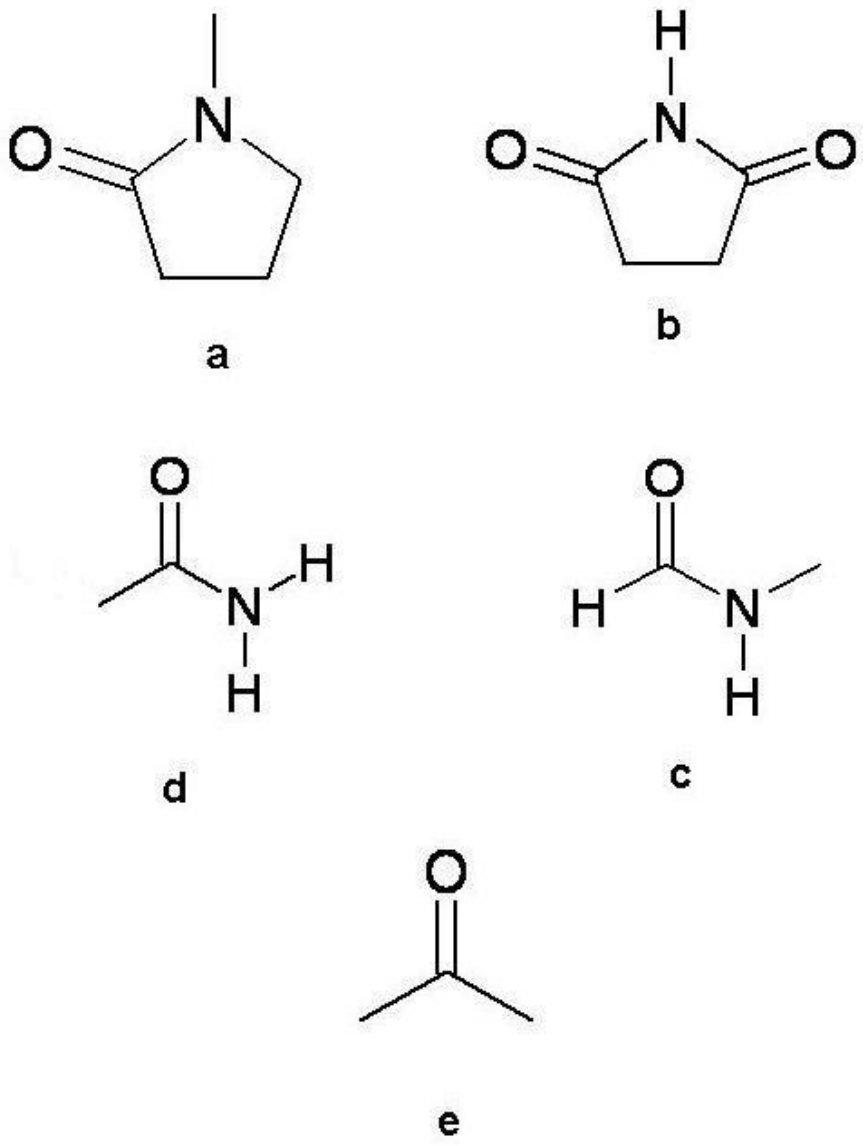

Figure 1-15 *DMSO and Nitrogen containing CPAs. a, N-methyl pyrrolidone, b, Succimide c, N-methyl acetamide d, acetamide e. Dimethyl sulfoxides (DMSO)*

1.4.1.4. Large molecules

Many large molecules like peptides, proteins are also used as CPAs. At concentration less than 4%, Serum Albumin is used for protecting viruses[102]. Gelatin is found to exhibit some protective ability in preservation of bacteria, E.Coli[103]. Even though glycoprotein is not widely used as an artificial CPA, it is very important for many species (fish or insects) to accumulate it, which help them survive extreme conditions like freezing[59].

In addition to the aforesaid CPA‟s, hormones can also act as CPAs, assisting plants to survive drought conditions, N-methyl formamide (NMF) being a notable example. This molecule is known to be a stress alleviator in the plants during hot summer, by inhibiting growth of plants (shedding leaves) and regulating plant stress responses [104-106]. Interestingly, a synthetic mimic of this hormone, a sulphonamide complex known as Pyrabactin, has been discovered very recently[107]. However, its commercial applications have not been completely explored yet.

1.4.1.5. Combined effects of CPAs

Cryoprotectants can also produce combined effect in certain cases - for example cryo preservation of bovine serum albumin. Fluorimetric studies indicate that addition of some CPAs even improve cryo protective ability of otherwise non-CPAs- for example addition of 10 percent of DMSO to Dextran improved the survival rate of biological materials[108]. The mechanism by which the mixture believed to act in the biological system is intriguing - higher molecular weight Dextran forms a complex inert substance, thereby shielding the membranes from any physical or chemical changes that might occur at extreme conditions. The most widely used and popular cryoprotectant mixture is PVS1 (plant vitrification solution), which is mixture of several known cryo protective agents- 22% glycerol, 15% ethylene glycol, 15% propylene glycol and 7% DMSO in 0.5M-sorbitol in Murashige-Skoog medium[109]. Several plant tissues have been successfully cryopreserved using PVS1 and its modified version- PVS2[110, 111] which contains 30% (w/v) glycerol, 15% (w/v) ethylene glycol and 15% (w/v) dimethylsulfoxide (DMSO) with 0.4 M sucrose (pH 5.8) in Murashige-Skoog medium.

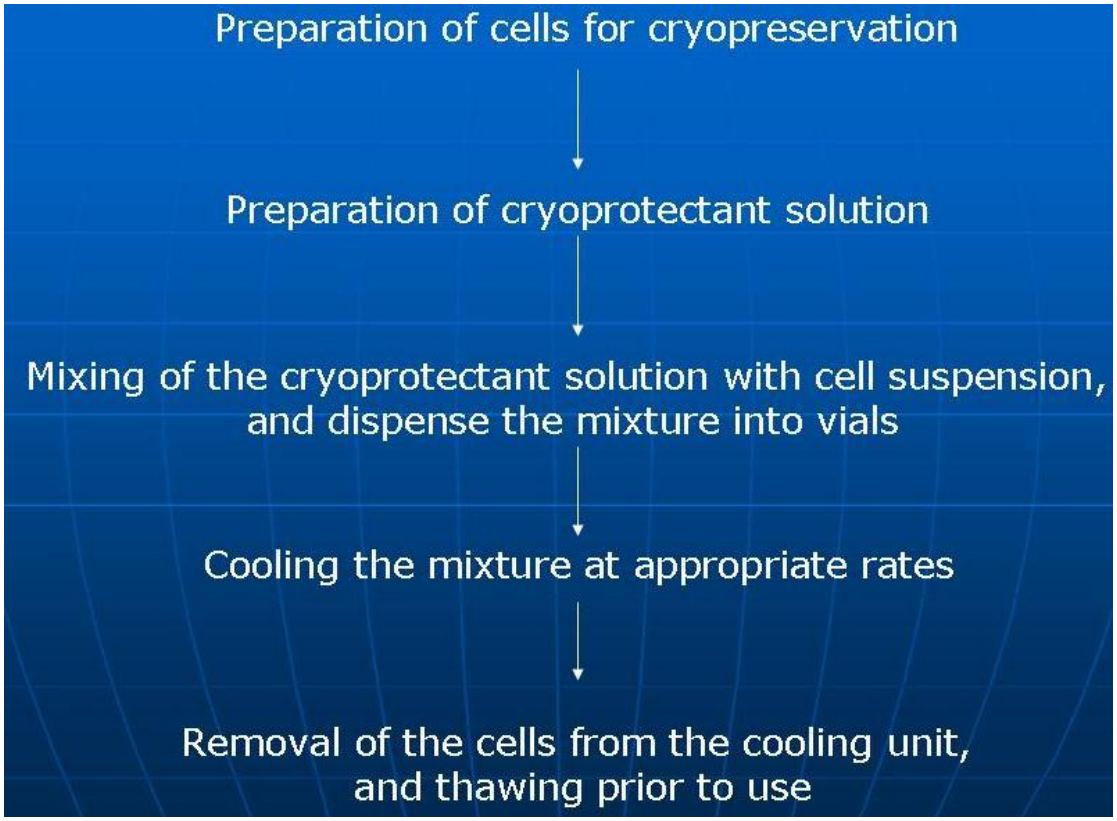

Figure 1-16 *Protocol for cryopreservation*

The cryopreservation procedure consists of five important steps[112]. First is the preparation of cells that are to be cryopreserved. Several factors such as type, nature and physiological state have to be considered while preparing the cells. Next step is preparation of cryoprotectant solutions (CPAs), choice of which depends upon the cell type. Thirdly, the CPA solution and cell suspension are mixed, followed by cooling at appropriate rates. Finally the sample is recovered and thawed before further use. Common cryopreservation protocol is outlined in Figure 1-16**.**

1.4.2. Mechanisms of Cryoprotection

Based on the interactions among the membranes, solutes and water molecules, solvent component in the aqueous solutions, there are several mechanisms have been put forward. The preferential exclusion model suggests that disaccharides interact with water and act as an additional protective layer[53, 113]. The stabilization of proteins by poly ethylene glycol is an example for this mechanism[114]. On the other hand,

preferential interaction model proposes three important hypotheses[115, 116 117] : water-replacement, water- entrapment, and vitrification.

Water replacement hypothesis suggests that disaccharides such as trehalose stabilises membrane structure via hydrogen bonding[115]. By replacing water molecules, sugars are found to cap the membranes by forming protective shells. This assists many natural sugar synthesizing plants in surviving freezing related deleterious effects. On the other hand, water entrapment hypothesis suggests that presence of sugars spurs on to increase the level of hydration near membrane[116]. Both these mechanisms are based on the interactions between water and the biological macromolecules; these interactions are primarily of two types- hydrogen bonds between polar groups and water molecules (hydrophilic interaction), and interactions between water and non polar residues in the system (hydrophobic interaction).

In the vitrification process CPAs function as vitrifying agents which protect biological membranes via formation of amorphous glass. Cryoprotectants such as disaccharides, by forming high viscous glassy matrix, hinder phase and conformational changes in the lipid bilayer[117]. The formation of glass, known as vitrification, takes place in three stages: first the cryoprotectant solution is transformed to a syrup, then to a visco elastic liquid and finally to a stable glass[117]. Due to high viscosity of the glass complex the membrane stacking is prevented, as a result elevation in transition temperature of membranes is decreased. Aqueous solutions of various cryoprotectants – dimethyl sulfoxides, glycerol, ethylene glycol – have also been found to be potential glass formers[118], and are believed to confer cryoprotection of organs and various plant tissues[119].

Prevention of homogenous and heterogeneous nucleation, thus precluding subsequent crystallisation, can be achieved via vitrification[120]. If the system cooled sufficiently fast, the liquid becomes more amorphous due to increase in viscosity. The rise in viscosity prevents water molecules having fast molecular rearrangement which inturn prohibits nucleation and crystal growth in the system. The amorphous state is characterised by the mechanical properties that is close to solid, and the system is said to be vitrified[10]. Figure 1-17 shown below illustrates the mechanism of vitrification.

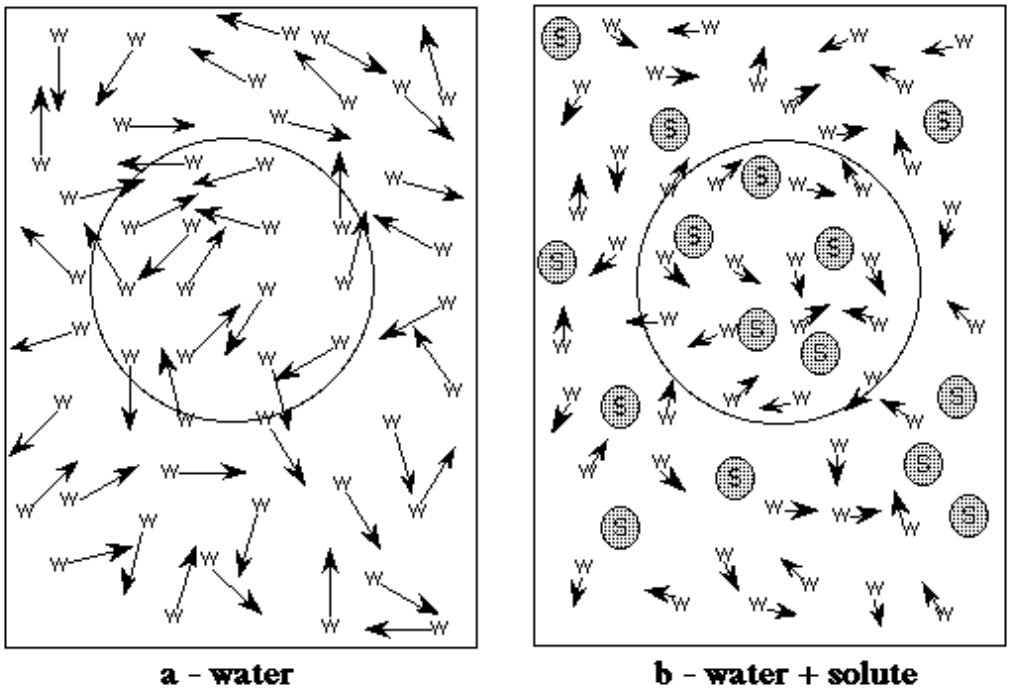

Figure 1-17 *Illustration of vitrification mechanism: w and s indicates water and solute molecules respectively, and arrows indicate the diffusion of the water molecules. The left panel represents the system with only water. The diffusion of water molecules is so high that they can nucleate themselves to the size indicated by the circle (critical nucleus) from which they can grow into crystals. On the other hand, with the addition of CPAs, as shown in the right panel, the viscosity of solutions increases dramatically. Due to intervention of solute molecules, the water molecules cannot form critical nuclei. The figure has been adapted from Wolfe et al[10] with the permission from Elsevier.*

The three aforementioned mechanisms can act together in some cases, especially during dehydration. At higher hydration, the population of hydrogen bonding between water and lipid head groups is more than that of sugar and lipid head groups; but, as the system dehydrates, more and more water molecules are removed from the membrane vicinity, more solute molecules come into contact with lipid head groups.

1.4.3. Chemical structure and vitrification

Addition of methyl group to a parent molecule, termed as methylation, has been shown to have profound effect on vitrification[121]. The concentration threshold for vitrification is decreasing as number of methyl groups is increased in a parent molecule. For

example, concentration threshold for N-methyl acetamide is almost as half as acetamide, because the former has one more methyl group. Formamide is, on the other hand, not a good vitrifying liquid. Similarly, smaller amount of 2,3 butane diol is required for vitrification than ethylene glycol, as the former has two more methyl groups[121]. It is believed that addition of methyl group to carbonyl carbon in formamide or N-methyl formamide strengthens basicity of the carbonyl oxygens and N-H protons, making its interacting with water molecules more feasible[122]. On the contrary, similar argument does not hold in the case of alcohols as C-H protons are less acidic than N-H protons. It is important to note that differential scanning calorimetry studies provide an evidence for enhanced glass forming ability of alcohols by the substitution of electron withdrawing groups[123]. A unified theory in the case of alcohol-water interactions has not been emerged yet, and this will be discussed in more detail in chapter 4.

1.4.4. Effect of solutes

The three mechanisms that are accounted for cryopreservation depend upon the type of solutes in the cryoprotectant solutions and hence their properties[124]. Solutes in aqueous solutions possess intriguing characteristics which affect membrane stability across wide range of temperatures: osmotic effect and solute partitioning. There are several properties of solutions that depend on the number of solutes in a given volume of solutions known as colligative properties. The action of cryoprotectant solution inside the cell can either be colligative or non-colligative, ie, dependent on the solute solvent ratio[125]. Both colligative as well as non colligative properties of aqueous solutions can influence bio protective action of aqueous cryoprotective solutions.

1.4.4.1. Colligative effects

Freezing point depression, due to colligative effect of solutes in a solution, mitigates issues related to freezing in the cellular structures[34]. Freezing occur during the transition from high entropic liquid phase to low entropic solid phase with liberation of heat. Freezing temperature is related to entropy by the equation $T\Delta S = L$, where T is the temperature at which freezing occurs, S is entropy and L is the heat liberated during the process or alternatively called as latent heat of fusion. With the addition of solute, preferably of moderate size, into the solvent, entropy increases naturally while L

remains to be a constant. When temperature drops down, more water content in the solution is converted into ice, which is a pure component. Consequently latent heat of fusion is unaltered even with further addition of solutes. In order to compensate for the increase in entropy, freezing temperature is depressed[10]. Of particular note is that high molecular weight solutes like hydroxyl ethyl starch (HES) do not depress the elevation of transition temperature.

From calorimetry experiments, it has been shown that macromolecules (having molecular weight around 40,000) are excluded from the membranes vicinity. Due to osmotic effect exerted by these heavy molecules, more water molecules are drawn from the vicinity of the membranes, resulting in a lower lipid hydration. This indicates that in the presence of macromolecules membranes are dehydrated than in its absence, leading to an increase in transition temperature than a pure lipid[126]. Both these colligative effects demonstrate that molecules of moderate size are generally preferable over large macromolecules as CPAs. Effect of solute size on membrane integrity is shown in the figure shown below.

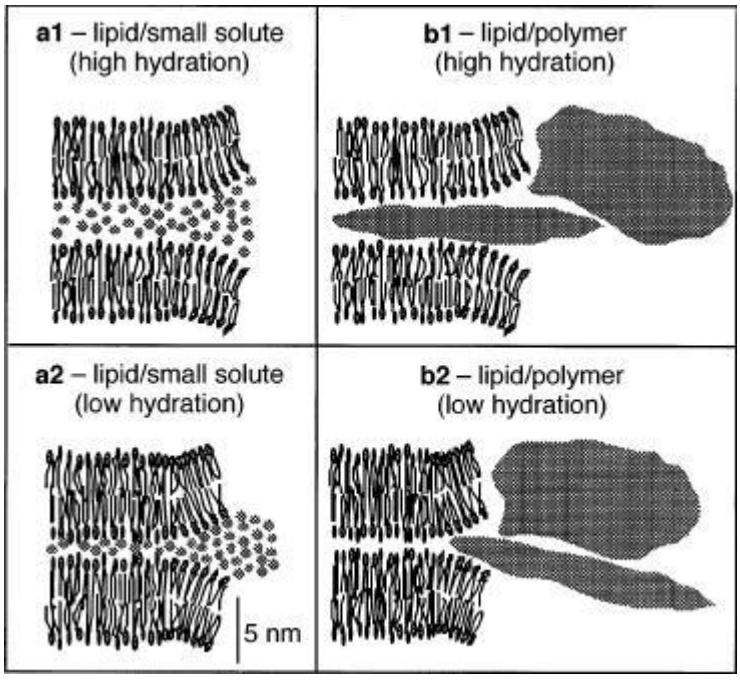

Figure 1-18 *Effect of solute size on membrane stability. In panel a1, a lipid with small solutes is shown at high hydration. At high hydration inter membrane space and membrane integrity are preserved since solutes occupy inter membrane space. In panel b1 (top right) lipid with large solutes like polymers at high hydration is shown. Like*

smaller solute, the macromolecular solutes too are able to occupy inter membrane space at this level of hydration. Figure on bottom right (b2) shows a system containing large solutes (polymer) and lipids at low hydration. Polymer molecules are excluded from the inter lamellar space at low hydration, whereas in the case of smaller solutes, they remain in inter lamellar space even at low hydration, preserving membrane integrity, as shown in figure a2. The figure has been adapted from Bryant et al[2].

1.4.4.2. Solute partitioning

Larger solutes such as polymers are not capable of permeating through membranes. Because of the size of solutes, they prefer not to occupy inter lamellar space but the bulk region. As freezing occurs, more water molecules in the bulk region are converted into ice, which results a partition between ice and solute in the bulk space. At the same time, the water is drawn from the inter membrane space due to osmotically, resulting in inter membrane stress[10]. Figure 1-19 illustrates the mechanism of solute partitioning.

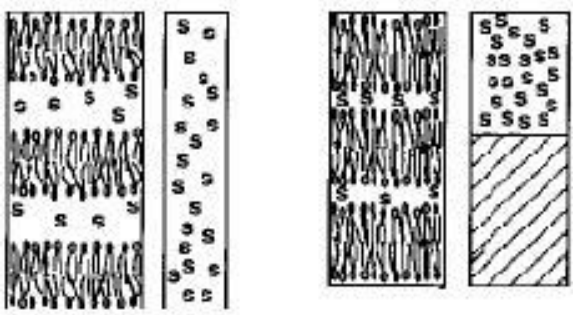

Figure 1-19 *Solute partitioning. The diagram in left side shows a membrane- solute – water system. Since the size of solute is big, most of the solutes occupy bulk region instead of inter lamellar space. As a result the bulk region becomes highly concentrated. As freezing occurs, water molecules in the bulk region are converted to ice, which causes partitioning of bulk region into ice and solutes. Large concentration of ice draws more water molecules from the inter membrane space, causing inter membrane stress and stacking. The figure has been adapted from Yoon et al[127].*

1.4.5. Experimental investigation of aqueous cryoprotectant solutions

Cryoprotective properties of aqueous disaccharide solutions measured using various experimental techniques have been reported in the literature[64, 128-130]. Advanced experimental techniques such as Quasi-Elastic Neutron Scattering (QENS) and Neutron Spin Echo (NSE) have been employed to study aqueous solutions of sugars. These

methods are extremely powerful such that structural confinement of solutes in solutions can effectively be probed to very minute detail[131]. The experiments reveal a slowing down mechanism exhibited in various disaccharide-water systems. A strong disaccharide-water interaction, especially in the case of trehalose, was observed causing the disruption of tetrahedral configuration arrangement. At lower temperature the number of water molecules bound to a trehalose molecule is very high, around 20, and as temperature increases, this tends to decrease. In addition, diffusion of trehalose molecules is reduced compared to other sugars such as maltose and sucrose[132].

Elastic Neutron Scattering experiments further show that in comparison to other aqueous disaccharide solutions, aqueous trehalose solutions appear to be more crystalline and therefore more structured, as evident by sharp peaks at the vibrational region[133]. A slightly higher dynamic transition temperature, obtained from the elastic incoherent neutron scattering data, for very dilute trehalose solutions indicates that even at very low concentrations aqueous solutions of trehalose can form glassy state at a higher temperature. This has a potential application in cryobiology as biological organs and membranes can be protected in the aqueous cryoprotectant solutions that can attain glass transition temperature at higher temperature. Trehalose"s superior glass forming ability is apparent even at very low concentrations: the glass transition temperatures at 5% aqueous solutions of trehalose, sucrose and glucose are 40^{o}C, 15^{o}C and -10^{o}C respectively. This indicates that even at very low hydration level trehalose protect membranes and other biological membranes by attaining glassy state, there by avoiding inter and intra membrane collapse.

1.4.5.1. Hydrogen bonding properties of sugars and glycerol

Sugars form hydrogen bonds with membranes- for example they interact with choline and phosphate groups via hydrogen bonding[134], through which they maintain membrane integrity. The abundance of hydroxyl groups in sugars help them form hydrogen bonds in order to replace water molecules during dehydration[135]. It is believed that due to excessive hydrogen bonding, sugar molecules in aqueous solutions hinder the translational as well as rotational motions of water molecules; this effect is more pronounced in concentrated region rather than bulk aqueous region[136]. The greater the number of pyranose or furanose rings in the sugar, the greater is the hindering of the movement of water molecules.

Trehalose has superior hydrogen bonding properties than other disaccharides, for example sucrose, in water. Probability distribution analysis of constituent oxygen atoms in aqueous sucrose solutions indicate that even at very low concentrations sucrose forms intra molecular hydrogen bonds, whereas trehalose only forms such hydrogen bonds at very high concentrations(50%), suggesting stronger interactions of trehalose with water[137]. In terms of interaction strength parameter and hydration number, measured by ultrasonic velocity measurements, trehalose has higher value than sucrose and maltose solutions[128]. Measurement of partial volume across wide range of temperatures indicates that trehalose has greater structural sensitivity to temperature changes than maltose and sucrose molecules. The superior protective ability of trehalose over other disaccharides is also supported, from the ultrasonic experiments, by the fact that trehalose has higher hydration number, indicative of more closed packing conformation[128].

Experimental techniques such as differential scanning calorimetry (DSC) as well as infra red spectroscopy (IR) also underpin the excellent cryoprotective abilities of aqueous trehalose solutions[50]. Three peaks have been reported in the range between 1180 cm^{-1} to 1280 cm^{-1} from the infra red spectrum – for a pure dry lipid, the highest peak around 1258 cm^{-1} was observed corresponding to the lipid that is not hydrogen bonded to water; a peak at 1229 cm^{-1} was observed indicating lipid – water hydrogen bonding in the hydrated state, and the lowest peak at 1227 cm^{-1} indicates a hydrogen bonded trehalose to lipid. The hydrogen bond between trehalose and the lipid helps the membrane stay apart at very dry conditions. This interaction prevents the membranes from stacking and there by decreases the phase transition temperature. This fact is supported by the DSC analysis that trehalose lowered the gel to fluid transition temperature well below the transition temperature when fully hydrated. DSC data further shows two sharp peaks at around 27^{o}C and 60 ^{o}C: former peaks corresponds to the melting transition of the lipid, where as the peak at higher temperature is an indication of glass transition with the addition of trehalose. This suggests that when temperature decreases, trehalose – membrane system attains glass transition temperature prior to the probable fluid- gel transition temperature.

Glucose, a mono saccharide, is another sugar molecule which has excellent protective properties against freezing and drying[131]. QENS studies reveals that diffusion rate of glucose molecules is inversely proportional to its concentration-doubling the concentration

reduces the diffusion rate by half. In addition, glucose molecules are found to be clustered in aqueous solutions. Small Angle Neutron Scattering (SANS) measurements also indicate clustering of glucose molecules on increasing the concentration. Rotational and translational motions slow down upon increasing the concentration, concomitant with the clustering of glucose molecules, as evidenced by the flat peaks in the spectroscopic data.

Glycerol, a polyhydric cryoprotectant, also exhibits excellent solvation properties in water: molecular dynamics studies reveal that there is significant increase in the number of hydrogen bonds upon increasing glycerol concentrations in the aqueous mixtures, indicating a linear relationship of the interactions between water and glycerol molecules. This trend is also reflected from the infra red spectroscopy studies that the frequency of hydrogen-oxygen-hydrogen (HOH) bending mode increases at the cost of decreasing frequency of OH stretching[138]. Moreover, it has to be noted that upon increasing concentration of glycerol in its aqueous mixtures, the water- water interactions are reduced, strengthening hydrogen bond network.

1.4.6. Computer simulation of cryoprotectant solutions

Experimental findings can be further verified by computer simulation analysis such as molecular dynamics methods. These techniques provide atomistic details such as solvation and dynamics properties around a solute which is probably experimentally inaccessible. Among the cryoprotectants, trehalose is one of the most widely studied molecule due to manyfold applications[54, 60, 139-142]. It has been shown that presence of a solute like trehalose has profound effect in orientation effects of water molecules, which tend to form tetrahedral clusters at lower temperature. At the same time, trehalose does not make any impact on bulk water molecules in the solution, indicating that rather colligative properties, due to distance dependent interactions between solute and solvent, play an important role in interactions existing in aqueous disaccharide solutions.

The rotational as well as translational motion of water molecules are also affected by sugar molecules, especially in their vicinity. From the molecular dynamics simulation analysis of various sugar molecules, it has been found that trehalose and glucose dampen

translational motion of water molecules at lower temperature more than sucrose molecules, whereas at a higher temperature (30^{o}C) reverse is the case, suggesting that trehalose and glucose can effectively interfere with the motion of water molecules as temperature decreases. In addition to that, the interaction is strong such that rotational and translational movement of water molecules within 5 Angstrom from the solute molecule are largely reduced[140].

Interactions exerted by various sugar solutes with water are more contrasted in the lower temperature region: glucose molecules are found to be less dampening the movements of water molecules than to sucrose and trehalose molecules. It is interesting to note that at higher temperature there is little to differentiate among glucose, trehalose and sucrose in slowing down of rotational motion of water molecules. Nonetheless, all three solutes are found to be engaged in forming hydrogen bonds with water that are more stable than hydrogen bonds existing between water molecules at various temperatures. This indicates that addition of sugar molecules in general disrupts the hydrogen bonding network in the water, echoed by the fact that the lifetime of water- water hydrogen bonds decays much faster than hydrogen bonds between water and sugar molecules. The calculation of rotational as well as translational diffusion coefficients provides further insights into the structural aspects of the binary mixtures: the calculation indicates that there occurs a decoupling of translational motions from the rotational motions, a signature of supercooled liquids [140].

It has been shown that sucrose molecules are less hydrated than trehalose molecules. The tendency of sucrose molecules to form more intra molecular hydrogen bonds via free hydroxyl groups and to be less hydrated than trehalose molecules indicates that trehalose has superior cryoprotectant ability than sucrose. In other words, a solute which can form more number of inter molecular hydrogen bonds is likely to interact with membrane and thus be a better cryoprotectant than a solute which prefer to form intra molecular hydrogen bonds[143].

Simulations of aqueous di methyl sulfoxide (DMSO) solutions also demonstrate how DMSO solutions effectively hinder the movement of water molecules[144]. This effect is not monotonous with increasing concentrations; at equimolar concentrations, the rotational motion of water molecules is found to be hindered the most as indicated by

the orientational time auto correlation functions (TACFs). Translational motion of water molecules follows the same trend as well, as indicated by the calculation of diffusion coefficient which is matched by the experimental values at various concentrations[145].

1.4.7. Experiments of cryoprotective action on membranes

The properties of cryoprotective agents on membranes can efficiently be investigated using experimental techniques such as differential scanning calorimetry (DSC). Since membrane largely contains phospholipids, many experimental as well as theoretical studies have been focussed on various types of phospho lipids[146]. Membrane stabilization properties of sugars, trehalose in particular, during dehydration are vindicated by the experiments[51, 147]. From the calorimetry experiments carried out by Bryant et al, it was shown that vitrified sugars diminish the increase in melting temperature from fluid state to gel state of the dehydrated membranes[148]. The experiment also confirms that transition temperature is a variant of the hydration and physical state of sugars. The decrease in melting point elevation was also observed differently in different types of lipids. The decrease was found to be in the decreasing order- dioleoyl-phosphatidylcholine (DOPC); 1-oleoyl-2-palmitoyl-phosphatidylcholine (OPPC); 1-steroyl-2-oleoyl-phosphatidylcholine (SOPC); 1,2-dimyristoyl-phosphatidylcholine (DMPC); 1,2 – diplamitoyl –phosphatidylcholine (DPPC), primarily due to different acyl chain composition in various lipids.

Fourier transform infrared spectroscopy analysis (FTIR) shows that the effect of trehalose in the membrane stabilisation is two fold: prevention of membrane fusion, and maintenance of membrane phase order. The analysis further reveals that trehalose"s interaction with membranes depends upon the nature of lipid components[149]. During dehydration trehalose molecules interact with the phosphate groups in the lipid very strongly, indicated by shift of asymmetric stretching peak towards the lower frequency region. FTIR spectral analysis also vindicates the role of hydrogen bonding in stabilizing the membrane structure in the presence of trehalose. Trehalose strengthens the interactions with the lipid layers by forming strong hydrogen bonding as evidenced by the higher steepness of OH stretching wave number in its presence.

1.4.8. Computer simulations of membrane cryoprotection

Simulations of various lipid bilayers provide further insights to the experimental findings[150]. It has been widely accepted that trehalose increases lipid head group width, suggesting that stacking of membrane is prevented upon increasing the trehalose concentration[151]. Furthermore, as temperature increases, entire membrane is destroyed without disaccharides, and membrane structure is almost retained in their presence. The increase in trehalose concentration ensures membrane integrity, indicating that trehalose establishes hydrogen bonding with the lipid matrix. It is generally believed, supported by the inter molecular radial distribution analysis, that at a given temperature sugars do not penetrate into the lipid bilayers; they only indulge in inter facial interactions with the lipid bilayers[146]. This clearly rules out the possibility of sugar - acyl groups (hydrophobic part of the lipid) interactions.

Supplementary to experimental findings, molecular dynamics simulations shed light on anisotropic nature of sugar- lipid interactions, similar to sugar – water interactions. Trehalose contains two glycosidic rings connected by an oxygen atom, with each ring contains four hydroxyl groups. However, interactions of all hydroxyl group are found not to be alike, as seen from the MD snapshots[146]. The hydroxyl groups that are directly connected to the glucose ring are found to be more interacting than the hydroxyl groups that are indirectly attached to the glucose ring, indicating glucose ring‟s self interaction with the lipid head groups.

1.4.8.1. Directional properties of hydroxyl groups in Trehalose

The interaction of trehalose with water is highly directional, evident by the fact that not all hydroxyl groups present in the trehalose molecules interact with the water molecules in the same fashion. Radial distribution analysis shows that the hydroxyl group in the glycosidic ring interacts with water less strongly, compared to the hydroxyl groups that are not directly attached to the ring[143]. The availability of free hydroxyl groups on the glucose rings leads into the high degree of hydration in the aqueous trehalose solutions compared to other sugar solutions. Water molecules, as a result, become isolated from the bulk solution which leads into unavailability of freezable water molecules[143].

Molecular dynamics simulation of DPPC layer shows that its head group can accommodate around 12 water molecules per head group in hydration layer[152]. Structural and dynamic properties of aqueous glycerol solutions have also been investigated using MD simulations[153]. Various lipids differ in certain aspects such as saturation that determines the stability of the membranes under certain conditions; molecular dynamics simulation reveals that dioleyl-phosphatidylcholine (DOPC) decreases the fluid to gel phase transition temperature considerably with respect to other lipids such as palmitoyl-oleyl phosphatidylcholine (POPC) and dipalmitoyl phophatidylcholine (DPPC), even though electron density and atom distribution profiles are similar.

Compared to sugars, DMSO molecules do not diminish the increase in melting temperature from gel to liquid phase during dehydration[154]. Also, DMSO dehydrates the bilayer surface, which may render DMSO ineffective in protecting membranes at low hydration, by drawing water molecules from the bilayer surface to itself since DMSO – water interactions are stronger than water – water interactions. Nevertheless it does possess excellent diffusive as well as membrane binding properties which could be very useful in cryo preservation of certain types of membranes. Potential mean force calculations indicate that DMSO penetrates much deeper into the bilayer region at 350K[154]. It prefers to stay in the aqueous region at 350K, whereas, at a higher temperature (450 K), DMSO molecules prefer to remain in the bilayer, a signature of hydrophobic character, suggesting highly temperature dependency of DMSO on bilayer systems.

1.5. VITRIFICATION

As mentioned in the previous section, vitrification is one of the successful methods to preserve biological as well as agricultural materials[1,2,16,121]. Successful cryopreservation of materials, in other words preventing crystallisation, is achieved through careful selection of vitrification solutions (mixture of CPAs in water) with moderate cooling rate[121]. Onset of crystallisation, threat to cells and membranes, during freezing is imminent under normal conditions[16]. However, vitrification is believed to prevent it with appropriate choice of cooling rates and CPAs. A vitrified and a non vitrified (crystallised) sample are shown in Figure 1-20.

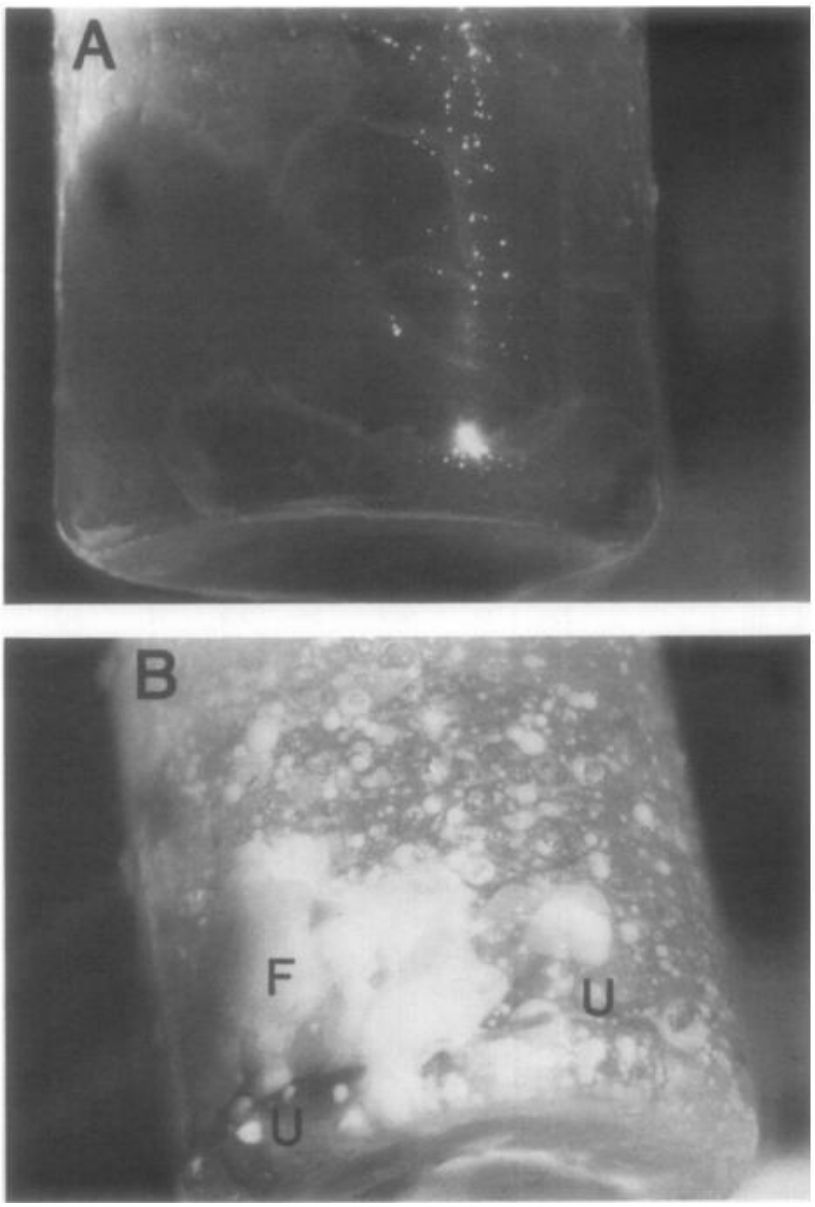

Figure 1-20 *Vitrification Vs Crystallisation. The upper panel (A) indicates the system that is successfully preserved via vitrification. The sample is very transparent without any tint of ice crystals. The lower panel shows the organ that was not preserved successfully. The white spots around the vessel indicate the growth of ice crystals which damage the organ. The figures have been adapted from Merryman etal*[16].

1.5.1. Supercooling

When cooled below the corresponding freezing point, liquids and aqueous solutions can even remain in liquid state, a phenomenon known as supercooling[15]. Supercooled materials will inevitably crystallise, unless it forms a vitreous substance called glass.

Supercooling range of all materials is not unique; some undergo supercooling far below the melting temperature, Tm, while some can only be supercooled to only 10-20 K below their melting temperature. Metals and inorganic liquids can generally be supercooled to couple of hundreds Kelvin below to their melting temperature. On the other hand, organic compounds can only be supercooled to less than 40K below their melting temperature. The melting temperature and corresponding supercooling temperature of some representative elements and compounds has been shown in Table below[155].

Table 1-2 *Crystallisation and supercooling temperatures of different materials*

Elements/compounds	Crystallisation Temperature	Supercooling Temperature
Metals		
Platinum	2043 K	1673 K
Palladium	1828 K	1496 K
Nickel	1725 K	1406 K
Iron	1803 K	1508 K
Gold	1336 K	1106 K
Inorganic compounds		
Sodium Chloride	1074 K	905 K
Sodium Bromide	1023 K	857 K
Potassium Chloride	1045 K	874 K
Lithium Fluoride	1121 K	889 K
Cesium Fluoride	955 K	823 K
Organic compounds		
Ammonia	195.5 K	155.2 K
Benzene	278.4 K	208 K
Chloroform	209.7 K	157.2 K
Carbon Tetrachloride	250.2 K	200.2 K
Methylamine	179.7 K	144 K

Supercooling behaviour of water is discussed in detail in section 01.4.1.6.3

1.5.2. Glass transition temperature

Glass transition temperature, characterised by a sudden change in thermodynamic response functions such as specific heats or coefficient of thermal expansion, is the temperature at which a supercooled liquid becomes glass[156,157]. Below the glass transition temperature, the system takes solid structure (glass), meta stable to crystallisation which can occur between T_g (glass transition temperature) and T_m (melting temperature)[158]. It is of high interest in material science in determining the temperature of the system undergoes a phase transition, glass transition temperature (Tg), due to diverse practical applications[121].

Experimental investigations on pure amorphous (supercooled) phase poses a severe challenge - since pure amorphous phase is inaccessible at very low temperature, only partially crystallised systems can normally be investigated[159]. Nevertheless Differential Scanning Calorimetry (DSC) and Elastic Neutron Scattering (ENS) techniques are often employed to measure the glass transition temperature, Tg, by analysing the step wise changes of heat flow during heating the sample[159].

Differential Scanning Calorimetry analysis asserts the importance of higher glass transition temperature in stabilizing the membranes during dehydration[117]. It has to be noted that the rate constant for the leakage of solutes in the protoplasm follows a linear relationship till the onset of the glass transition temperature. After attaining Tg, a marked deviation from the linear behaviour has been observed, with 50% increase in the activation energy below Tg, indicating that attainment of glass transition temperature reduces the membrane damage by increasing the energy barrier.

1.5.2.1. Sugars and glass transition temperature

Saccharides are known to have high glass transition temperatures[10, 160, 161]. Due to their peculiar glass forming property, sugars, disaccharides in particular, are very effective in preserving cell structure in dry conditions[162]. Nevertheless the exact mechanism by which these saccharides act in order to alleviate stress in the membranes during dehydration are still subjected to controversy- some argues that higher the glass transition temperature is,

the more effective the solute (saccharide) becomes against the increase in fluid to gel transition temperature[163]. On the contrary, calorimetry scan reveals that glucose, despite its glass transition temperature of being the lowest of the tested sugars, reduces the transition temperature the most[164].

The glass forming tendency of sugars like trehalose and its implications in cryobiology have been discussed in the previous sections. Their glass forming properties are so remarkable such that addition of small amount of water does not diminish the glass transition temperature of trehalose as it forms hydrates upon addition of water molecules[165]. State diagram of glass transition temperature against hydration indicates that glass transition temperature of anhydrous trehalose is much higher than sucrose, 115^0C and 65^0C respectively[165]. High glass transition temperature at a higher hydration is believed to have contributed to exceptional cryo protective ability of trehalose.

Some compounds, for example dextran, are found to be less effective cryoprotectant than trehalose, though they have higher glass transition temperature than the disaccharide[132]. This suggests that vitrification may be inextricable with other mechanisms in protecting membranes at drastic conditions. Sugars also play an vital role in sustaining the life by preventing uncoupling (destruction) of ATP synthesis, vital for all organisms[115].

1.5.3. Fragility

Glass transition is an important property that classifies materials into strong glass formers and weak (fragile) glass formers. The distinction between strong glass former and fragile glass former can be made by measuring fragility index, m[166]. Fragility is defined in two ways, thermodynamically and kinetically (dynamic)[167]. Dynamic fragility index indicates deviation from the Arrhenius behaviour (linear) in terms transport or diffusion properties, for example diffusion coefficient and viscosity. Mathematical formulation of dynamic fragility index (m) in terms of viscosity, for example, can be given as

$m = \frac{d(\log(\eta))}{d\left(\frac{T_g}{T}\right)}$ at T = Tg.,

where η is viscosity at corresponding temperature and Tg is the glass transition temperature of the corresponding liquid[168]. Equivalent relationships in terms of relaxation times or diffusion coefficient are valid as well.

On the other hand, thermodynamic fragility can also be explained on the basis of thermodynamic variable such as entropy. Mathematically, it is given as

$m = \frac{d\left(\frac{\Delta S(T_g)}{\Delta S(T)}\right)}{d\left(\frac{T_g}{T}\right)}$, (ΔS = entropy difference).

Alternatively, fragility is given as the ratio of heat capacities of liquid and glassy states, $\frac{C_{pliquid}}{C_{pglass}}$. Higher the value of m, the more fragile the liquid is.

Fragile liquids are thermodynamically very distinct from strong liquids, in terms of configurational states. In fragile liquids, number of these states is very high and structural changes can easily be occurred, whereas strong liquids are resistant towards thermally induced changes, and the number of configurational states is very low[169]. The diagram given below, Figure 1-21, illustrates the basic difference in the energy profiles of strong and fragile system. In the case of strong system, there is only one energy minima is observed, whereas in the case of fragile system, there are several energy minima is seen[170].

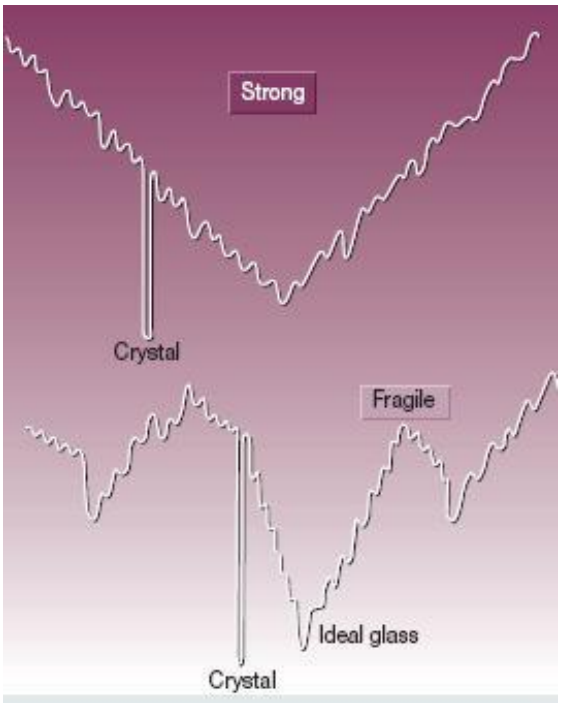

Figure 1-21 *Energy spectrum of a strong and a fragile systems. Energy profile of a strong system is depicted above. Symmetry in energies of different configuration can clearly be seen, whereas in the case of a fragile system as shown below, proliferation of "mega basins" is observed without any symmetry. The figure has been adapted from Debenedetti et al*[170].

The fragility index can be directly measured from experiments[171]. Experimental techniques including Differential Scanning Calorimetry (DSC) have been proved to be an efficient tool for investigating the correlation between viscosity and mean square displacement at atomic level[133]. By plotting these in a 2D plot one can calculate fragility index. Alternatively, the data obtained by the dielectric relaxation experiments can be fitted into the Vogel- Fulcher- Tamman (VLF) equation, which correlates the dielectric relaxation times to temperature. The equation reads, $\eta = \eta_0 \exp [DTo/(T-To)]$, where To is the temperature at which relaxation times (η_o) diverges and D is a constant. The fragility can directly measured using the relationship between relaxation times, obtained from the dielectric relaxation experiments, and the corresponding temperature: ie, $\log_{10}(\eta)$ vs Tg/T . A straight line indicates a strong Arrhenius behaviour, whereas the VLF equation, characterised by stretched exponential, does represent the behaviour of more fragile liquids[172].

Liquids have been classified into six according to the Dynamic Fragility Index (DFI): 1. Polymers, 2. small organic liquids, 3. small hydrogen bonding liquids, 4. inorganic glass formers, 5. ionic glass formers, 6. metallic glass formers.[167] Dynamic Fragility indices of polymer glasses lie in between 25 to 200, with their glass transition temperatures lying from150K to 450K; by contrast metallic glasses possess high glass transition temperature range (300K to 1000K) and lower dynamic fragility indices, (25 to 100). On the other hand, glass transition temperatures of organic glass formers and inorganic glass formers lie in the range from 70K to 350K, however there is a marked difference between the organic glass formers and inorganic glass formers: glass transition temperatures of inorganic glasses are inversely related to fragility- lower the fragility, higher the glass transition temperature is. Examples of six types of glass formers with glass transition temperatures and corresponding dynamics fragility values have been shown in the following table.

Table 1-3 *Glass transition temperature and fragility indices of various glass formers*

Glass formers	**Glass transition temperatures**	**Dynamic Fragility index**
1.Polymers		
Polystyrene	375	139
Polyethylene	237	46
Polypropylene	263	137
2. Metallic glasses		
$Fe_{83}B_{17}$	760	103
$Pd_{82}Si_{18}$	657	106
$Fe_{80}P_{13}C_7$	736	102
3. Ionic glass formers		
ZnCl2	380	42.5
$2BiCl_3.KCl$	306	85
$H_2SO_4.3H_2O$	158	95
4. Inorganic glass formers		
B_2O_3	554	32
$CaAl_2Si_2O_8$	1118	53

As_2S_3	455	36
5. small organic glass formers		
Toluene	126	59
Propylene Carbonate	157	93
Ortho terphenyl	246	81
6.Hydrogen bonded organic glass formers		
Ethanol	92.5	55
n- Propanol	97	35
Glycerol	190	53

1.5.3.1 Fragility index of aqueous sugar solutions

Glass forming ability of aqueous solutions can also be quantified by measuring their fragility index. Aqueous solution of trehalose (20%) has the lowest fragility index among the aqueous solutions of other sugars such as maltose and sucrose at same concentration[171]. Fragility data obtained from the elastic incoherent neutron scattering indicates that at very dilute concentrations, aqueous trehalose has the least fragility index value, indicating its stronger glass forming capability and hence better cryoprotective property[171]. It is interesting to note that at very low concentrations of various sugar solutions, difference in fragility index is higher, and as concentration increases this difference is diminished. For instance, fragility index of aqueous trehalose solutions (trehalose + 19 water molecules) is 302 and sucrose solution at the same concentration has a value of 355. At a relatively higher concentration, with the solute – solvent ratio 1:6, fragility indices of aqueous trehalose and sucrose solutions read 241 and 244 respectively.

1.6. WATER AND ITS PROPERTIES

Discussions pertaining to properties of aqueous cryoprotectant solutions is incomplete without mentioning the properties of the only inorganic liquid which occurs naturally on earth and the only compound that exists in all three physical states (gas, liquid, solid), water[173]. Water is also important for animals and plants alike as it catalyses

many physiological cycles in both creatures. In addition, water is an excellent solvent and being used extensively in natural bio chemical reactions. Plants make use of wetting properties of water to deliver nutrient to its leaves. Due to zero contact angle between water and surface of xylem tube a capillary force is generated in the column, and water is transported from bottom to top. By this, even leaves of tall trees can get enough water and other nutrients to grow further.

1.6.1. Chemical structure of water

Water, in terms of chemical formula, is one of the simplest chemical structures. However electron density surface calculations suggest a quite complex structure of water molecules. According to this model, water can be treated as four point charge tetrahedral with a pair of both positive and negative charges occupy the vertices of a Tetrahedron[173]. Water also shows cooperative properties, i.e. the tendency to form clusters with more molecules (dimers, trimers and tetramers). The interactions among the water molecules, in terms of oxygen- oxygen atomic distance, tend to change upon change of phase (liquid to solid), as evidenced from the X-ray diffraction data. Water exists in different isotopic combinations – $^{1}H^{16}O$, $^{2}H^{17}O$, $^{3}H^{18}O$; among these $^{1}H^{16}O$ is the most abundant, around 99.9 percent of water molecules seen on earth[173].

1.6.2. Physical states of water

Water principally exists in three forms at normal temperatures and pressures- vapour (at higher temperatures), liquid (in between 273 K and 373 K) and ice (at lower temperatures)[174]. Adding to this, water undergoes enormous changes at normal atmospheric pressure, 1 bar, and over a wide range of temperature[174].

The transition from liquid to solid phase is well defined- at freezing point temperature where liquid phase and solid phase exactly intersect. However, water, like many liquids, can also exist in liquid form to some extent even under the freezing transition point, known as super cooling, till 231K (nucleation temperature of water), as supercooled. Like many other liquids, when water is further cooled to a lower temperature, a transition from liquid state to more ordered amorphous state takes place. This

amorphous state is termed as meta stable state since it is very unstable to crystalline phase[155]. Meta stability is so transient that even minor amounts of impurities present in the vessel can convert the system into more stable crystalline state[174].

Below 231K, water can no longer exist in a supercooled state due to nucleation of water molecules. The clusters of the nucleated water molecules, in analogue to ice, form and break continuously as temperature drops. When any of these nuclei reach critical size, other water molecules will grow on this nucleus and this process becomes energetically favourable for crystallisation, but becomes arrested at the temperature nearing 140K, below which water remains as glassy water[174]. Since meta stability is not well defined, the exact value of glass transition temperature of water is still under debate[175]. Experimental and computational investigations related to glass transition in water have been explained in considerable detail in chapter 5.

On the other hand water can also be heated to a liquid even above its boiling point (373K), a process called superheating. Until 553K, known as superheating limit, water can exist as a liquid. In other words, water can remain in as a liquid till a temperature that is 180K higher than its melting point. From 273K to 373K water is found in its stable region- i.e., existing as pure liquid. The physical states of water are depicted in Figure 1-22**.**

1.6.3. Supercooled water

Due to the homogenous nucleation at 240K, however, liquid water cannot directly be supercooled[175]. Therefore supercooled water is prepared by an indirect way – by heating the glassy water, existing as several polymorphs – hyper quenched glassy water (HGW), low density amorphous ice (LDA), amorphous solid water (ASW). Hyper quenched glassy water is formed by cooling the water at a high cooling rate, whereas low density ice and amorphous solid water are formed by high pressure treatment of amorphous ice and depositing water vapour to cold substrate respectively.

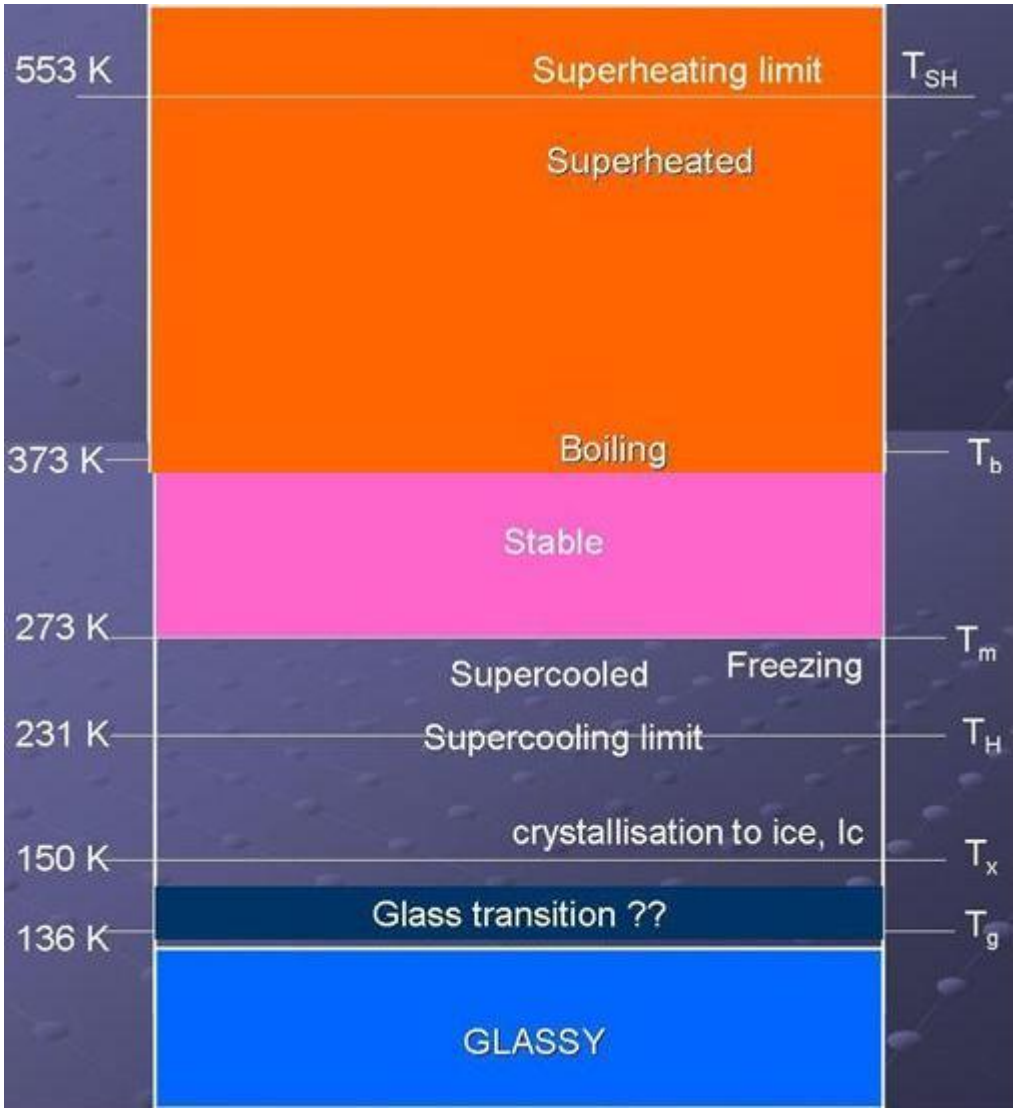

Figure 1-22 *Physical state of water. Region between Tm and Tb, water exists as normal liquid. At Tb (373) water becomes vapour and remains in the state till 553K, super heating point, TSH. Below the freezing point of water, 273K, water can exist in a supercooled state till 231K (TH), under which water molecules nucleate themselves. Crystallisation of ice, Ic, occurs at Tx (150K). At 136, water becomes an amorphous solid- the most abundant form of water in the universe. The figure has been adapted from Stanley et al*[174].

This suggests that the estimation of glass transition temperature reported for water can vary according to the methods employed for preparation of supercooled water. Recently, it has been proposed that the already proposed glass transition temperatures, 136K and 165K, correspond to two different phenomena that manifests the existence of liquid -

self diffusion of water molecules corresponds to the value of 136 K, and desorption of water droplets from a surface corresponds to the value of 165K[175]. This further indicates that the glass transition temperature may take place in two steps: at 136K Low density liquid (LDL) is formed from low density amorphous ice (LDA ice), and at 165K, low density liquid (LDL) is transformed to supercooled water.

1.6.4. Anomalous physical properties of water

Physical properties of water also play an important role in sustaining animal life in both water and land. In general water exhibits three kinds of anomalies- thermodynamic, dynamic and structural[176]. Density of water shows a remarkable deviation from the expected monotonic behaviour: it decreases during freezing; at 4^{o}C water exhibits the maximum density, which shifts towards lower temperature upon increasing pressure. Dependence of pressure on temperature at constant densities is shown in Figure 1-23.

In a standard liquid, increase in volume is accompanied by an increase in entropy as the number of configurations of the molecules increases correspondingly. However, water shows an anti correlated behaviour of entropy and volume, when cooled: an increase in volume reduces entropy[174]. This anomaly is attributed due to the existence of hydrogen bonds - entropy is reduced upon decrease in temperature, at the same time, water structure attains relatively stable tetrahedral hydrogen bond network at this tempreature than at normal temperature. This increases volume around the water molecule; hence entropy and volume are anti correlated when water is cooled. It is cogent from this explanation that hydrogen bond formation in water plays crucial role for water having numerous anomalies compared to other liquids, for example SiO_2.

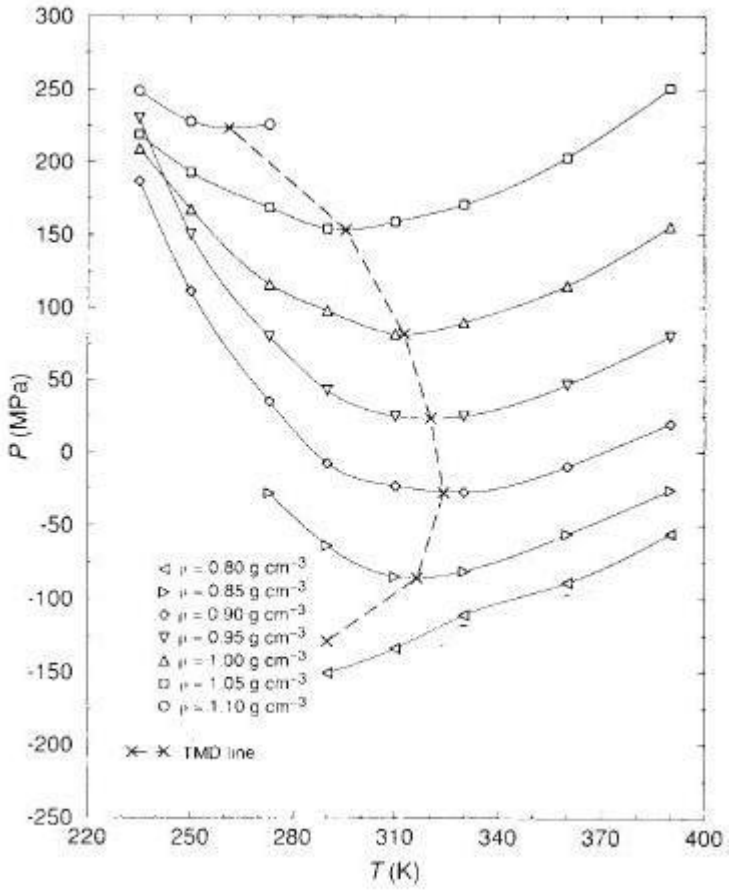

Figure 1-23 *Pressure versus temperature at constant density of pure water tabulated from computer simulations. The vertical line shows the temperature of maximum density at corresponding densities. The figure is taken from Poole et al*[177].

Water also shows some other anomalous behaviour: high heat capacity, melting and boiling points, expansion upon cooling, and contraction upon melting. It does exhibit exceptional dielectric properties as well. Water becomes more compressible upon cooling and less viscous upon compression[174]. Thermodynamic response functions (compressibility, heat capacity and coefficient of thermal expansion) obtained by differentiating thermodynamic state functions (energy, pressure or volume), of water clearly manifest very intriguing properties compared to other liquids[155, 178]. Schematic dependence of temperature on these functions has been shown in Figure 1-24.

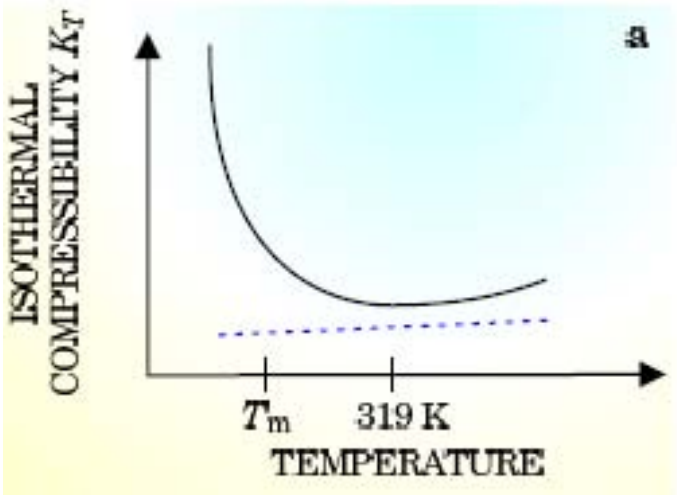

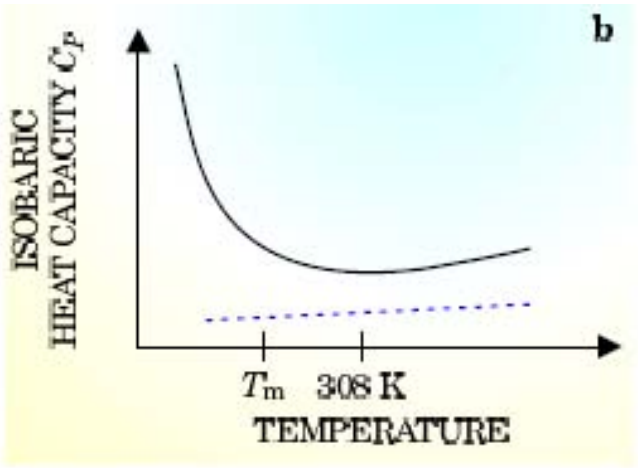

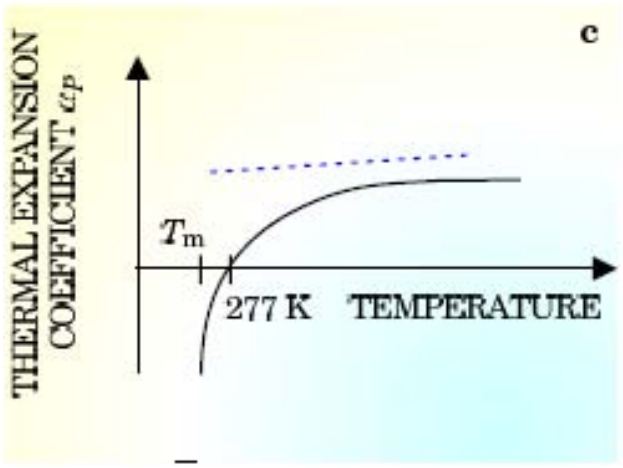

Figure 1-24 *Illustration of dependence of temperature on thermodynamic response functions. Variations in isothermal compressibility, isobaric heat capacity and thermal expansion coefficient of water with respect to temperature are shown (thick black lines) in panel a, b and c respectively. The blue dotted lines indicate assumed values of normal liquids at these temperatures. The discrepancy in these thermodynamic*

response functions is clearly evident in the supercooling region. Figures have been adapted from Stanley et al[174].

In a typical liquid, compressibility (the derivative of volume with respect to pressure) decreases upon lowering the temperature due to decrease in the number of molecular fluctuations in the liquid. Water, however, exhibits an opposite effect - compressibility increases upon the decrease in temperature - almost twice than one would expect for a standard liquid. But this effect is not appeared to be monotonous - it reaches to a minimum value prior to attaining as twice as this value at 233K. Another response function specific heat, which is the derivative of energy with respect to temperature, follows similar trend - it increases upon decreasing the temperature with a minimum at 308K. Coefficient of thermal expansion, response function of volume with respect to temperature, of most liquids shows an increase upon increase in the temperature due to positive changes of specific volume[178]. On the contrary, a decrease in coefficient of thermal expansion is observed in the case of water in lower temperature region, and coefficient of expansion attains a value of zero at 4^0C. All anomalies reported on water can be attributed into three different, yet inclusive, effects- structural, kinetic and thermodynamic[176].

Anomalous behaviour of water is further revealed by structure factor analysis. It has been shown that in low density amorphous water, first peak, known as low q- range, appears nearer with respect to other molecules than its higher density analogue[179]. By contrast, there are several crystalline polymorphs of water, around 13, have been identified so far, nine of which are very stable at moderate pressure and temperature ranges[174].

1.6.5. Amorphous water

X-ray investigation on polymorphs of water indicates existence of several forms of water, in terms of number unique among all liquids - high density amorphous (HDA), low density amorphous (LDA), cubic (Ic) and hexagonal ice (Ih) for example[179]. All these polymorphs were investigated from a continuous process from a single sample, starting from pure water. High density amorphous ice (HDA) can be prepared after cooling of water to 77K at a pressure range 1-1.3GPa; which after been heated to 140K,

and upon subsequent cooling to 77K becomes low density amorphous water (LDA). Crystalline ice, Ic, can be made when Low Density Amorphous Ice (LDA) is heated and then cooled to 190 K and 77 K respectively. Ic can be transformed to its polymorphic form Ih by heating to 250k and subsequent cooling to 77K. All these inter conversions between different forms of water show the complexity of water structure which depends upon the previous history of the system. Samples of low temperature forms of water – amorphous water and ice, are shown in Figure 1-25.

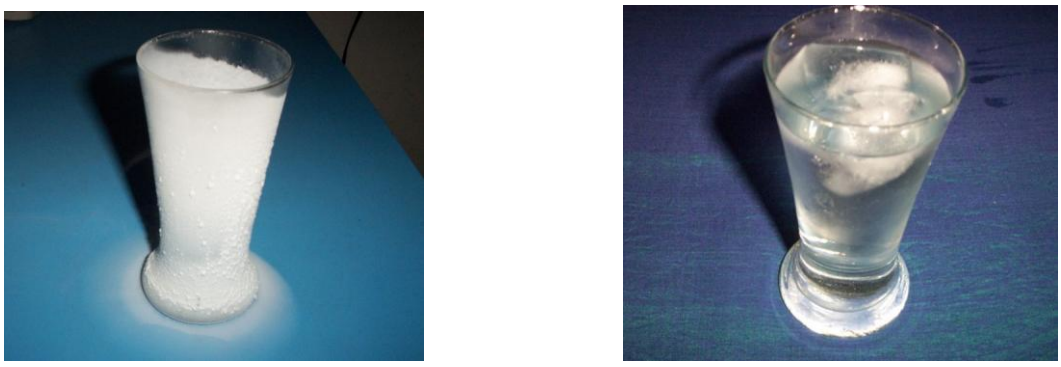

A **B**

Figure 1-25 *Low temperature forms of water - amorphous water (panel A) and ice floating on cold liquid water (panel B). The figures have been adapted from* http://www.iisc.ernet.in/researchhigh/amorphous.shtml

Different water forms can be characterised by X-ray diffraction measurements - for example crystalline state of water exhibits a series of sharp peaks indicating high order, while relatively broader peaks are seen in the case of amorphous samples. Different polymorphs corresponding to different phases can clearly be distinguished by the X-ray spectrum- crystalline nature of polymorphs is followed in the order: hexagonal ice, cubic ice, low-density amorphous and high density amorphous.

1.6.6. Experimental investigations on pure water

Various experimental methods have been used in order to elucidate the water structure; among these X-ray and Neutron Scattering techniques are the most informative and widely used for unfolding the properties of water, the most anomalous liquid on earth[180]. There are several structural quantities can be measured using these techniques: pair

distribution functions, self distribution functions and cross distribution functions. The correlations between identical atoms can be measured by the self distribution functions, whereas correlations between various atoms can be measured from cross distribution functions. Another important structural quantity that can be obtained is structure factor, by which one can probe into the polymorphism exhibited by water. Experiments also revealed the existence of water as a tetrahedral species even at supercritical temperature and high pressures[180].

1.6.7. Simulations of pure water

In complimentary to the experimental findings, computer simulation investigations also support the existence of hydrogen bonding network in water[181]. Phenomenon such as tetrahedral arrangement of water molecules was also confirmed with the aid of molecular dynamics simulations, which underpins the importance of molecular dynamics based techniques as indispensable tools for elucidating structure and dynamics of water and aqueous solvents. Computational analysis has been further extended to study deeply supercooled water, which indicates that the density and critical point of water are interlinked : slight changes in density has profound effect in phase transformation between different poly morphs of water[177]. This phase transformation occurs as a result of structural reorganisation of water.

Further simulations explore the anomalous behaviour of water density, by drawing pressure density phase diagram[177]. Using various models the temperature of maximum density of water has been calculated. It has been found that this temperature, abbreviated as TMD, is negatively sloped at positive pressures and vice versa. Determination of the phase diagram of water is relatively straight forward using molecular dynamics simulations.

Various polymorphs of water and ice have been investigated using different water models - the coexistence region of high density amorphous ice and low density amorphous ice has been determined at pressures of 150Mpa or above[177]. Along with temperature, pressure can also influence the stability of polymorphs of water. Computer simulation can provide information at various thermodynamic ranges where

experiments are often inaccessible, for example it is very complicated to conduct an experiment on liquids at -200 MPa[182]. Comparison of structural factor and pair distribution function indicates the existence of high density amorphous ice at 600 MPa and low density amorphous ice (LDA) at -200MPa, which is independent of temperature – existence of HDA ice is also supported by the experimental findings, but the experiments at very low pressure has not yet materialised.

One of the major advances that computer simulations have made on water studies is quantifying the structural, thermodynamic and kinetic anomalies by a set of order parameters[183]. These order parameters are translational and orientational; the former measures preferential separation of a pair of molecules, while the latter measures the tetrahedral arrangement around a molecule. According to this method, region where water shows thermodynamic anomalies is bounded by the region where water exhibits kinetic anomalies, which is in turn bounded by the region water shows structural anomalies.

The exact boundary where all three anomalies occur can be located by drawing a temperature density plot. The structural anomalous region, bounded by density from 0.9 to 1.2 g/cm^3 and temperature 200K to 330K, is characterised by a maxima in orientational order parameter and a minima in translational order parameter. In this region, water becomes more disordered upon increase in compression. On the other hand, kinetic anomalous region, for which density lies between 0.91 to 1.18 g/cm^3 and temperature, from 200K to 310K, is bounded by the loci of maximum and minimum diffusivity. Within this region, diffusion is correlated with density. The thermodynamic region, bounded by the other two, is the loci of the temperature of maximum density, TMD. Within this limit, density of water increases at constant pressure.

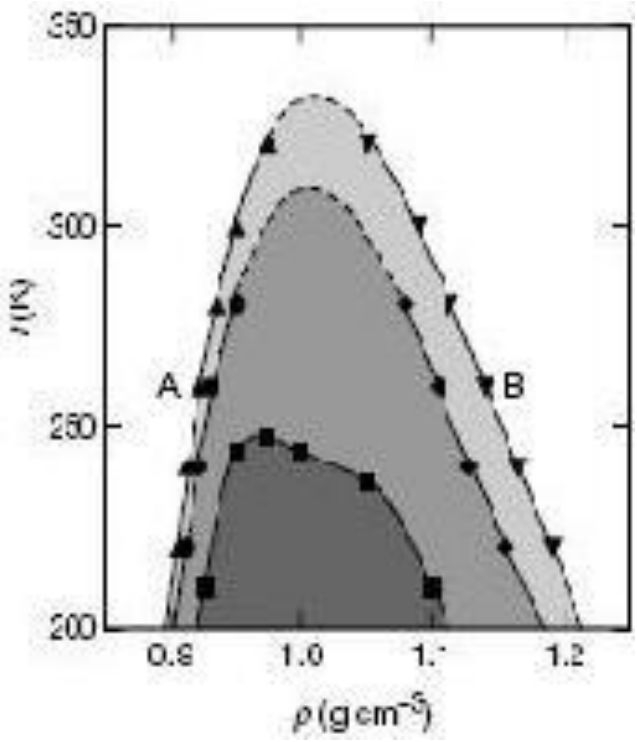

Figure 1-26 *Relationship between structural, dynamic and thermodynamic anomalies. X and Y axes denote density in g/cm^3 and temperature in Kelvin scale respectively. The outer shaded region (triangles) indicates structural anomaly of water where water is more disordered upon compression. In the central region, bounded by circles and diamonds, where water shows anomalous dynamic behaviour - diffusivity increases with density. Water behaves thermodynamically anomalous in the innermost region, bounded by squares- its density increases upon heating at constant pressure. TheFigure has been taken from Errington et al [184].*

1.6.7.1 Tetrahedral structure of water

Computer simulation also reveals that at high pressure, tetrahedral structure of water does not possess multiple configurations in comparison with the water at low pressures[185]. Simulations suggest that hydrogen bonding pattern within the local tetrahedral varies with respect to changes in pressures: at low pressures, there exist water pentamers consisting of five water molecules, four of which occupying the corners of a regular tetrahedron and the remaining water molecule occupying the central position. At low pressures there may exist several hydrogen bonds per water molecule, whereas at higher pressures, hydrogen bonds between the water molecules is

significantly reduced. This underpins the notion of structural heterogeneity of liquid water under pressure.

Other valuable information that can be obtained from simulations is the dependence of diffusion coefficient on density. Extensive picture of density dependence of diffusion have not yet obtained from experiments as minimum in the diffusion coefficient has not been recorded due to inaccessibility. Simulations along isotherms, constant temperature plots, of diffusion coefficient and density indicate that as temperature drops by, clearer minima of diffusion coefficient is observed at density around 0.9 g/cm^3, a fact supported by the order parameter analysis.

1.6.8. Water anomaly – hypotheses

Experimental findings and supporting computer simulation studies mentioned in the previous sections have led into the development of various theoretical frameworks to describe the anomalous properties of water[186]. Three prominent hypotheses have been put forward in order to explain the water anomalies[187]: the stability limit hypothesis, singularity free hypothesis, and liquid – liquid phase transition hypothesis.

1. Stability limit hypothesis states that there exists a spinodal temperature line in the Pressure – Temperature phase diagram, beyond which liquid water cannot exist when cooled.

2. Singularity- free hypothesis posits that there exist local network of hydrogen bonded sub domain within the system (water) that leads into fluctuations in specific volume, resulting in anomalous decrease of response function such as coefficient of expansion.

3. Whereas liquid- liquid transition hypothesis suggests that there exists two distinct phases, LDL (corresponding to lower pressures) and HDL (corresponding to higher pressures), beyond the lower critical point that appeared in the phase diagram of water.

Data obtained from computer simulation established the well known liquid- liquid transition hypothesis which explains the phase separation of water at various pressure ranges where temperature plays an irrelevant role[178, 182, 188, 189]. These polymorphs are known as Low Density Amorphous water (LDA) and High Density Amorphous water (HDA), existing at low pressures and high pressures respectively. The phase separation is characterised by the Oxygen- Oxygen neighbour distance in the liquids: molecules with distance higher than 4.4 were found to exists in the high density liquid, whereas neighbour distance less than 4.4 were found to be present in its low pressure analogue[189].

Temperature domains of the various hypotheses have been shown in the figure below.

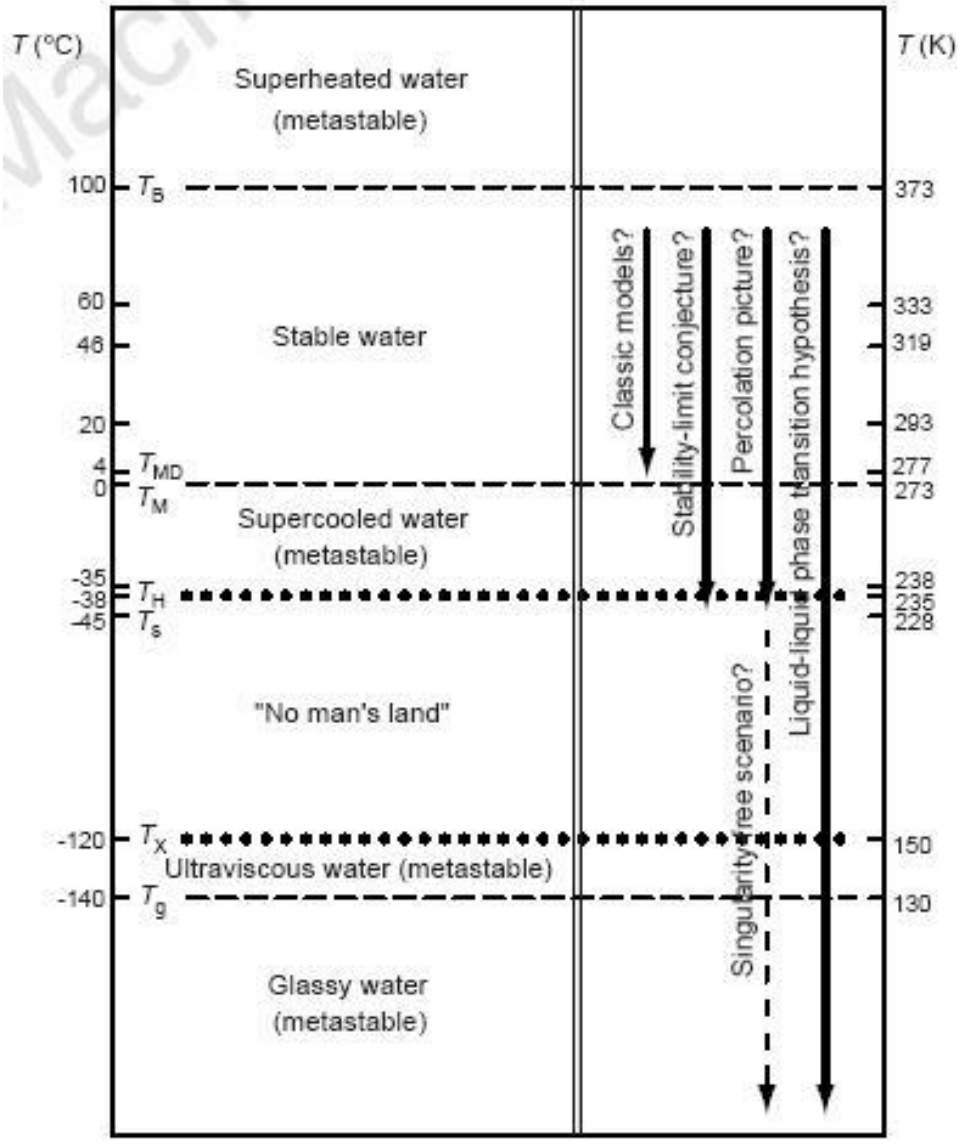

Figure 1-27 *Schematic illustrations of different temperature domains of water at atmospheric pressure. Temperatures in Celsius scale and Kelvin scale are given in left and right sides respectively. (Starting from the upper part of the diagram)* T_B *indicates temperature at which water boils, 100K, above which water exists as vapour under normal conditions;* T_{MD} *is the temperature at which water exhibits its maximum density (277K), and anomalies in water set in;* T_M *is temperature of freezing (273K);* T_H *is the temperature at which homogenous nucleation occurs;* T_s *is the temperature at which thermodynamics response functions such as constant pressure heat capacity becomes infinite;* T_X *is the crystallisation curve; and Tg is temperature of glass transition. The temperatures 333K, 319K, 293K indicate the onset in anomalies in sound velocity, isothermal compressibility and shear viscosity respectively. Most of the computational water models are designed to reproduce properties above* T_{MD} *as indicated by an arrow. The stability limit hypothesis and the singularity free hypothesis (hypotheses 1 and 2) are proposed to account of properties of water between* T_B *and* T_H*. The figure has been taken from Mishima et al*[187].

SIGNIFICANCE OF THE STUDY

This project will investigate the structural and dynamical behavior of aqueous solutions of CPAs at low temperatures in order to rationalize the differences in cryoprotective properties seen experimentally between various organic molecules. Importantly, this project will help determine the molecular mechanism by which CPAs alter the properties of liquid water in order to prevent crystallisation and lead to the formation of a glassy state. In conjunction with an understanding of the physical and chemical properties that make an organic molecule a suitable CPA, this will be crucial for the future rational design and optimisation of cryoprotective mixtures, which currently remains an empirical practice. This may also help determine the optimum cooling/heating rates in various cryobiological applications. A proper understanding at the molecular level of the phenomenon of cryoprotection by organic molecules will be an important biotechnological breakthrough in cryobiology because of its broad applications in medicine, pharmaceutics, ecology, agriculture and the food industry.

Chapter 2

METHODOLOGY

This chapter discusses the theoretical background of molecular dynamics simulations and various analyses, and a brief overview of water forcefields.

2.1. INTRODUCTION

Computer simulation methods including molecular dynamics simulations are widely employed to probe into various types of systems ranging from atomic to macromolecular scale[190]. When experimental measurements become expensive or difficult, computer based experiments, otherwise known as computer simulations, can complement them for providing better understanding of macroscopic and microscopic processes. Two molecular dynamics techniques employed in this study are equilibrium molecular dynamics and simulated annealing. The basic algorithm for these methods will be explained in the following section.

2.2. MD SIMULATION ALGORITHM – EQUILIBRIUM MOLECULAR DYNAMICS

Time dependent behaviour of the system under investigation can be obtained from molecular dynamics simulation by solving Newton‟s equations of motion coupled with accurate potential energy functions (forcefields). The outcome of simulations is a time series of conformations called trajectory which is analysed to obtain estimate of desired quantities of interest.

Molecular dynamics simulation set-up contains several steps. First, initial configuration of the system is chosen, which is then minimised for several hundreds of pico seconds for getting rid of artifacts such as bad atom contacts. Then the system is set for equilibration, during which the thermodynamic quantities such as temperature and/or pressure attain stable values. In the production phase, simulations are performed for longer time, and the resulting trajectories are considered for analysis. Important steps during a molecular dynamics simulation have been highlighted in Figure 2-1

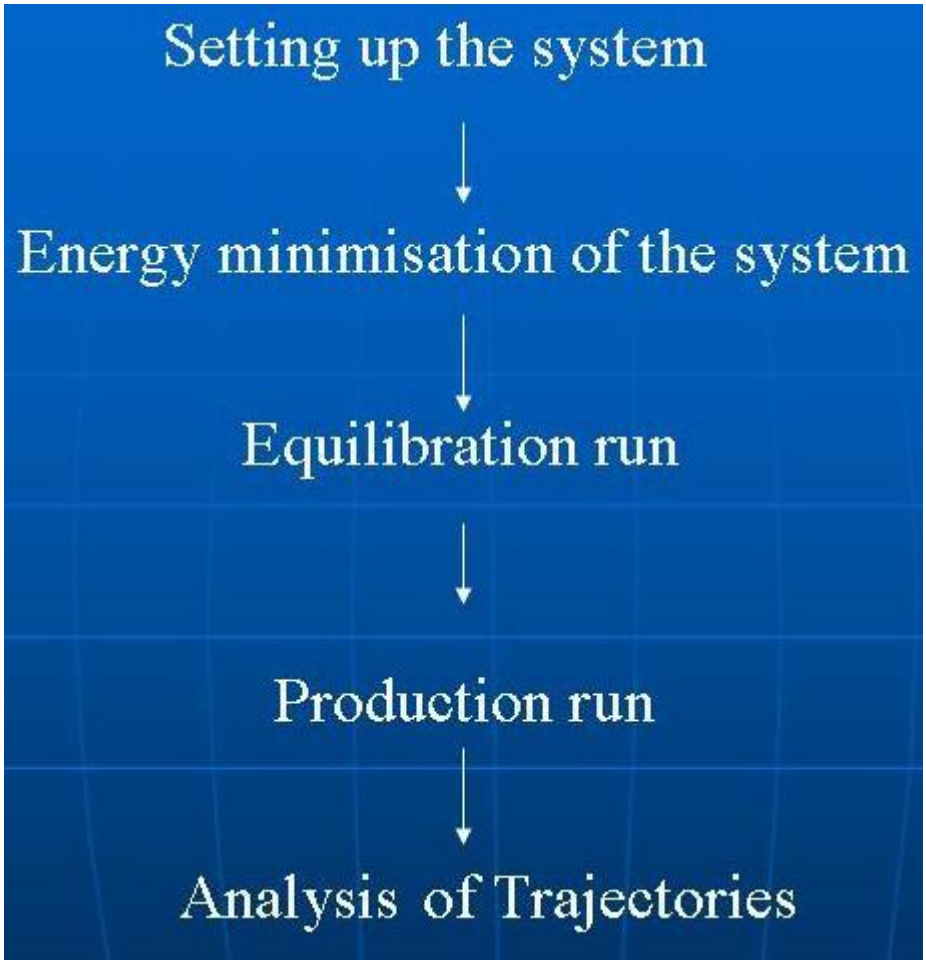

Figure 2-1 *Setting up and running molecular dynamics simulation*

2.2.1. Classical mechanics

Molecular dynamics simulation methods provide valuable information about time dependent evolution of the positions of the particles governed by Newton‟s second law of motion, mathematically represented by

$F = ma$, (1)

where F and a are the force exerted by the particles in the system and acceleration due to the motion respectively, whereas M is the total mass of the particles in the system. Acceleration is defined as time dependent derivative of velocity, $a = \frac{dv}{dt}$,which can in turn be represented by similar fashion, taking derivative of displacement with respect to time as shown below,

$$v=\frac{dx}{dt} \quad (1)$$

Integrating this equation yields, $x(t) = vt + x(0)$ (3)

With equations (2) and (3), one can write a combined form to denote displacement in terms of acceleration,

$$x(t) = at^2 + v(0)t + x(0) \quad (4)$$

,

v(0) denotes initial velocity.

Acceleration, a**,** can be defined as the derivative of energy as indicated in equation 5,

$$a = -\frac{1}{m}\left(\frac{dE}{dr}\right) \quad (5)$$

Equations from (2) to (5) indicate that in order to obtain a trajectory one needs to know initial position of particles, initial distribution of velocities and acceleration. Initial distribution of velocities can be obtained from well known Maxwell- Boltzmann distribution law, which is written according to the mathematical formula given below.

$$P(v) = \left(\frac{m_i}{2\pi K_B T}\right)^{1/2} exp^{-1/2(m_i v_i^2)/K_B T} \quad (6)$$

It is to be noted that temperature, T, and velocity, v are connected by the following relation,

$$T = \frac{1}{(3N)}\sum_1^N \frac{P_i}{2m_i} \quad (7)$$

N and *p* denotes number of atoms in the system and momentum of the system respectively.

Since analytical solutions are practically impossible for the complex many body classical mechanics problems, the equations of motions have to be solved numerically. Different numerical routines have been developed for the evaluation of these equations, including Leap-frog, Velocity Verlet and Beeman algorithms.

In **GROMACS** molecular dynamics package[191] used throughout this study, Leap frog algorithm is employed to solve equations of motion using following equations:

$$r(t+\Delta t) = r(t) + v(t + \tfrac{1}{2}\Delta t)\,\Delta t, \quad (8)$$

where r and v are displacement and velocity respectively;

$$v(t + \tfrac{1}{2}\Delta t) = v(t - \tfrac{1}{2}\Delta t) + a(t)\Delta t, \quad (9)$$

Velocities can explicitly be calculated combining equations (7) and (8).

$$v(t) = \tfrac{1}{2}[\, v(t - \tfrac{1}{2}\Delta t) + v(t + \tfrac{1}{2}\Delta t)] \quad (10)$$

One can clearly see from the equations from 8 to10 that given the initial displacement and velocity, the phase difference between these two variables always be half of the time step, Δt/2. Hence this routine is called leap frog algorithm, and has several advantages over other schemes employing for numerical approximation such as Runge-Kutta and Euler algorithms since it ensures angular momentum conservation and invariant time reversal of the system under consideration.

2.2.2. Potential energy function (Force fields)

Accuracy of the molecular dynamics simulations heavily depends upon the choice of intermolecular potential, *E(R)*, commonly referred as force fields or potential energy function. The energy *E(R)* is function of atomic positions *R* of the all particles (atoms) in the system. The potential function comprises of bonded and non-bonded terms.

$$E(R) = E_{bonded} + E_{non\text{-}bonded} \quad (11)$$

Bonded term, E_{bonded}, describes bond, angle and dihedral angles in a molecule, whereas the non bonded term, $E_{non\text{-}bonded}$, accounts for interactions between non bonded atoms separated by three or more covalent bonds.

$$E_{bonded} = E_{bond\text{-}streching} + E_{angle\text{-}bending} + E_{dihedral} \quad (12)$$

The first term in the equation (12) is $E_{\boldsymbol{bond\text{-}streching}}$ which is a harmonic potential representing the interactions between atomic pairs whose atoms are separated by a covalent bond.

$$E_{bond\,stretching} = \sum K_b\,(b - b_0)^2 \quad (13)$$

where K_b is the force constant which determines the strength of the bond, and $(b\text{-}b_0)$ denotes the displacement from an ideal bond length b_0. K_b is often evaluated using either highly accurate quantum mechanical calculations or infra red experimental data.

The second term, also represented by a harmonic potential, is associated with deviation of bond angles from an ideal value, θ_0.

$$E_{angle\ bending} = \sum K_\theta\ (\theta - \theta_0)^2 \qquad (14)$$

The third term denotes the torsion angle potential function which accounts for the presence of steric barriers between atoms separated by three covalent bonds. Rotational motion is represented by this function, described by coefficient of symmetry, n**,** around the central bond, and a dihedral angle. An additional term included in the equation incorporates planarity and chirality.

Mathematically torsional angle potential is given by the following equation.

$$E_{dihedral} = \sum_{1,4\ pairs}(1 - cos(n\varphi)), \qquad (15)$$

where n and θ represent coefficient of symmetry and dihedral angle respectively.

In the simulations, a constraint algorithm such as **SHAKE**[192] is employed to satisfy bond geometry specified, implemented using Langrage multipliers.

For a given set of n linear constraints at a time t, the constraint equation is formulated by a set of equations given below.

$$\sigma_k\ (t) := 0 = \left\|X_{k\alpha}\ (t) - X_{k\beta}\ (t)\right\|^2 - d_k^2 \qquad (16)$$

where $X_{k\alpha}$ and $X_{k\beta}$ are the positions of two particles involved in the k^{th} constraint (σ_k) at time t, d_k is the inter particle distance.

The constraint condition in equation (16) is added to equations (5) and (11), which results in a second order differential equation.

$$m_i \left(\frac{\partial^2\ x_i(t)}{\partial t^2}\right) = -\frac{\partial}{\partial x_i}\left[V(x_i(t)) + \sum_{k=1}^{n}(\lambda_k \sigma_k\ (t))\right] \qquad (17)$$

Integrating the above equation twice yields the particle position subject to the constraints, resulting in the following equation

$$X_i(t+\Delta t) = X_i'(t+\Delta t) + \left[\sum_{k=1}^{n}\left(\lambda_k \frac{\partial \sigma_k}{\partial x_i}(\Delta t^2)\right)\right] m_i^{-1}{}_{i=1,\ldots N} \quad (18)$$

$X_i(t + \Delta t)$ and $X'_i(t + \Delta t)$ are constrained and unconstrained positions of i^{th} particle after time t respectively. λ_k is Langrange multiplier by which optimization of a function subject to constraints can be made. The mathematical operation described in the equation (16) is performed until constraints at each time step are solved to a given SHAKE tolerance.

2.2.3. Non-bonded interactions

Non bonded interactions include two interactions, electrostatic and Van der Waals.

$$\mathbf{E}_{non\text{-}bonded} = \mathbf{E}_{electrostatic} + \mathbf{E}_{Van\ der\ Waal} \quad (19)$$

Electrostatic interactions between pairs of atoms, treated as point charges, are calculated using Coloumb‟s law,

$$E_{electrostatic} = \sum\sum_{pairs} \frac{Q_i Q_j}{4\pi\varepsilon_0} \quad (20)$$

Q_i and Q_j are the charges associated with each site.

Van der Waals interactions are calculated using the relationship,

$$E_{Van\ der\ Waal} = 4\varepsilon_{ij}\left[\frac{\sigma_{ij}}{r}^{12} - \frac{\sigma_{ij}}{r}^{6}\right] \quad (21)$$

ε_{ij} and ζ_{ij} are the Lennard Jones parameters : the former determines attractive part of the potential $\mathbf{E}_{Van\ der\ Waal}$, while the latter represents molecular diameter. The Van der Waal‟s interaction between two atoms arises from a balance between attractive forces which are dominant at larger distances, and repulsive forces experienced at shorter distances due to strong electron-electron. The attractive force, alternatively termed as dispersion force, arises due to uneven distribution of electrons around each atom, causing instantaneous dipoles which triggers induced dipole in neighbouring atom. Van

der Waals interaction can be modelled using Lennard Jones potential given as equation (21).

Non- bonded energy terms between every pair of atoms must be evaluated, and number of interactions increases as the square of number of particles, N^2, where N is number of particles in the system. Therefore, to speed up the computation for practical applications, a cutoff radius Rc is implemented and interactions between atoms separated by more than Rc is neglected. Interactions between the pairs can effectively be computed using combination of various techniques – Periodic boundary conditions (PBC), minimum image convention, and Ewald summation, to handle long range interactions between charge pairs.

2.2.4. Periodic boundary conditions

Excessive computational cost demands number of particles necessary to extract the desired properties from a simulation as small as possible, yet without losing original properties of the real system - for example a cube of 1 litre water molecules containing approximately $3x10^{25}$ molecules. A simulation can be performed using as small number of molecules as they were in a bulk fluid, if periodic boundary conditions are employed. A cubic box of particles, replicated in all directions giving a periodic array, is normally used to simulate liquids and solutions. In such a three dimensional set up, every single box is surrounded by 26 nearest neighbours. The coordinates of the particles in the neighbouring boxes (image of the particles in the central box) can be calculated by simple arithmetical operations. The number of particles in the central box is kept constant by imposing minimum image convention, which guarantees every molecule that leave the box being replaced by its image particle entering from opposite side.

Periodic boundary condition transforms equation (20) into

$$E_{electrostatic} = {}^{1}/_{2}\left[\sum_{n}'\sum_{j=1,..N}\frac{Q_iQ_j}{4\pi\varepsilon_0 r}\right] \quad (22),$$

where n is a cell coordinate vector which is equal to $n_1 L_x + n_2 L_y + n_3 L_z$, with x, y and z representing three dimensional Cartesian coordinate unit vectors. The original cell is located at n = (0,0,0), while the image cells are located at L_n intervals in all three dimensions. Prime in the first sum of the above equation indicates that the term with i=j

are omitted when n=0. In MD simulations, calculation of Coloumb interactions is the most time consuming, and hence robust methods for enhancing computation of Coloumb‟s interactions are needed.

2.2.5. Particle Mesh Ewald (PME)

Ewald summation[193] is a technique to sum Coloumb interactions between particles and all their infinite periodic images efficiently. Ewald summation recasts equation (20) into two series of rapidly converging series and a constant term[194].

$E_{Ewald} = E_{real} + E_{img} + E_{constant}$, (23)

E_{real}, E_{img} and $E_{constant}$ are real space sum, imaginary space term and constant respectively.

E_{real} and E_{img} are expanded as shown in equations (24) and (25).

$$E_{real} = \frac{1}{2}\sum_{i,j}^{N'}\Sigma_n q_i q_j \frac{(erfc\,\alpha r_{ij,n})}{r_{ij,n}} \quad (24)$$

$$E_{img} = \frac{1}{2\pi V}\sum_{i,j} q_i q_j \sum_{m\neq 0} exp\left(\left(\frac{-\pi m}{\alpha}\right)^2 + 2\pi i m(r_i - r_j)\right)\Big/_{m^2} \quad (25)$$

V and *m* are volume of the box and reciprocal space vector respectively. The forces are calculated by differentiating and summing equations 24 and 25, and adding a correction term (E constant) to account for self interaction of charge points.

The convergence of Ewald summation is determined by three parameters: *n*, the integer which defines the number of image cells; *m* which defines the summation in reciprocal lattice; and α, the convergence parameter that determines relative rate of convergence between real and reciprocal terms (equations 24 and 25). According to various systems of interests, these parameters are carefully chosen. For instance a system with large particles (N is high), a high value of α is normally assigned for rapid convergence of real space term and taking higher values of α, *n* and *m* yields more accurate results.

With the aid of Fast Fourier Transformation (FFT) techniques, charges can be interpolated into a three dimensional grid, which can reduce the perplexity of Ewald summation. Particle Mesh Ewald (PME)[195] is one of the FFT based techniques which aids faster computation of electrostatic interactions. In this method, real space sum, E_{real}, is explicitly evaluated, whereas imaginary term (equation 25) is approximated using FFT, with convolutions on the grid where charges are interpolated to the grid points. Thus in PME, equation (25) is transformed into

$$E_{img} = \frac{1}{2\pi V}\sum_{m\neq 0} S_m S_{-m}\, exp^{(-\pi m/\alpha)^2)/m^2} \quad (26)$$

S_m is structural factor defined by $\sum_{k=1,N} q_k\ exp^{(-2\pi i m.r_k)}$, where r is defined as the relative charge position in Gaussian charge distribution.

The structural factor, *Sm*, is related to charge matrix, Q, by the following formula

$$S_m = \sum_{k1,k2,k3} Q exp^{2\pi i m_{ki}} \quad (27)$$

The Q matrix or charge matrix is the three dimensional matrix that is obtained by interpolating the point charges to the dimensions of the simulation box.

2.2.6. Controlling thermodynamic variables

Using a thermostat, temperature can be modulated, rather than keeping it constant which would set kinetic energy to a constant value in molecular dynamics simulations. There are several methods have been proposed to achieve this: velocity rescaling, Berendsen and Nose-Hoover temperature coupling[196]. Berendsen thermostat has been widely used throughout the work presented in the thesis, since it has several advantages over the other methods. Velocity-rescaling leads to discontinuities in the momentum part of trajectory due to rescaling at every time step. Employing Noose Hover thermostat on the other hand may lead to higher kinetic energy transfer time to the system due to additional constraints in the system Hamiltonian. In Berendsen method, the temperature is allowed to fluctuate while keeping the average temperature of the system to a constant value. At the same time by setting the frequency term to appropriate values, the system can be simulated in various thermodynamic ensembles.

According to Berendsen formalism, velocities are rescaled at each step equating rate of change of temperature to the difference in temperature, $T_0 - T_t$ as given in equation 28,

$$\frac{dT(t)}{dt} = \frac{1}{\tau}(T_0 - T_t) \quad (28),$$

where τ is coupling parameter which determines how tightly the bath and the system are coupled together.

Berendsen pressure coupling method is used for reaching target pressure in molecular dynamic simulations described in the thesis[196]. The algorithm employs a scaling matrix to rescale the coordinates and box vectors in conjunction with the time step assigned in the input file. The target pressure, P_o is achieved by introducing the scaling matrix which is computed using following relationship:

$$\mu_{ij} = \delta_{ij} - \frac{\Delta t}{3\tau}\left[\beta_{ij}\left\{P(0)_{ij} - P(t)_{ij}\right\}\right] \quad (29),$$

where scaling matrix and isothermal compressibility are denoted by μ_{ij} and β_{ij} . $P(0)_{ij}$ and $P(t)_{ij}$ are target and instantaneous pressures respectively, and the frequency of coupling is specified by a variable η, the pressure coupling constant.

2.3. Simulated annealing molecular dynamics simulations

While equilibrium molecular dynamics methods deal with systems that stay in equilibrium, many natural process are away from equilibrium. These processes may alter with respect to variables like time. The glass transition of molecular systems is such a scenario. One can investigate such systems by employing simulated annealing molecular dynamics simulations. The basic algorithm for the simulation is almost identical to equilibrium simulation methods explained in the previous section. The prime difference lies in introduction of an additional variable which controls the targeted temperature in a fixed cycle of time specified during the simulation run.

The system is first cooled from a higher temperature, with the targeted temperature constantly changed by a variable δt which multiplied by the cooling rate gives the targeted temperature in each cycle of simulations. Mathematically it reads $T = \delta t$ x

cooling rate[197]. This means that after certain number of steps the system will reach the final targeted temperature. The reverse heating scan is resumed by inverting initial and final targeted temperatures and the energies are saved during this run. The protocol of simulated annealing simulations has been explained in detail in chapter 5.

2.4. WATER MODELS

Due to its key role in physical and biological sciences, water is the most computationally studied liquid. Even though computer simulation methods have their own limitations such as small system size and short timescales, the properties water at ambient and non ambient conditions including its anomalous thermodynamic and kinetic properties have been reproduced with the choice of better water potentials[198,199]. Despite modifications of the water model that was used in the first molecular dynamics simulations of water by Stillinger et al,[200] accurate descriptions of important physical properties such as liquid-liquid coexistence diagram, diffusivity and dielectric properties have not been achieved by a single model all together[201]. There were several potential models that had been in use at various times. These models can be categorised into three based on different aspects considered during parameterisation – rigid, flexible and polarisable[199]. Most important models appeared in the literature so far is shown in Table 2-1.

Table 2-1 *Water models*

Potential	Type	Year of introduction
BF[202]	rigid	1933
R	rigid	1951
BNS	rigid	1971
ST2[203, 204]	rigid	1973
MCY[205]	rigid	1976
SPC[206]	rigid	1981
TIP4P[207]	rigid	1983
WK [208]	rigid	1989
NSPCE [209]	rigid	1998

TIP5P[210]	rigid	2001
SPC/HW[211]	rigid	2001
DEC[201]	rigid	2001
CF[212-214]	flexible	1975
BJH[215]	flexible	1983
SPC/F[216]	flexible	1985
MCYL[217]	flexible	1986
CKL[218]	flexible	1990
SPC/FP[219]	flexible	1991
NCCvib[220]	flexible	1992
MCHO[221]	polarisable	1990
NCC[222]	polarisable	1990
NEMO[223]	polarisable	1990
PTIP4P[224]	polarisable	1991
KJ[225]	polarisable	1992
ASP-W[226]	polarisable	1992
RPOL[227]	polarisable	1992
PPC[228]	polarisable	1994
SPC/FQ[229]	polarisable	1994
SQPM[230]	polarisable	1995
SCPDP[231]	polarisable	1996
TAB/10D[232]	polarisable	1998
TIP4P-EW[233]	rigid	2004
TIP4P-FQ[229]	polarisable	1994
TIP4P/ice[234]	rigid	2005
TIP4P/2005[235]	rigid	2005
TIP5P[210]	rigid	2001
TIP5P-Ewald[236]	rigid	2004

The potential models shown above are constructed with three, four, five or six interaction sites. Three site models were some of the first derived potentials for water – SPC[237], TIP3P[207]. These models have charges on both hydrogen and oxygen atoms.

Another important class of water potentials is 4 point models including BF, TIPS2 and TIP4P. These models have charges on 4 sites - negative charge is given at a point which is slightly moved off oxygen atom along the bisector of H-O-H angle. Five point models include ST2 and TIP5P models proposed by Stillinger and Jorgensen et al respectively[200, 210]. In these five point models, charges are on Hydrogen atoms and two lone pairs of oxygen atom, while oxygen carries zero charge. Recently Nada and Van der Eerden have proposed a six-site model for water[238]. Similar to the TIP5P model, positive charges are placed on Hydrogen sites, and negative charges on lone pair sites. In addition, the negative charge is also placed on the bisector of the HOH angle, at a distance M away from the oxygen atom. The geometry and parameters for the most popular potential models have been given in Table 2-2.

Table 2-2 *Geometry and parameters for the most popular models currently in use*

Water models	SPC[206]	SPC/E[237]	TIP3P[207]	TIP4P[207]	TIP5P[210]
r (OH) Å	1.0	1.0	0.9572	0.9572	0.9572
< HOH deg	109.47	109.47	104.52	104.52	104.52
q(O)	-0.82	-0.8476	-0.834	0.0	------
q(H)	0.41	+0.41	0.417	0.52	0.241
q(M)	-------		0.0	-1.04	-0.241
r(OM) Å	--------		0.0	0.15	0.70

Among aforesaid water models, TIP4P and TIP5P are the two notable water models that are widely being used in molecular simulations. TIP4P and its parameterised version to treat long range electrostatics, TIP4P-EW, give better estimates of heat of vaporisation than TIP5P and its variant, TIP5P-EW[239]. In addition, TIP4P water model has been found to reproduce the experimental phase diagram of water[240], and potentials based on TIP4P model (for example TIP4P-EW) in general yield better experimental Temperature of Maximum Density (TMD) curve than other potential models[241]. Also, structural properties such as oxygen-oxygen radial distribution function predicted by the model match with the experimental measurements[240, 242]. Furthermore, Ayala et al.

have found out that experimental densities of several polymorphs of water have been reproduced by TIP4P model[243]. What is more, molar potential energy of TIP4P model gives good estimate with respect to the experimental values[244]. Considering superior performances over other popular models, TIP4P model is chosen to investigate properties of water and aqueous solutions described in this study.

2.5. ANALYSIS

In this section, a brief overview of the methods that are used to analyse molecular dynamic simulation trajectories in order to extract various physical properties is discussed.

2.5.1. Radial distribution function

Radial distribution function (RDF), or alternatively known as pair distribution function, is a measure of the correlation between particles within the system. In other words, RDF measures, on average, the probability of finding a particle at a distance away from a given reference particle, relative to an ideal gas. The radial distribution function is determined by calculating the distance between all particle pairs and binning them into a histogram which is normalised. The normalising factor is calculated the following equation.

$$N = 4\pi r^2 \, \rho dr \tag{30}$$

where N and ρ denote normalisation factor and number density.
Then, the radial distribution function, g(r), is given by the formula:

$$g(r) = n(r) / N \tag{31}$$

2.5.2. Hydrogen bond analysis

Hydrogen bond is a type of attractive intermolecular force that exists between two partial electric charges of opposite polarity. Hydrogen bonding plays a crucial role in the behaviour of water and its aqueous mixtures, proteins and other macromolecules.

The definition of a hydrogen bond is not fixed, however water is normally taken with respect to Oxygen-Oxygen distance equal to 3.5 Å, from two neighbouring water molecules[245]. In addition, the angle a hydrogen bond would form between the O-H axis and neighbouring oxygen has been taken to 30°.

Dynamic property of hydrogen bonds, measured as hydrogen bond life time, has been calculated by well known Luzar model[246]. In this model non exponential behaviour of hydrogen bonds at longer time scales has been incorporated. In molecular dynamics simulations, an instantaneous position configuration r(t) denotes the positions of all atoms in the system at time, t. A configurational criterion of whether a particular pair of water molecules is bonded allows one to define hydrogen bond population operator, h[r(t)]=h(t). This operator takes a value of one if a pair of molecules is bonded, and zero otherwise. The probability that the hydrogen bond is intact at time t, given that the bond exists at time t=0 is characterised by a correlation function c(t), which can be mathematically represented by the equation[247],

$$c(t) = \frac{\langle h(0)h(t)\rangle}{\langle h\rangle}, \qquad (32)$$

h(0) and *h(t)* denote hydrogen bond population operator at time 0 and *t* respectively, where <*h*> stands for the average for time t.

At equilibrium, following relation can be written connecting *h(0)* and *h(t)* as

$$k(t) = -\frac{\langle h(0)[1-h(t)]H(t)\rangle}{\langle h\rangle}, \qquad (33)$$

where *k(t)* is time correlation function. *H(t)* takes the value of 1 if Oxygen-Oxygen distance of the tagged pair lies within R=3.5Å and zero otherwise.

The probability, n, at time t that a pair of initially bonded water molecules are separated without making bonds within the distance R is calculated using the relationship,

$$n(t) = \int_0^t k(t)dt \qquad (34)$$

Time dependence on hydrogen bond correlation function, c, can be calculated combining equations 33 and 34, which yields

$$\frac{dc}{dt} = -kc(t) + k'n(t) \quad (35)$$

where *k* and *k`* are rate constants for bond breaking and making between a pair of water molecules within a bond making distance[246]. The hydrogen bond life time can be obtained from equation (35) by finding inverse of *k*.

2.5.3. Self diffusion coefficient

Self diffusion coefficient of atoms or molecules can be obtained by monitoring the displacement of the species as a function of time and averaging over all atoms (in case of a molecule). The diffusion coefficient (*D*) is then calculated using the Einstein"s formula,

$$D = \frac{1}{6}\lim_{t\to\infty}\frac{d\,\langle|R(t)_i - R(0)_i|\rangle}{dt} \quad (36)$$

$R(t)_i$ and $R(0)_i$ are the positions of the particle at two different times.

2.5.4. Rotational correlation function

Relaxation process of molecules can effectively be characterised by rotational correlation functions, which can also studied using experimental techniques such as Nuclear magnetic spectroscopy (NMR)[248]. Rotational correlation time, perpendicular to the molecular plane of a molecule, for instance water, is defined as vector product of bond length of each O-H bond in the water molecule, r_{OH1} x r_{OH2}.

Rotational correlational times can be estimated from time autocorrelation functions $C_\alpha l$[249,] where *l* stands for the Legendre polynomials of angle, α, subtended by the z axis perpendicular to molecular plane at time t with respect to t=0, which is mathematically represented by the following equation.

$$C_\alpha l = \langle P_l(e_\alpha(t).e_\alpha(0)) \rangle \quad (37)$$

Equation (37) can conveniently represented, using Fourier transformation, by the following form, $C_\alpha l = A_\alpha^l \, exp^{\left(-\frac{t}{t_\alpha^l}\right)}$, from which rotational correlational times, η_l, can be evaluated.

Chapter 3

MOLECULAR DYNAMICS SIMULATIONS OF SUPERCOOLED AQUEOUS DMSO SOLUTIONS

Molecular dynamics simulations of DMSO in water elucidating its structural, dynamic and hydrogen bonding properties are described in this chapter. Comparison with its chemical analogue, Acetone, is made in an attempt to rationalise DMSO‟s exceptional properties in a wide range of temperatures.

3.1. PROPERTIES OF AQUEOUS DMSO SOLUTIONS

Intriguing properties of aqueous Dimethylsulfoxide (DMSO) solutions at subzero temperatures are manifested by their use as cryoprotectants[5, 250, 251], a class of compounds that allow prolonged storage of biomaterials at very low temperatures[250, 252]. DMSO‟s capability to interact with membranes and ability to vitrify aqueous solutions[253] are attributed to its cryoprotective action[254, 255]. Solutes like DMSO contain both hydrophobic (methyl group)[256] as well as hydrophilic part (sulfinyl group) that helps them interact with water [257], and interact[258] and permeate through membranes[259-261].

Mixtures of water and dipolar liquids such as DMSO exhibit a large deviation from ideal behaviour, such as positive heat of mixing. Numerous experiments [257, 262-274] as well as quantum and classical molecular dynamics simulations[144, 145, 267, 275-285] indicating intriguing physical as well as chemical properties of aqueous DMSO solutions have been reported in the literature. Of particular interests are structural, dynamic and hydrogen bond properties.

Water is considered to be a tetrahedral coordinated infinite network connecting individual water molecules[286]. Density measurements of various solvents in sulfoxide family suggest that DMSO enhances this water network[287]. Calorimetric experiments [288] indicate that addition of DMSO into water enhances the water-water network in

aqueous solution, as a further evidence. Simulation reveals that even at a higher concentration of DMSO (χ = 0.3 to 0.5), tetrahedral structure among the water molecules is retained[267]. It has to be noted that a thermodynamics response function adiabatic compressibility has a minimum value at χ = 0. 30 mole fraction of DMSO[271]. Moreover, the DMSO-water mixtures exhibit the most static and dynamic dielectric perturbations at this concentration[275].

However, a clear picture has not yet emerged from the simulations regarding the dependence of structural enhancement and breaking of water network on DMSO concentration : Berkovitz and Vaizman have shown that at very low concentration (χ = 0.005) DMSO retains the water structure, whereas at higher concentrations(χ = 0.04,0.2), a breakdown of water structure is observed[289]. In addition, there are reports which suggest that enhancement is only found locally in the solution and that the tetrahedral structure of water is retained only within the first coordination shell[257, 268]. A flattening of the second hydration shell was observed for a concentration of χ=0.33 DMSO in water, suggesting a perturbation of the water structure[268].

Plot of distribution of tetrahedrality in aqueous DMSO solution by Berkowitz et al, employing statistical geometry approach[289], suggests that distortion of the water structure less visible in non polar region, implying water structure promotion of hydrophobic groups. Simulations using P2 (for DMSO) and TIP4P (for water) correlate the strong water-water interactions, varying significantly with temperature, with hydrophobic effect[281]. On the other hand, it has been demonstrated that the association between methyl and water molecules is weaker, as water forms a distorted cage around methyl groups. Spatial distribution function analysis by Laaksonen et al indicates that the preferential orientation of water molecules towards methyl groups is either weak or absent[290]. By contrast, enhancement of water structure around sulfinyl oxygen is evidenced by a sharper peak of corresponding radial distribution functions[267]. Radial distribution analysis suggest a strong correlation existing among DMSO oxygen[267]. On the contrary this effect is weaker in aqueous solution of its chemical analogue, acetone[268]. The interactions of water with sulfur atom of DMSO, however, are less pronounced in the spectroscopic measurements[278].

Despite these contrasting observations, it can be argued that water network may be perturbed upon addition of DMSO, without the water structure being completely distrupted[291], drawing a difference between aqueous DMSO and other common aqueous mixtures[292].

Hydration and hydrogen bonding are two major intermolecular interactions influencing structural and thermodynamical properties of water[181] and aqueous solutions alike[293]. Hydration around DMSO molecules is primarily observed around non polar methyl groups, whereas polar sulfinyl group interacts strongly with water via much stronger interaction, hydrogen bonding[281, 293]. Structuring of water molecules (hydration) upon addition of DMSO molecules[291] is also evident by the fact that the water – water hydrogen bond life time is higher in aqueous DMSO solutions than in neat water. Nevertheless, lifetime of water-water hydrogen bonds is almost as half as that of DMSO-water hydrogen bonds[247]. Molecular dynamics simulation reveals that water is more bonded to sulfinyl oxygen than to itself upon addition of DMSO, indicating transference of more water- water bonding to water-sulfinyl bonds[267]. Estimation of excess enthalpy and free energy of mixing corroborate the existence of strong hydrogen bonds between both DMSO and water[291, 294].

Strength of water-water hydrogen bonds is attenuated upon addition of DMSO molecules as evidenced by bond angle distribution analysis[267]. With an increase in DMSO concentration, more number of DMSO-water hydrogen bonds is formed in the solution[247]. Total number of hydrogen bonds in the solutions, however, remains constant irrespective of the concentration of the mixture[247].

The interaction of DMSO towards itself, known as clustering, has also been reported, based on X-ray Diffraction studies[295]. The studies show that DMSO molecules are bound by dipole attraction of sulfinyl groups, excluding hydrophobic methyl groups. The associated behaviour is also echoed from the dipolar symmetry projected data from MD simulations - even at low concentrations, relative orientation between DMSO molecules is preserved as that of pure liquid[275].

There are conflicting reports found in literature regarding translational and rotational motion of water molecules in the aqueous mixtures. Neutron scattering studies indicate

that the diffusive motion of both DMSO and water molecules decreases with respect to the pure liquids[257]. The addition of DMSO molecules to water further decreases the diffusion of water molecules[296]. The rotational motion of water molecules is affected upon increase in the concentrations of DMSO - at higher concentrations rotational mobility is greatly hindered[257].

On the other hand, some argues that rotational and translational mobility strictly depends upon concentration range. At equimolar concentration, both rotational and translation motions are found to be the slowest[145]. Quasi elastic neutron scattering study by Levinger et al. indicates that the rotational correlation time has its highest value at DMSO mole fraction χ=0.33[296,] suggesting competing effects between formation of DMSO-water complexes and tetrahedral water networks[275]. They also observed that diffusion of water molecules at χ=0.5 is the slowest at room temperature, clearly indicating relative stability of DMSO-water complex at this concentration.

Water – DMSO hydrogen bonded aggregates, otherwise known as complexes, influence the non ideal behaviour of aqueous DMSO solutions[267, 289]. By employing linear response theory of dielectric relaxations, Skaf has proposed aggregates of 1DMSO: 2water for water rich mixtures and aggregates of 2DMSO:1water for DMSO rich mixtures[275]. The aggregation of a DMSO molecule with two water molecules is further supported by the measurement of order parameter[291]. Stability of such complexes, found to be the highest at equimolar concentration, has profound effect on the thermodynamics of the solution as maximum in the density and stability of complexes has been correlated by experiments[297]. Thermal conductivity data also show a distinctive minimum at this concentration, suggesting that transport properties of the mixture is also affected by the complex formation[291]. Along with 1:2 DMSO-water complexes proposed from thermodynamic measurements, Glasel suggested a complex of 1:3 DMSO-water complexes based on dielectric measurements[95]. His findings indicate a co-existence of 1:2 and 1:3 DMSO-water aggregates in the solution. Laaksonen et al. proposes the existence of 1DMSO:2water aggregates[290]. They also suggest that the complex may link to additional DMSO and water molecule each to form longer chains of DMSO-water bonds, leading to much larger complex of 2DMSO-3H_2O. Existence of DMSO-water complexes was also proposed in low temperature

region: on the basis of structural and hydrogen bonding analysis Rasmussen and MacKenzie have proposed that DMSO forms only 1:3 clusters with water at this temperature regime[298].

Preferential conformations for the DMSO-water aggregates has been proposed by Han et al., based on their all atom simulation study[277]. This indicates that hydrogen atom of the water molecules faces the oxygen atom of DMSO and oxygen atoms of water molecules interact preferentially with methyl groups in DMSO. This observation contradicts Luzar"s model based on mean field approximation[293] which considers the DMSO-water mixture as an ensemble of water-DMSO oxygen and water-water hydrogen bonds.

Despite plethora of data found in the literature on DMSO-water binary mixtures, investigation on aqueous DMSO solutions at sub zero temperature is scarcely reported in the literature. Westh has studied thermodynamics properties of the system at low temperature using calorimetric experiments; he found out that enhancement of water structure by DMSO is more pronounced at lower temperature, characterised by a negative slope of heat capacity increases upon decrease in temperatures[299]. A study of aqueous DMSO solutions near their glass transition temperature revealed the existence of 2DMSO:1water complexes[300].

In order to provide a detail account of structural and dynamical properties of aqueous DMSO solutions, a series of molecular dynamics simulations have been conducted above and below room temperature, and compared with its chemical analogue acetone. Aqueous acetone solutions have also been studied in a considerable detail, both by experimental[301-310] as well as computational methods[268, 285, 302, 311-319]. A rigorous molecular model of aqueous acetone solution has been developed based on infrared spectroscopy analysis[303]. The model proposes an extensive hydrogen bond network in the mixture in which both acetone and water Oxygens compete with each other for accepting hydrogen atoms supplied by hydroxyl groups in water. There are many types of complexes found to exist in aqueous DMSO solutions by both experimental as well as computational studies as mentioned before. On the contrary according to the molecular model proposed by Chapados et al[303] such complexes are absent in the

aqueous acetone solutions, being the notable difference between these two aqueous mixtures. Absence of such networks in aqueous acetone solutions leads into the self aggregation of water molecules[285]. A detail overview is not given here on aqueous acetone solutions since it is not the focus of this chapter. Although the difference between these two solutes lies only on central atoms, this has profound effect in differentiating the properties of their aqueous solutions. DMSO is a triagonal pyramid due to the lone pair electrons at sulphur atom, whereas the geometry of acetone is planar due to non availability of lone pair of electrons on the central carbon atom.

3.3. SIMULATION DETAILS

A series of molecular dynamics (MD) simulations from 230K to 300K at interval of 10 Kelvin were performed in the NVT ensemble using **GROMACS 3.3.3**[191]. A time step of 2fs and 1fs were employed at lower temperatures (below 270K) and higher temperatures (above 270K) respectively. Periodic boundary conditions were applied throughout the simulations, with a cutoff radius of 10Å. To treat long range electrostatic interactions, the technique of Particle Mesh Ewald (PME) was used[320]. The intermolecular potentials used in the simulations were four point transferable intermolecular potential (TIP4P) for water[321] and OPLS- All Atom for DMSO[322] and Acetone[322]. The TIP4P model of water is chosen because it is found to reproduce experimental data for thermodynamic properties[323], in particular main characteristics of experimental phase diagram of water[240, 243, 324-327], and to be the least affected by the cut off problems[244]. Moreover, the focus of this study is on the solution properties at very high dilution. The choice of potentials is crucial in the simulation of mixtures, as the properties of the individual potentials may not be additive in most of the cases[311]. TIP4P/AA OPLS combined potentials are found to give significantly good estimates of solution properties of binary mixture of DMSO and water, and similar systems of other organic liquids[282, 328]. The simulation boxes, containing 500 molecules in total, were built up using **PACKMOL**[329], ensuring a realistic packing of binary mixtures. For lower concentration (8% by weight) 13 and 10 solute molecules, and for higher concentration (27% by weight) 52 and 40 solute molecules were used for acetone and DMSO respectively. Since solutions above a concentration threshold (33% by weight) were reported as toxic as in the case of DMSO and other cryoprotectants of similar size,

we limited our study within this concentration range[5]. The simulation box is minimised from 5000 steps, followed by 1ns to 2ns equilibration in NPT ensemble at higher and lower temperatures respectively. Subsequently, a 2-5ns production runs in NVT ensemble (at interval of 10 K from 230K to 300K) were carried out, saving the trajectories at every 10fs. The data were divided into part of 250ps for analysis. The temperature and pressure were controlled using Berendsen thermostat and barostat respectively [330].

3.3. RESULTS AND DISCUSSIONS

Effect of temperature on structural and hydrogen bonding properties and dynamics of aqueous acetone and DMSO solutions with respect to pure water is discussed here. First, solution structure is elucidated by employing radial distribution functions (RDFs), followed by an extensive analysis of hydrogen bonding properties, and then an account of translational and rotational mobility in the solutions is given. Finally density analysis is presented in an attempt to investigate glass transition properties of the mixtures.

3.3.1. Water structure

Figure 3-1 - Figure 3-3 depict the water-water radial distribution functions of 27% aqueous DMSO and acetone solutions, compared with pure water. As temperature decreases, the water becomes more structured as expected in the case of the three systems investigated. It is interesting to note that in terms of height of the peak oxygen-oxygen RDFs in both aqueous acetone and DMSO solutions varies the most upon decrease in temperature, where as the hydrogen-hydrogen orientation varies the least. The position of first peak of oxygen-oxygen radial distribution functions (gO-O) in all three simulated systems (pure water, aqueous mixtures of DMSO and Acetone) as shown in Figure 3-2 is unaltered, in contrast to the gO-O of ice wherein a slight shift towards a lower value indicating crystal ordering is observed[331]. Furthermore, the intensities of the peak increase from pure water to acetone, which indicates acetone enhances structuring of water the most. The structural difference in aqueous acetone and DMSO solutions is more evident from a higher peak in the oxygen-oxygen radial distribution function of the former corresponding to the second hydration shell at 4.5 Å that is attributed to the tetrahedral network of water[267].

Calculation of coordination number, obtained by integrating up to the first minima of the respective RDF, provides a lucid picture regarding solute solvent interactions; the coordination number between oxygen atoms calculated for pure water is 4.56 at 300K, 4.29 at 270K, and 4.17 at 240K, the numbers very close to the reported values for TIP4P model[332], suggesting a perfect tetrahedral network of water at its supercooling limit. The corresponding coordination numbers for DMSO solution is 4.00, 3.88 and 3.75, and for acetone it reads 3.95, 3.90 and 3.82. It can be seen that the difference in coordination numbers for DMSO at 240K and 300K is 0.25, while this difference for aqueous acetone solution is 0.17. This clearly indicates that DMSO perturbs water structure than acetone does in the vicinity of supercooling limit of water, 230 K.

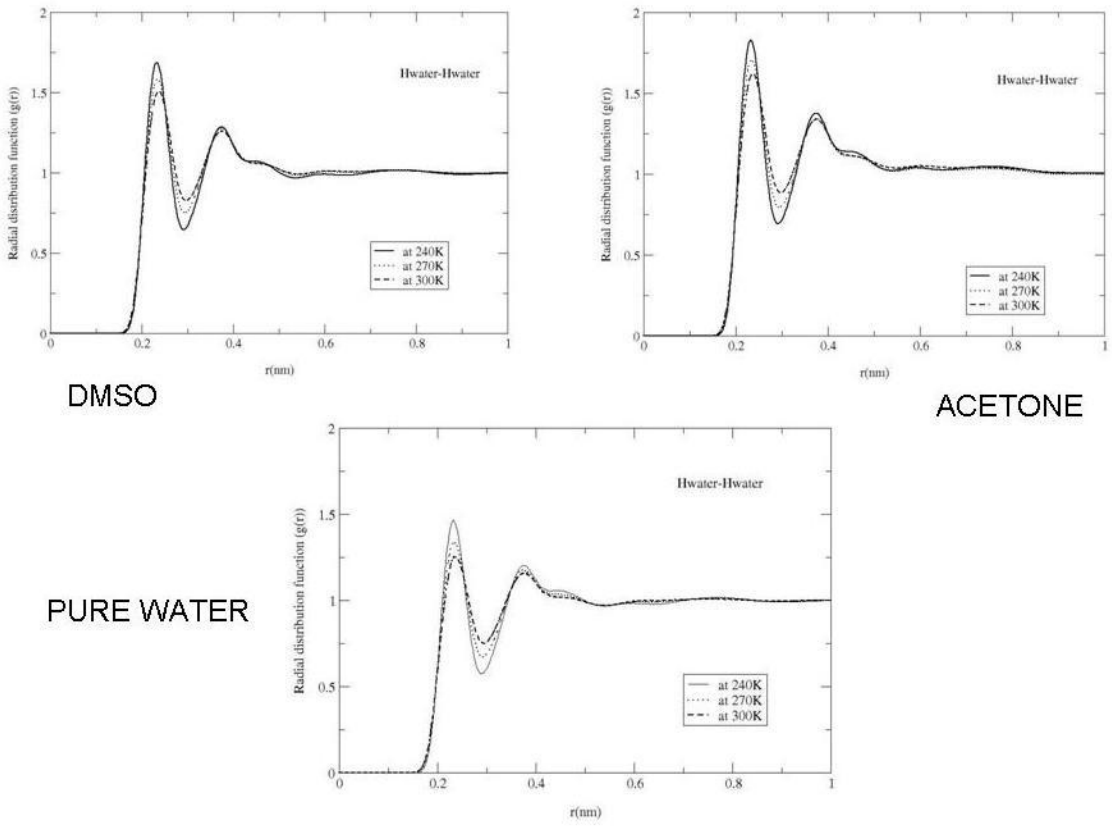

Figure 3-1 *Hydrogen-Hydrogen Radial distribution functions of 27% aqueous DMSO and Acetone solutions, and pure water*

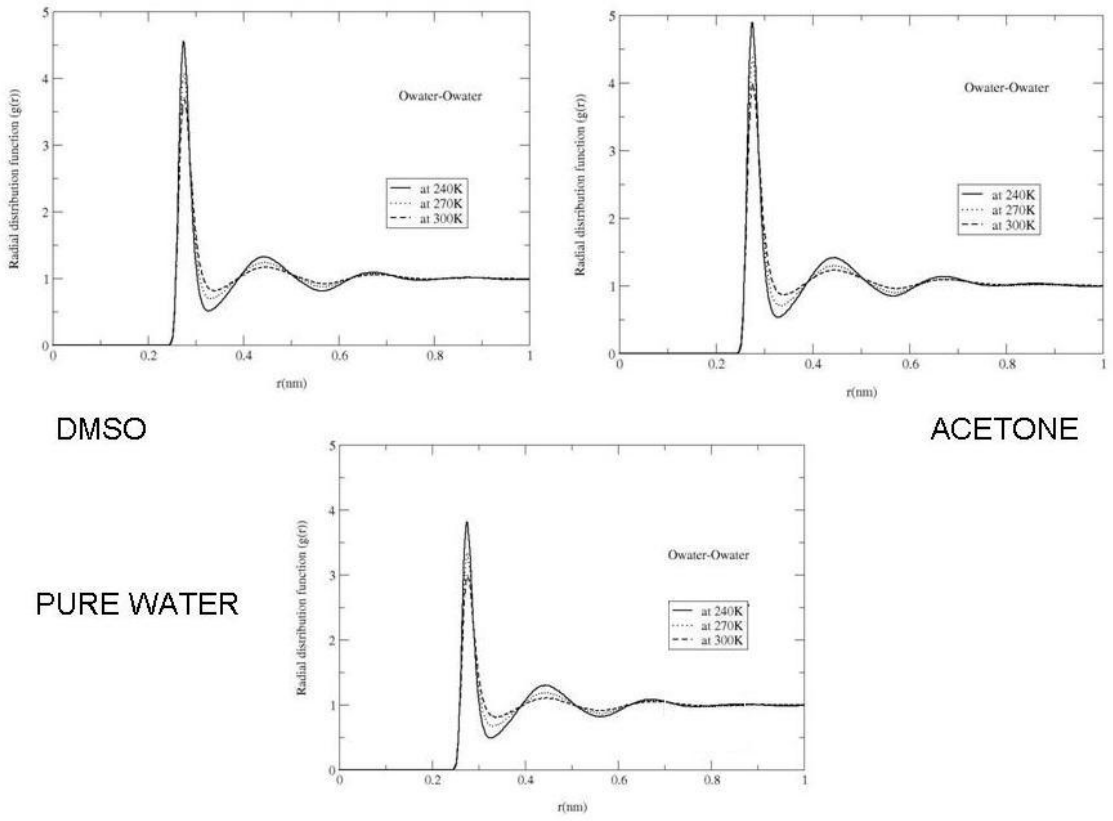

Figure 3-2 *Oxygen-Oxygen Radial distribution functions of 27% aqueous DMSO and Acetone solutions, and pure water*

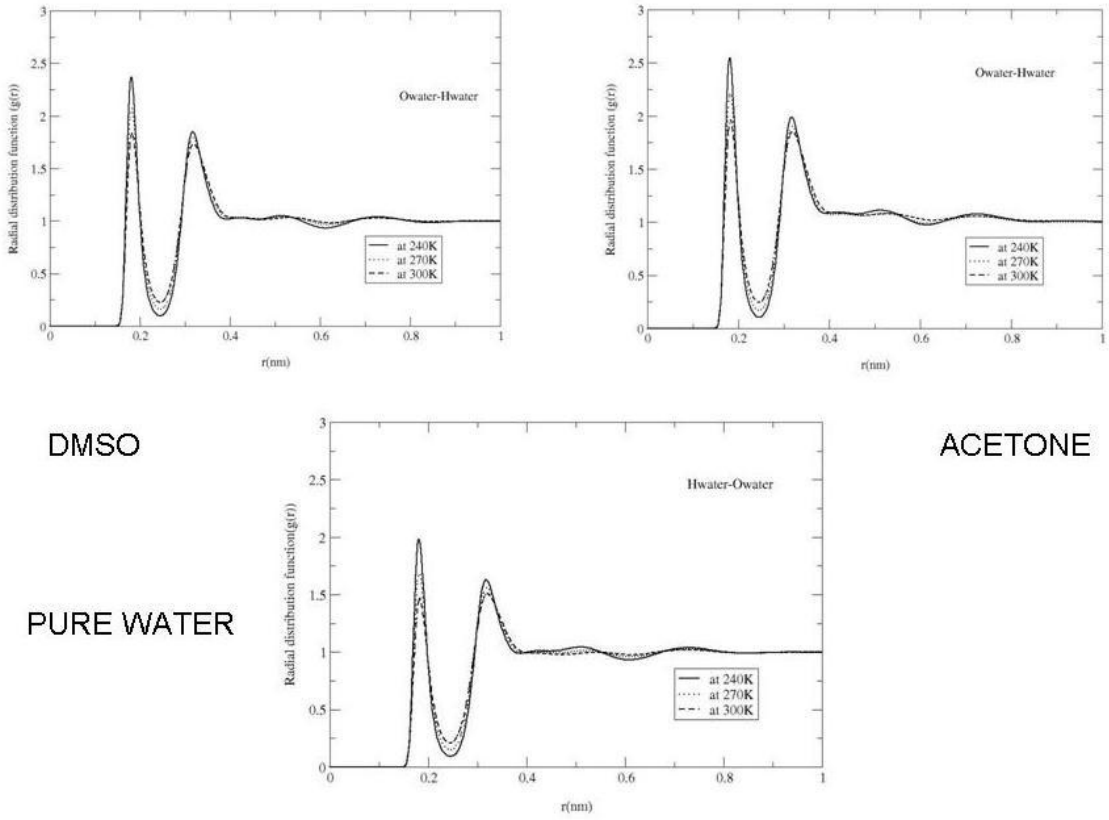

Figure 3-3 *Oxygen-Hydrogen Radial distribution functions of 27% aqueous DMSO and Acetone solutions, and pure water*

3.3.2. Solute-solvent structure

Figure 3-4 - Figure 3-7 show the intermolecular radial distribution functions of the two solute-solvent systems under investigation. An additional peak, centred at 4.5Å, is observed in the sulfinyl- water hydrogen RDF of DMSO solution. In the case of aqueous acetone solution this second peak is not so evident suggesting higher inter molecular interactions of sulfinyl groups in DMSO with water hydrogen atoms. Thus radial distribution functions indicate stronger association of sulfinyl groups than carbonyl group with water hydrogen, consistent with previous neutron diffraction and computer simulation studies[268]. This effect is more pronounced upon decrease in temperature. Another striking effect is featured in the methyl-water oxygen radial distribution functions. The second peak has been disappeared in the DMSO rdf, while a characteristic second peak is observed in the case of acetone solution at around 5Å, similar to the rdf of the mixture simulated using united atom OPLS/TIP4P

combination[313]. The flattening of the peak corresponding to second hydration shell in DMSO mixture has been attributed to water structure perturbation of DMSO[268], in conformity with previous simulations[267]. A peak around 3.5Å is observed in both DMSO and acetone methyl- water oxygen rdfs, indicating an interaction of methyl hydrogen with oxygen of water molecules; NMR spectroscopic investigations establishing the C-H…OH_2 interactions in acetone solutions corroborate the hydrophobic hydration in the aqueous acetone solution[307].

Methyl- water H pair correlation function indicates perturbation of water structure around the methyl group as evident by the broader peaks. It has been already established that at higher temperature, the methyl-hydrogen peak broadens suggesting a tangential orientation of water hydrogen towards methyl group in DMSO solutions[281]. Thus, this study confirms the finding that hydrogen molecules around methyl group promotes hydrophobic hydration in the mixture[281]. However, this confronts with the findings of the recently published neutron scattering experiments performed at room temperature, in which a sharp peak around 4Å for methyl carbon – water hydrogen has been reported[268], and a previous molecular dynamics simulation study using P2/SPC potentials combination. This points out that the choice of water potential indeed marks a difference in structural properties of aqueous solutions. On the contrary, temperature is not found to play a major role in the orientation of hydrogen water around methyl groups in acetone solution - the peaks observed remains the same in terms of the location and the intensity.

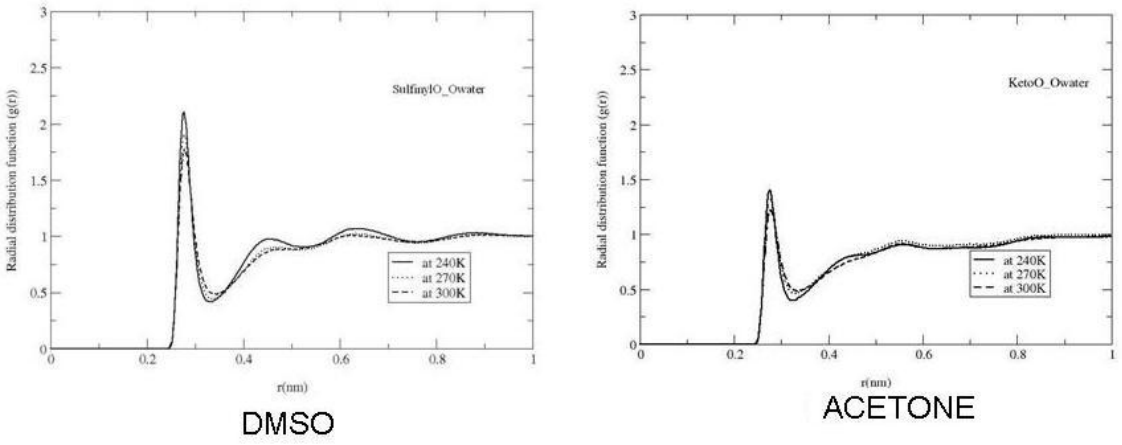

Figure 3-4 *Sulfinyl /Carbonyl oxygen – water oxygen radial distribution functions in 27% DMSO and acetone solutions*

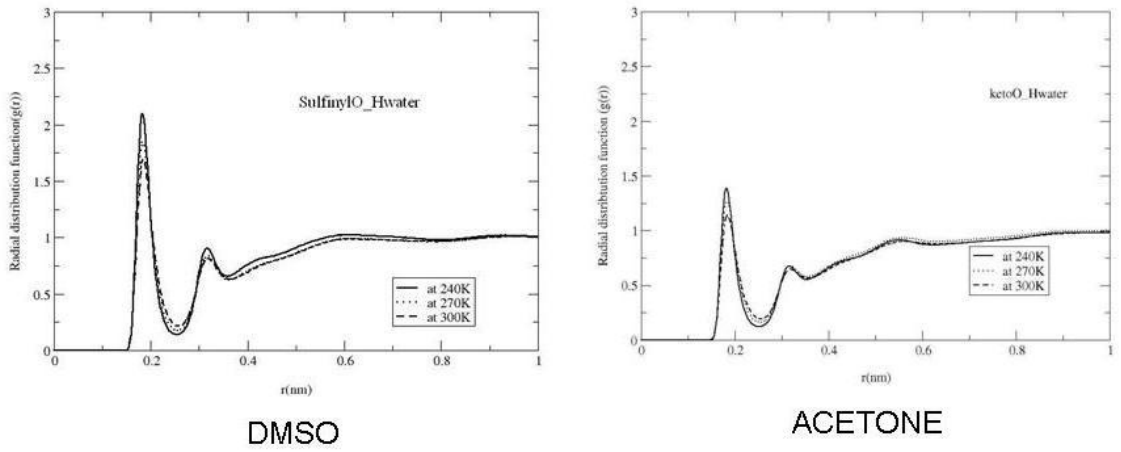

Figure 3-5 *Sulfinyl/carbonyl - water hydrogen radial distribution functions in 27% aqueous DMSO and Acetone solutions*

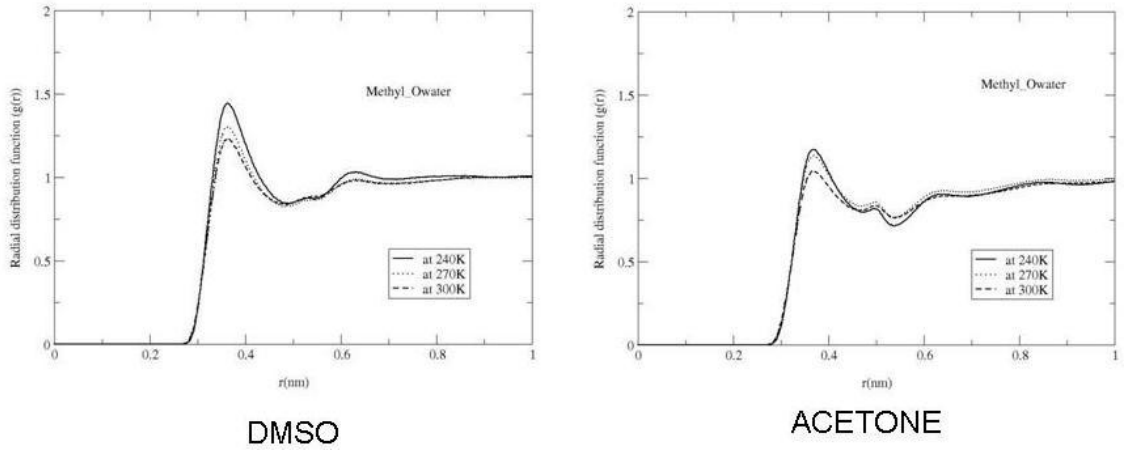

Figure 3-6 *Methyl - water Oxygen radial distribution function in 27% aqueous DMSO and Acetone solution*

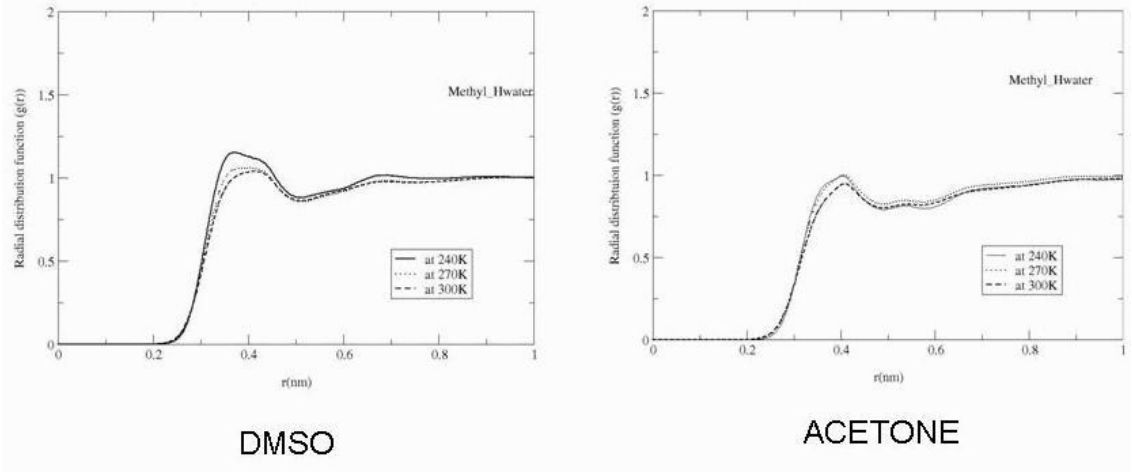

Figure 3-7 *Methyl- water hydrogen radial distribution function of 27% aqueous DMSO and Acetone solution*

3.3.3. Solute-solute structure

Figure 3-8- Figure 3-9 show solute - solute radial distribution functions of aqueous DMSO and acetone solutions. Contrary to a previous neutron diffraction investigation[268], RDFs obtained in this study demonstrate opposite trends in orientation of methyl groups as indicated by methyl-methyl pair correlation functions. In the aqueous acetone solutions, the first peak around 4Å is enforced towards lower temperature, indicating an increase in clustering in acetone solutions. The shape and location of the peak is similar to what has been obtained by using SPC/P1 potential combination[247]. On the other hand, the corresponding peak in DMSO solution is attenuated upon decrease in temperature. Carbonyl oxygen- methyl pair interaction in acetone is found to be strongly dependent on temperature - as temperature decreases the intensity of the peak increases; whereas in DMSO solutions the peaks obtained at 240K and 270K are found to be similar in their intensity. The most striking difference is seen in the case of second peak of the same radial distribution functions - the location of second peak is found at 6.1Å in DMSO and 5.6Å in acetone, implying a stronger interaction of methyl and carbonyl group in the latter. In addition, the intensity of second peak is more pronounced in acetone solution. This indicates that interactions between methyl and carbonyl group cannot be considered negligible, which echoes to the simulation findings on the pure liquid systems of acetone and DMSO[333]. Although the location of the carbonyl-methyl peak is same with the rdf obtained from TIP5P/AAOPLS simulations[312], the rdf derived from this work differs from those in intensity. Apart from that an additional flattened peak was also observed in that work around 7.5Å, indicating more structural order between solutes.

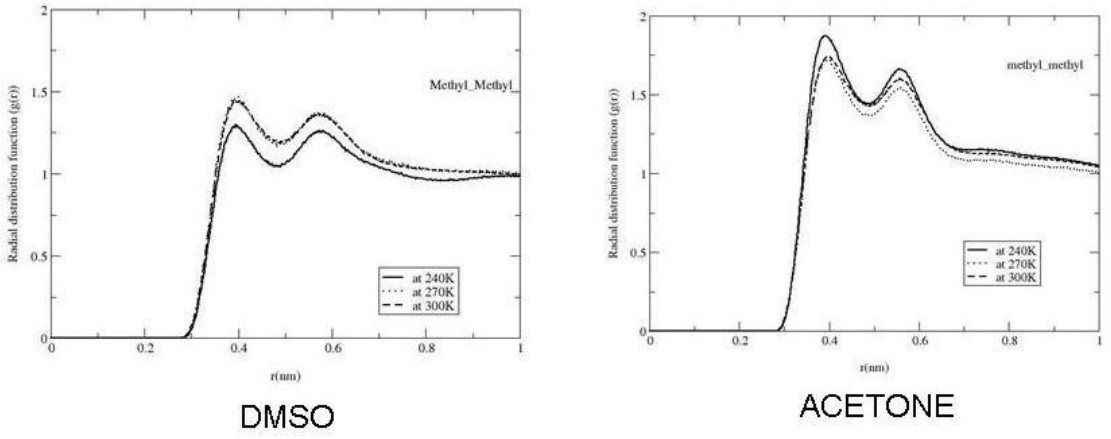

Figure 3-8 *Methyl-Methyl radial distribution function of 27% aqueous DMSO and Acetone solutions*

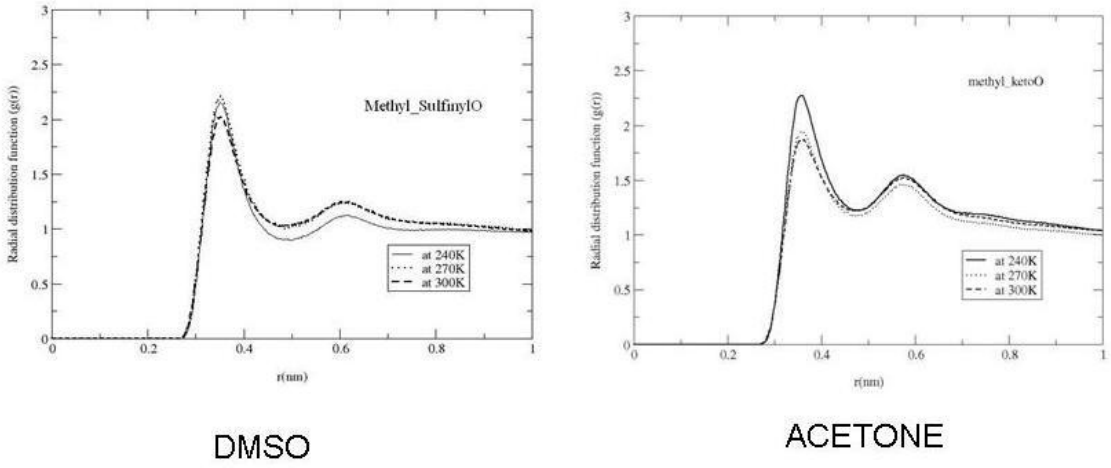

Figure 3-9 *Methyl-Sulfinyl/Keto oxygen radial distribution function in 27% aqueous DMSO solution*

Radial distribution functions (RDFs) play a significant role in elucidating solution structure in liquids and mixtures. Cross correlation functions obtained from a previous study employed using TIP5P/OPLS combination potentials by Han et al indicates existence of preferential conformation in aqueous DMSO solutions: oxygen atom of DMSO face hydrogen atoms of water, while methyl groups in DMSO are located opposite to oxygen atoms in water[277]. At the same time the interaction between methyl groups in DMSO and Hydrogen in water appears to be very weak as characterised by broad peaks in the corresponding radial distribution functions. The RDFs obtained in this work also reveal these three distinct interactions in the aqueous DMSO solutions - methyl groups in DMSO with oxygen of water, sulfinyl group in DMSO with hydrogen atoms in water, and sulfinyl group in DMSO with oxygen of water. A broad peak in the

methyl-water hydrogen distribution function implies weak interactions existing between these groups. A comprehensive comparison of radial distribution functions with the work done by Han et al[277] was not possible due to non availability of complete set of radial distribution functions in that paper.

Analogous interactions of the above three pairs are present in dilute acetone solutions, as revealed by corresponding radial distribution functions. The major difference between these two aqueous solutions lies in methyl-water hydrogen correlation functions - the interaction between two groups is stronger in aqueous acetone solutions as characterised by a sharper peak. It is very interesting to note that, as observed in pure acetone and DMSO, methyl - sulfinyl/carbonyl interactions are retained to a greater extent even in aqueous mixtures of the two solvents. In pure liquids (acetone and DMSO), in the absence of water, this interaction is the strongest, as evident by the sharper peaks, of all molecular interactions observed in these liquids[333].

3.3.4. Hydrogen bonding properties

A rigorous analysis of hydrogen bond properties of both the aqueous DMSO and acetone solutions at different concentrations has been made, in an attempt to quantify the strength of hydrogen bonds. A hydrogen bond is defined within the cut off radius of 3.5Å from the molecule that is considered and the cut off angle between Acceptor and donor is 30°.

3.3.4.1. Hydrogen bonding statistics

The number of hydrogen bonds between solute and solvent (water) in the solution is plotted in the Figure 3-10. The figure clearly indicates that the average number of solute-solvent hydrogen bonds is always higher in aqueous DMSO solutions than aqueous acetone solutions. Around 2 hydrogen bonds per DMSO are found in aqueous DMSO solutions and, at a higher concentration, the average number of hydrogen bonds hover around 1.8. On the other hand, the number of hydrogen bonds per acetone was found to be much lower- 1.3 and 1.2 in dilute and concentrated solutions, respectively, which is in close agreement with a previous molecular dynamics simulations of aqueous acetone solution[292]. Notably, the number of hydrogen bonds in the dilute

acetone solution shows a distinctive maximum (1.6) at 270K and a minimum (0.9) at 240K. Thus stronger water binding capacity of DMSO molecules can be inferred from hydrogen bonding statistics. It is interesting to note that number of hydrogen bonds between water and DMSO changes little with temperature compared to hydrogen bonds in pure water, confirming the assumption of a previous neutron scattering studies on aqueous DMSO solution[257].

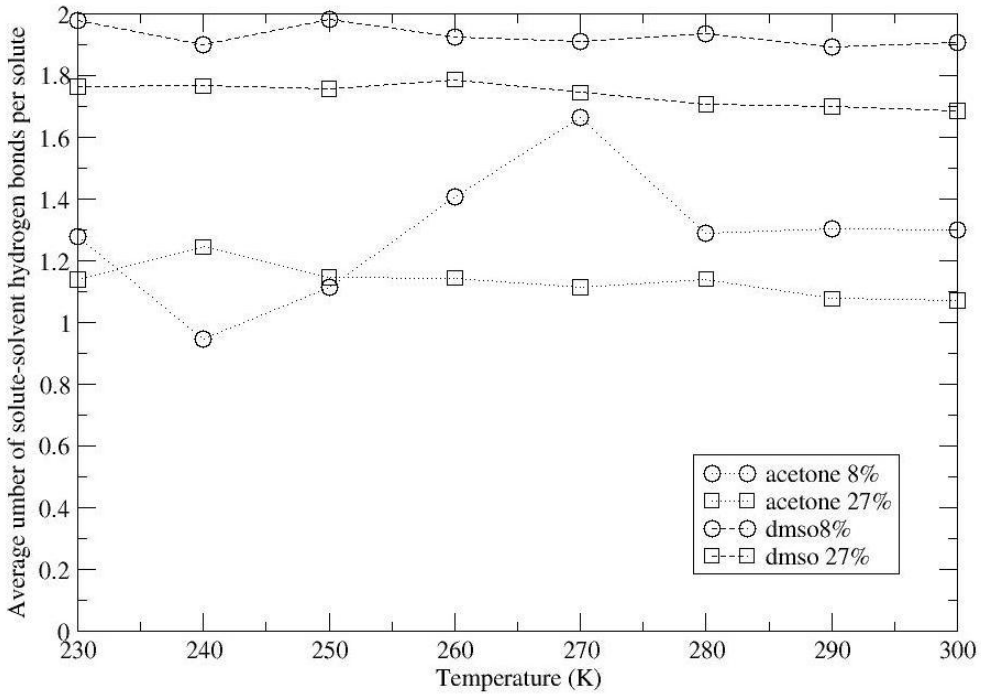

Figure 3-10 *Average number of solute –solvent hydrogen bonds per solute molecule*

A similar distinction, however, cannot be drawn from the estimation of solvent-solvent hydrogen bonds between two aqueous systems shown in Figure 3-11. A steady increase in the number of hydrogen bonds occurs from higher temperature region to lower temperature region in most of the cases. Clearly, the average number of water-water hydrogen bonds is found to be decreasing upon the addition of acetone and DMSO: this is due to the formation of more number of solute- solvent hydrogen bonds at the expense of water-water hydrogen bonds in the mixtures. The plot shows that this decrease is seen in concentrated DMSO solutions marginally higher than in acetone solutions at same concentration. In the concentrated DMSO solution the average number of water – water hydrogen bonds are found to be 3.3 at 298K, where as in the case of water it is 3.57, in consistent with previously reported value for TIP4P water[207].

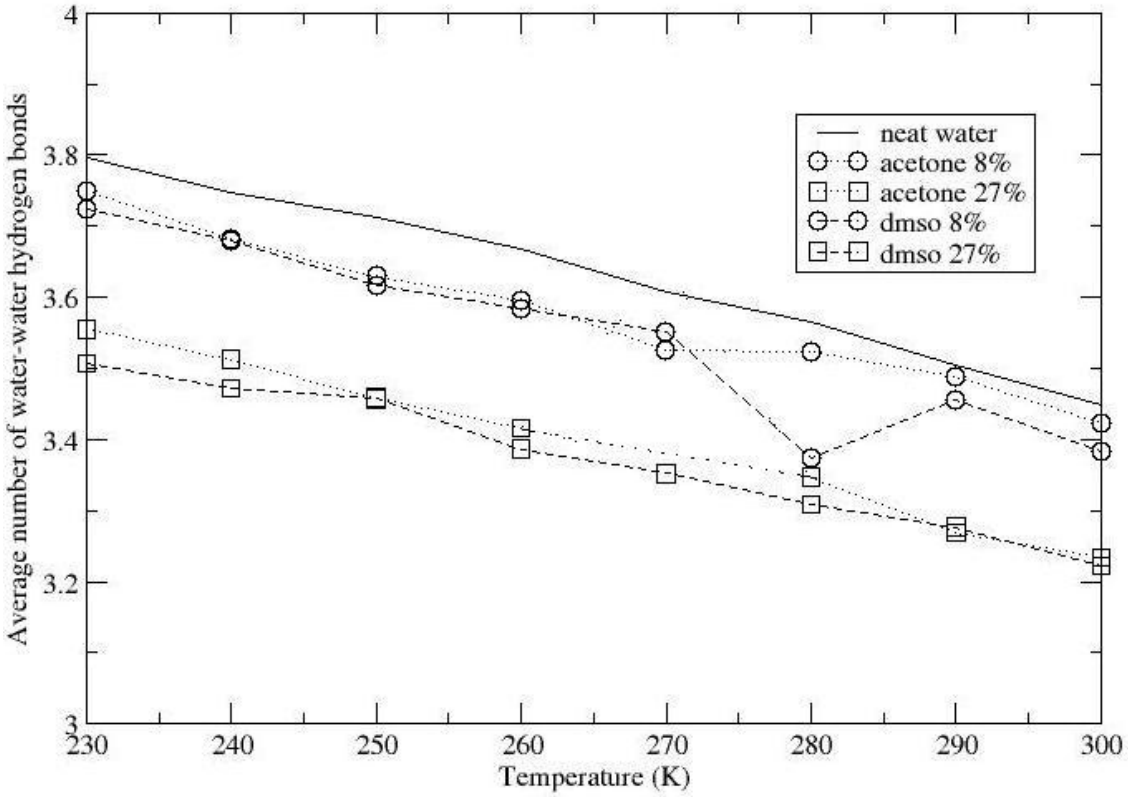

Figure 3-11 *Average number of water- water hydrogen bonds*

3.3.4.2. Hydrogen bond dynamics

In order to measure the strength of the hydrogen bonds, hydrogen bond lifetimes between solute and solvent, and solvent and solvent have been computed, which provides a quantitative estimation of the strength of hydrogen bonds in acetone and DMSO solutions. Solute- solvent hydrogen bonding lifetime shown in Figure 3-12 indicates that DMSO- water hydrogen bonds are kinetically more stable compared to corresponding concentrations of acetone solution, whilst this difference being notable at lower temperature. Figure 3-13 depicts solvent-solvent hydrogen bond lifetimes in the two systems investigated compared to pure water. Interestingly water-water hydrogen bond lifetime is found to be the shortest at higher temperature region among the systems investigated. Increasing the concentration of acetone, as data indicates, clearly increases the lifetime of the water- water hydrogen bonds in the solution, while addition of DMSO into water only moderately increases water-water hydrogen bond lifetimes. The plot (Figure 3-13) clearly demonstrates that both acetone and DMSO enhances water-water network, in accordance with previous observations[268].

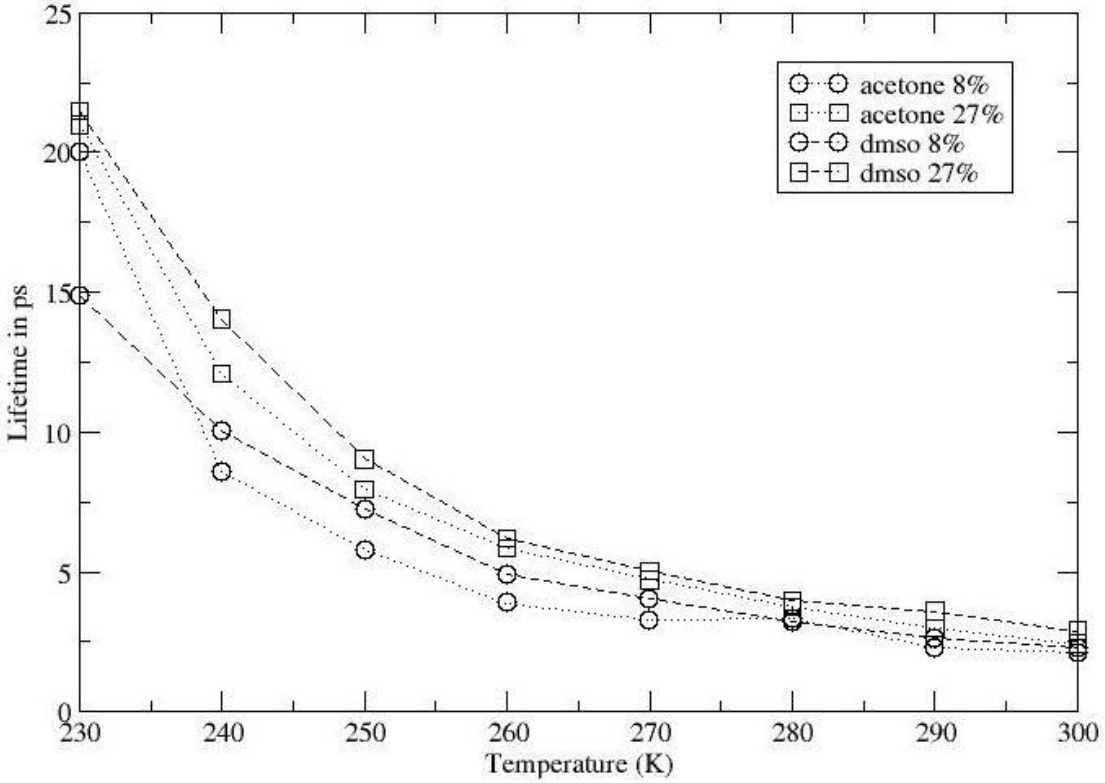

Figure 3-12 *solute-solvent hydrogen bond lifetimes in acetone and DMSO solutions*

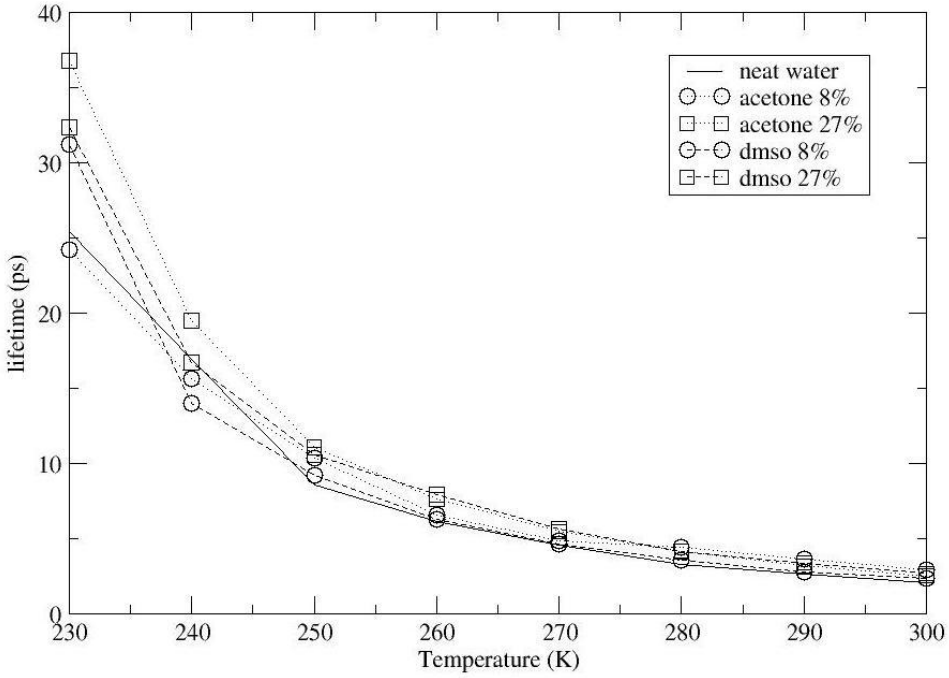

Figure 3-13 *Water-water hydrogen bond lifetimes in pure water, aqueous DMSO and acetone solutions*

Several authors have reported hydrogen bond lifetimes of various components in aqueous DMSO solutions. In conformity with a previous estimation of hydrogen bond lifetimes, employing P2/DMSO combination for DMSO-water mixture[291], water-water hydrogen bond lifetimes calculated in this study are found to be higher in mixtures than in pure water. DMSO-water hydrogen bond life times and water-water hydrogen bond lifetimes in the DMSO-water mixture read around 3ps at 300 K, which is contrary to the previous simulation findings by Luzar and Chandler (4.8 ps and 3.3 ps at 298K respectively)[247].

3.3.4.3. Hydrogen bond angle distribution

Figure 3-14 to Figure 3-17 show the hydrogen bond angle distribution of the two mixtures studied. In both solutions, at both concentrations investigated, the proportion of hydrogen bonds with smaller angle between acceptor and donor increases upon decrease in temperature, indicating formation of stronger, linear hydrogen bonds formed at lower temperature. The difference between aqueous solutions of acetone and DMSO is negligible in this aspect.

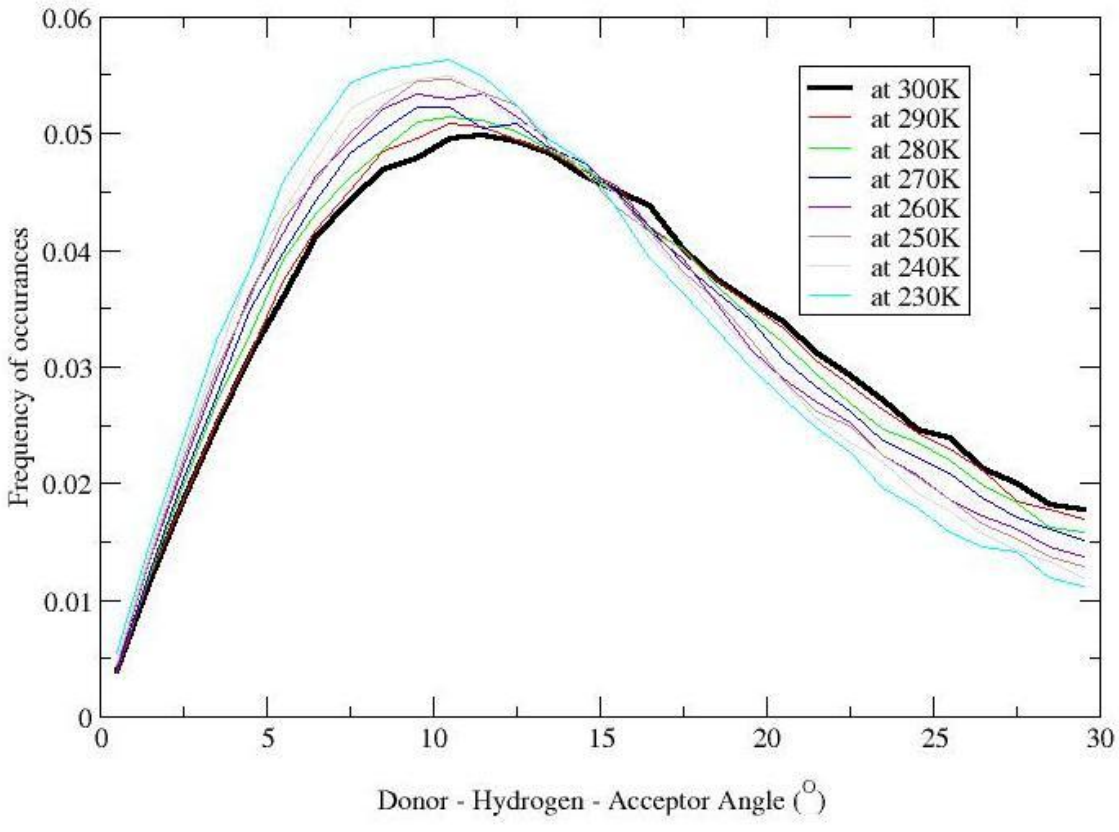

Figure 3-14 *Hydrogen bond angle distribution of 8% aqueous DMSO solution*

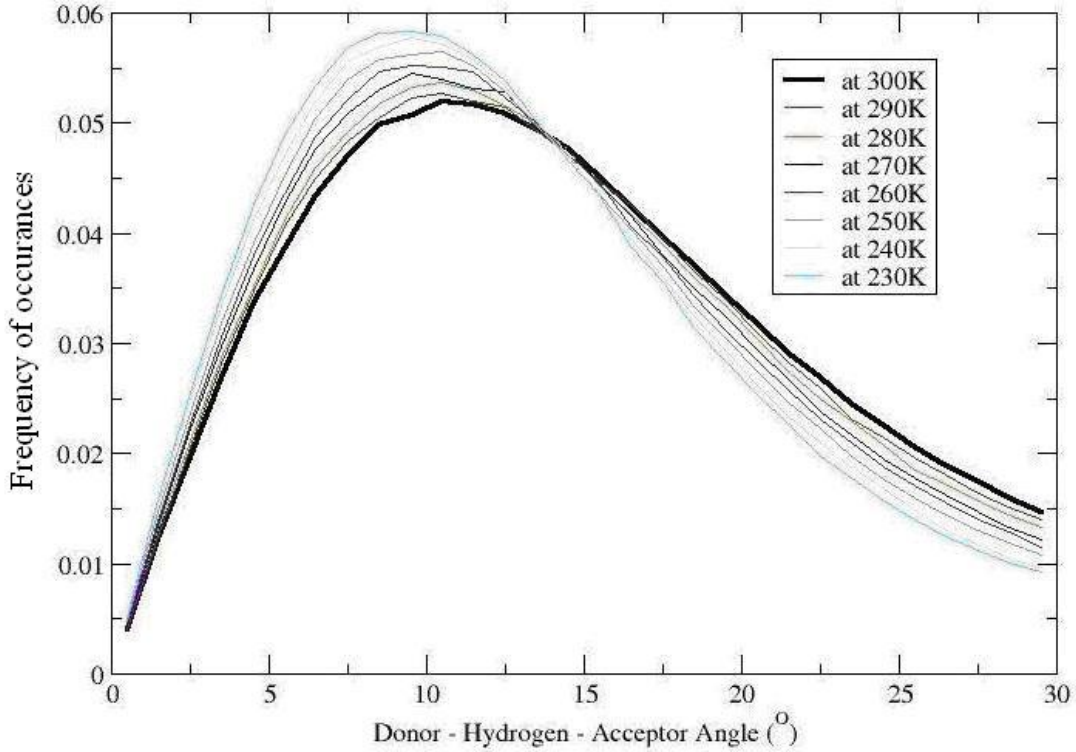

Figure 3-15 *Distribution of donor-acceptor hydrogen bond angle of 27% DMSO solution*

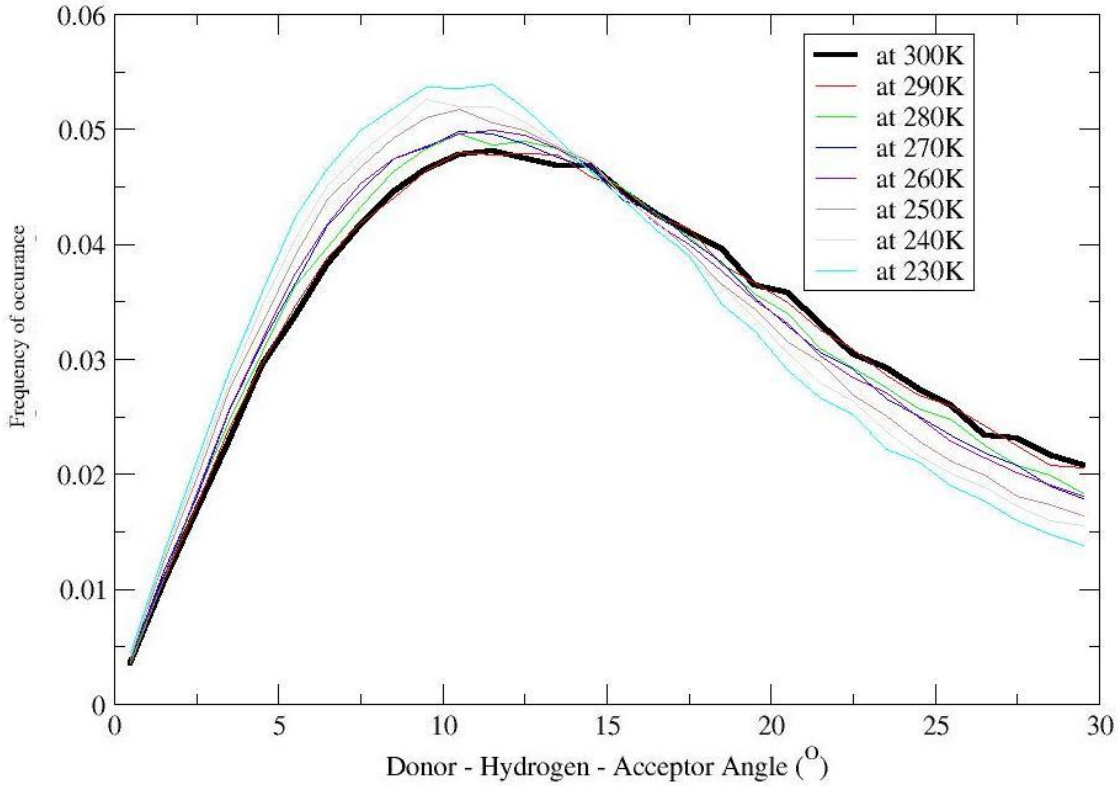

Figure 3-16 *Hydrogen bond angle distribution of 8% acetone solution*

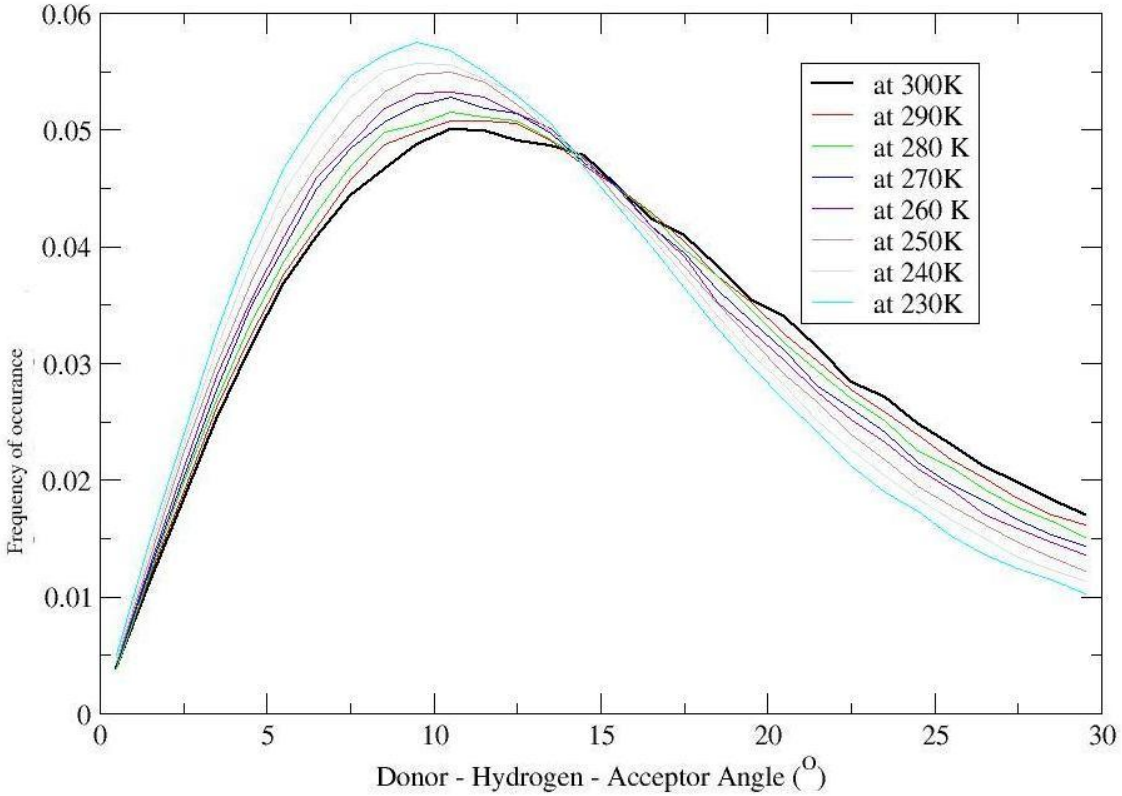

Figure 3-17 *Hydrogen bonding angle distribution of 27% aqueous acetone solution*

3.3.4.4. Hydrogen bond distance distribution

Figure 3-18 to Figure 3-21 indicate the distribution of hydrogen bonding distance. As seen from the plots the length of the hydrogen bonds slightly varies in proportion to the decrease in the temperature, in consistent with a previous observation[281]: at 230K, the highest proportion of hydrogen bond distance is 1.8Å, whereas at higher temperatures this value shifts towards 1.9Å. This indicates that the hydrogen bonding is progressively becoming stronger as temperature decreases. This shift occurs in regardless the systems and concentrations.

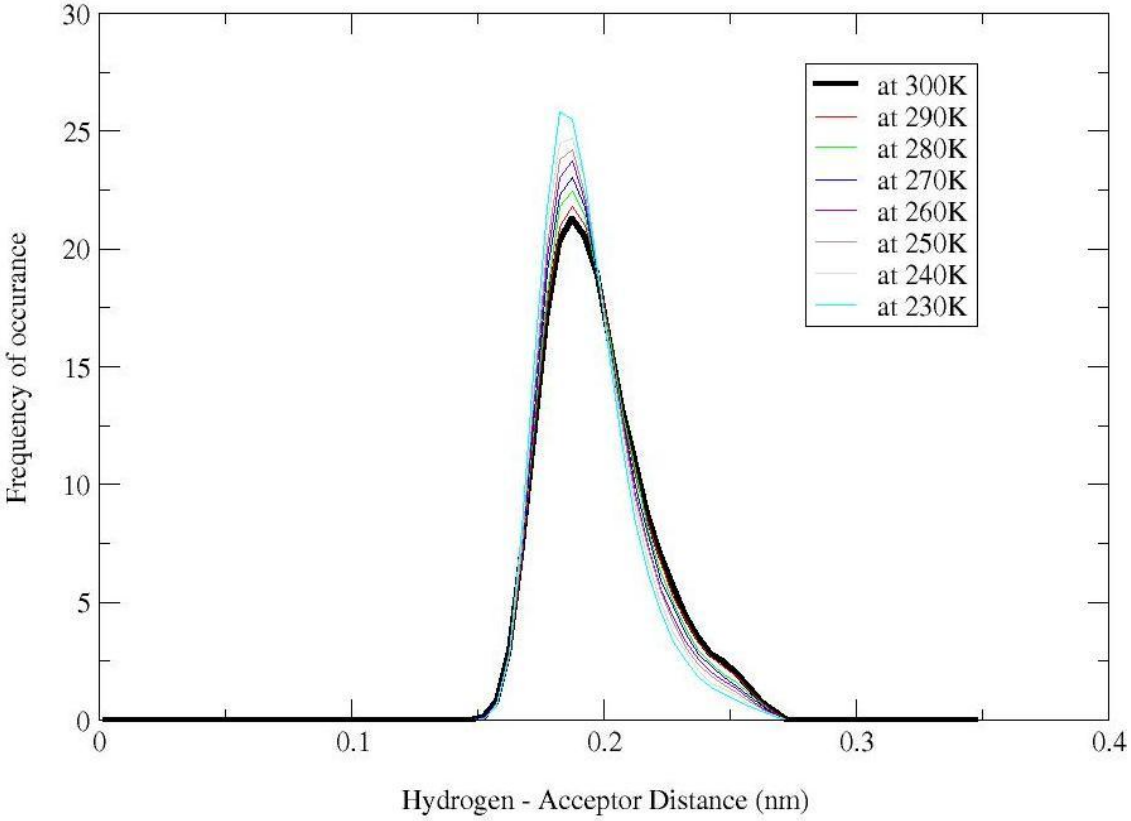

Figure 3-18 *Hydrogen bond distance distribution of 8% aqueous DMSO solutions*

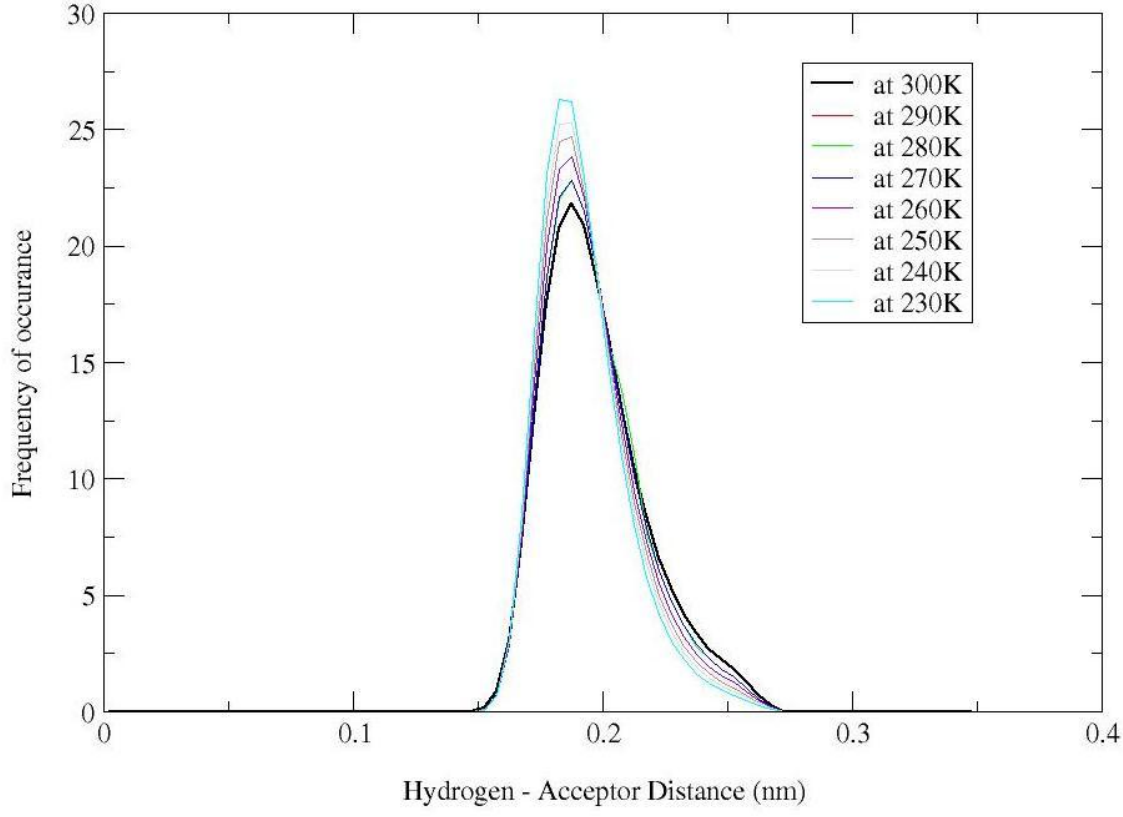

Figure 3-19 *Hydrogen bond distance distribution of DMSO 27% solution*

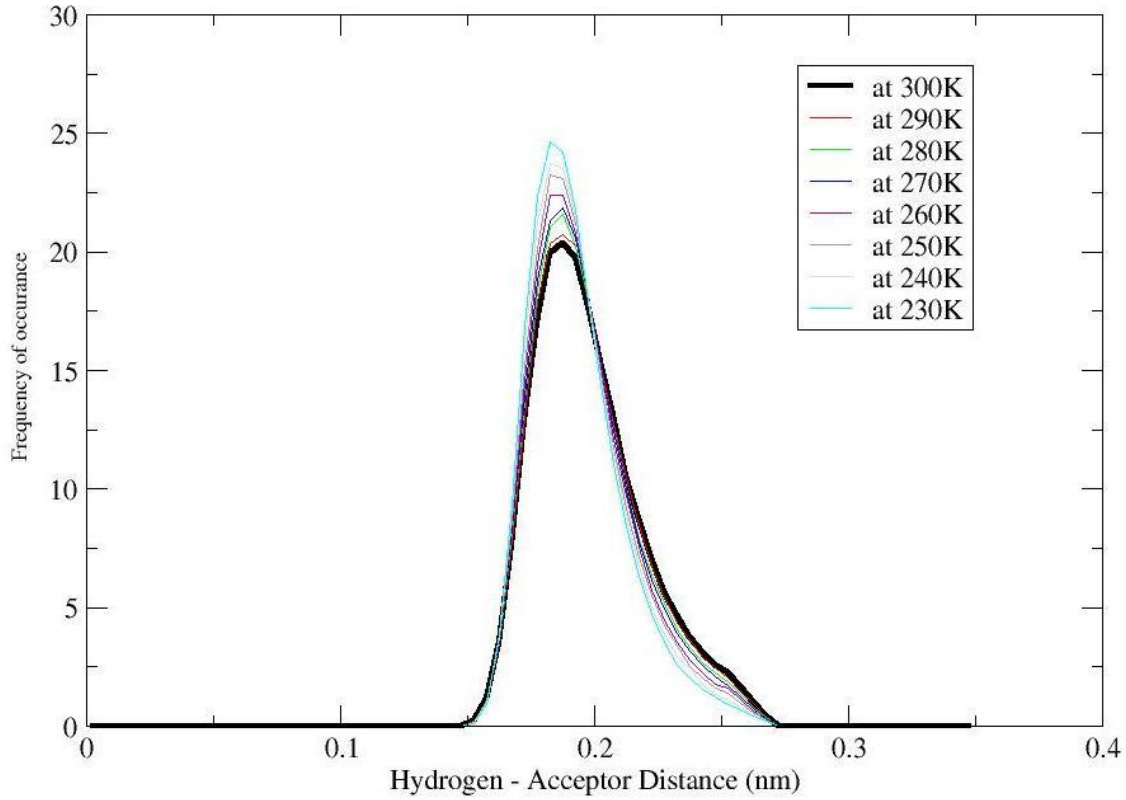

Figure 3-20 *Distribution of bond distance in 8% aqueous Acetone solutions*

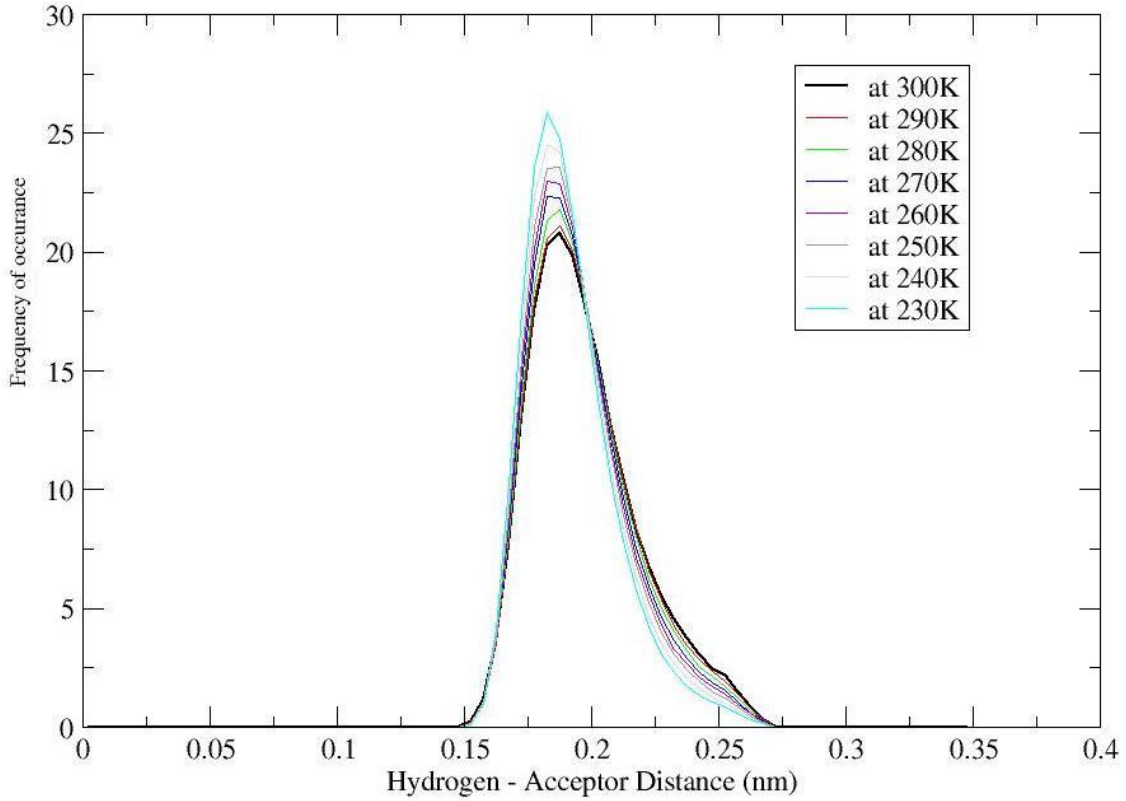

Figure 3-21 *Distribution of hydrogen bond distance of 27% aqueous Acetone solution*

Neat water, in particular at low temperature, exists as tetrahedral network linked by four hydrogen bonds[286]. Two hydrogen atoms of a central water molecule are hydrogen-bonded to the oxygen of neighbouring molecules, and one hydrogen atom each of two other neighbour molecules is inturn hydrogen bonded to the central water molecule. Number of free hydroxyl groups, widely thought to exist in neat water, decreases upon addition of molecules that have excess H-bond acceptor lone pairs on their oxygen[303, 304]. DMSO and acetone, being strong acceptor of hydrogen bonds, will form hydrogen bonds with water molecules until available hydroxyl groups in the solution are consumed. It can be seen, as mentioned previously, that as concentration of solutes increases, the average number of hydrogen bonds between solutes and water rises proportionately. Addition of Acetone, DMSO too, to a solvent like water naturally adds more number of solute-water hydrogen bonds in the solution[303, 304]. Theoretically an isolated water molecule can form two hydrogen bonds with acetone molecules, as carbonyl oxygen can form hydrogen bonds with a water molecule at either side of the molecular plane. Nevertheless even at very dilute concentrations, acetone forms very less number of hydrogen bonds than the expected number, as shown in Figure 3-10, which is in good agreement with previous computer simulations findings[313].

A previous molecular dynamics simulation study suggested that addition of DMSO weakens hydrogen bond network of water at room temperature at the expense of DMSO-water interactions[289]. Despite of these interactions, as characterised by a negative slope towards temperature as shown in Figure 3-11, an inverse relationship can be deduced between average number of water- water hydrogen bonds and temperature, implying an increase in mean force for water – water hydrogen bonding, hence structuring of water[247] towards lower temperature.

DMSO and water compete as acceptors of hydrogen bonds donated by water molecules. Interaction of DMSO with water occurs through the two lone pairs of DMSO oxygen atom, which is capable of accepting two hydrogen bonds from neighbouring water molecules[264]. This notion is supported by infrared spectrum of aqueous DMSO solution. Appearance of band at 1041cm^{-1} is reported in the infrared spectrum pertaining to

water-DMSO hydrogen bonds. At the same time much higher band width that would correspond to a non hydrogen bonded Sulfinyl group (S=O) was not present in the spectrum[264].

Compared to Neutron diffraction experiments which are widely used to probe liquid structure, computational methods are very useful tools for extracting better estimate of hydrogen bonding structure as neutron diffraction data are not sensitive to potential hydrogen bonding sites on solute molecules[247]. The maximum possible hydrogen bond between a DMSO and water molecules in very dilute solutions that has been predicted by the neutron experiments is two which is closely matched by the molecular dynamics simulations[247]. Average number of DMSO-water hydrogen bonds estimated in this study is slightly below this predicted value. Though such estimation heavily depends upon the potential employed in the simulations and the concentration of the solute, it does not alter the final conclusion much. It is interesting to note that average number of hydrogen bonds between solute and solvent in the DMSO/water mixture is independent of temperature, whereas average number of hydrogen bonds per water molecule in pure water increases monotonically towards lower temperature. Monotonic increase in average number of hydrogen bonds in pure water suggests Arrhenius dependence of number of hydrogen bonds with temperature[170]. On the other hand, calculations shown in Figure 3-13 and Figure 3-12 suggest that relaxation times (hydrogen bond life times) associated with breaking of hydrogen bonds between water and water, and solute and water follow weak Arrhenius behaviour.

Superior hydrogen bonding property of DMSO over acetone is reflected in higher molecular dipole moment of the constituents in DMSO[285]. While traditional molecular dynamics methods are not suitable to accurately measure electronic properties in solutions, more sophisticated methods such as Car Parinello molecular dynamics (CPMD) can be employed to achieve such task. CPMD simulations combined with dipole moment calculations using Wannier formalism, analogue of localised molecular orbitals, reveals that upon dilution total dipole moment of DMSO is drastically increased[334]. Sulfinyl group in DMSO is highly polarised leading to a large increase in negative charge on oxygen atom, whereas dipole moments of methyl groups decreases in water[334]. Hence it can be concluded that sulphur - oxygen dipole contributes primarily to the overall dipole moment of DMSO.

Computer simulations can complement NMR experiments in great detail for elucidating hydrogen bond structure in systems such as aqueous DMSO solutions. Dependence of DMSO-water hydrogen bonds and Nuclear magnetic resonance (NMR) chemical shift in aqueous mixtures on concentration demonstrates non ideal behaviour of aqueous DMSO solutions[277]. Highly polarised and anisotropic sulfinyl group (S=O) in DMSO readily forms hydrogen bonds when mixed with water. This hydrogen bond interaction is the major contributor of NMR chemical shift in the aqueous solutions.

Two competing effects – increase in attractive potential of mean force between pairs of water in the presence of a solute[257], alternatively known as enhancement of water network, and strong hydrogen bonding between DMSO and water, are dominant in aqueous DMSO mixtures. But both these effects are favourable due to energetic and entropic requirements. Formation of DMSO-water hydrogen bonds is energetically favourable for about -2Kcal/mol than water-water hydrogen bonds[263], while structuring of water around methyl groups is made up for entropic expense for inserting a solute molecule within the network of water molecules. Weak interaction of acetone with water compared to the interactions between water molecules themselves facilitates the process of opening up cavities close to acetone molecules in the mixture. On the other hand, DMSO due to stronger interaction with water suppresses density fluctuations that open up cavities around the solute molecules[285].

3.3.5. Translational and rotational dynamics of aqueous solutions

Figure 3-22 represents the self diffusion coefficient of solute molecules in the aqueous mixtures. Self diffusion coefficient of all five systems simulated is appeared to be converged within the range of 0.10-0.2 x 10^{-9} m^2/sec after fluctuated values in the higher temperature region. In general, upon increasing the concentration of Acetone and DMSO, diffusion decreases; this effect is more pronounced with DMSO. On the other hand, Acetone diffuses slower than DMSO at all temperatures at low concentration, but this trend is reversed in concentrated solutions as shown in Figure 3-23. Hydrogen bonding alone cannot explain the lower diffusion coefficient of DMSO at a higher concentration as the number of hydrogen bonds per DMSO decreases from 2.0 to 1.8 upon increase in its concentration. Hence, this prompts one to suggest the

formation of much larger DMSO-water complexes that can exist in the solution.[275] On the other hand, increase in concentration of acetone does not significantly alter the solute diffusion coefficient. This may be attributed to its weaker interaction with water as the concentration increases.

In Figure 3-23, a comparison of the diffusion coefficients of water in the mixtures to pure water is given. It can be seen from the plot that pure water has a higher diffusion than in the solutions. In addition, the figure provides a general feature that solutes like DMSO and acetone considerably reduce the translational mobility of water molecules, in consistent with the experimental findings[296]. Water in DMSO solutions diffuses slower than pure water, which becomes much more pronounced at high DMSO concentration. Water in acetone solutions on the other hand diffuses slower than 8% DMSO solution, but a higher concentration of acetone does not result in a substantial drop in diffusion, as is the case of solutions of DMSO at 27%. Increase in concentration of DMSO has notable effect in reducing the diffusive motions of water molecules, which may be an indication of the formation of complexes containing DMSO and water molecules[275]. Non dependence of concentration on water diffusion in aqueous acetone solution is suggestive of the fact that acetone does not form clusters with water[304].

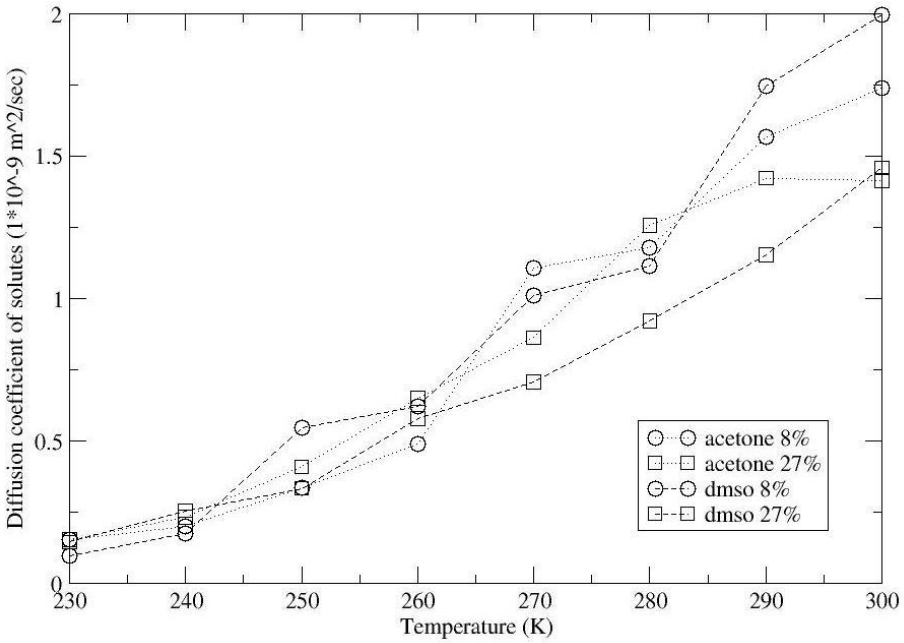

Figure 3-22 *Diffusion coefficients of solutes in the aqueous DMSO and acetone solutions*

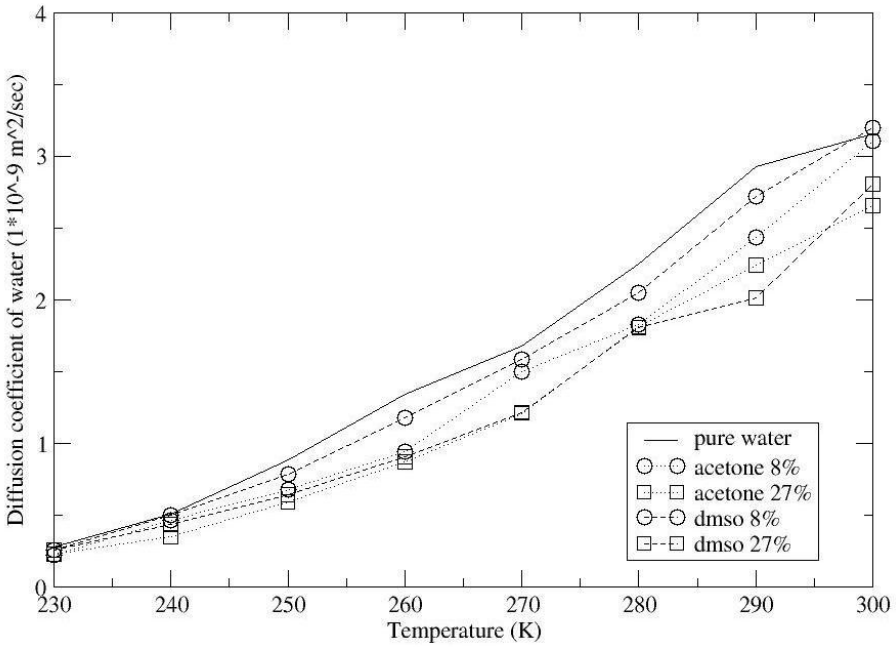

Figure 3-23 *Diffusion coefficients of solvent molecules in pure water and aqueous mixtures*

In Figure 3-24, the rotational correlation times of solvent molecules (water) in the mixtures and in pure water are plotted. The simulated rotational correlation times of the aqueous DMSO solutions is much lower than quasi elastic neutron scattering measurement at 295K[296]. However, qualitative description of rotational correlation times is in agreement with the experiment at room temperature[296]. Addition of either DMSO or acetone does not alter the rotational correlation times of water considerably at normal temperature. A substantial increase in rotational correlation times can be seen in all systems investigated. At both concentrations, increase in rotational correlation times is more in acetone solution in the low temperature region, from 280K to 230K.

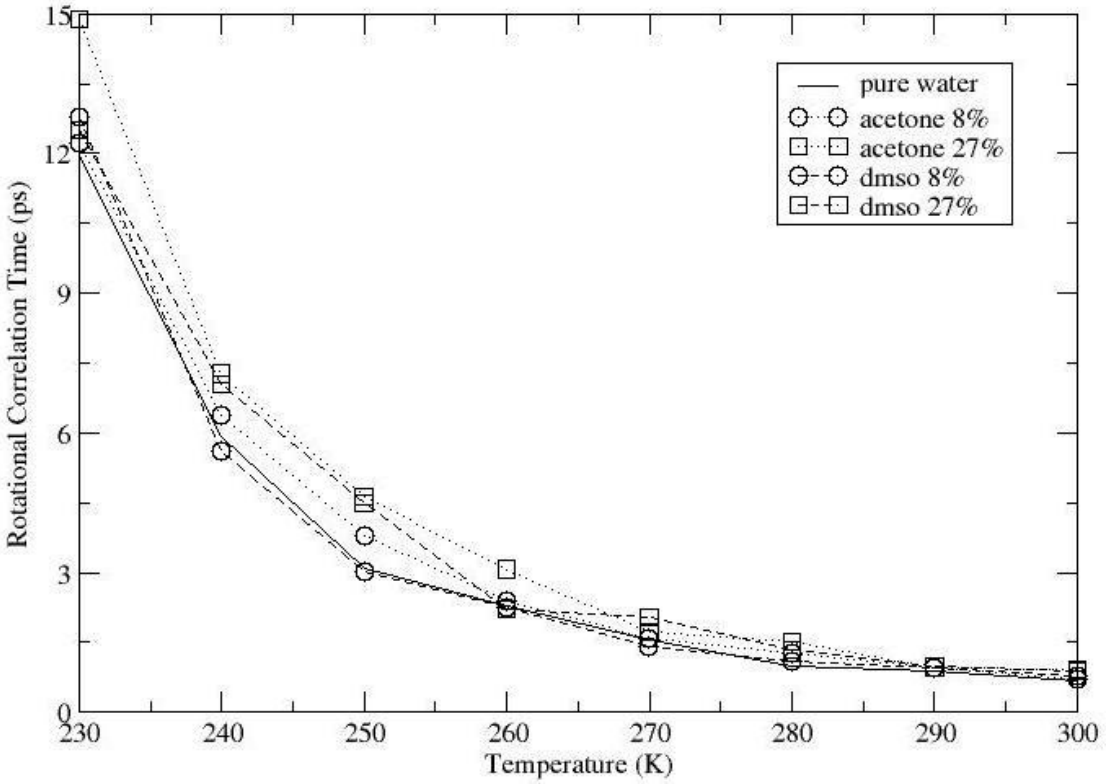

Figure 3-24 *Rotational correlational times of aqueous solutions of DMSO and acetone, compared with that of pure water*

Feller and Strader have reported a higher rotational correlation times for water in the aqueous solutions, which has been attributed to the existence of short water chains connected by hydrogen bonds[335]. Rotational correlation data shows that water in the concentrated acetone solutions has the highest relaxation times, suggesting that short solute-water chains linked by hydrogen bonds may exist throughout in the mixture. This confirms that availability of such water chains is larger in acetone mixtures than in aqueous DMSO solutions as more water molecules are incorporated in DMSO-water complexes. By contrast, acetone molecules, being planar, do not form such complexes when mixed with water; infra red spectroscopic studies have ruled out the possibilities of acetone–water complexes[303]. Furthermore Fourier Transform Infrared Attenuated Total Reflectance Spectroscopy (FTIATRS) studies clearly indicate that acetone molecules do not promote large complexes of acetone and water[304].

3.3.6. Density analysis of aqueous solutions

In this section, density profiles of two systems, aqueous acetone and DMSO, at five different concentrations are compared, following the work of Grigera et al, in which observed a characteristic minimum in the plot, which was assigned as glass transition temperature[336].

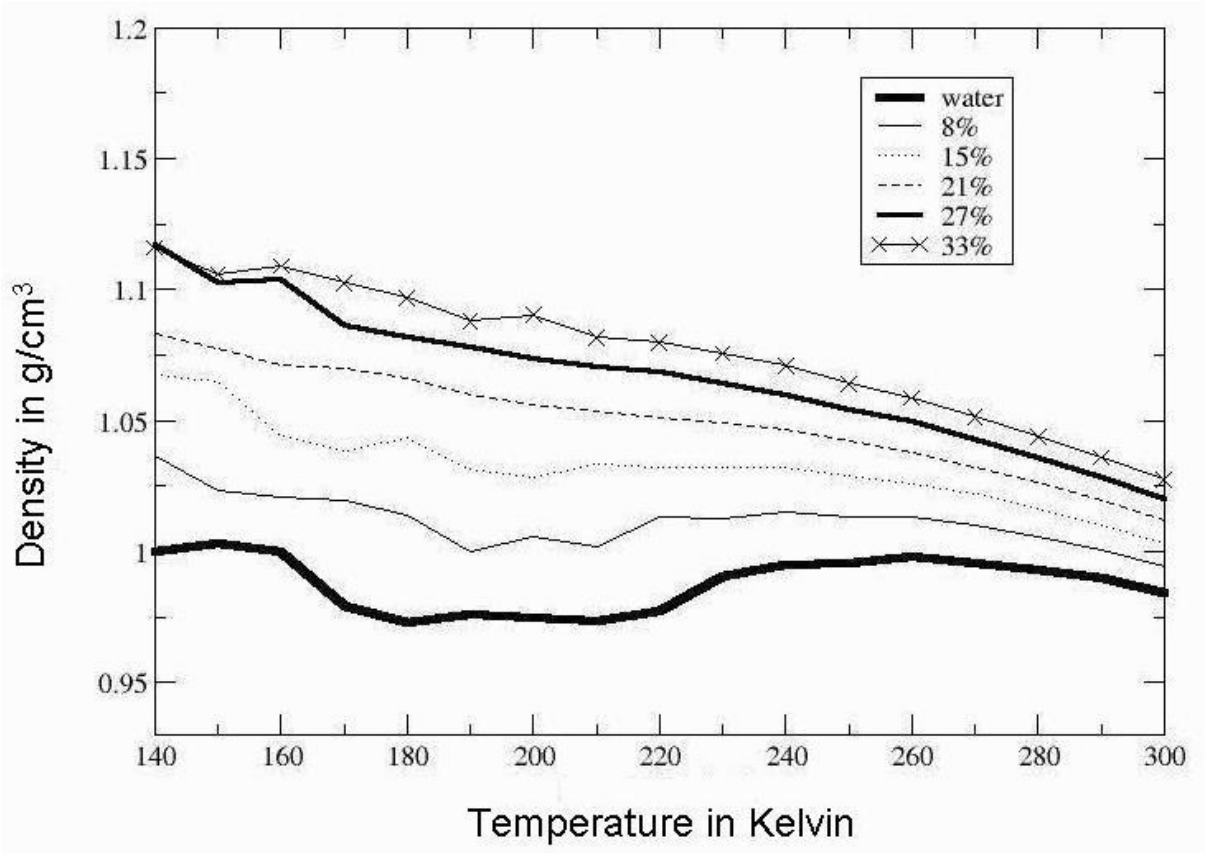

Figure 3-25 *Density-Temperature profile of aqueous DMSO solutions at five different concentrations compared with pure water. From the figure it can be seen that a minimum in the profile is observed in the case of pure water. On the contrary, as the concentration of DMSO increases, this minimum diminishes, leading to a smooth decrease in the density upon change in temperature.*

Figure 3-25 and Figure 3-26 show density temperature profile of aqueous DMSO and acetone solutions at five different concentrations, viz. 8%, 15%, 21%, 27%, 33% by weight. As depicted in the figures, density profile of pure water shows a higher order polynomial (non exponential) behaviour with a distinct minimum around 200K. Interestingly this value is found to be in very good agreement with the measured density minimum for heavy water by employing Small Angle Neutron Scattering (SANS) experiments[337]. Density-temperature profile has been reported in the literature for TIP5P-Ewald model which is claimed to represent properties of water at a wide

range of temperature accurately. The density minimum for TIP5P-E water however is slightly higher than that of TIP4P water obtained in this study[338].

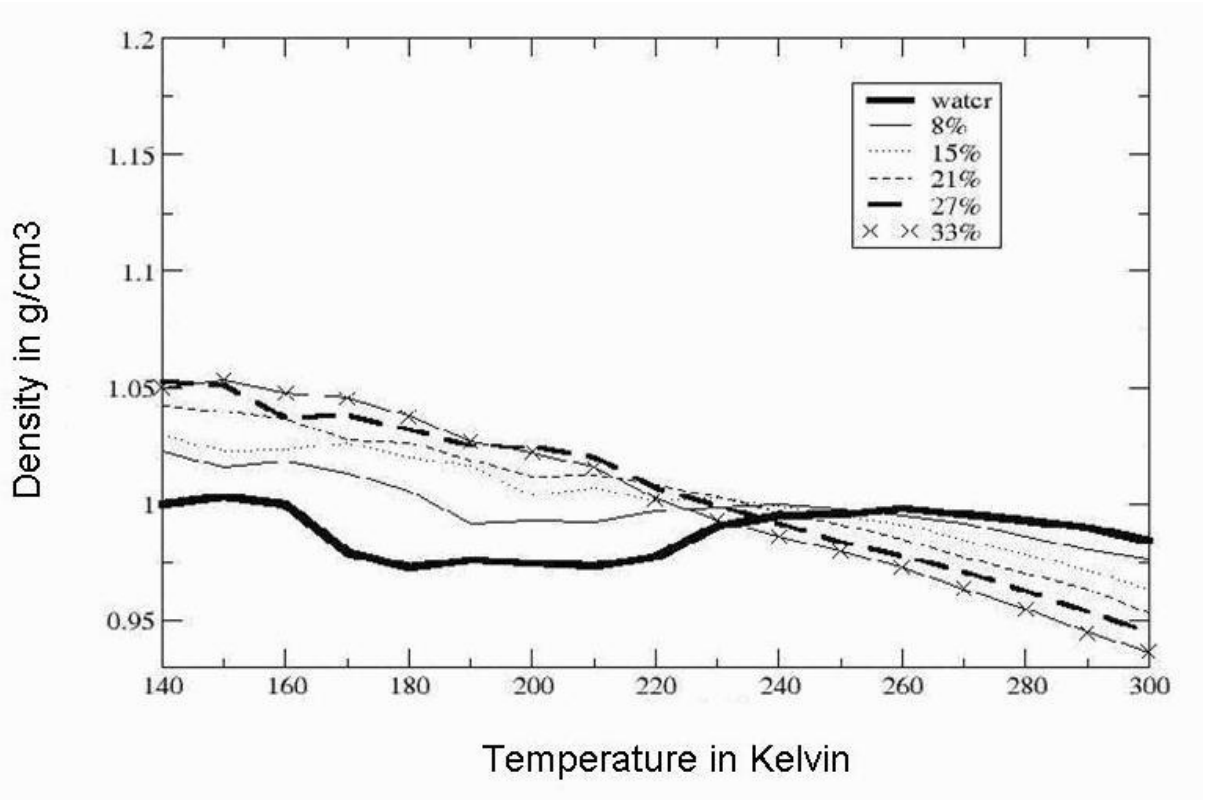

Figure 3-26 *Density-Temperature profile of aqueous acetone solutions at five different concentrations compared with pure water. As can be seen from the figure, density of water shows distinctive minimum around 200K. As the concentration of acetone increases, the minimum disappears.*

The plots clearly demonstrate increase in density at lower temperature region in both DMSO and acetone mixtures, echoing the fact that cooling at constant pressure usually increases the density of the system[339]. Conversely, density of pure water goes through a distinct minimum at around 200 K as shown in the figures. Discontinuities in the density-temperature profile of single component systems such as molten glucose has been correlated with the onset of glass transition temperature[336]. The plots do not indicate density minimum in the case of aqueous mixtures, in particular at higher concentrations. Density plots also indicate that addition of DMSO transforms low density liquid water into high density mixture. It has to be noted that densities of DMSO – water mixture are always higher than that of pure water, whereas densities of aqueous acetone solutions are found to be higher than pure water only below its supercooling temperature, 230K. Exponential dependence of density with respect to temperature is observed in both the systems. The exponential decrease in the density

towards higher temperature rather than density minimum within the range of temperature investigated is observed in the concentrated solutions, implying that water anomalies are generally absent in the concentrated solutions of DMSO and Acetone. In the light of molecular dynamics simulations described in this chapter, it can be concluded that water-water interactions are supplanted to a greater extent by hydrogen bonding interactions between these solutes, DMSO in particular, and water in the aqueous solutions leading to the suppression of water anomalies in its supercooling region[170].

3.4. CONCLUSIONS

Molecular dynamics simulations on aqueous mixtures of DMSO and acetone at two different concentrations and for a wide range of temperatures have been performed using widely accepted TIP4P potential for water and OPLS potential for the solutes, in order to extract characteristic differences in structural, dynamic and hydrogen bonding properties. Solvent -solvent radial distribution functions provide an evidence for an enhancement of water structure in acetone than DMSO. Inter molecular radial distribution functions suggest that sulfinyl group in DMSO interacts with water more than carbonyl group in acetone; this effect is particularly more pronounced in the lower temperature region. Furthermore, both DMSO and acetone promote hydrophobic hydration as evident from inter molecular radial distribution functions. Solute - solute radial distribution functions indicate that clustering of acetone molecules occurs at very low temperature, in contrast to DMSO molecules.

Hydrogen bond analysis indicates that DMSO forms more hydrogen bonds with water per molecule (2.0 and 1.8) than acetone (1.3 and 1.2) at both concentrations studied. At the same time, average number of water – water hydrogen bonds per water molecule is found to be higher in acetone solution, indicating stronger enhancement of water network in the presence of acetone molecules. On the other hand, DMSO molecules are likely to be incorporated in water network resulting in three dimensional DMSO-water complexes, as suggested by Vishnyakov et al[290]. In addition, statistics of DMSO – water hydrogen bonds points out to the fact that these complexes do exist regardless of the temperature range studied in this work. Water – water (despite having better correlations between water molecules as seen in water-water radial distribution

functions of aqueous acetone solutions) and water-solute interactions are kinetically found to be stronger in the DMSO mixtures as evidenced by the higher hydrogen bond lifetimes.

Computation of self diffusion coefficient, shown in Figure 3-22 and Figure 3-23, suggests a systematic decrease in diffusive motions of both solute and solvent. The difference between the two solutions is very subtle, implying that water dynamics play a major role in the dampening diffusive motions in the aqueous mixtures. Longer rotational correlation times are observed for the concentrated acetone solutions, indicating the presence of homogenous acetone-water chains in the mixture.

The present study reveals the quantitative and qualitative aspects of interactions that exist between amphiphile solutes like DMSO and acetone with water. Radial distribution analysis combined with hydrogen bonding calculation indicate existence of three dimensional DMSO-water complexes by which cryoprotective ability of DMSO molecules can be explained. Such complexes cannot exist in aqueous acetone solutions due to planarity of acetone molecule and lower hydrogen bonding number between acetone and water molecules. Occurrence of such three dimensional structures can trap more water molecules, thereby inhibiting water from nucleation and subsequent crystallisation. Stronger interactions of DMSO with water that are observed across a wide range of temperature have profound impact on medicinal applications as DMSO is widely used as a cryoprotectant. Stronger interactions of DMSO with water resulting in larger three dimensional complexes prevent water nucleation, prologue to crystallisation which is detrimental to cells and biological organs in freezing conditions.

Chapter 4

Molecular dynamics simulations of supercooled aqueous methanol and ethanol solutions

Structural and hydrogen bonding properties of aqueous ethanol and methanol solutions are described in this chapter.

4.1 INVESTIGATIONS OF AQUEOUS METHANOL AND ETHANOL SOLUTIONS

Over the years binary mixtures of water and alcohols instilled interests in researchers primarily due to their applications in areas like cryobiology[5]. Smaller alcohols like ethanol and methanol in aqueous phase are capable of interacting with membranes[340, 341], thereby preventing membrane damage during freezing. In addition, aqueous solutions of alcohols can form inert glassy matrix at low temperature[342], inhibiting crystallisation that damages the system under cryopreservation. To probe into these intriguing properties, aqueous methanol solutions have been investigated by various experimental[343-353] as well as computer simulation methods[341, 343, 354-366]. Aqueous mixtures of ethanol have also been studied in detail by different experimental techniques, including spectrospcopic,[345, 367, 368] scattering,[369, 370] dielectric[371-373] as well as molecular dynamics simulations[356, 357, 374-382].

Alcohols are also amphiphile in nature, containing both hydrophilic and hydrophobic groups. In aqueous solutions, amphiphile may either self aggregate[383] or participate in infinite network of water molecules through hydrogen bonding[384]. Addition of alcohol has a profound impact on the water structure by reducing density-density fluctuations that occurs in neat water over a wide range of temperatures[369]. At the same time, self aggregation induced by alcohol - alcohol affinity tends to increase as the size of the hydrophobic tail increases[344].

Computer simulations show that even at a low concentration, methanol tends to aggregate, which, known as hydrophobic interaction, is reflected in an increase of thermodynamic response function heat capacity[354]. Experimental investigations supported by computational studies suggest that within a particular concentration limit, χ=0.27–0.54, aqueous methanol solutions exhibit intriguing properties where thermodynamic and kinetic functions, namely compressibility, entropy, viscosity and diffusion coefficient, attain extreme values[343]. Water and methanol form concomitant self aggregates in their mixture within this concentration range: below χ=0.27 only water molecules are found to form aggregates, whereas above this threshold concentration, methanol forms self aggregates[343]. These simultaneous percolating networks of both components existing in the alcohol-water mixtures are accounted for ambiguous thermodynamic and diffusive properties.

Self aggregation of solutes, otherwise known as clustering, is found to predominantly exist in highly concentrated methanol solutions[385]. Molecular dynamics cluster analysis has revealed that methanol forms small and large clusters, ranging from 3 to 50 molecules per cluster[385], and the proportion of larger clusters was found to decrease with the increase in the number of clusters. Average lifetimes of the clusters were found to be of hundreds of picoseconds. It is important to note that lifetimes of larger methanol clusters are higher than the three or four member clusters. Interestingly, the cluster analysis of methanol rich solution indicates the existence of water clusters solvated by the hydrophobic tail of methanol molecules. In addition, water-water clustering at high water concentration has been experimentally observed by Redlin etal[386].

It has been found that even in methanol rich solution, long range water-water interactions can exist, which may lead to feeble percolated networks of water[358], along with the linear chain of methanol-water networks. On the other hand, structural enhancement in water (tetrahedral arrangement) is naturally retained in water-rich solution[387]. This underlines the impact of concentration on the qualitative nature of percolating networks in the mixture. Notwithstanding some disagreements, it has been suggested that iceberg structures, due to water enhancement, is found to be in water-rich alcohol mixtures[388].

Both water and methanol molecules are capable of forming hydrogen bonds in their pure state[198, 389]. Number of hydrogen bonds in aqueous solutions is higher than pure methanol but lower than pure water[390]. Upon mixing, the hydrogen bond network among the pure components (alcohol and water) is broken, in concomitant with the formation of water – methanol hydrogen bonds[390]. It has been suggested that hydrogen bonds between water and alcohols are responsible for complete miscibility of alcohols with water at any proportion in wide range of temperatures. Molecular dynamics simulation reveals that hydrogen bonding between water and alcohol hydroxyl group has longer lifetimes than that of water –water hydrogen bonds[292], indicating stronger inter molecular interaction existing in the mixture. Hydrogen bonding interaction of methanol with water is also prominent in the mixtures in very dilute solutions. This has been marked with a decrease in diffusion coefficient of water molecules around χ=0.25[345].

Hydrogen bonding also influences the solvation properties of ethanol, the next higher homologue of methanol. Radial distribution analysis shows pronounced peaks in the intermolecular pair distribution functions of water and hydroxyl group of ethanol, a signature of strong hydrogen bonding between the solute and the solvent[374]. Nuclear Magnetic Resonance (NMR) experiments indicate that both hydroxyl oxygen and hydrogen atoms in ethanol participate in hydrogen bonding[391]. Upon dilution average number of hydrogen bonds per ethanol is found to be increasing, from 1.65 to 2.23, at the expense of decreased number of water-water hydrogen bonds[392]. It has been suggested that there may exist four types of hydrogen bonds in the ethanol-water mixtures - between two water molecules and two ethanol molecules; in addition ethanol incorporated hydrogen bonded water network as well as water incorporated hydrogen bonded ethanol network are observed in the mixtures[391].

Hydrogen bonding in the binary mixtures of water and alcohols in general have been found to be dependent extensively on the concentration, viz. extreme (either water or alcohol rich) and intermediate regions[393]. At molar concentration of alcohol below 0.2, considered as the water rich region, structure making on water is observed[367]. Even at this concentration, ethanol molecules are incorporated into the water network as suggested by the density functional based Car Parinello molecular dynamics simulation studies[374]. The highest number of water-water hydrogen bonds is naturally found in this

concentration region, below 0.2[392]. At molar concentration around 0.3, a minimum in self diffusion coefficients is observed[376], which has been attributed to the formation of clathrate like hydrates.

As alcohol molecules become more numerous, preponderance of alcohol-water hydrogen bonds is naturally observed in the mixture, which results an increase in heat of hydration of ethanol at infinite dilution. At very high alcohol concentrations, χ>0.8, the mixture exhibits an intriguing phenomenon - water molecules are accommodated between alcohol molecules, establishing entropy favoured alcohol-water-alcohol network. This inevitably minimize the chances of formation of water-water network in the solution[367]. At higher concentration, ethanol, like other monohydric alcohols, exhibits self aggregation where polar hydroxyl groups point towards the interior of the cluster, while the non polar part oriented towards exterior[375].

In order to elucidate the effect of low temperatures on water-alcohol mixtures, several studies have been conducted[394, 395]. Kanno et al has reported supercooling enhancement of alcohols, deriving a relationship between the number of hydroxyl group in a compound and nucleation temperature, the temperature below which water is supposedly to be nucleating prior to crystallisation[394]. Inhibition of ice formation and ensuing crystallisation is achieved with the substitution of the hydroxyl groups of alcohols since more hydrogen bonds can be formed between water and alcohols at the expense of water-water hydrogen bonds.

Recently Stanley et al have investigated the properties of methanol solutions for a wide range of temperatures using Nuclear Magnetic Resonance (NMR) technique[395]. Spin lattice relaxation times derived from the NMR provides shorter relaxation times than pure water and methanol at ambient temperatures, indicating that interaction between them is stronger in the solution. This effect is more pronounced around hydroxyl group, suggestive of stronger hydrogen bonds between alcohol and water molecules. At lower temperature below 265K, it is interesting to note that hydrogen bond network between hydroxyl group and water molecules be stabilized, resulting in an exclusion of methyl groups from the network. This forces methyl group to form aggregates as in the case of pure methanol[395]. At further lower temperature, around 245K, the difference in rotational and translation movements of functional groups in the solution do not make

any significant deviation from pure solvents. This clearly indicates that a structural reorganisation is taking place as temperature decreases- from stable water-alcohol network at room temperature to two distinct clusters of water and methanol in the mixture. Molecular dynamics simulations and neutron diffraction studies also reflect the existence of two distinct clusters upon cooling, with an increase in the size of the clusters[396]. On the other hand, an opposite trend is observed in the case of aqueous ethanol solution. It has been reported that addition of ethanol to water in the supercooled region decreases the density fluctuation, a phenomenon that occurs as a result of coexistence of intact and weakly bound hydrogen bond networks[369]. This may suggest that ethanol-water complexes are more in number in aqueous mixtures than homogenous clusters of water or ethyl alcohols.

In spite of the significant research into the nature of monohydric alcohol-water mixtures at ambient conditions, there is very little known about their structural properties at sub zero temperatures. An atomistic understanding of the interactions that play a major role in these mixtures is expected to improve our understanding of the interactions that underpin their applications as cryoprotectants. Molecular dynamics simulations of aqueous ethanol and methanol solutions at two different concentrations (9 and 23 w/w % in water) are performed and described in detail. Extensive analysis has been carried out, aimed at providing molecular level interpretation of structure and dynamics of these mixtures.

4.2. SIMULATION PROTOCOL

Classical molecular simulations in the NVT and NPT ensembles have been performed for a wide range of temperatures. The simulations utilized well known potentials for water (TIP4P)[207], and methanol and ethanol (All Atom OPLS)[322], in accordance with the simulations of aqueous DMSO and acetone solutions described in the previous chapter. The exact simulation protocol described in the chapter three is also followed in the simulations. Ethanol and methanol with 9% and 23% by weight in water are only considered for the simulations described in this chapter due to toxicity effects of highly concentrated alcohol solutions in cryopreservation.

4.3. RESULTS AND DISCUSSIONS

In this section, extensive analysis of structural and dynamic properties of aqueous solutions of methanol and ethanol in a wide range of temperatures – from 230 K to 300K, is described. The structural properties will be discussed first, followed by hydrogen bonding and finally rotational and translational dynamics. Instead of presenting density analysis of the mixtures as described in chapter three, a more successful annealing method which can explain the glass transition in aqueous solutions will be described in the next chapter in detail.

4.3.1. Water structure

Figures from Figure 4-1 to Figure 4-3 show the solvent – solvent radial distribution functions of 23% aqueous methanol and ethanol solutions. Systems of lower concentrations were not considered for radial distribution analysis due to their resemblance of pure water. Heights of the peaks are found to be higher in all the solvent-solvent RDFs of the two mixtures compared to pure water (see previous chapter). Since the heights and widths of the two systems investigated are almost identical, no structural differences between these systems can be deduced from the water-water radial distribution functions. Second peaks observed at around 4.5 Å in oxygen - hydrogen (Figure 4-3) and hydrogen – hydrogen (Figure 4-1) radial distribution functions are also found to be unaltered compared to those of pure water. It is interesting to see that at lower temperature there exists a sharper peak at 4.5 Å. In a previous study using empirical potential structure refinement (EPSR), this has been identified as a promotion of tetrahedral structure by water[396]. Average number of neighbour water molecules from a reference water molecule, quantified by the computed coordination numbers, reads for aqueous methanol solutions as 3.76 at 300K, 3.58 at 270K and 3.54 at 240K. The corresponding numbers for the ethanol mixtures are 3.917 (300K), 3.7925 (270 K) and 3.64 (240K). This suggests that water structure in aqueous methanol solution is more perturbed than in ethanol solution. Nevertheless it can be seen that temperature has a more profound impact on aqueous ethanol solutions than on methanol solutions in perturbing water structure. The coordination numbers corresponding to both systems indicate the deviation from tetrahedral network of water molecules, as mentioned in the previous chapter.

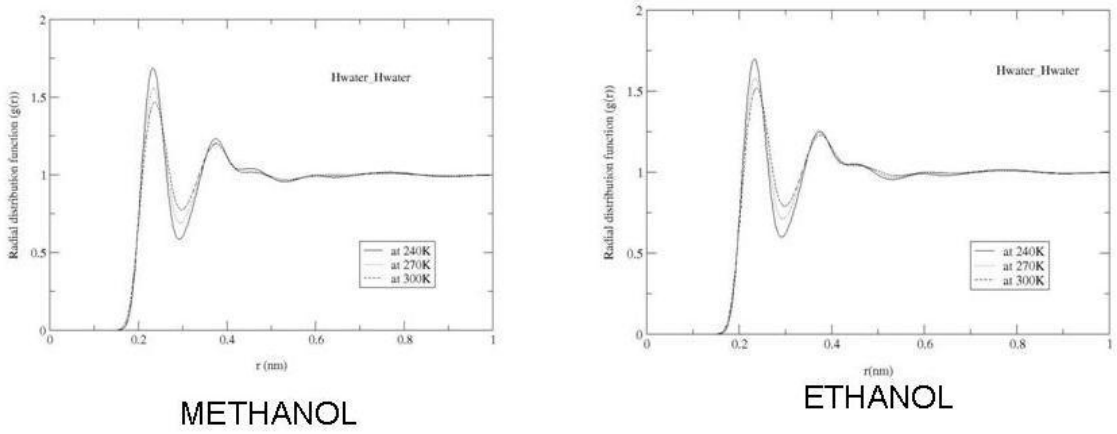

Figure 4-1 *Hydrogen-Hydrogen Radial distribution functions of 23% of aqueous methanol and ethanol solution*

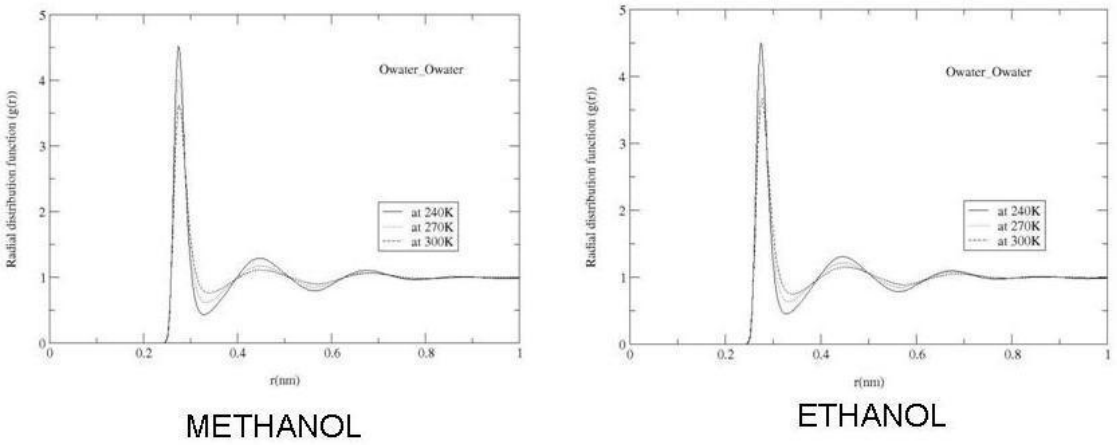

Figure 4-2 *Oxygen-Oxygen radial distribution function of 23% of aqueous methanol and ethanol solutions*

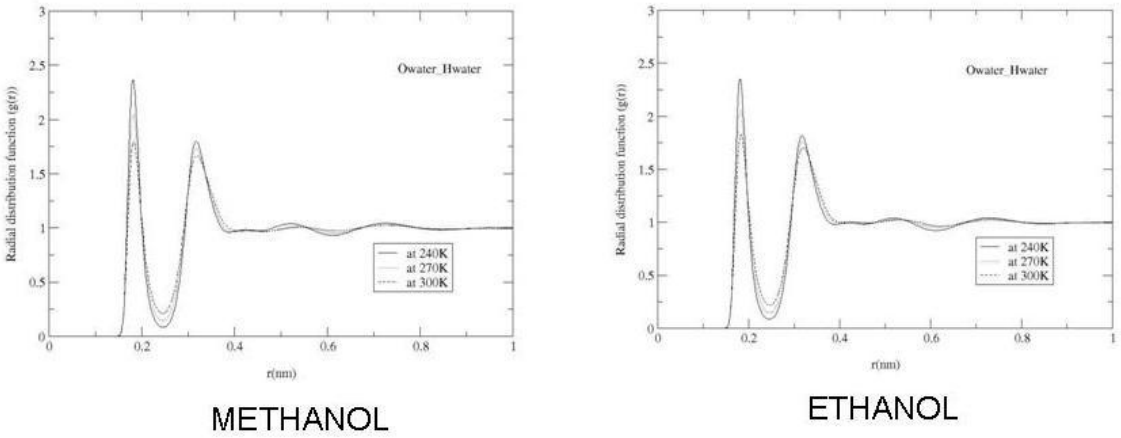

Figure 4-3 *Oxygen-Hydrogen radial distribution function of 23% aqueous methanol and ethanol solutions*

4.3.2. Solute-Solvent structure

The hydration structure around the solutes was examined by various alcohol-water intermolecular pair correlation functions. Hydroxyl-water oxygen correlation functions of methanol and ethanol aqueous solutions (23% w/w) are shown in Figure 4-4. A peak corresponding to first coordination shell is higher more pronounced in aqueous ethanol solution, indicating structuring around hydroxyl group. The corresponding peak in the hydroxyl – oxygen radial distribution function in methanol solution is located at the same distance as that of previously reported simulations using MCY/ST2 potentials[360]. However, subsequent peaks seem to be less sharp, and lie farther from the RDF. A general trend can be deduced in the case of both systems is that as temperature decreases structuring around hydroxyl groups increases**.** Hydroxyl - water hydrogen intermolecular radial distribution functions, shown in Figure 4-5, also indicate a higher structuring of water around hydroxyl group, as evidenced by sharper peaks, in both mixtures. A well defined third peak can be found at around 5 Å, contrary to a previous molecular dynamics simulation of aqueous ethanol solution[374]. This peak is sharper in the aqueous methanol solution, suggestive of higher long range structure.

Methyl - water oxygen radial distribution functions of both methanol and ethanol solutions are shown in Figure 4-6. Structuring of water molecules around hydrophobic methyl group in aqueous methanol solution is evident by a peak around 3.5Å, in close agreement with simulations of aqueous methanol solutions performed using MCY-OPLS potential combinations[360]. The height of the peak however is found to be attenuated in comparison to previously reported molecular dynamics simulations using united Atom OPLS – TIP4P combination[356]. Methyl- water oxygen first hydration shell in aqueous ethanol solutions is different in terms of the location and number of peaks compared to methanol: the peak is found to be shifted to 4Å, accompanied by a small shoulder at 5Å, which closely resembles the results of *ab initio* simulations[374]. It has to be noted that in a previous simulation using united atom OPLS-TIP4P potential combination this feature has not been reported[356]. From Figure 4-6, it can be seen that

first peak in methanol solution has higher intensity than that of ethanol mixture, indicating that enhancement of water structure around methyl group.

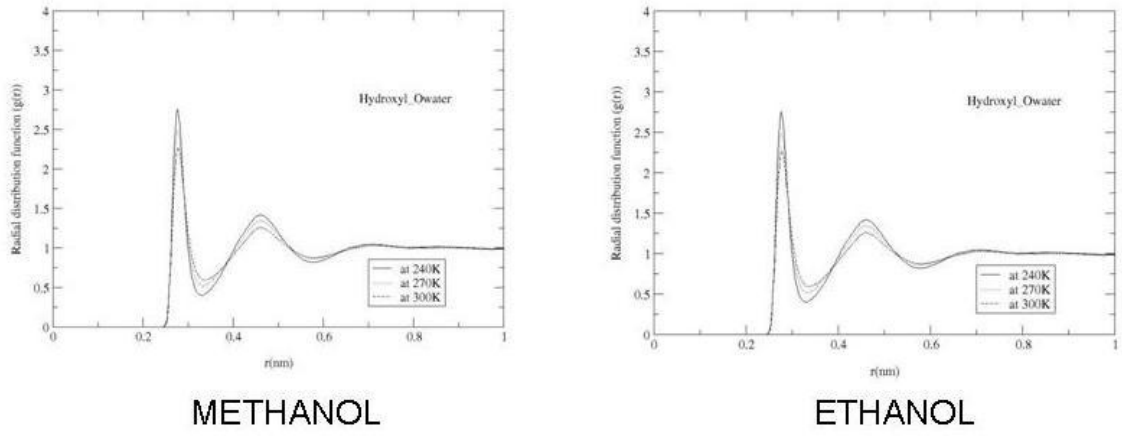

Figure 4-4 *Hydroxyl-water Oxygen radial distribution functions of 23% aqueous methanol and ethanol solutions*

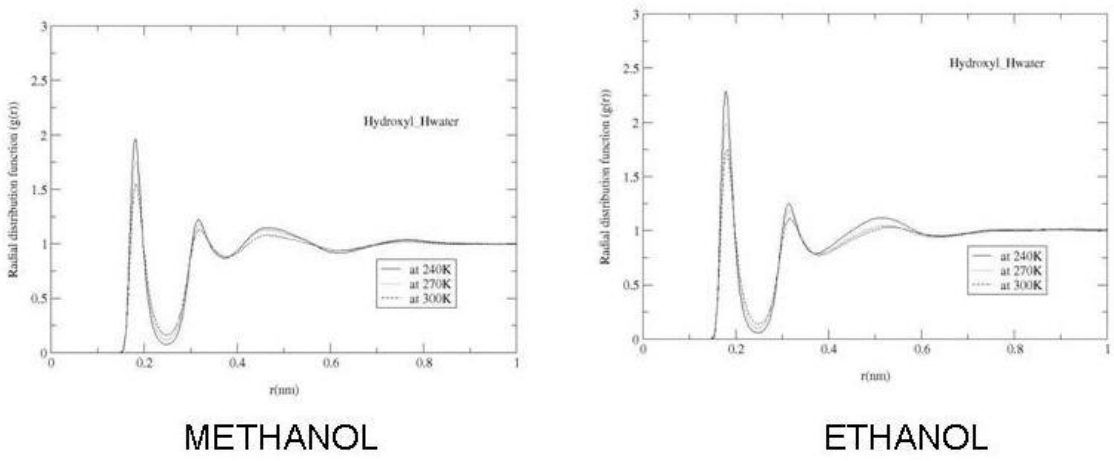

Figure 4-5 *Hydroxyl – water Hydrogen radial distribution function of 23% aqueous methanol and ethanol solutions*

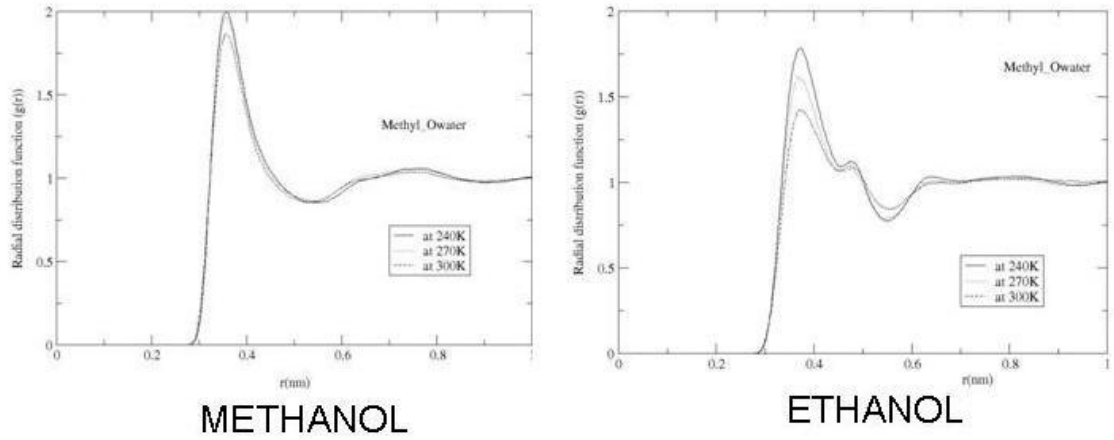

Figure 4-6 *Methyl – water Oxygen radial distribution function of 23% aqueous methanol and ethanol solutions*

Figure 4-7 depict methyl – water hydrogen pair correlation function of both the systems simulated. A small peak at 2.5 Å followed by a broad peak around 4Å of higher intensity can be identified from the radial distribution function of methanol solution, with sharpening of peaks upon decrease in the temperature. On the contrary, the radial distribution function of ethanol solution bears little resemblance to this; a broadened peak is observed between 3 - 4 Å. Thus, a structure enhancement of water molecules around the methyl group in methanol, as opposed to weakly bound water molecules to the hydrophobic part in ethanol, can be inferred from methyl-water radial distribution functions.

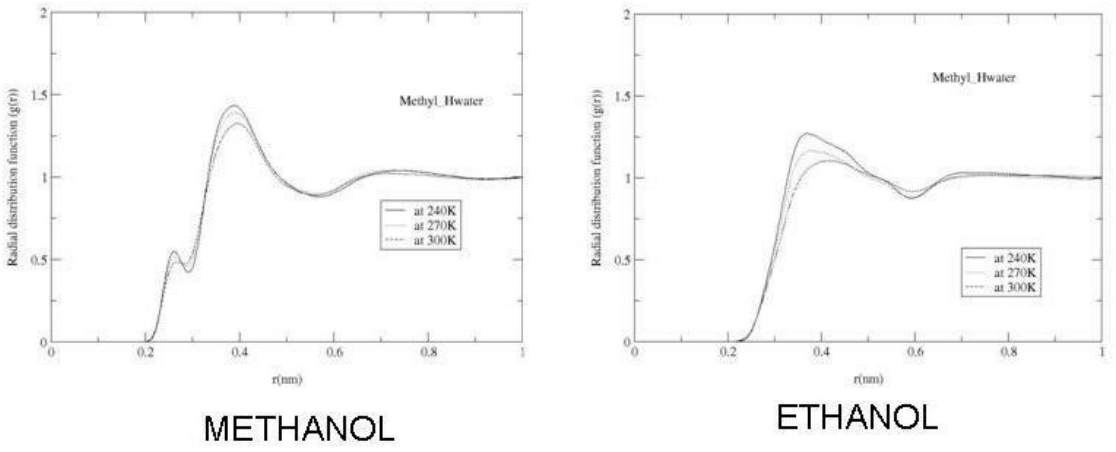

Figure 4-7 *Methyl- water Hydrogen radial distribution functions of 23% aqueous methanol and ethanol solutions*

The alcohol methyl-water radial distribution functions reveal a contrasting solution structure in the two alcohol systems studied. Multiple peaks of lower intensity are observed in the methyl – water oxygen RDFs in the ethanol mixture, similar to the findings of Meijer et al[374], as opposed to a single sharper peak in methanol solution. This implies that that orientation of methyl hydrogen atoms towards water oxygen is more pronounced in methanol solutions. Strong methyl- water hydrogen interactions as characterised by two peaks within 4Å in the methyl- water hydrogen pair correlation function in aqueous methanol solution suggests hydrophobic hydration of water molecules around methanol methyl groups. Weaker peaks resulting from the corresponding pair correlation function rule out such an arrangement in aqueous

ethanol solutions. A molecular level explanation can be given as to why ethanol methyl is moderately hydrated by water: the methyl group which has proximal hydroxyl group in ethanol are not the same as that of methanol, the one that has the hydroxyl group in ethanol is sandwiched between the hydroxyl and the terminal methyl group, having a reduced surface area but being more difficult for water to hydrophobically hydrate.

4.3.4. Solute-Solute structure

Self interaction of solutes can be measured by solute – solute radial distribution functions, viz methyl-methyl, methyl-hydroxyl and hydroxyl-hydroxyl pair distribution functions. Figure 4-8 shows methyl – methyl pair correlation functions of aqueous methanol and ethyl-ethyl pair correlational functions of ethanol solutions. Two distinct peaks, at 4 Å and 7 Å, are observed in the pair correlation functions of methanol solution. It is clear from the plot that temperature does not make any significant impact on the solute-solute structure in methanol. On the other hand, two peaks centred at 4 Å and 5 Å (due to methylene group sandwiched between methyl and hydroxyl groups in ethanol), is found in the corresponding pair correlation function of aqueous ethanol solution. Furthermore, temperature is not found to play a key role in shaping the rdfs in the methanol solutions, whereas methyl- methyl association in ethanol solution exhibits a sharp decrease at 240K, indicated by lower height of the peaks.

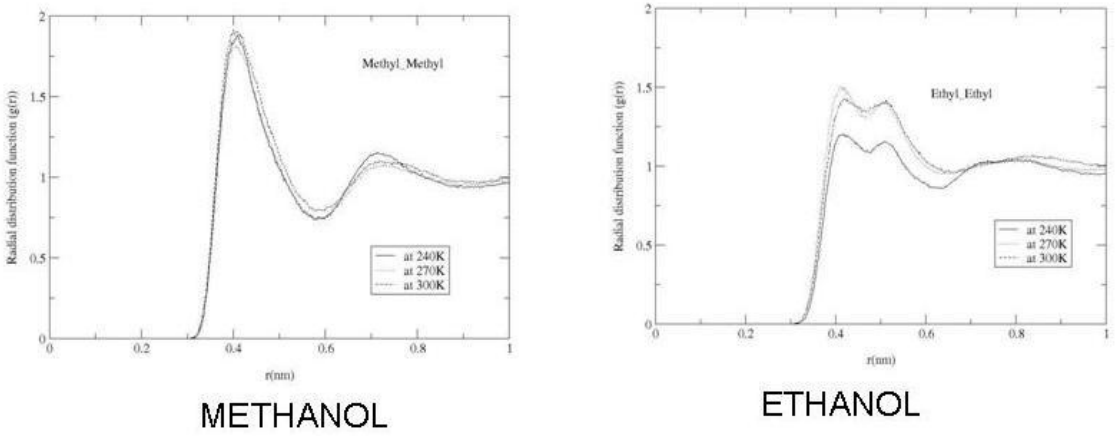

Figure 4-8 *Methyl-Methyl radial distribution function of 23% aqueous methanol and Ethyl-Ethyl radial distribution functions of 23% aqueous ethanol solutions*

Two contradictory observations have been reported regarding the solute structure of aqueous methanol solutions in the literature: methyl- methyl pair correlation functions

shown by Allison et al suggest that methyl- methyl correlation is weaker, indicated by a broad peak around 4Å in a highly concentrated methanol solution (methanol and water in 7:3 ratio)[385]; on the contrary, the neutron diffraction as well as molecular dynamics studies conducted by Soper et al at a comparable concentration has observed rather sharp peak centred at 4Å[343, 390]. This has been attributed to the fact that methanol molecules tend to be squeezed by water molecules[343]. A recent neutron scattering study of aqueous butanol solutions by Finney et al[397] has suggested that this structuring of water around the alcohols in general varies with temperature: there appears a temperature maximum, at which water is increasingly excluded from the vicinity of solute-aggregates, and after which water begins to penetrate through the alcohol clusters leading to the breaking of alcohol-alcohol aggregates.

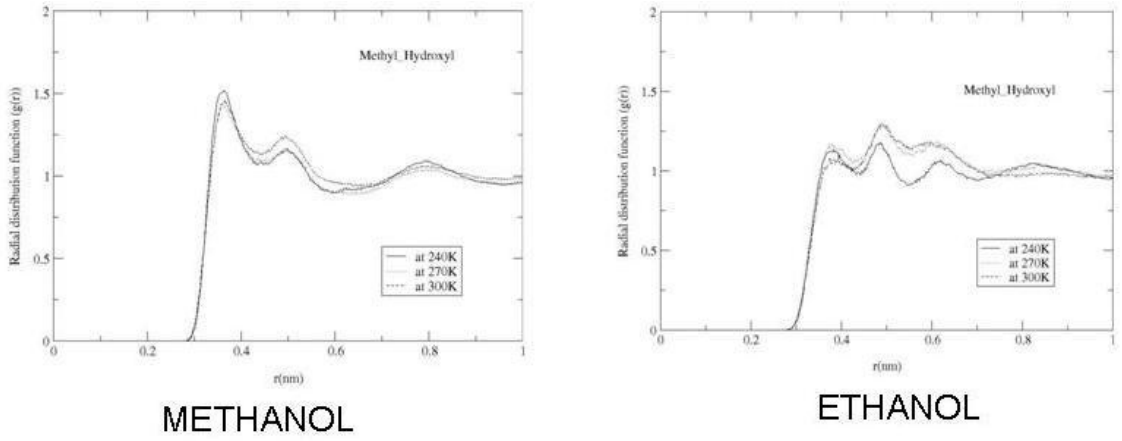

Figure 4-9 *Methyl-hydroxyl radial distribution function of 23% aqueous methanol and ethanol solutions*

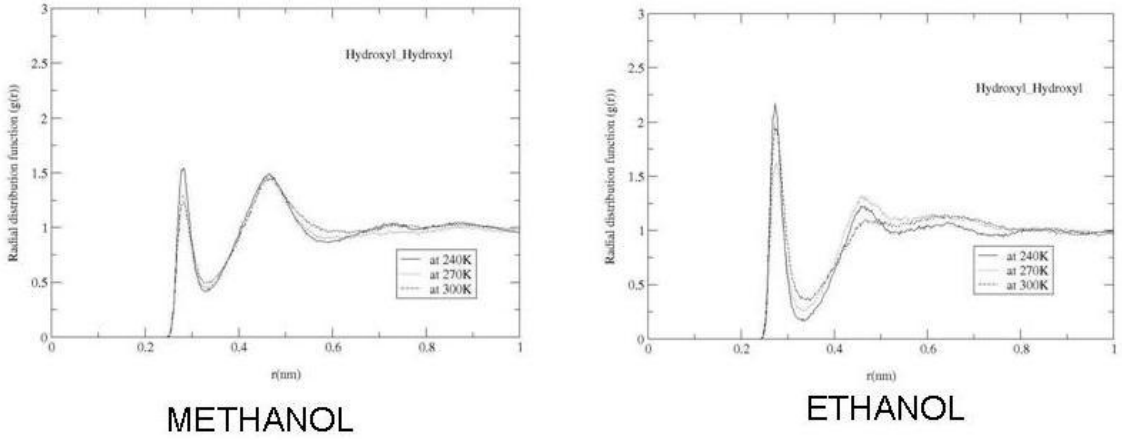

Figure 4-10 *Hydroxyl-Hydroxyl radial distribution function of 23% aqueous methanol and ethanol solutions*

Figure 4-9 depicts methyl-hydroxyl radial distribution functions of aqueous methanol and ethanol solutions. Since a preferential interaction between a hydrophobic methyl and hydrophilic hydroxyl group in alcohol is not likely to happen, the peaks seen in the figure may be attributed to the self aggregation of solute molecules (alcohol) where the hydroxyl groups happen to end up in relative close proximity to methyl groups. Such interactions are found to play a larger role in aqueous methanol solutions as characterised by sharper first peak. Shown in Figure 4-10 is hydroxyl- hydroxyl RDFs of both ethanol and methanol solutions. In aqueous ethanol solution, the RDF is found to be sharpened at lower temperature region than in methanol-water mixture, indicating alcohol-alcohol interactions that exist in the solution. The interactions cannot not be attributed to either alcohol-alcohol hydrogen bonding or proximity of alcohol groups with respect to each other (due to self aggregation of alcohols in water) since both these effects are dominant in aqueous methanol solutions than in ethanol solutions (A comparison of hydrogen bond statistics between aqueous ethanol and methanol solutions is followed after this section). A plausible explanation for this enhanced hydroxyl - hydroxyl peaks in ethanol solutions is the existence of ethanol-water hydrogen bonded random networks as proposed by Mizuno et al[391]. According to this model ethanol and water can be randomly connected by hydrogen bonds. A second peak in hydroxyl-hydroxyl radial distribution function (Figure 4-10) can be seen at 5Å in both solutions, but more evident in aqueous methanol solutions. The first peak in methanol solutions is found to be strengthened upon decrease in temperature, while the second peak remains to be undiminished. This suggests that upon decrease in temperature hydroxyl groups remain to be clustered, and methyl groups do not push the hydroxyl group apart as observed in the case of dilution of pure methanol by water [390].

Radial distribution analysis, as shown from Figure 4-1 to Figure 4-3, reveals an enhancement of water structure in the presence of methanol and ethanol molecules. This result contradicts with previous computer simulations carried out at 298 K by Fidler et al[356] and neutron diffraction experiments[350] that water structure is only moderately affected by presence of alcohol molecules and that any change in water structure due to hydration effect affects only very small percentage of water molecules in the system. Nevertheless, the result obtained in this study is in close agreement with a recently employed Empirical Potential Structure Refinement (EPSR) analysis[396]. The simulation results by Fidler et al[356] seem to be very surprising, considering the fact that

the simulation reported by Fidler[356] and the present work employ same potential combination, OPLS/TIP4P. However, one can see that the data reported in reference[356] were from a total run of only 40-50 pico seconds, and require better sampling.

Methyl-water intermolecular radial distribution functions, shown in Figure 4-4 - Figure 4-7, clearly indicate that hydroxyl of water orients towards methyl group in methanol and ethanol, whereas orientation of water hydrogen towards methyl group can be observed only in methanol solutions. This implies that a preferential conformation, methyl groups facing water oxygen, exists in the case of ethanol solutions. By contrast, interactions of methyl group with both water oxygen and hydrogen are prominent in methanol solutions, echoing neutron diffraction experiments indicating that water forms a distorted cage, connected by loose hydrogen bonds, around the methyl groups of methanol[350].

All three solute-solute radial distribution functions, in particular methyl-methyl radial distribution function, suggest a stronger correlation between methanol molecules in the mixture. This has been attributed to methanol-water segregation existing in the solutions in almost any proportion[348]. On the other hand, it can be seen from the ethyl-ethyl radial distribution functions ethyl – ethyl correlation does not occur in aqueous ethanol solution compared to methanol in water. Weaker alcohol – alcohol association found in aqueous ethanol solutions is in good agreement with Small Angle X-ray Scattering (SAXS) experiments[370], but not with Kirkwood-Buff integral analysis suggesting that alcohol-alcohol association increases as the size of the non polar part (alkyl part) increases[344].

Addition of small alcohols including ethanol and methanol to water sees only a moderate increase in entropy of the system than expected for ideal solutions. This is primarily due to the cohesion of hydrophobic head groups in water[390]. This cohesion, alternatively known as alcohol-alcohol association, has been experimentally detected; a infra red spectral analysis indicates that transition from alcohol monomer to micelles (alcohol-alcohol clusters) is accompanied by large shifts (approximately $10cm^{-1}$) in alkyl stretching bands[346].

4.3.4. Hydrogen bonding analysis

Radial distribution function analysis, despite its usefulness, does not reveal complete structural features of the aqueous mixtures. Hydrogen bonding properties have been thoroughly investigated in order to obtain further structural characteristics. In this section, a quantitative estimate of hydrogen bonding between various components in the mixture, their life times, and distribution of bond angle and distance are described.

4.3.4.1 Hydrogen bonding statistics

Figure 4- 11 shows the total number of hydrogen bonds formed between solute and solvent in the aqueous alcohol solution as a function of temperature. The number of hydrogen bonds between solute and solvent in ethanol solutions is always higher than that of aqueous methanol solutions, as figure indicates. In addition, the figure reveals that upon increase in the concentration, the solute-solvent hydrogen bonds decrease in both systems. As expected, the number of hydrogen bonds decreases upon increase in temperature. Thus the data clearly indicates stronger interaction between ethanol and water in aqueous mixtures.

In Figure 4- 12, number of water – water hydrogen bonds in aqueous methanol and ethanol solutions is shown. As the plot suggests, water-water hydrogen bonds are found to be the highest and the lowest in pure water and concentrated methanol solutions respectively. Comparing the two alcohol systems, it can be seen that increasing the concentration of alcohol solution further decreases the number of water-water hydrogen bonds in the mixtures, and water- water hydrogen bonds are more abundant in the aqueous ethanol solutions. This gives strong evidence that water structure is more perturbed in the presence of methanol, and this effect is considerably evident upon increase in concentration of methanol.

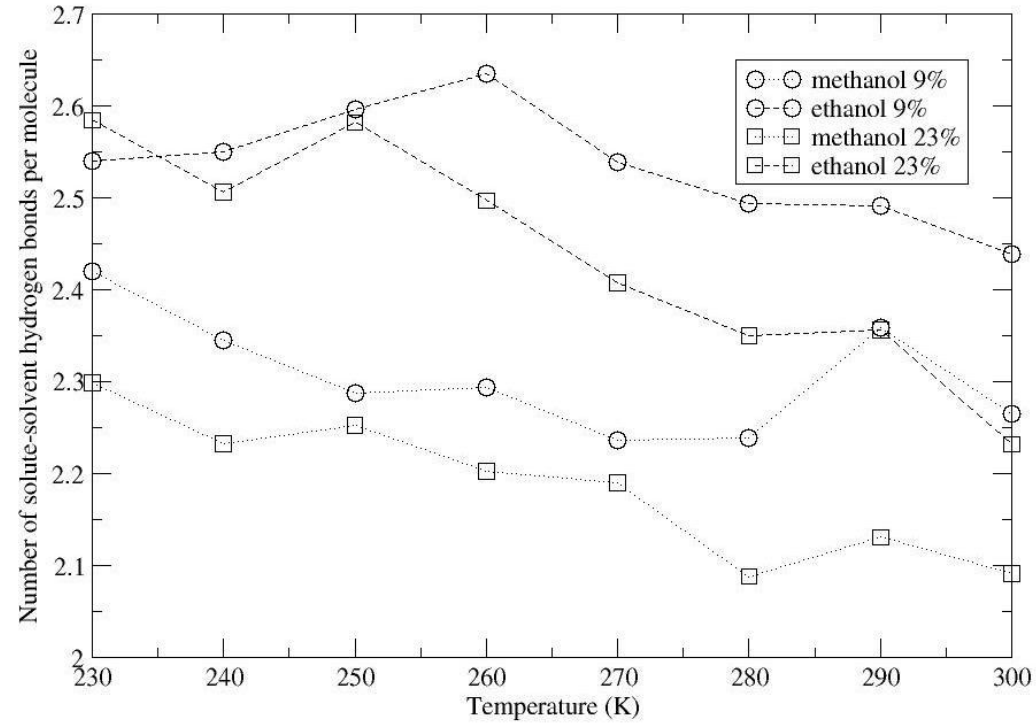

Figure 4- 11 *Average number of solute-solvent hydrogen bonds in aqueous methanol and ethanol solutions*

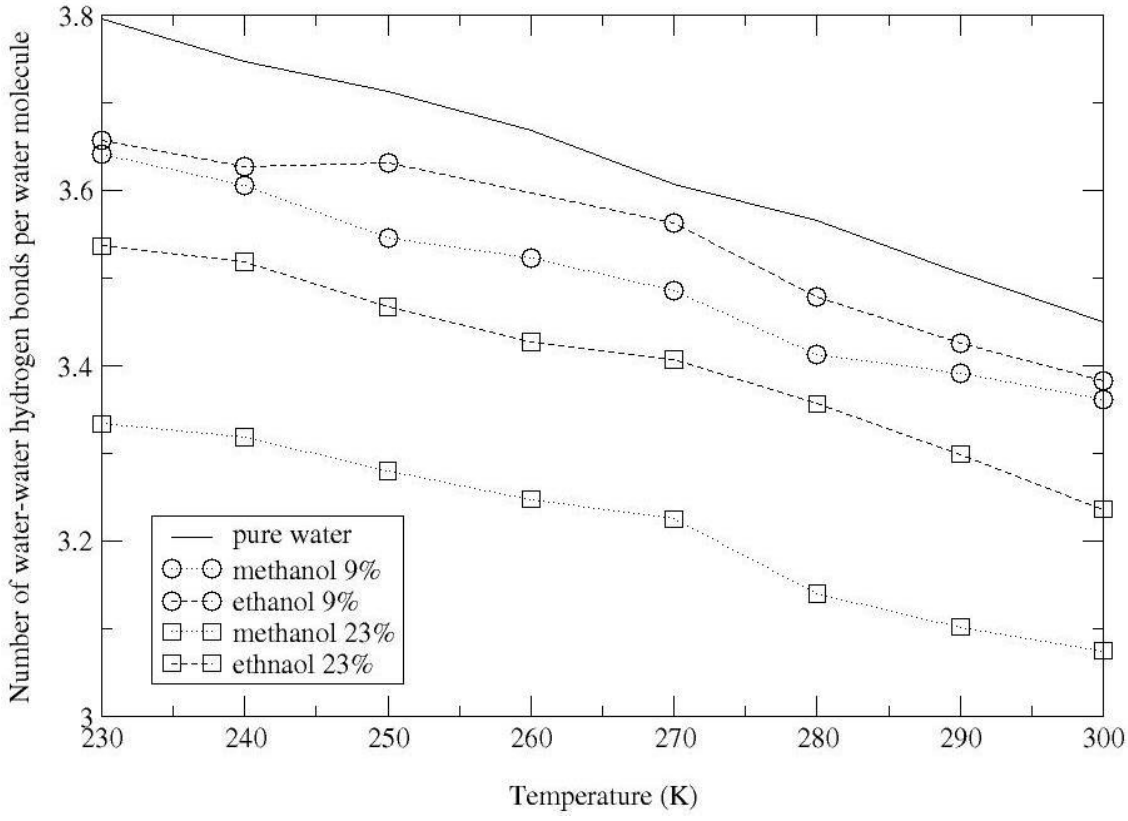

Figure 4- 12 *Average number of solvent-solvent hydrogen bonds in aqueous methanol and ethanol solutions*

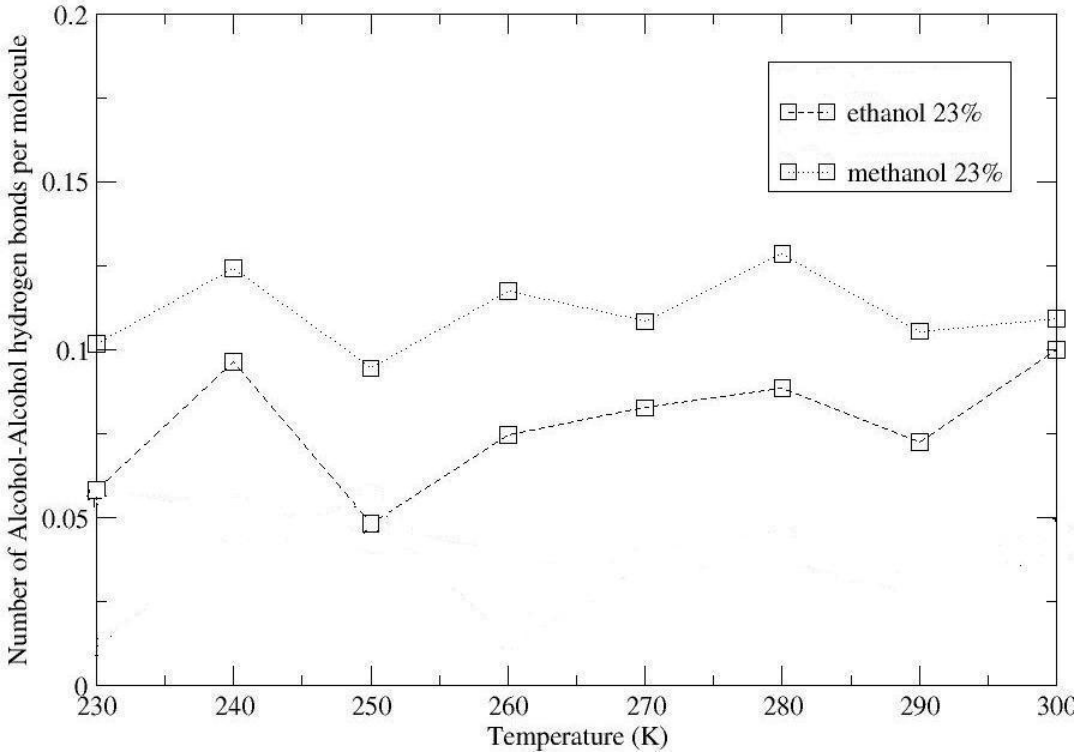

Figure 4-13 *Average number of alcohol-alcohol bonds in the aqueous methanol and ethanol solutions*

Figure 4-13 shows the number of alcohol-alcohol hydrogen bonds found in the concentrated ethanol and methanol solutions. Statistics for lower concentrations was not shown because of the insignificant number of hydrogen bonds found in respective solutions. The data shows that the number of alcohol-alcohol hydrogen bonds is negligible compared to water-water, and water – alcohol hydrogen bonds discussed previously. Higher number of solute-solute hydrogen bonds is formed in the concentrated methanol solution, which could, in part, suggest higher self association between methanol molecules. The number of alcohol-alcohol H-bonds is lower than that of a highly concentrated methanol solution reported by Soper et al[390]. They observed that 1.2 hydrogen bonds are formed among methanol molecules in 7:3 methanol-water binary mixtures (~81%)[390].

4.3.4.2. Hydrogen bond dynamics

In order to investigate the stability of three types of hydrogen bonds previously discussed, their hydrogen bond life times are computed. Figure 4-14 shows solute-solvent hydrogen bond life times in the aqueous solutions. At room temperature region (290K to 300K) the differences in the life times are relatively small. But as temperature decreases, hydrogen bond lifetime in concentrated (23%) ethanol solution increases significantly - from around 5 ps at 300 to >100 ps at 230K. On the other hand, the difference in life times of solute-solvent hydrogen bonds in dilute and concentrated methanol solutions is negligibly small for a wide temperature region, from 300K to 240K. It is interesting to note that solute – solvent hydrogen bond life times in dilute ethanol solutions are higher than both methanol systems within the temperature range. The data reveals that ethanol- water hydrogen bond is stronger than corresponding hydrogen bonds in the aqueous methanol mixtures. Interestingly the alcohols systems investigated here have higher solute-solvent hydrogen bonding lifetimes than acetone and DMSO, described in the previous chapter.

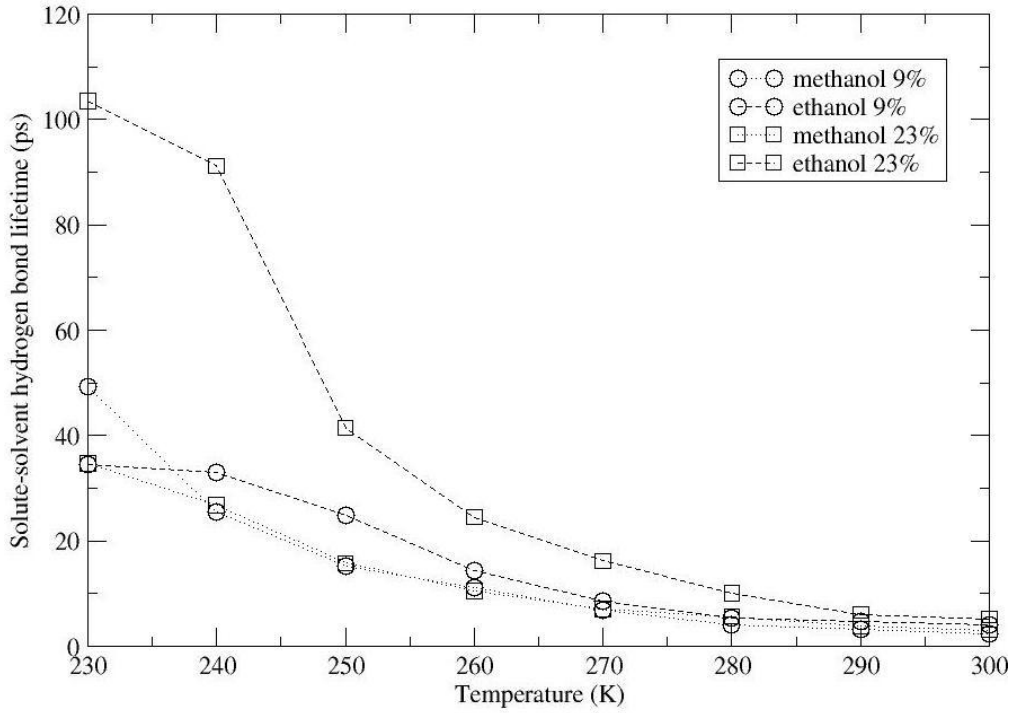

Figure 4-14 *Solute-Solvent hydrogen bond life times in aqueous methanol and ethanol solutions*

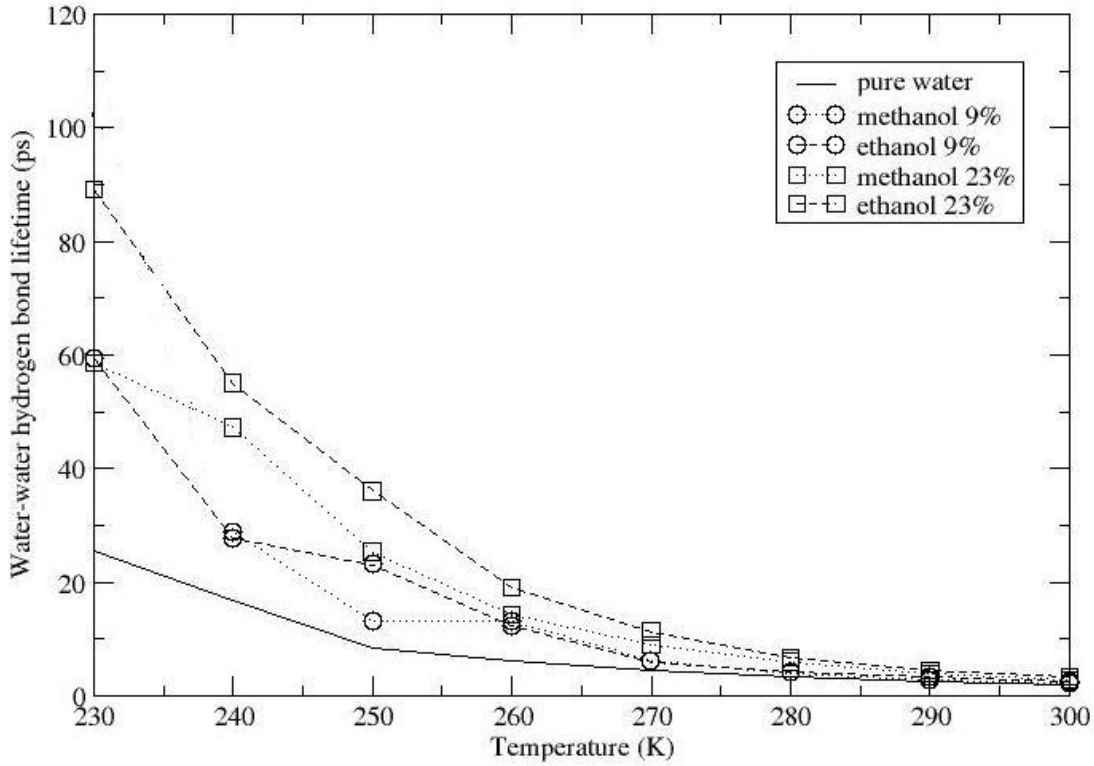

Figure 4-15 *Solvent-Solvent hydrogen bond lifetimes in aqueous ethanol and methanol solutions*

Solvent – solvent hydrogen bond lifetimes in the aqueous systems are shown in Figure 4-15. As seen in the figure, the lifetimes begin to diverge much at lower temperatures, while the magnitude of the difference between the systems is very small at higher temperature. The data clearly indicates that the lifetimes of solvent - solvent hydrogen bonds in aqueous solutions are much higher than that of pure water, which has values in the range of 2 to 25 ps for the whole temperature range investigated. Lifetimes of ethanol and methanol solutions have higher values as well than aqueous DMSO and acetone solutions, as in the case of solute-solvent hydrogen bond lifetimes.

Figure 4-16 shows hydrogen bond lifetimes between solute molecules (alcohols). It can be seen that ethanol-ethanol hydrogen bond lifetimes are found to be higher than that of in aqueous methanol solutions and this trend is more apparent in the supercooling temperature of pure water. The notable difference between aqueous ethanol and methanol solutions is that hydrogen bond lifetimes increase with increase in ethanol concentration, whereas decrease in lifetimes upon increase in concentration is observed in aqueous methanol solutions.

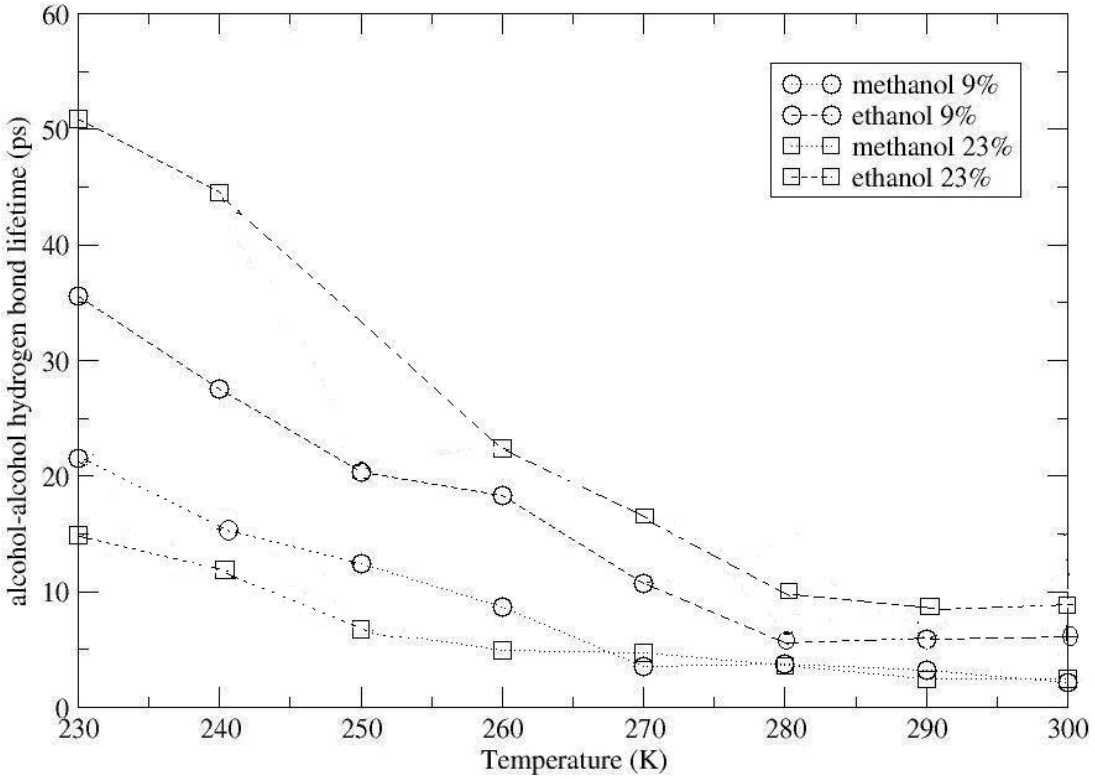

Figure 4-16 *Alcohol-alcohol hydrogen bond lifetime in aqueous methanol and ethanol aqueous solutions*

4.3.4.3. Hydrogen bond angle

Solvent- Solvent hydrogen bond angle distributions of the two systems investigated are shown in figures Figure 4-17 to Figure 4-20. As observed in the cases of aqueous acetone and DMSO solutions (see previous chapter), as temperature decreases, a larger number of hydrogen bonds become linear, evident from shift of the distribution peak towards smaller angle. Change in concentration does not seem to affect this trend in either system.

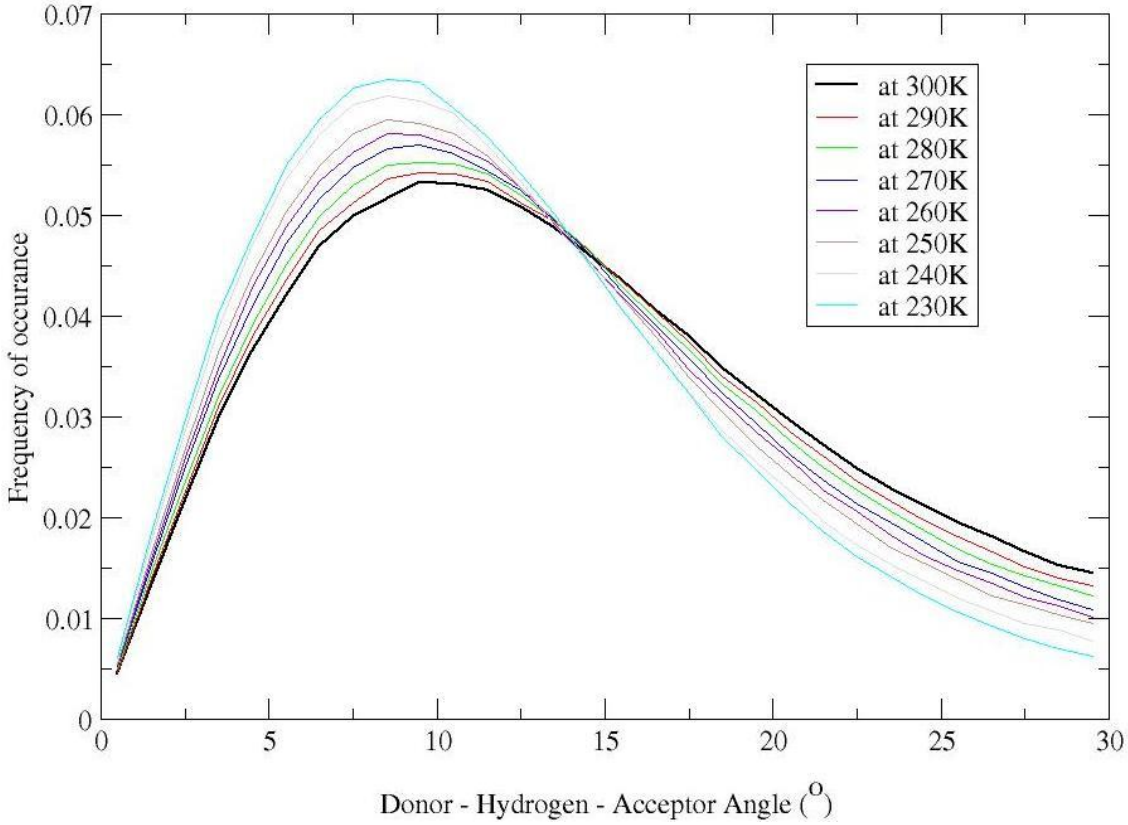

Figure 4-17 *Hydrogen bond angle distribution of 9% aqueous methanol solution*

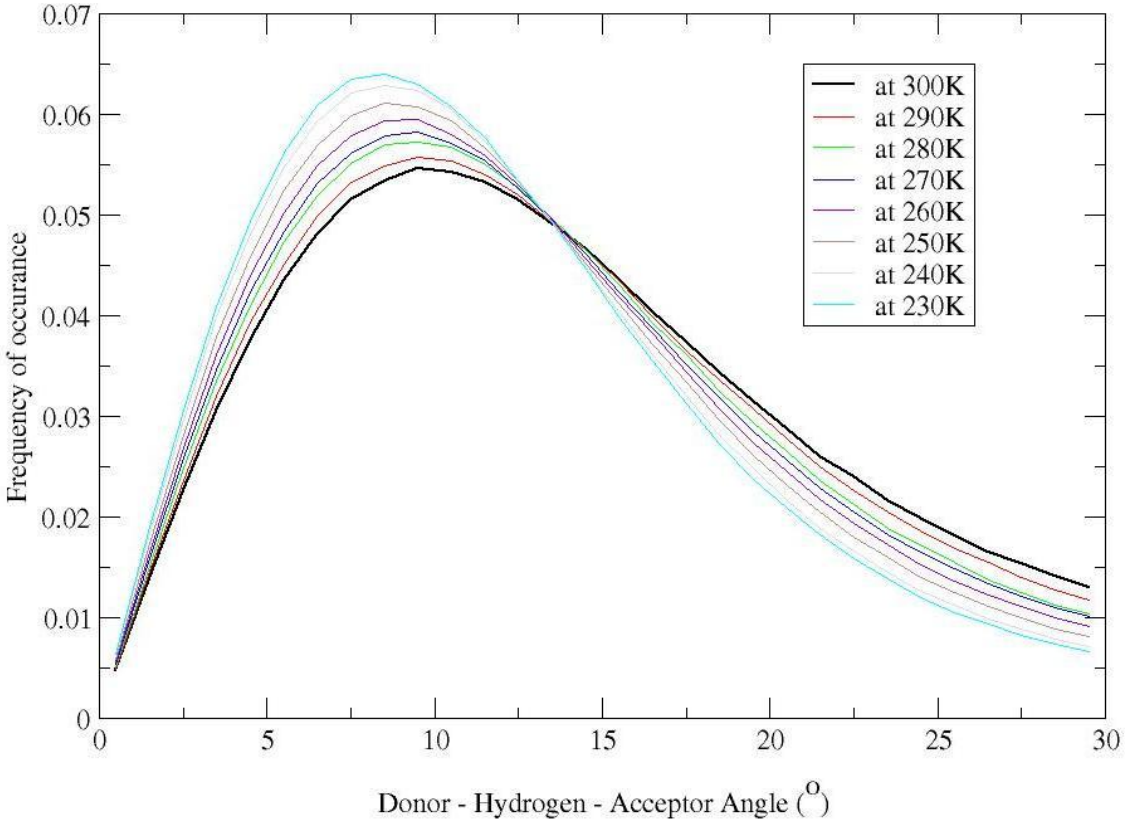

Figure 4-18 *Hydrogen bond angle distribution of 23% aqueous methanol solution*

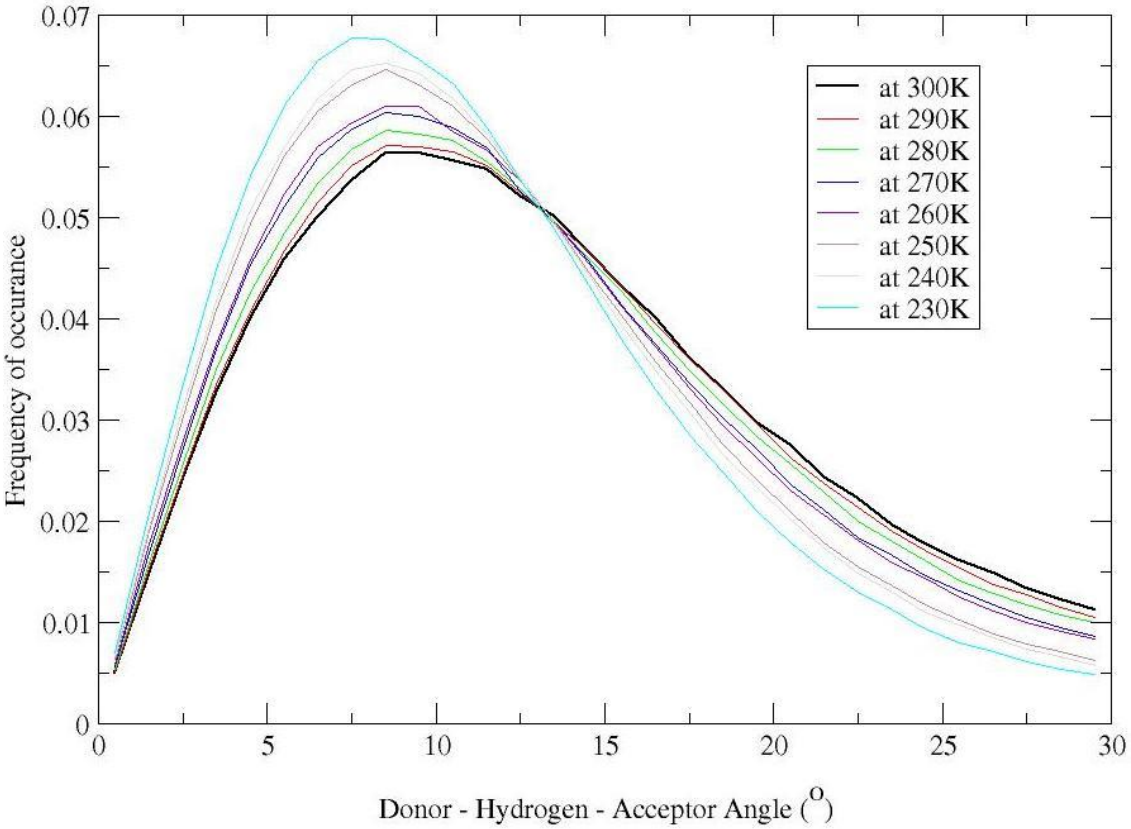

Figure 4-19 *Hydrogen bond angle distribution of 9% ethanol solution*

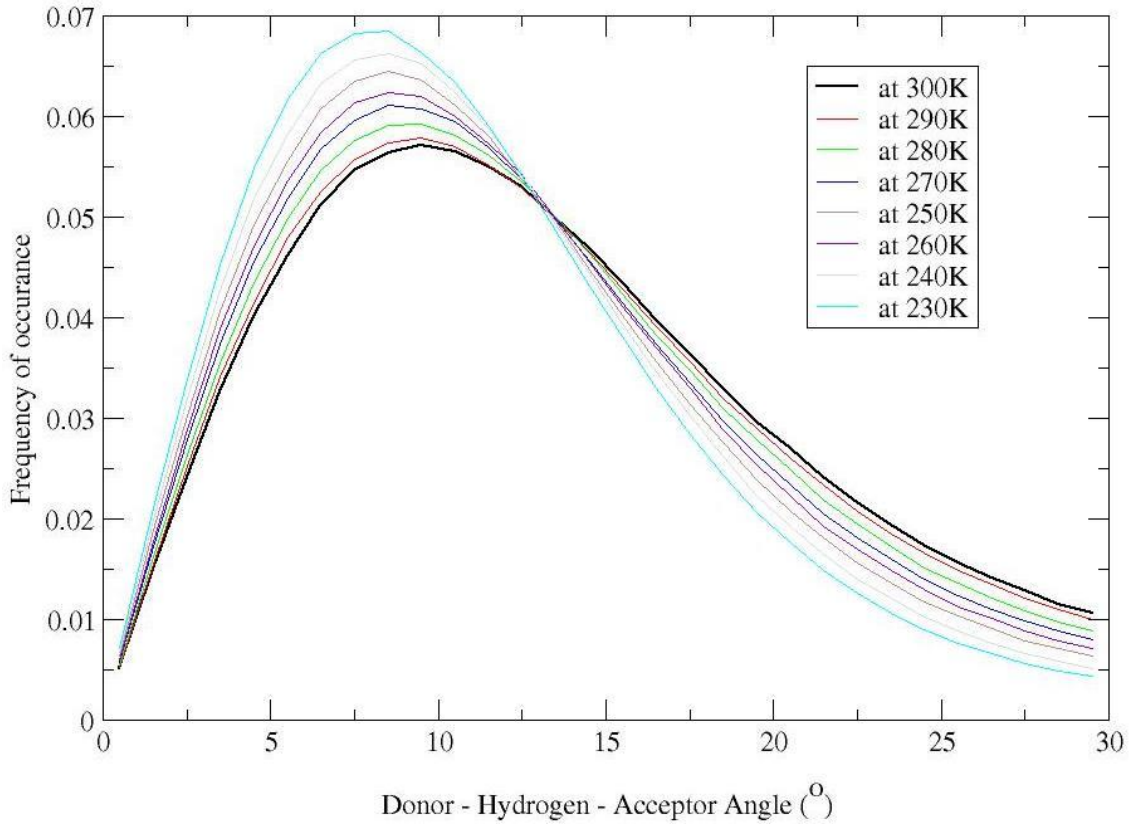

Figure 4-20 *Hydrogen bond angle distribution of 23% ethanol solution*

4.3.4.4 Hydrogen bond distance distribution

In Figure 4-21 to Figure 4-24, water- water hydrogen bond distance distribution of the systems studied are shown. In all cases, it can be seen that the most frequent hydrogen - acceptor distance is 1.9, occurrence of which is found to be higher is aqueous ethanol solutions, and as temperature decreases from 300K to 230K, this becomes more pronounced, as indicated by sharper peaks.

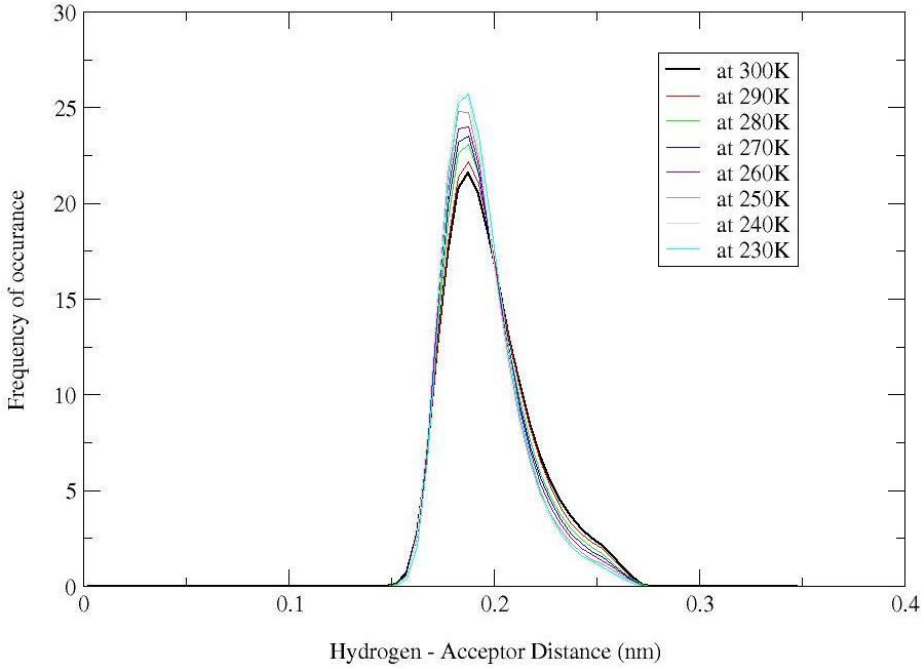

Figure 4-21 *Hydrogen bond distance distribution of aqueous 9% methanol solution*

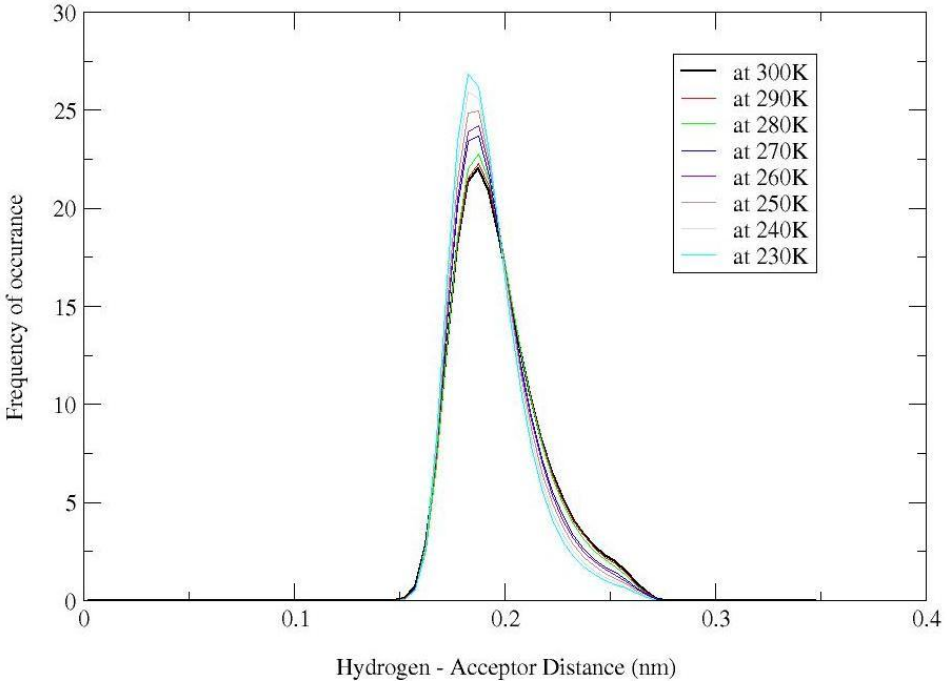

Figure 4-22 *Hydrogen bond distance distribution of aqueous 23% methanol solution*

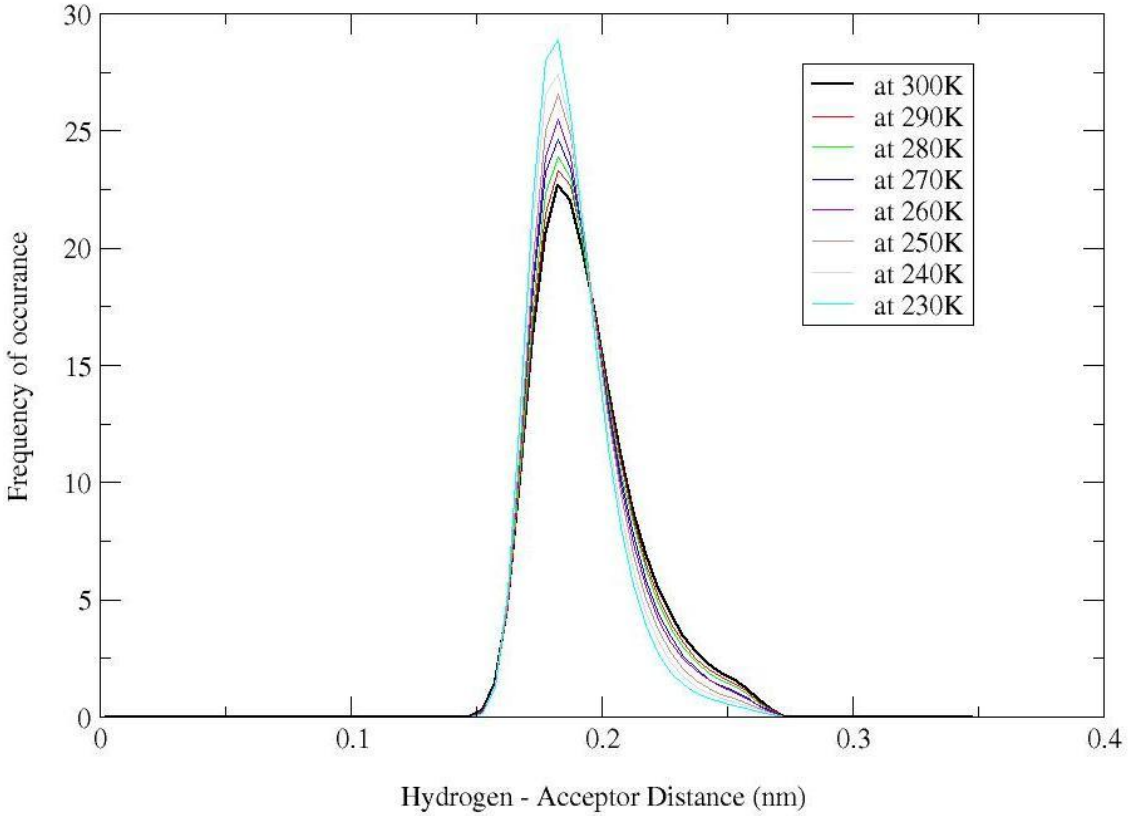

Figure 4-23 *Hydrogen bond distance distribution of aqueous 9% ethanol distribution*

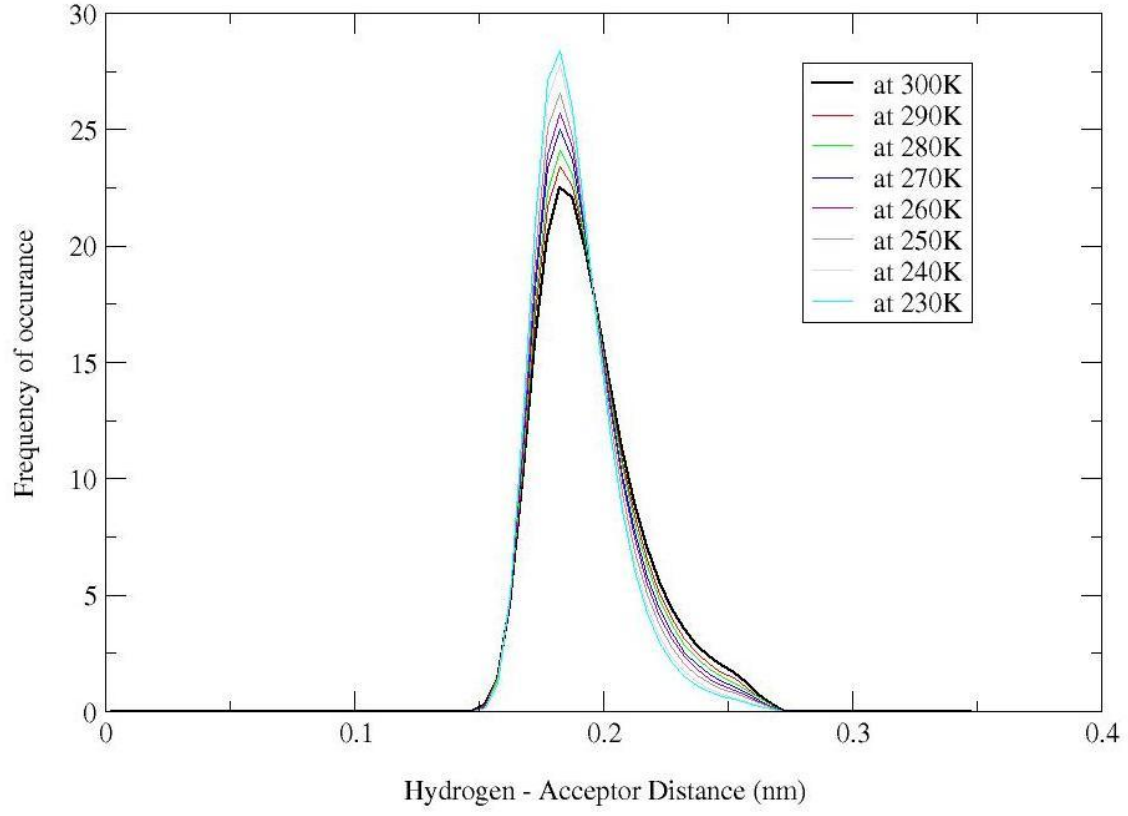

Figure 4-24 *Hydrogen bond distance distribution of 23% aqueous ethanol solution*

Hydrogen bonding statistics (Figure 4- 11) suggests that average number of solute (methanol/ethanol) - solvent (water) hydrogen bonds tends to increase as solute concentration decreases[364]. Hydrogen bond plays a pivotal role in determining physical properties of aqueous alcohol solutions at wide temperature range. It can be seen that even at supercritical temperature, hydrogen bond interactions still exist in aqueous ethanol and methanol solution[398]. Statistics of average number of hydrogen bonding between alcohols and water are shown in Figure 4- 11. The figure clearly indicates a steady increase in number of hydrogen bonds between the solute and solvent upon decrease in temperature. In both the concentration studied ethanol forms more hydrogen bonds than methanol.

The large increase of hydrogen bonds in water is attributed to the increase of free hydrogen donors of water surface at the expense of excess hydrogen-bond acceptors of ethanol. Furthermore, analysis of electronic charge distribution using Wannier functions shows that upon solvation the dipole moment of ethanol increases from 1.8 D to 3.1 D[374]. This increase, however, is found to be less than what has been reported for aqueous DMSO solutions[334]. It is interesting to compare the hydrogen bonding statistics of aqueous alcohol solutions with that of aqueous DMSO and acetone solutions described in chapter 3. The general pattern of average hydrogen bonding exhibits characteristic difference in both sets of solutions. In the case of aqueous acetone and DMSO solutions, the average number of hydrogen bonds per solute molecules remains to be same in most of the cases. By contrast, aqueous solutions of methanol and ethanol exhibit increase in average number of hydrogen bonds from higher temperature region to lower temperature region. Another striking feature is that average number of hydrogen bonds is higher in aqueous alcohol solutions than in DMSO solution despite increase in dipole moment of the solute upon dilution is much higher in DMSO than simple alcohols. This clearly indicates that electronic properties alone cannot explain hydrogen bonding properties of solutes in aqueous solutions.

Infrared spectroscopic experiments suggest that structural transformation occurs in aqueous alcohol solutions at a critical concentration corresponding to distinctive minimum of change in mean molar extinction coefficient (quantifying the changes in

hydrogen bonding equilibrium between solute and solvent molecules)[353]. This transition is attributed to structural changes within the hydration sphere of alcohol molecules. When alcohol is added to water, some hydrogen bonds among water molecules are replaced by alcohol-water hydrogen bonds. Above the critical concentration range water-alcohol interactions dominate, whereas water-water interactions controls solution dynamics below the critical concentration range.

As shown in Figure 4- 11, the average number of hydrogen bonds per solute is higher in aqueous ethanol solutions than methanol-water mixture, which can also be explained with the help of infrared spectroscopic measurements. The experiment suggests that the amount of solute molecules that is required to reach the afore mentioned critical concentration is inversely proportional to the chain size of monohydric alcohols[353].This implies that ethanol, being higher homologue of methanol, is required only in smaller amounts in order to attain the critical concentration at which solute-solvent hydrogen bonding interactions start to operate in the aqueous alcohol solutions. Hydroxyl – water radial distribution functions also highlight stronger interactions between hydroxyl group and water molecules in ethanol solutions, as shown in Figure 4-8 and Figure 4-10.

The characteristic difference between ethanol and methanol solutions at higher concentrations can be noted in terms of water-water hydrogen bonding in the mixtures, as shown in Figure 4- 12. Average number of water-water hydrogen bonds is found to be lower in aqueous methanol solutions than in pure water, suggestive of relatively high perturbation of water structure in the presence of methanol. While both types of hydrogen bonding exhibit a monotonous increase towards lower temperature, a third type hydrogen bond between two alcohol molecules does not exhibit such trend[343], rather it hovers around a particular value as seen from alcohol-alcohol hydrogen bonding statistics (see Figure 4-13). In addition, the probability of such alcohol percolating networks is relatively low as the data suggests. Alcohol – alcohol hydrogen bond lifetime is found to be longer in aqueous ethanol solutions. The difference is conspicuous at higher concentrations and lower temperature as Figure 4-16 shows. Although average number of alcohol-alcohol hydrogen bonds in aqueous ethanol solutions is lower than methanol-water mixture, stability of hydrogen bonds is found to be higher in the former.

4.3.5. Translational and rotational dynamics of aqueous alcohol solutions

Self diffusion coefficients of the various species in the two alcohol systems at two different concentrations were computed from 230K to 300K, in an interval of 10 K. Translational mobility of molecules is best described by the diffusion coefficient. Figure 4-25 shows the diffusion coefficients of alcohol molecules in the aqueous solutions as a function of temperature. The diffusion coefficients of solutes in methanol solutions do not differ significantly at 300K, in contrast to aqueous ethanol solutions. The figure also indicates that increasing concentration makes an impact on the diffusive motion of ethanol molecules, more so than in methanol. Across the temperatures studied, the translational mobility of solutes is found to be lower in ethanol solutions, primarily due to its high molecular weight and stronger interaction with water. The calculated value for ethanol in aqueous solutions at the corresponding concentrations at 300K are in close agreement with a previous molecular dynamics computation[377]. However, the values obtained using TIP4P/OPLS combination potentials[399] are found to be much higher than that of experimental measurements such as NMR[345] and magnetically stirred diaphragm cell techniques[351].

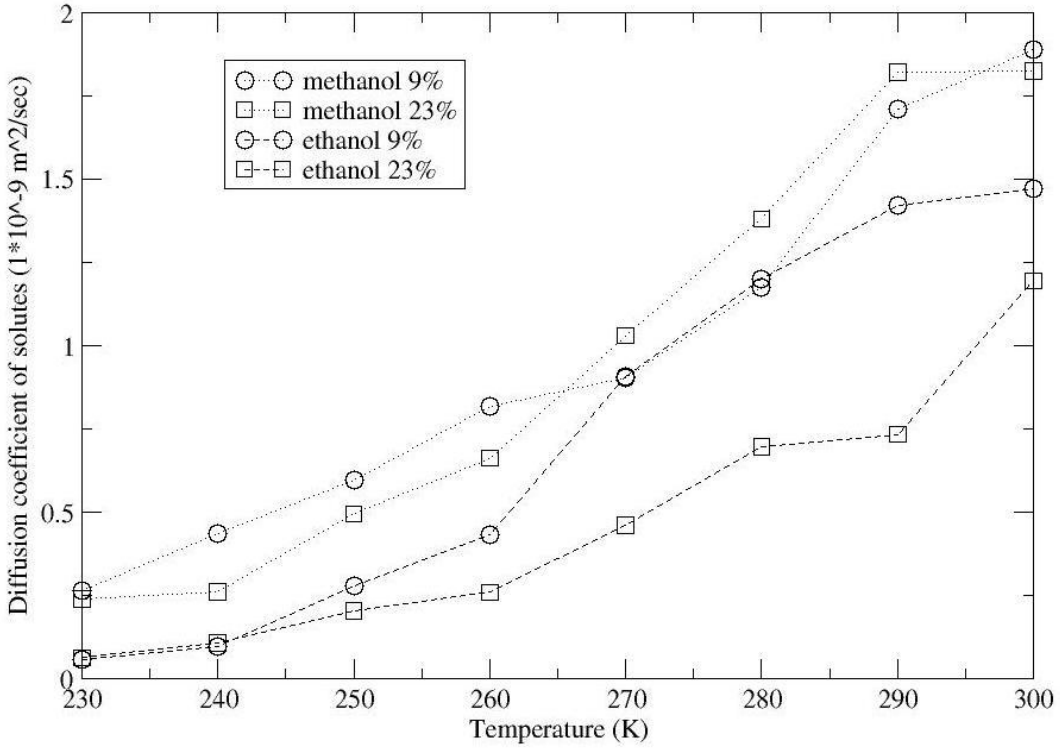

Figure 4-25 *Diffusion coefficient of solute in aqueous methanol and ethanol solutions*

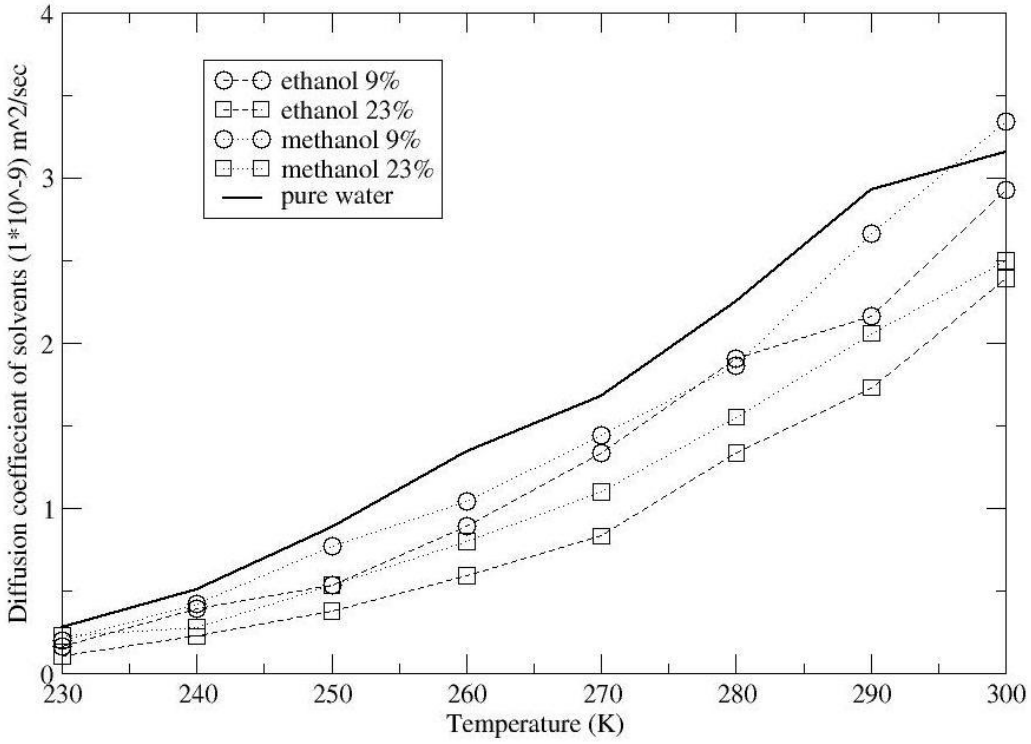

Figure 4-26 *Diffusion coefficient of solvent in aqueous methanol and ethanol solutions*

In Figure 4-26, diffusion coefficient of water molecules (solvent) in the mixtures is compared with pure water. As seen in the figure, the diffusion coefficients of all systems naturally decrease upon decrease in temperature. The plot clearly indicates the existence of higher diffusion coefficients for water molecules in pure water than in binary mixtures at all temperatures. The translational mobility of water molecules is found to be lower in aqueous ethanol solutions; since self diffusion coefficient is a measure of solute-solvent interactions[345], the decrease in diffusion coefficient of water molecules in concentrated ethanol solutions indicate stronger solute-solvent association. Stronger hydrogen bonding interactions between water-ethanol molecules are also demonstrated by self diffusion coefficient calculations.

Rotational correlation times of water molecules in the binary mixtures are shown in Figure 4-27. The calculated correlation times of solvents in both ethanol and methanol aqueous solutions are found to be in good quantitative agreement with the simulated values at ambient conditions obtained by Van der Spoel et al employing TIP4P-OPLS potential combination for water and alcohol[399]. At room temperature, the differences in correlation times of two solutions with that of pure water are relatively small. However, as temperature decreases, the correlation times increase dramatically for the

concentrated solutions. It can be seen that addition of alcohol to water increases the correlation times of the solvent molecules, up to more than two fold at 230K. Methanol is also found to increase the correlation times of the solvent molecules in par with ethanol. The increase in correlation times is another indication of stronger association of alcohols, in general, with water molecules.

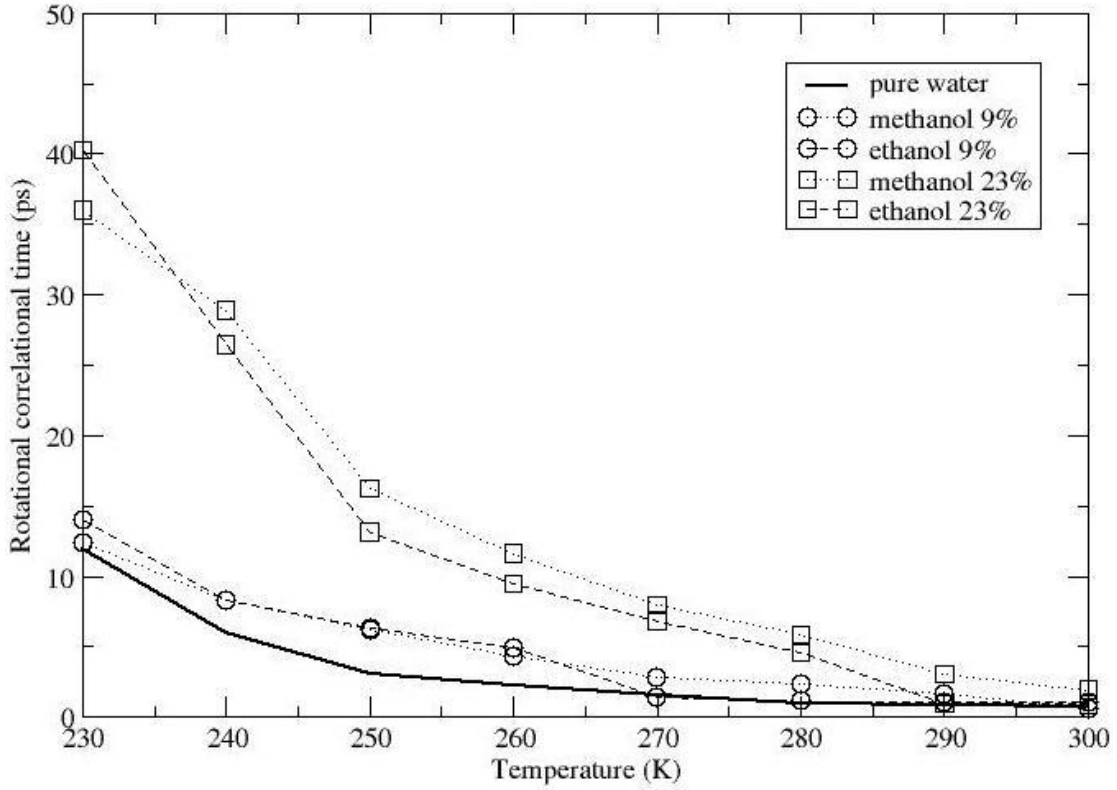

Figure 4-27 *Rotational correlation times of water molecules in aqueous methanol and ethanol solutions*.

Rotational correlation times on the other hand suggest a higher relaxation time for water in the presence of methanol. As in the case of aqueous acetone solutions, this is primarily due to the existence of more number of short water-alcohol chains in the methanol-water mixture resulting in higher relaxation times for the solvent molecules. The networks existing in aqueous ethanol solutions, on the other hand, are larger and kinetically stable.

4.4. CONCLUSIONS

Molecular dynamics simulations of aqueous ethanol and methanol solutions at two different concentrations using all atom OPLS/TIP4P potential combination are reported

in this chapter. Structural, hydrogen bonding and diffusive properties of these solutions are compared in an attempt to characterise the differences between the two systems. Calculation of coordination number suggests that methanol molecules perturb water more than ethanol does. Evidence of structuring of water molecules around the polar hydroxyl groups can be deduced from hydroxyl-water radial distributions. It has to be noted that alcohol hydroxyl- water oxygen interaction are stronger in the ethanol solution. Orientation of water molecules around the non polar part is entirely different in both solutions - in ethanol solution, methyl group interacts strongly with oxygen atom of water, evidenced by sharper peaks in the solute-solvent RDFs, whereas such preferential orientation is absent in the case of methanol solutions.

Self association of methanol molecules is further evidenced by the solute-solute radial distribution functions. Existence of well structured peak at 4Å regardless the temperatures in the methyl-methyl radial distribution function suggests that methanol generally prefers to form self aggregates, in conformity with the previous study by Noskov et al[354]. By contrast ethanol-ethanol self association is found to be weaker, indicated by the weakening of the corresponding peak in the ethyl-ethyl RDFs as temperature decreases. This finding contradicts to a previous experimental observation that self association increases as hydrophobic tail increases[344]. Methyl - hydroxyl association can also be characterised in the aqueous methanol solution, indicated by strengthening of peaks in the corresponding radial distribution function.

In order to obtain a quantitative picture of interactions between water and alcohols, extensive hydrogen bond analyses were performed. The data indicates that as the concentration of alcohol increases number of hydrogen bonding between water and alcohol decreases, which is more pronounced in the aqueous methanol solutions. In addition, ethanol forms more hydrogen bonds than methanol on average, indicating stronger interaction of ethanol molecules with water which is also reflected by sharper peaks in the hydroxyl - water hydrogen radial distribution function. It has also to be emphasized that there are fewer water-water hydrogen bonds in methanol solutions. These observations relate to the fact that methanol molecules prefer to form self aggregates especially in the lower temperature domain, whereas water structuring and ethanol – water hydrogen bonding interplay in the ethanol-water binary mixtures, in conformity with the previous observations[369, 395]. Percolating network of alcohols in

water, methanol in particular, has been reported in the literature[343]. Estimation of the number of hydrogen bonds that exist between alcohol molecules shows that methanol has a tendency to make such networks by forming more alcohol-alcohol hydrogen bonds. On the other hand, hydroxyl-hydroxyl correlations found in ethanol-water mixtures corroborate the existence of alcohol-water random networks in the solution as revealed by NMR and FT –IR experiments[391].

The lifetimes of various hydrogen bonds were also computed in order to measure their strength. It has to be noted that ethanol- water hydrogen bond lifetimes increase upon the addition of more ethanol molecules to the mixture. On the contrary, addition of methanol molecules to the solution does not seem to have any effect in increasing the solute-solvent hydrogen bond lifetimes. Increased lifetimes seen in concentrated ethanol solutions while moving towards lower temperature regions suggest that addition of ethanol stabilises water-water hydrogen bonds. Nevertheless, such distinction cannot be made with very dilute solutions.

Addition of alcohols, as estimation of self diffusion coefficients indicates, decreases the mobility of water molecules in the solution. This supports the previous radial distribution and hydrogen bonding analysis which reveals stronger interaction of ethanol with water molecules. Nevertheless the same difference cannot be seen in the case of rotational correlation functions. Of particular note is that the rotational correlation functions of the aqueous alcohol solutions- ethanol and methanol- were found to be higher than that of DMSO and acetone solutions described in the previous chapter.

The analysis described so far provides insights into the interactions that govern the solution properties of the simplest monohydric alcohol (ethanol and methanol) – water mixtures. From the simulations, characteristic differences between aqueous ethanol and methanol solutions can be made - ethanol prefers to form hydrogen bonds with water, where as methanol tends to form self aggregates. Strong interactions with water, by forming hydrogen bonds, will reduce the availability of water molecules that are likely to undergo nucleation at lower temperatures. On the other hand, though methanol forms more hydrogen bonds with water than another notable cryoprotectant DMSO, its associative behaviour may negate its hydrogen bonding properties, which can result in

the loss of its ability to trap water molecules, making methanol ineffective in preventing nucleation and subsequent crystallisation.

Chapter 5

Determination of glass transitions of aqueous cryoprotectant solutions

Estimation of glass transition temperatures of aqueous mixtures of DMSO, acetone, ethanol, methanol and water using simulated annealing molecular dynamics techniques has been described in this chapter.

5.1. INTRODUCTION

Avoiding the formation of intracellular ice, as mentioned earlier in chapter 1, is essential for the successful storage of cells at very low temperatures and can be achieved through the vitrification of water[16]. The so-called vitrification hypothesis suggests that certain cryoprotective agents (CPAs), such as DMSO, methanol and ethanol, protect biological structures not only colligatively by depressing the freezing point of water, but also by promoting the formation of the amorphous glassy state of water, thereby preventing the formation of ice, reducing structural fluctuations, denaturation and/or mechanical disruption[16].

Neat water can remain in the liquid state below its freezing temperature, in what is known as supercooled water[174, 400]. The supercooling limit of water is reached at its homogeneous nucleation temperature, T_H (231K), below which it is readily crystallised[174]. At the further lower temperature of approximately 165K[401] (the glass transition temperature or T_g) water can reach a glassy state if it is cooled very rapidly[174, 187]. Glassy water is a non-equilibrium state, which makes its physical properties dependent on the method by which vitrification is reached[174]. In neat water, molecules can diffuse freely and can arrange themselves at low temperature to form a critical nucleation radius, whereupon ice crystals are easily formed[5]. On the other hand, in the presence of CPA solutes, the viscosity of the solution increases leading to a decrease in the diffusion of water molecules.

The crystallisation of water in aqueous solutions of CPAs is restricted to the region above T_g, where water remains in the liquid state. Consequently, achieving a higher T_g is required for better cryopreservation, leading to the onset of vitrification at a higher temperature and closer to the freezing point of water with appropriate cooling rates[10, 16]. In addition, the number of water molecules available to form a critical nucleus is small due to strong interactions with CPA molecules, retarding the onset of nucleation[5].

The experimental determination of T_g has been controversial as its value differs depending on the technique used: although glass transition temperature of pure water was earlier assigned to 136K[402], it has now been recognised as the pre-peak preceding the glass transition which has been determined by hyper-quenching experiments, 165K[402, 403]. On the other hand, molecular dynamics (MD) annealing simulations predict T_g to be 188K using SPC/E water model[404]. Noting the variation of potential energy with respect to temperature, Oleinikova et al have predicted the glass transition temperatures for various water models employing Monte Carlo simulations in density restricted NPT ensembles[405] - 235K using ST2 water model, 255K using ST2RF water model, 180K using TIP4P water model, 215K using TIP5P water model, and 220K using SPC/E water model.

There have also been previous attempts to study experimentally the glass forming properties of aqueous DMSO[253, 300] and other cryoprotectant solutions[406, 407]. However, the use of low cooling rates in these studies is unlikely to have avoided significant crystallisation of the samples, raising questions about the extent of true vitrification achieved. Molecular dynamics annealing method is described in this chapter in an attempt to estimate glass transition temperatures of aqueous solutions following prediction of glass transition temperature of liquid water by Stanley et al[197]. In the annealing simulations, generic relationships between thermodynamic response functions such as the heat capacity (C_V) and the energy of the system allow the use of MD simulations to determine discontinuities in plots of C_V versus temperature, revealing the appearance of a second order transition at a temperature corresponding to the onset of vitrification[197]. Though time scale that is possible with available computer power cannot match with experimental time scales, meta stable

systems like glasses, property of which is determined by kinetic effects (rate of cooling or heating for example), can be studied using the annealing method.

The first computational predictions of the glass transitions of aqueous DMSO, ethanol, methanol and acetone solutions are reported in this chapter. DMSO, ethanol and methanol are very common CPAs[408, 409] that are used at various concentrations[5] and are exceptionally effective for the cryopreservation of a variety of biological tissues[10, 110, 409, 410]. They are miscible with water in all proportions and hence aqueous solutions of these solvents constitute excellent systems to investigate in detail. Acetone, a structural analogue of DMSO that is not used as a CPA due to its reactivity and toxicity, is also a useful system to investigate. We have thus conducted a number of MD annealing simulations of water at different DMSO, ethanol, methanol and acetone concentrations to study any changes to the T_g that may corroborate the hypothesis that a CPA like DMSO can increase the T_g of water. For further comparison, we have also performed simulations of water at different concentrations of tetrahydrofuran (THF), a solvent that is also miscible with water in all proportions but that does not have cryoprotective abilities.

5.3. SIMULATION METHODS

Molecular dynamics annealing simulations in the isobaric-isothermal canonical ensemble (constant number, pressure and temperature) were carried out at 1 atm of pressure. Initial molecular configurations in cubic simulation boxes were generated using Packmol[329] and were subsequently energy minimised and equilibrated at 360K for 1.0-3.0 ns. The Berendsen thermostat and barostat[330] were used for controlling the temperature and pressure, respectively. A cooling rate of $-3*10^{10}$ K/s was used to bring the systems from the initial temperature of 360K down to 0K. This was followed by heating back to 360 K at the same rate. The heat capacity (C_V) was calculated by numerical differentiation of the total energy, saved at every 10fs, with respect to the temperature. The energy data was divided into the blocks of 10000 and averaged. The onset of the glass transition was determined to occur when a sudden increase in C_V upon heating was observed[404, 411, 412]. All simulations were carried out with GROMACS 3.3.3 using a time step of 1 fs[413] The TIP4P water potential[207] and the OPLS potentials for DMSO[277], acetone[322], ethanol[322],

methanol[322] and THF[322] were used. Aqueous solutions at different DMSO, acetone and THF number concentrations were simulated: 0, 1, 4, 8, 25, 40, 80 and 100 DMSO molecules; 1, 10, 20, 40 ,60, 80, 100 ethanol molecules; 1, 10, 20, 40, 60, 80 100 methanol molecules; 0, 1, 4, 13, 25, 52, 80 and 100 acetone molecules; and 1, 10, 25, 50, 80 and 100 THF molecules, with additional water molecules filling up a cubic box up to a total of 500 molecules. Long range interactions were measured using the PME method[414] with a cut off of 10.0 Å. The total simulation time for each system was 24.0 ns, with 12.0 ns each for cooling and subsequent heating.

5.3. RESULTS AND DISCUSSIONS

Figure 5-1 shows plots of C_V versus temperature for neat water and for each DMSO concentration. A broad but well defined peak corresponding to the onset of the glass transition of neat water (T_g) appears to occur at 193 K. This value, calculated using the TIP4P water potential[23] is in good agreement with the reported T_g of 188K using the SPC/E water potential[14]. Upon addition of DMSO, the glass transition of the solutions broadens significantly, both towards lower and higher temperatures (the latter promoted by an increase in the heat capacity of liquid phase). Therefore the glass transition of aqueous DMSO solutions occurs over a wide range of temperature range, indicating an increase in its thermodynamic stability[415,416]. This suggests that a stronger glass is formed in increasingly concentrated aqueous DMSO solutions. This is likely to result in a reduced tendency for the nucleation and subsequent crystallisation of water above the Tg of pure water. This would explain, at least qualitatively, the cryopreservation properties of DMSO.

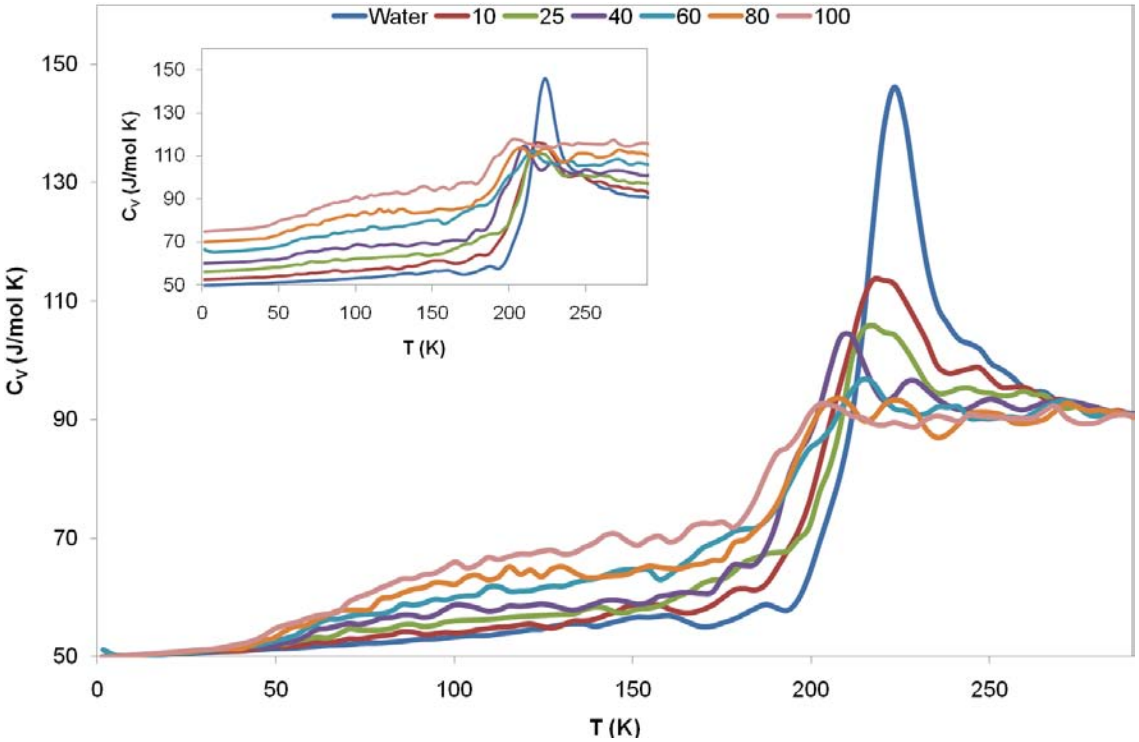

Figure 5-1 *Prediction of the glass transition temperatures of aqueous DMSO solutions. Plots of C_V as a function of temperature were obtained for pure water and aqueous solutions at five different number concentrations of DMSO (10:490, 25:475, 40:460, 60:440, 80:420 and 100:400 DMSO: water ratio), which are shown shifted to the initial C_V value of water for comparison and in their original form (inset). The predicted glass transition temperature of neat water (T_g) is ~193K. As the concentration of DMSO increases, the overall glass transition of the solution broadens, corresponding to a glass transition that occurs over a wider temperature range and suggesting the formation of a thermodynamically stronger glassy state and, therefore, a decrease in the chance of ice formation. Consequently, the addition of DMSO to liquid water improves its vitrification properties. The figure has been adapted from Mandumpal et al[417] with the explicit permission from PCCP owner societies.*

The broadening of the glass transition of water is analogue to the so-called fragile-strong crossover (FSC), a thermodynamic transition from a fragile to a strong glassy system which confers thermodynamic and kinetic stability against crystallisation at low temperature upon cooling[416, 418]. This phenomenon has been observed in a variety of glass forming systems such as hydrazine hydrates and inorganic compounds like BeF_2 and SiO_2[415]. Fragile glasses have relaxation times that change very rapidly with temperature, resulting in a characteristic very sharp increase in the heat capacity at Tg that is complete in just a few degrees. On the other hand, non-fragile glasses exhibit glass transitions that require tens of degrees to complete[419]. There has been controversy as to whether water should be regarded as fragile or strong liquid near Tg, depending on the temperature and cooling rate[419]. However it

appears that it may be considered to be a moderate glass former on the basis of an order-disorder transition above Tg[419]. Consequently, while the broadening of the glass transitions of the aqueous DMSO solutions reported here cannot be described as a FSC, it can be understood as the formation of a stronger glass.

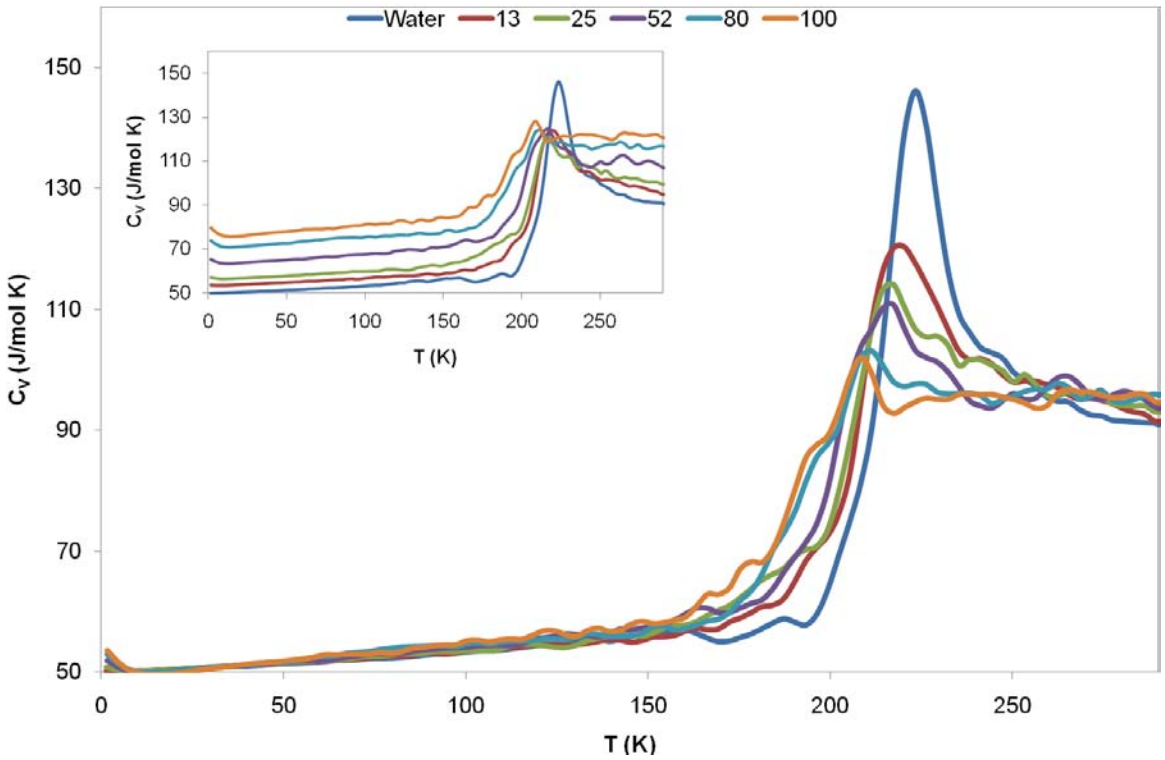

Figure 5-2 *Prediction of the glass transition temperatures of aqueous acetone solutions. Plots of C_V as a function of temperature were obtained for pure water and aqueous solutions at five different number concentrations of acetone (13:487, 25:475, 52:448, 80:420 and 100:400 acetone:water ratio), which are shown shifted to the initial C_V value of water for comparison and in their original form (inset). As the concentration of acetone increases, the overall glass transition of the solution broadens but to a lesser extent than that seen in aqueous DMSO solutions. Consequently acetone would not be expected to improve the vitrification properties of water to the same degree as DMSO. The figure has taken from Mandumpal et al[417],with the explicit permission from PCCP owner societies.*

Figure 5-2 shows the corresponding plots of C_v versus temperature for each acetone concentration. As the concentration of acetone increases the glass transition of the solution broadens, in analogous to aqueous DMSO solutions. Nevertheless this effect is less pronounced than that observed in aqueous DMSO solutions. Moreover, the relatively well-defined shape of the glass transition of water retained even at the highest concentration of acetone studied. This suggests that there is only limited broadening of the glass transition upon addition of acetone and hence that there is

modest thermodynamic strengthening of the glassy state. Consequently acetone would not be expected to improve the vitrification properties of water to the same level of effectiveness as DMSO.

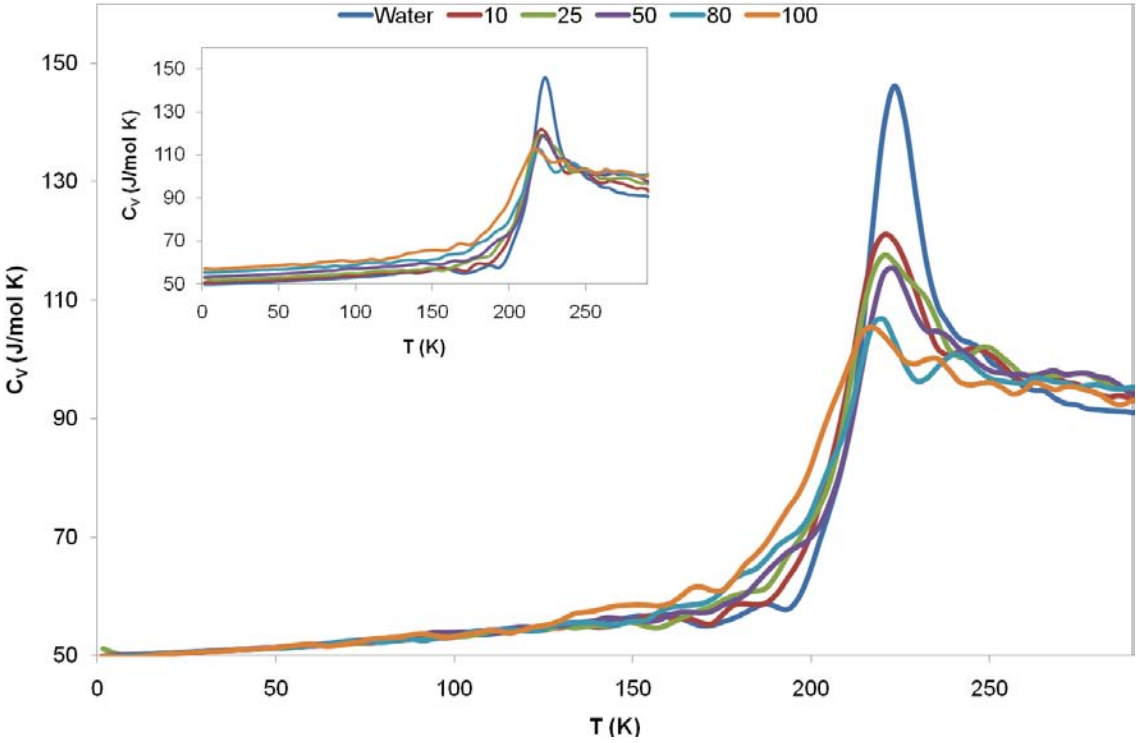

Figure 5-3 *Prediction of the glass transition temperatures of aqueous THF solutions. Plots of C_V as a function of temperature were obtained for pure water and aqueous solutions at five different number concentrations of THF (10:490, 25:475, 50: 450, 80:420 and 100:400 THF:water ratio). As the concentration of THF increases, the glass transition broadens only slightly. The position and relative shape of the well-defined transition peak are retained at all THF concentrations. These findings suggest that THF would not be expected to significantly improve the vitrification properties of water. The figure has been adapted from Mandumpal et al[417], with the explicit permission from PCCP owner societies.*

The Figure 5-3 shows the plots of Cv versus temperature for each THF concentration. It can be seen that the addition of THF to water broadens the width of the glass transition to some extent but mostly towards lower temperatures, as indicated by the slanted arrow. In addition, the position and relative shape of the well-defined peak of the glass transition are retained at all THF concentrations. These findings suggest that there is very limited if any thermodynamic strengthening of the glassy state upon addition of THF to water. Consequently the addition of THF would not be expected to increase the tendency for vitrification of water.

The annealing simulations were also carried out for aqueous ethanol and methanol solutions, shown in Figure 5-4 and Figure 5-5. As seen in the case of aqueous DMSO solutions, broadening of glass transition is observed in both alcohol solutions. In most of the cryoprotectant solutions discussed in this chapter, the glass transition temperatures are found to be decreasing with respect to the concentration of the solutes, in accordance with an earlier Differential Thermal Analysis (DTA) investigation on aqueous solutions[420].

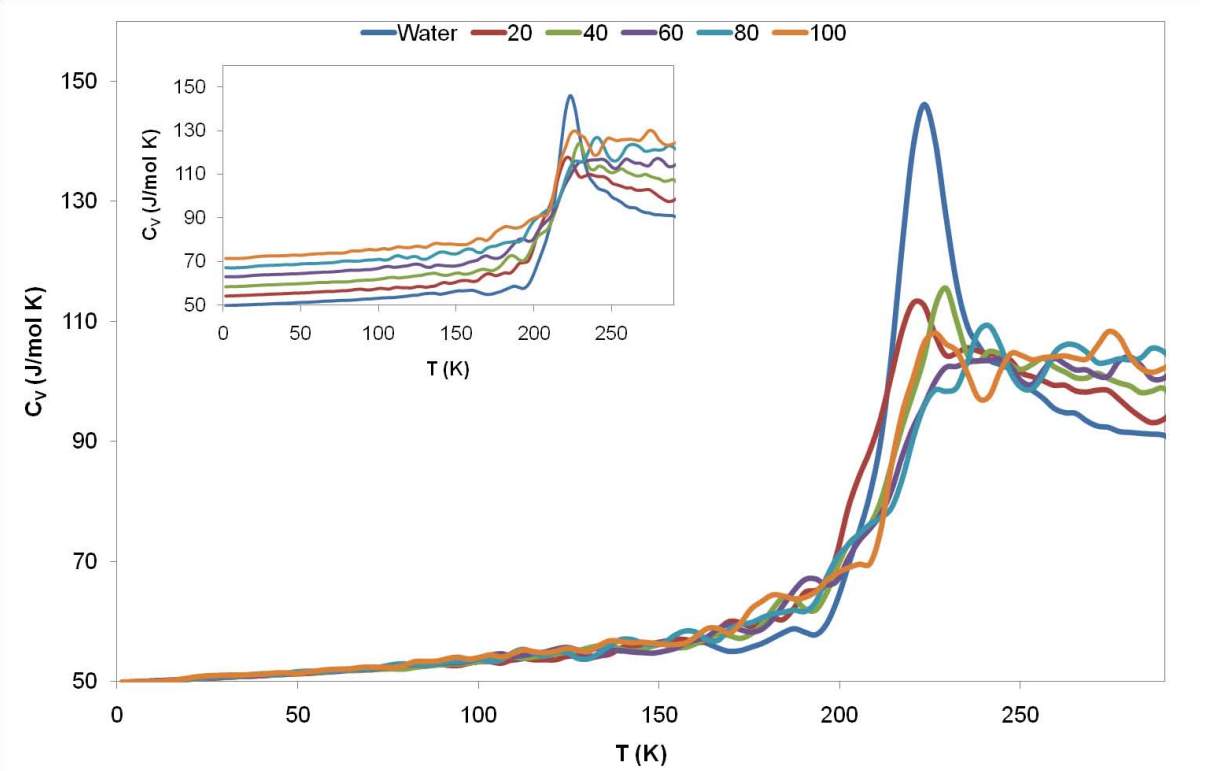

Figure 5-4 *Prediction of the glass transition temperatures of aqueous ethanol solutions. Plots of C_V as a function of temperature were obtained for pure water and aqueous solutions at five different number concentrations of ethanol (20:480, 40:460, 60:440, 80:420 and 100:400 ethanol:water ratio), which are shown shifted to the initial C_V value of water for comparison and in their original form (inset). As the concentration of ethanol increases, the overall glass transition of the solution broadens as seen in aqueous DMSO solutions.*

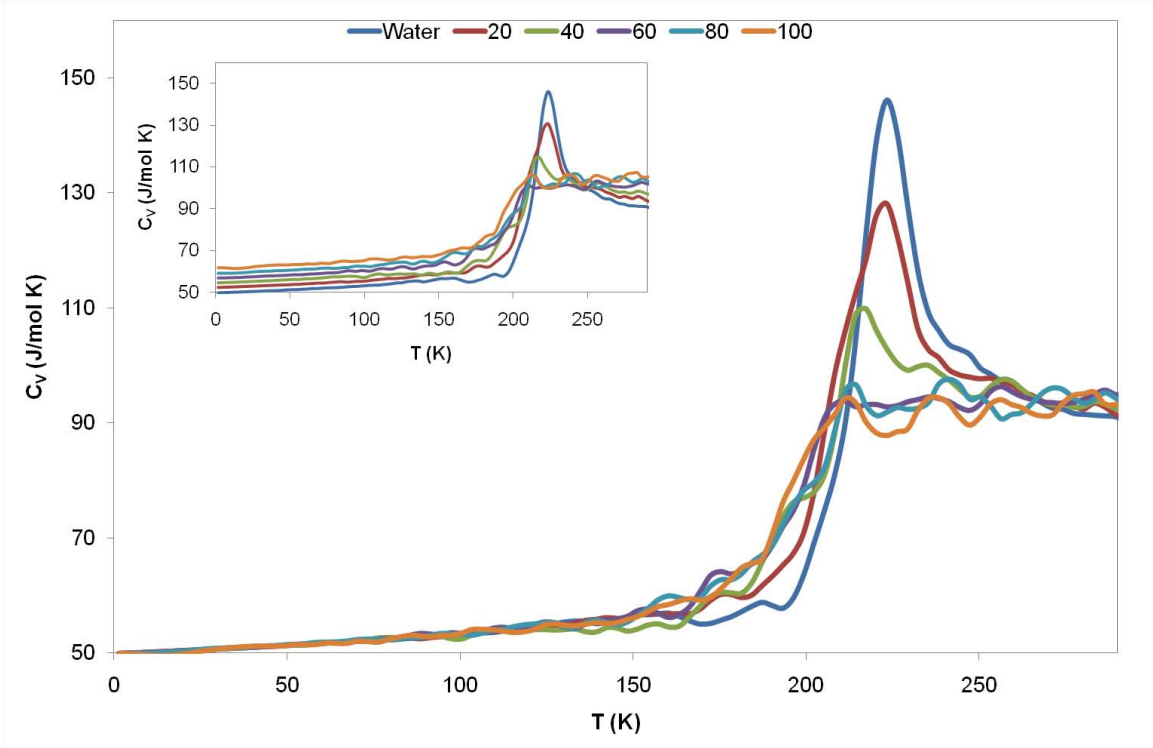

Figure 5-5 *Prediction of the glass transition temperatures of aqueous methanol solutions. Plots of C_V as a function of temperature were obtained for pure water and aqueous solutions at five different number concentrations of methanol (20:480, 40:460, 60:440, 80:420 and 100:400 ethanol: water ratio), which are shown shifted to the initial C_V value of water for comparison and in their original form (inset). As the concentration of methanol increases, the overall glass transition of the solution broadens as seen in aqueous DMSO solutions.*

Annealing simulations provide a qualitative description of the glass transition in aqueous cryoprotectant solutions. The apparent broadening of glass transition curves in the mixtures, indicated by only small heat capacity jumps, is observed in variety of glass forming systems such as hydrazine hydrates and inorganic compounds such as BeF_2 and SiO_2[415]. This suggests that the glass formed in the presence of CPAs like DMSO would be able to withstand thermodynamic or kinetic perturbations that may alter glassy state leading to formation of ice crystals in the samples. Structure of such strong glass, due to their strong network[156], does not change much with temperature as opposed to fragile glass. By employing self consistent phonon theory, it has been demonstrated that the decrease in fragility is attributed to increasing connectivity of network forming liquids and solutions[421], suggesting that CPAs can act as strong network maker when they mix with water.

The strong- fragile classification of the liquids and solutions can be explained on the basis of fluctuation range of coordination number of the solute. Strong glass

formers will have their coordination number intact, leading to stable networks, whereas fragile glass formers show a large deviation in the coordination number, suggestive of unstable networks in the system[422]. The interactions existing between molecules in a fragile system are non-directional; due to this glass transition temperatures of fragile liquids are accompanied by abrupt changes in heat capacities within small range of temperature[156]. Furthermore, experimental investigations employed by Low frequency Raman spectra suggests that the driving force acting within a strong system (liquids or solutions) is low energy vibrational motions, whereas high energy relaxational motions, often known as β relaxations, are dominant in fragile systems[423]. Cornucopia of these unstable interactions is the primary cause of instability observed in fragile systems.

Heat capacity curves derived from molecular dynamics annealing simulations indicate that there exists only one distinct peak indicating the onset of glass transition temperatures in aqueous solutions. Thus absence of any sub peaks reflects in the formation of stable complexes or two dimensional networks in the supercooled mixtures, hence suggest higher degree of mixing in the cryoprotectant solutions as connoted by dielectric relaxation experiments[424]. From the heat capacity curves it is clear that the sharpness of the peaks corresponding to the glass transition recedes in the concentrated solutions. In the light of Differential Scanning Calorimetry (DSC) experiments on aqueous Lithium Chloride, ethanol and ethylene glycol solutions, this effect has been attributed to the crossover from non Arrhenius behaviour to Arrhenius behaviour pertaining to the stability of a system against any thermodynamic or kinetic variations[342]. In another DSC study, it has been shown that aqueous solutions of Poly Glycol (PG) separate into water rich and solute rich phases as evident by two separate peaks[424]. On the contrary, heat capacity-temperature plots as shown in the figures exhibit only a single peak. This difference is primarily attributed to the crystallisation of water rich region in the experiments, which is unavoidable during DSC scans at low temperatures, whereas the formation of ice is suppressed in computer simulations in which high cooling and heating rates are normally achieved.

From the plots one could see that the fragile strong cross over is observed in increasing order among all five aqueous solutions described in this chapter: THF <<

Acetone < DMSO ~ ethanol = methanol. Formation of stronger glass observed in aqueous DMSO and alcohol solutions predominantly occurring at higher concentrations can be explained in terms of molecular interactions existing in these mixtures. Alcohols are capable of forming multiple hydrogen bonds with water due to their hydroxyl groups, as indicated by hydrogen bonding analysis described in chapter 4. Addition of alcohol into water enhances ordered molecular interactions through hydrogen bonding, which results in highly directional stronger network of molecules that are unperturbed by variations in thermodynamic variables such as temperature or pressure. Small alcohols like ethanol and methanol form more than two hydrogen bonds on average, and as temperature decreases the number of alcohol-water hydrogen bonds increases up to 2.6 and 2.3 respectively. Hydrogen bonding analysis also indicates self association of water molecules in aqueous solutions - molecular dynamics simulations suggest that upon addition of alcohol into water, interactions between water molecules become stronger as characterised by increasing number of hydrogen bonding lifetimes. Both these types of interactions, alcohol-water and water-water, contribute to directional nature of the interactions occurring in aqueous alcohol solutions justifying the transition from a fragile to strong glass upon their addition into water.

DMSO is also capable of interacting strongly with water due to the formation of two strong hydrogen bonds with its sulfinyl group (S=O)[425, 426], which contributes to the structuring of the first hydration shell of DMSO. In addition, the methyl groups of DMSO are hydrophobically hydrated, as evidenced by further structuring of water in their vicinity[247, 283,281]. While the addition of DMSO decreases the number of water-water hydrogen bonds , there is an overall increase in water-water and DMSO-water correlations with increasing DMSO concentrations[247, 267, 281, 283] as well as an increase in the number of DMSO-water hydrogen bonds[268]. These observations indicate that DMSO is strongly hydrated by water.

Acetone is also capable of forming strong interactions with water through its carbonyl group, but this interaction is weaker as it forms on average fewer hydrogen bonds with water than DMSO[268, 292]. While the addition of acetone also decreases the number of water-water hydrogen bonds, the increases in acetone concentrations, in contrast to DMSO, results in significant decrease in number of

acetone-water hydrogen bonds. Higher water-water coordination in aqueous solutions of acetone compared to DMSO has indicated the existence of a significant level of segregation of water upon addition of acetone[268], whereas DMSO is known to form clusters with water. All these facts suggest that acetone is not as strongly hydrated as DMSO.

In the case of THF, the cyclic ether oxygen can form only one hydrogen bond with neighbouring water molecules[427]. Furthermore, water in aqueous THF solutions has a significantly lower number of hydrogen bonds compared to pure water, even after taking into account its hydrogen bonding to THF. This is due to the fact that THF molecules can compete with water through their ability to accept but not donate hydrogen bonds, resulting in an overall disruption of the tetrahedrally-coordinated network of water[427], which is not observed in aqueous solutions of DMSO or acetone.

These findings reveal that stronger glass is formed upon addition of cryoprotectants such as DMSO and alcohols than acetone and THF, thereby increasing thermodynamic as well as kinetic stability of the glass over a wide range of temperatures. The fact that fragile strong crossover (*FSC)* is more pronounced in alcohols and DMSO solutions than other two at comparable concentrations demonstrates superior cryoprotective ability of these solvents over common solvents such as acetone and THF. Acetone shows an intermediate trend while THF demonstrate a weaker fragile to strong transformation. The results provide direct evidence of the molecular mechanism of solvent cryoprotection related to changes to the vitrification properties of water.

5.4. CONCLUSIONS

The enhancement of the glass transition peak as observed in the annealing plots has implications in the observed cryoprotective ability of DMSO and alcohols at higher concentrations, as it demonstrates that cryoprotectants stabilize the vitrification over a wide range of temperature. The simulations qualitatively provide a rationale at the molecular level of the mechanism of cryopreservation of CPAs including DMSO, ethanol and methanol. It is important to note that the addition of CPAs

would prevent the formation of ice by modifying vitrification properties of water in cryopreserved biological tissues; whereas aqueous Acetone and THF solutions, despite their moderate glass enhancement behaviours, are not widely used supposedly due to their toxicity and formation of moderately strong glass.

Chapter 6

Conclusions and scope of future work

SUMMARY OF MAIN FINDINGS

Molecular dynamics simulations methods have been used to investigate molecular mechanism of selected cryoprotectants. The primary focus of this study is on the structural elucidation of smaller cryoprotectants like DMSO, ethanol and methanol in water for obtaining a definitive understanding of underlying mechanism of their solvation in water. These CPAs are very commonly used in cryobiology for preserving biological materials and seeds, and are less studied by means computer simulations at cryopreservation conditions than their sugar counterparts such as trehalose and glucose. In addition, employing simulated annealing techniques, vitrification properties of these solvents (one of the proposed mechanism of cryopreservation), is compared with respect to non cryoprotectants such as acetone and Tetra Hydro Furan (THF)

Radial distribution functions and hydrogen bonding analyses provide vital information regarding the solution properties of the solvent studied. Solvent-Solvent radial distribution functions indicate that structural enhancement of DMSO in water is limited in comparison with its chemical analogue, acetone. Solute-Solvent radial distribution function suggests that the sulfinyl group in DMSO interacts more strongly with water molecules than the carbonyl group in acetone, and this is particularly notable in the lower temperature region. Radial distribution function analysis suggests that clustering of acetone molecules occurs in the lower temperature region compared to DMSO. Hydrogen bond analysis suggests that DMSO forms more hydrogen bonds with water on average than acetone. A smaller number of hydrogen bonds between acetone and water is suggestive of self-aggregation at lower temperatures. On the other hand, the number of water-water hydrogen bonds is found to be higher in aqueous acetone solutions, indicating the stabilisation of water structure in the solution. Higher number of DMSO-water hydrogen bonds and longer hydrogen bond life times indicate existence of stronger and relatively stable DMSO-water network in their mixtures,

which will prevent the tendency of water molecules to self aggregation, leading into nucleation and eventual crystallisation. This has implications in cryobiological applications as formation of ice can be prevented by insertion of solutes like DMSO, preventing self aggregation of water molecules.

The structure and dynamics of aqueous solutions of methanol and ethanol were also investigated using classical molecular dynamics simulations. Radial distribution function analysis reveals that structuring of water molecules around hydroxyl groups occurs for the whole range of temperatures studied. A distinction between the two systems can be deduced in terms of water orientation around the non polar methyl group: a stronger methyl-water oxygen interaction is seen in aqueous ethanol solutions, whereas such preferential orientation is found to be absent in the case of aqueous methanol solutions. Another notable difference refers to the self interaction of solutes- this is a striking feature in aqueous methanol solutions. This effect, on the other hand, is found to be weaker in its higher homologue ethanol.

Hydrogen bonding analysis suggests that the number of hydrogen bonds that are formed between alcohol and water decreases upon addition of alcohol molecules, an effect which is stronger in aqueous methanol solutions. An important difference between these two alcohol mixtures is that alcohol-water hydrogen bond life times vary directly with the concentration of ethanol solutions, whereas alcohol-water hydrogen bond life times are found to be largely independent of the concentration of aqueous methanol solutions. In addition to solute-solvent and solvent-solvent hydrogen bonds, solute-solute hydrogen bonding is also found to exist in aqueous alcohol solutions. However, the latter is found to be numerically insignificant compared to the other two types of hydrogen bonding interactions. The ability to form multiple hydrogen bonds with water, could explain enhanced cryoprotective activity of these amphiphile molecules. However, the tendency of methanol molecules to self-aggregate in water may reduce its cryoprotective ability, apart from being toxic.

To investigate the glass forming characteristics exhibited by aqueous cryoprotectant solutions, molecular dynamics annealing simulations were conducted. These simulations, for the first time, reveal that cryoprotectants such as DMSO, ethanol and methanol exhibit the formation of stronger glass than non-cryoprotectant solutions,

such as acetone and tetrahydrofuran (THF). The predicted glass transition temperature of pure water is in good agreement with the recently proposed glass transition temperature of pure water.

In conclusion, molecular dynamics annealing simulations of aqueous cryoprotectant solutions provide further understanding of the glass transitions that occur in these mixtures, underlying their cryoprotective ability. The study of the unique properties of water, such as the formation of its glassy state, has been a central theme in chemistry, physics and biology. The so-called vitrification hypothesis was proposed decades ago, whereby the formation of a glassy state in water avoids the formation of ice crystals inside cells, which would result in their death. Elucidating in detail the physical chemical mechanism of how cryosolvents promote the vitrification of water advances our fundamental understanding of the behaviour of water, which is important in many fields and has multiple technological applications.

SCOPE FOR FUTURE WORK

There is scope for extending simulation time scales to ensure better thermodynamic control, which particularly is essential when dealing with properties like the glass transition in water. The simulation times employed in this work to predict the glass transitions of aqueous solutions were only nanoseconds long, resulting in extremely fast and unrealistic annealing times, compared to real experiments. Hence, slower cooling/heating rates should be used in future to simulate the formation of glassy water under realistic conditions.

Another area that needs refinement is the development of accurate forcefields that can exactly reproduce physical as well as chemical properties of the solutes and solvents. So far, no consistent mathematical model has been emerged to accurately describe the properties of the molecules that were studied, in particular water, under various thermodynamic conditions. This means that simulation findings could be biased depending upon the choice of the potential. Given the fact that water exhibits numerous

anomalous properties within the temperature regime in which the current investigations have been carried out, this is very important area that needs improvement.

Another important future direction will be to extend the study into other types of cryoprotectants, in particular polyalcohols, sugars and polysaccharides. In addition, the investigations of cryoprotectant mixtures in aqueous solution are likely to provide insight into the likely synergistic effects of such combinations. This is important because in most of the cases combination of several cryoprotectants (for example PVS) are used for preservation of the materials. With the advent of the state of the art computer architectures simulating these multi component systems for longer timescales will be possible.

REFERENCES

1. Jacobsen, A.& Pegg, D.E. (1984). Cryopreservation of Organs: A review. *Cryobiology,* 21, 377-384.
2. Bryant, G., Koster, K.L. & Wolfe J. (2001). Membrane behaviour in seeds and other systems at low water content: the various effects of solutes. *Seed Science Research*, 11, 17-25.
3. Fennema, O. (1966). An Overall view of low temperature food preservation. *Cryobiology*, 3, 197-213.
4. Takagi, H., Thinh, N.T. & Kyesmu, P.M. (1998).Cryopreservation of vegetatively propagated tropical crops by vitrification. *Proceedings of International symposium, Biotechnology*, 461, 485-491.
5. Hubalek Z. (2003) Protectants used in the cryopreservation of microorganisms. *Cryobiology*, 46, 205-229.
6. Edashige, K., Yamaji, Y., Kleinhans, F.W. & Kasai, M. (2003). Artificial Expression of Aquaporin-3 improves the survival of mouse oocytes after cryopreservation. *Biology of Reproduction*, 68, 87-94.
7. Engelmann, F. (2004). Plant Cryopreservation: Progress and Prospects. *In Vitro Cellular and Developmental Biology - Plant,* 40, 427-433.
8. Singhal, P.K. & Shrivastava, P. (2004). Challenges in sustainable development New Delhi: Anmol Publications PVT. LTD.
9. Rubinsky, B. (2003). Principles of Low Temperature Cell Preservation. *Heart Failure Reviews*, 8, 277-284.
10. Wolfe, J. & Bryant, G. (1999) Feezing, drying and/or vitrification of membrane-solute-water systems. *Cryobiology*, 39, 103-129.
11. Mazur, P. (1963) Kinetics of water loss from cells at subzero temperatures and likelihood of Intracellular Freezing. *Journal of General Physiology*, 47, 347-371.
12. Meryman, H.T. (1974). Freezing injury and its prevention in living cells *Annu Review of Biophysics and Bioengineering*, 3, 341-363.
13. Meryman, HT, Williams, R.J. & Douglas, M.S.(1977). Freezing injury from solution effects and its prevention by natural or artificial cryoprotection. *Cryobiology*, 14, 287-302.
14. Mazur, P., Seki, S., Pinn, I.L., Keinhans, F.W. & Edashige, K. (2005). Extra and intracellular ice formation in mouse oocytes. *Cryobiology*, 51, 29-53.
15. Zachariassen, K.E. & Kristiansen, E. (2000). Ice nucleation and Anti nucleation in Nature. *Cryobiology*, 41, 257-279.
16. Fahy, G.M., MacFarlane, D.R., Angell, C.A. & Meryman, H.T. (1984). Vitrification as an approach to Cryopreservation. *Cryobiology*, 21, 407-426.
17. Burke, M.J. & Lindow, S.E. (1990). Surface properties and size of the ice nucleation site in ice nucelation active bacteria: theoretical considerations. *Cryobiology*, 27, 80- 84.
18. Zachariasen, K.E., Pedersen S.A. & Hammel, H.T. (2004). Ice nucleation in solutions and freeze-avoiding insects-homogeneous or heterogeneous? *Cryobiology* , 48, 309-321.
19. Wolfe, J. & Bryant, G. (2001). Cellular cryobiology: thermodynamic and mechanical effects. *International Journal of Refrigeration*, 24, 438-450.
20. Bigg, E.K. (1953). The supercooling of water *Proceedings of Physical Society B* 66, 688-694.

21. Jaeger, M., Carin, M., Medale, M., & Tryggvason, G. (1999). The osmotic migration of cells in a solute gradient *Biophysical Journal* , 77, 1257-1267.
22. Slade, L. & Levine, H. (1988). Non equilibrium behaviour of small carbohydrate-water systems. *Pure and Applied Chemistry*, 60, 1841-1864.
23. Mazur, P., Rall, W.F. & Rigopoulos, N. (1981). Relative contributions of the fraction of unfrozen water and of salt concentration to the survival of slowly frozen human erythrocytes. *Biophysical Journal*, 36, 653-675.
24. Acker, J.P. & Mcgann, L.E. (2003). Protective effect of intracellular ice during freezing. *Cryobiology*, 46, 197-202.
25. Weiser, C.J. (1970). Cold resistance and injury in woody plants. *Science*, 169, 1269-1278.
26. Lovelock, J.E. (1953). The haemolysis of human red blood cells by freezing and thawing *Biochimica et Biophysica Acta*, 10, 414-426.
27. Lovelock, J.E. (1953) The mechanism of the protective action of glycerol against haemolysis by freezing and thawing. *Biochimica et Biophysica Acta* 11, 28-36.
28. Meryman, H.T. (1968). Modified model for the mechanism of freezing injury in erythrocytes. *Nature*. 218, 333-336.
29. Steponkus, P.L. (1984) Role of Plasma Membrane in Freezing Injury and Cold Acclimation. *Annual reviews of plant Physiology*, 35, 543-584.
30. Zimmerman, U., Scheurich, P., Pilwat, G. & Benz, R. (1981). Cells with Manipulated Functions: New Perspectives for Cell Biology, Medicine, and Technology. *Angewandte Chemie International Journal*, 20, 325-344.
31. Mazur, P. (1977). The role of intracellular freezing in the death of cells cooled at supraoptimal rates. *Cryobiology*, 14, 251-272.
32. Dowgert, M.F. & Steponkus, P.L. (1983). Effect of cold acclimation on intracellular ice formation in isolated protoplasts *Plant Physiology*, 72, 978-988.
33. Levitt, J.A. (1962). Sulf hydryl- Disulfide Hypothesis of Frost Injury and Resistance in Plants. *Journal of Theoretical Biology*, 3, 355-392.
34. Burke, M.J., Gusta, L.V., Quamme, H.A., Weiser, C.J. & Li, C.H. (1976). Freezing and injury in plants. *Annual reviews of plant Physiology*, 27, 507- 528.
35. Steponkus, P.L. (1996). Advances in Low Temperature Biology, Springer Verlag
36. Mazur, P. (1984). Freezing of living cells: mechanisms and implications. *American Journal of Physiology*, 247, C125- C147.
37. Muldrew, K. & Mcgann, L.E. (1990). Mechanisms of intracellular ice formation. *Biophysical Journal*, 57, 525-532.
38. Acker, J.P. & McGann, L.E. (2000). Cell- Cell Contact affects membrane integrity after intracellular freezing. *Cryobiology*, 40, 54-63.
39. Sherman, J.K. & Liu., K.C. (1973). Ultrastructural cryoinjury and cryoprotection of rough endoplasmic reticulum *Cryobiology*, 10, 104-118.
40. Sasikumar, R., Ramamohan, T.R. & Pai, B.C. (1989) Critical velocities for particle pushing by moving solidification fronts. *Acta Metallica*, 37, 2085-2091.
41. Bronstein, V.L., Itkin, Y.A. & Ishkov, G.S. (1981). Rejection and capture of cells by ice crystals on freezing aqueous solutions. *Journal of Crystal Growth* 52, 345-349.
42. Ishiguro, H. & Rubinsky, B. (1994). Mechanical interactions between ice crystals and red blood cells during directional solidification. *Cryobiology*, 31, 483-500.

43. Rubinsky, B. & Ikeda, M.A. (1985) . A cryomicroscope using directional solidification for the controlled freezing of biological material. *Cryobiology,* 22, 55-68.
44. Mazur, P. & Cole, K.W. (1985). Influence of cell concentration on the contribution of unfrozen fraction and salt concentration to the survival of slowly frozen human erythrocytes. *Cryobiology*, 22, 509-536.
45. Leebo, S.P. (1976). Freezing damage of bovine erythrocytes: simulation using glycerol concentration changes at subzero temperatures. *Cryobiology*, 13, 587-598.
46. Bryant, G., Pope, J.M. & Wolfe J. (1992). Low hydration phase properties of phospholipid mixtures - Evidence for dehydration-induced fluid fluid seperations. *European Biophysics Journal*, 21, 223-232.
47. Bryant, G. & Wolfe, J. (1989) Can hydration forces induce lateral phase seperations in lamellar phases? *European Biophysics Journal*, 16, 369-374.
48. Crowe, J. H., Oliver, A.E. & Tabin, F. (2002). Is there a single biochemical adapatation to anhydrobiosis? *Integral and Computational Biology*, 42, 497-503.
49. Wolfe, J. & Bryant, G. (2001). Cellular cryobiology: thermodynamic and mechanical effects. *International Journal of Refrigeration*, 24, 438-450.
50. Crowe, L.M. (2002). Lessons from nature: the role of sugars in anhydrobiosis. *Comparative Biochemistry and Physiology Part A*, 131, 505-513.
51. Koster, K.L., Lei, Y.P., Anderson, M., Martin, S. & Bryant, G. (2000). Effects of vitrified and non vitirfied sugars on Phosphatidylcholine Fluid to Gel Phase Transitions. *Biophysical Journal*, 78, 1932-1946.
52. Giles, C.H. & Mackay, R.B. (1962). Studies in hydrogen bond formation- XI. Reactions between a variety of carbohydrates and proteins in aqueous solutions. *Journal of Biological Chemistry,* 237, 3388-3392.
53. Leekumjorn, S. & Sum, A.K. (2006). Molecular invetigation of the interactions of trehalose with lipid bilayers of DPPC, DPPE and their mixture. *Molecular Simulation*, 32, 219-230.
54. Crowe, J.H, Hoekstra, F.A. & Crowe, L.M. (1992). Anhydrobiosis. *Annual Review of Physiology*, 54, 579-599.
55. Koster, K.L & Leopold, A.C. (1988). Sugars and dessication tolerance in seeds. *Plant Physiology*, 88, 829-832.
56. Meryman, H.T., Williams, R.J. & Douglas, M.S. (1977). Freezing injury from solution effects and its prevention by natural or artificial cryoprotection. *Cryobiology*, 14, 287-302.
57. Meryman, HT. (1971). Cryoprotective agents. *Cryobiology*, 8, 173-183.
58. McGann, L.E.(1978). Differing actions of penetrating and nonpenetrating cryoprotective agents. *Cryobiology*, 15, 382-390.
59. Zachariasen, K.E, Kristiansen, E., Pedersen, S.A. & Hammel, H.T. (2004) Ice nucleation in solutions and freeze-avoiding insects-homogeneous or heterogeneous? *Cryobiology*, 48, 309-321.
60. Conrad, P.B. & de Pablo, J.J. (1999). Computer simulation of the Cryoprotectant Disaccharide alpha, alpha- Trehalose in Aqueous Solution (change alpha to greek letter). *Journal of Physical Chemistry B*, 103, 4049-4055.
61. Vitkova, V., Genova, J., Mitov, M.D. & Bivas, I. (2006). Sugars in the aqueous phase change the mechanical properties of lipid mono and bilayers. *Molecular crystals and liquid crystals*, 449, 95-106.
62. Lee, B.W., Faller, R., Sum, A.K., Vattulainen, I., Patra, M. & Karttunen, M. (2005). Structural effects of small molecules on phospholipid bilayers

investigated by molecular simulations. *Fluid Phase Equilibria*, 228-229,135-140.

63. Crowe, J.H., Crowe, L.M., Carpenter, C.A. & Wistrom, C.A. (1987). Stabilization of dry phospholipid bilayers and proteins by sugars *Biochemical Journal*, 242, 1-10.
64. Branca, C., Faraone, A., Magazu, S., Maisano, G., Mangione, A., Pappas, C. & Triolo, A. (2002) Characterization of trehalose aqueous solutions by neutron spin echo. *Applied Physics A,* 74, S461 - S462.
65. Gupta, C.K., Leszczynski, J., Gupta, R.K. & Siber, G.R. (1996). Stabilization of respiratory syncytial virus (RSV) against thermal inactivation of freeze thaw cycles for development and control of RSV vaccines and immune globulins. *Vaccine*, 14, 1417-1420.
66. Breierova, E. (1994). Cryoprotection of psychrophilic yeast species by the use of additives with cryoprotective media. *Cryoletters*, 15, 191-197.
67. Declerck, S. & Coppenolle, A. (2000). Cryopreservation of entrapped monoxeniacally produced spores of an arbuscular mycorrhizal fungus. *New Phytologist*, 148, 169-176.
68. Feofilova, E.P. (2003) Deceleration of vital activity as a universal biochemical mechanism ensuring adaptation of microorganisms to stress factors : A review. *Applied Biochemistry and Microbiology,* 39, 1-18.
69. Turner, S., Senaratna, T., Touchell, D., Bunn, E., Dixon, K. & Tan, B. (2001). Stereochemical arrangement of hydroxyl groups in sugar and polyalcohol molecules as an important factor in effective cryopreservation *Plant Science,* 160, 489-497.
70. Postgate, J.R. & Hunter, J.R. (1961). On the survival of frozen bacteria. *Journal of General Microbiology*, 26, 367-378.
71. Tsuji, K. (1966). Liquid Nitrogen preservation of Saccharomyces carlsbergensis and its use in a rapid biological assay of Vitamin B6 (pyridoxine). *Applied Microbiology*, 14, 456-461.
72. Doebbler, G.F. (1966). Cryoprotective compounds: review and discussion of structure and function. *Cryobiology*, 3, 2-11.
73. Sehgal, O.P. & Das, P.D. (1975). Effect of freezing on conformation and stability of the virions of southern bean mosaic virus. *Virology*, 64, 180-186.
74. Calcott, P.H. & Macleod, R.A. (1975). Survival of Escherichia coli from freeze thaw damage. *Canadian Journal of Microbiology*, 21, 1960-1968.
75. Daily, W.A.& Higgens, C.E.(1973). Preservation and storage of microorganisms in the gas phase of liquid nitrogen. *Cryobiology*, 10, 364-367.
76. Bodas, K., Brenning, C., Diller, K.R. & Brand, J.J. (1995). Cryopreservation of blue-green and eukaryotic algae in the culture collection at the University of Texas at Austin. *Cryoletters*, 16, 267-274.
77. Lewis, J.G., Learmonth, R.P. & Watson, K. (1994). Cryoprotection of yeast by alcohols during rapid freezing. *Cryobiology*, 31, 193-198.
78. Levine, N.D. & Marquardt, W.C. (1955). The effect of glycerol and related compounds on survival of Trichomonas foetus at freezing temperatures. *Journal of Protozoology*, 2, 100-107.
79. Sakurada, M., Tsuzuki, Y., Morgavi, D.P., Tomita, Y. & Onodera, R. (1995). Simple method for cryopreservation of an anaerobic rumen fungus using ethylene glycol and rumen fluid. *FEMS Microbiology Letters*, 127, 171-174.
80. Sandskar, B. & Magalhaes, B. (1994). Cryopreservation of Zoophthora radicans in liquid Nitrogen. *Cryobiology*, 31, 206-213.

81. Boutron, P. & Arnaud, F. (1984). Comparison of the cryoprotection of red blood cells by 1,2-Propanediol and Glycerol. *Cryobiology*, 21, 348-358.
82. Boutron, P. & Arnaud, F. (1984). Comparison of the cryoprotection of red blood cells by 1,2-Propanediol and glycerol. *Cryobiology*, 21, 348-358.
83. Francis, E. (1932). Duration of viability of Pasteurella Pestis. *Public Health Reports*, 47, 1287-1294.
84. Hollander, D.H & Nell, E.E. (1954). Improved preservation of Treponema pallidium and other bacteria by freezing with glycerol. *Applied Microbiology,* 2, 164-170.
85. Fahy, G.M., Wowk, B., Wu, J., Phan, J., Rasch, C., Chang, A. & Zendejas, E. (2004). Cryopreservation of organs by vitrification: perspectives and recent advances. *Cryobiology*, 48, 157-178.
86. Kono, S., Kuwano, K., Ninomyia, M., Onishi, J. & Saga, N. (1997). Cryopreservation of Enteromorpha intestinalis in liquid Nitrogen. *Journal of Marine Biotechnology* , 6, 220-223.
87. Moore, A.I., Squires E.L. & Graham, J. K. (2005). Adding cholesterol to the stallion sperm plasma membrane improves cryosurvival. *Cryobiology*, 51, 241-249.
88. Greiff, D. & Rightsel, W. (1964). Effects of freezing, storage at low temperature, and drying by sublimation in vacuo on the activities of measles virus. *Nature,* 202, 624-625.
89. Meyle, J.S. & Kempf, J.E. (1964). Preservation of T2 bacteriophage with liquid Nitrogen. *Applied Microbiology*, 12, 400-402.
90. Gibson, C.A., Landerkin, G.B. & Morse, P.M. (1966). Effects of additives on the survival of lactic streptococci in forzen storage. *Applied Microbiology,* 14, 665-669.
91. Nash, T., Postgate, J. R. & Hunter, J.R. (1963). Similar effects of various neutral solutes on the survival of Aerobacteraerogenes and of red blood cells after freezing and thawing. *Nature*, 199, 1113.
92. Collins, W.E. & Jeffrey, G.M. (1963). The use of dimethylsulfoxide in the low temperature frozen preservation of experimental malarias. *Journal of Parasitology*, 49, 524-525.
93. Gurtovenko, A.A. & Anwar, A. (2007). Modulating the structure and properties of cell membranes: the molecular mechanism of action of dimethyl sulfoxide. *Journal of Physical Chemistry B*, 111, 10453-10460.
94. Vaisman, I.I. & Berkovitz, M.L. (1992). Local strucutral order and molecular associations in water-DMSO mixtures. Molecular dynamics study. *Journal of American Chemical Society*, 114, 7889-7896.
95. Glasel, J.A. (1970). Deutron magnetic relaxation studies on the solution properties of some denaturing agents and surfactants. *Journal of American Chemical Society*, 92, 372-375
96. Lovelock, J.E. (1954). The mechanism of the protective action of glycerol against haemolysis by freezing and thawing. *Biochemical Journal*, 56, 265-270.
97. Alvarenga, M.A., Papa, F.O., Landim-Alvarenga, F.C. & Mendeiros, A.S.L. (2005). Amides as cryoprotectants for freezing stallion semen:a review. *Animal Reproduction*, 89, 105-113.
98. Fahy, G.M. & Wowk, B. (2007). Inventor Methods and compositions for the cryopreservation of organs. United states.
99. Johanssen, E. (1972). Malt extract as protective medium for lactic acid bacteria in cryopreservation. *Journal of Applied Bacteriology*. 35, 423-429.

100. Vitanov, T. & Petukhov, V.G. (1973). Effect of low temperature on bacteria and protective effect of polyvinylpyrrolidone of different molecular weight. *Mikrobiologia*, 42, 647-650.
101. Morris, G.J., Clarke, A. & Fuller, B.J. (1980). Methanol as a cryoprotective additive for Chlorella. *Cryoletters*, 1, 121-128.
102. Bovarnick, M.R., Miller, J.C. & Synder, J.C. (1950). The influence of certain salts, amino acids, sugars, and proteins on the stability of rickettsiae. *Journal of Bacteriology*, 59, 509-522.
103. Takano, M., Sado, J.I., Ogawa, T. & Terui, G. (1973). Freezing and freeze drying of Spirulina plantesis. *Cryobiology* , 10, 440-444.
104. Ma, Y., Szostkiewicz, I., Korte, A., Moes, D. & Yang, Y. (2009). Regulators of PP2C Phosphatase Activity Function as Abscisic Acid Sensors. *Science,* 324, 1064-1067.
105. Notman, N. (2009). Organic compound aids thirsty plants. *Chemistry World,* 6, 22.
106. Pennisi, E. (2009). Stressed Out Over a Stress Hormone. *Science*, 324, 1012-1013.
107. Park, S.Y., Fung, P., Nishimura, N., Jensen, D.R., Fujii, H., Zhao, Y., Lumba, S., Santiago, J., Rodrigues, A., Chow, T.F., Alfred, S.E., Bonetta, D., Finkelstein, R., Provart, N.J., Desveaux, D., Rodrigues, P.L., McCourt, P., Zhu, J., Schroeder, J.L., Volkman, B.F. & Cutler, S.R. (2009). Abscisic Acid Inhibits Type 2C Protein Phosphatases via the PYR/PYL Family of Start proteins. *Science*, 324, 1068-1071.
108. Ruwart, M.J., Holland, J.F. & Haug, A. (1975). Flurimetric Evidence of Interactions Involving Cryoprotectants and Biomolecules. *Cryobiology*, 12, 26-33.
109. Uragami, A., Sakai, A., Nagai, M. & Takahashi, T. (1990). Cryopreservation by vitrification of cultured cells and somatic embryos from mesophyl tissues of Aspraragus. *Acta Horticulture*, 271, 109-116.
110. Volk, G.M. & Walters C. (2006). Plant vitrification solution 2 lowers water content and alters freezing behaviour in shoot tips during cryopreservation. *Cryobiology*, 52, 48-61.
111. Hirai, D., Shirai, K., Shirai, S. & Sakai, A. (1998). Cryopreservation of in vitro-grown meristems of strawberry (Fragaria * ananassa Duch.) by encapsulation-vitrification. *Euphytica*, 101, 109-115.
112. Cryopreservation manual. *Nalge Nunc International*.
113. Leekumjorn, S. & Sum, A.S. (2008). Molecular dynamics study on the stabilisation of dehydrated lipid bilayers with glucose and trehalose. *Journal of Physical Chemistry B*, 112, 10732-10740.
114. Tormanen, C.D. (1992). Cryoprotection of purified rat kidney transamidinase by Polyethylene Glycol. *Cryobiology*, 29, 511-518.
115. Heber, U.W. & Santarius, K.A. (1963). Loss of Adenosine Triphosphate Synthesis caused by Freezing and its relationship to Frost Hardiness Problems. *Plant Physiology*, 712-719.
116. Belton, P.S. & Gill, A.M. (1994). IR and Raman spectroscopic studies of the interaction of trehalose with hen egg white lysozyme. *Biopolymers*, 34, 957-961.
117. Sun, W.Q., Leopold, A.C., Crowe, L.M. & Crowe, J.H. (1996). Stability of Dry Liposomes in Sugar Glasses. *Biophysical Journal*, 70, 1769-1976.

118. Markarian, S.A., Bonora, S., Bagramyan, K.A. & Arakelyan VB. (2004). Glass-forming property of the system diethyl sulphoxide/water and its cryoprotective action of Escherichia coli survival. *Cryobiology* , 49, 1-9.
119. Ryynaenen, L. & Aronen T. (2005). Vitrification, a complementory cryopreservation method for Betula Pendula Roth. *Cryobiology*, 51, 208-219.
120. Wowk, B., Leitl, E., Rasch, C.M., Mesbah-Karimi, N., Harris, S.B. & Fahy, G.M. (2000). Vitrification enhancement by synthetic ice blocking agents. *Cryobiology*, 40, 228-236.
121. Fahy, G.M., Levy, D.I. & Ali, S.E. (1987). Some emerging principles underlying the physical properties, biological actions, and utility of vitrification solutions. *Cryobiology* , 24, 196-213.
122. Spencer, J.N., Berger, S.K., Powell, C.R., Henning, B.D., Furman, G.S., Loffredo, W.M., Rydberg, E.M., Neubert, R.A., Shoop, C.E. & Blauch, D.N. (1981). Amide interactions in Aqueous and Organic Medium. *Journal of Physical Chemistry* , 85, 1236-1241.
123. Baudot, A., Cacela, C., Duarte, M.L. & Fausto, R. (2002). Thermal study of simple amino-alcohol solutions. *Cryobiology*, 44, 150-160.
124. Wolfe, J. & Bryant, G. (1999). Feezing, drying and/or vitrification of membrane-solute-water systems. *Cryobiology*, 39, 103-129.
125. Santarius, K.A. & Bauer, J. (1983). Cryopreservation of Spinach chloroplast Membranes by low- molecular weight carbohydrates. *Cryobiology*, 20, 83-89.
126. Crowe, J.H., Crowe, L.M., Wolkers W.F., Oliver, A.E., Ma X., Auh, J.H., Tang M., Zhu S., Norris J. & Tablin, F. (2005). Stabilization of Dry Mammalian Cells : Lessons from Nature. *Integral and Computational Biology*, 45, 810-820.
127. Yoon, Y.H., Pope, J.N. & Wolfe, J. (1998). The effects of solutes on the freezing properties of and hydration forces in lipid lamellar phases. *Biophysical Journal*, 74, 1949-1965.
128. Branca, C., Magazu, S., Maisano, G. & Migliardo, P. (2000). Experimental study of the hydration properties of homologues disaccharides. *Journal of Biological Physics*, 26, 295-306.
129. Williams, R.J. & Leopold, A.C. (1989). The glassy state in corn embryos. *Plant Physiology*, 89, 977-981.
130. Crowe, J.H., Crowe, L.M. & Chapman, D. (1984). Preservation of Membranes in Anhydrobiotic Organisms: The role of Trehalose. *Science*, 223, 701-703.
131. Lelong, G., Price, D.L., Douy, A., Kline, S. & Saboungi, M. (2005). Molecular Dynamics of confined glucose solutions. *The Journal of Chemical Physics,* 122, 164504.
132. Magazu, S., Migliardo, F. & Telling, M.T.F. (2007). Study of the dynamical properties of water in disaccharide solutions. *European Biophysics Journal* 36, 163-171.
133. Magazu, S., Maisano, G., Migliardo, F. & Mondelli, C. (2004). Mean square Displacement Relationship in Bioprotectant Systems by Elastic Neutron Scattering. *Biophysical Journal*, 86, 3241-3249.
134. Constaca, C. & Hincha D.K. (2006). Monosaccharide composition, chain length and linkage type influence the interactions pf oligosaccharides with dry phosphatidylcholine membranes. *Biochimica et Biophysica Acta*, 1758, 680-691.
135. Ullrich, H. & Heber U. (1961). Ursachen der Frostresistenz bei Winterweizen. IV Mitteilung Das Verhalten von Fermenten und Fermentsystemen gegenuber tiefen Temperaturen *Planta*, 57, 370-390.

136. Umemura, M., Hayashi, S., Nakagawa, T., Urakawa, H. & Kajiwara, K. (2003). Structure of water molecules in aqueous solutions od i- and penta-D-glucopyranoses using Molecular dynamics simulaiton. *Journal of Molecular Structure (Theochem)*, 639, 69-86.
137. Ekdawi-Sever, N.C., Conrad, P.B. & Pablo JJd. (2001). Molecular Simulation of Sucrose Solutions near the Glass Transition Temperature. *Journal of Physical Chemistry A*, 105, 734-742.
138. Dashnau, J.L., Nucci, N.V., Sharp, K.A. & Vanderkooi, J.M. (2006). Hydrogen bonding and the cryoprotective properties of Glycerol/Water Mixtures. *Journal of Physical Chemistry B*, 110, 13670-13677.
139. Cottone G, Cordone, L. & Ciccoti, G. (2001). Molecular dynamics simulation of carboxy-myoglobin embedded in a trehalose , *Biophysical Journal,* 80, 931-938.
140. Lee, S.L., Debenedetti, P.G. & Errington, J.R. (2005). A Computational study of hydration, solution structure, and dynamcis in dilute carbohydrate solutions. *The Journal of Chemical Physics*,122, 204511.
141. Branca, C., Magazu, V., Maisano, G., Migliardo, F. & Soper, A.K. (2002). Study on Destructuring effect of trehalose on water by neutron diffraction. *Applied Physics A Material Science & Engineering*, 74, S450 - 451.
142. Crowe, J.H., Crowe, L.M. & Chapman, D. (1984). Preservation of membranes in anhydrobiotic organisms: the role of trehalose *Science*, 223, 701-703.
143. Dashnau, J.L., Sharp, K.A. & Vanderkooi, J.M. (2005). Carbohydrate intramolecular hydrogen bonding cooperativity and its effect on water structure. *Journal of Physical Chemistry B*, 109, 24152-24159.
144. Rao, B.G. & Singh, U.C. (1992). A free energy perturbation study of solvation in methanol and dimethyl sulfoxide. *Journal of American Chemical Society,* 112, 3803-3811.
145. Harpham, M.R., Levinger, N.E. & Ladanyi, B.M (2008). An investigation of Water Dynamics in Binary Mixtures of Water and Dimethyl Sulfoxide. *Journal of Physical Chemistry B*, 112, 283-293.
146. Sum, A.K., Feller, R. & Pablo, J.J. (2003) Molecular Simulation Study of Phospholipid Bilayers and Insights of the Interactions with Disaccharides. *Biophysical Journal*, 85, 2830-2844.
147. Koster, K.L., Webb, M.S., Briant, G. & Lynch, D.V. (1994). Interactions between soluble sugars and POPC during dehydration : vitrification of sugars alters the phase behaviour of the phospholipid *Biochimica et Biophysica Acta* 1193, 143-150.
148. Koster, K.L., Yoon, P.L., Anderson, M., Martin, S. & Bryant, G. (2000). Effects of vitrified and non vitirfied sugars on Phosphatidylcholine Fluid to Gel Phase Transitions. *Biophysical Journal*, 78, 1932-1946.
149. Ricker, J.V., Tsvetkova, N.M., Wolkers, W.F., Leidy, C., Tablin, F., Longo, M. & Crowe, J.H. (2003). Trehalose Maintains Phase Seperation in an Air Dried Binary Lipid Mixture. *Biophysical Journal,* 84, 3045-3051.
150. Chiu, S.W., Jacobsson, E., Subramanian, S. & Scott, H.L. (1999). Combined Monte Carlo and Molecular Dynamics Simulation of Fully hydrated Dioleyl and Palmitoyl-oleyl Phosphatidylcholine Lipid Bilayers. *Biophysical Journal,* 77, 2462-2469.
151. Pereira, C.S., Lins, R.D., Chandrasekhar, I., Freitas, L.C.G. & Huenenberger, P.H. (2004). Interaction of the Disaccharide Trehalose with a Phospholipid bilayer: A Molecular Dynamics Study. *Biophysical Journal*, 86, 2273-2285.

152. Mashl, R.J., Scott, H.L., Subramaniam, S. & Jakobsson E.(2001). Molecular dynamics simulation of Dioleolphosphatidylcholine lipid bilayers at differing levels of hydration. . *Biophysical Journal,* 81, 3005-3015.
153. Blieck, J., Affouard, F., Bordat, P., Lerbret, A. & Descamps, M. (2005). Molecular dynamics simulations of glycerol glass- forming liquid. *Chemical Physics*, 317, 253-257.
154. Sum, A.K. & Pablo, J.J. (2003). Molecular Simulation Study on the Influence of Dimethyl Sulfoxide on the structure of Phospholipid Bilayers. *Biophysical Journal*, 85, 3636-3645.
155. Debenedetti P.G. (1996). Metastable liquids: Princeton University Press.
156. Angell, C.A. (1995). Formation of Glasses from Liquids and Biopolymers. *Science*, 267, 1924.
157. Gutsow, I., Grigorova, T.S. & Todorova, S. (2002). Kinetics of vitirification, glass relaxation and devitrification: a unified treatment. *Journal of Non-crystalline Solids*, 304, 4-18.
158. Slade, L. & Levine H. (1988). Non-equilibrium behaviour of small carbohydrate - water systems. *Pure and Applied Chemistry*, 60, 1841-1864.
159. Gao, C., Zhou, G.Y., Xu, Y. & Hua, T.C. (2005). Glass transition and enthalpy relaxation of ethylene glycol and its aqueous solution. *Thermochimica Acta,* 435, 38-43.
160. Green, J.L. & Angell, C.A. (1989). Phase Relations and Vitrification in Saccharide-Water Solutions and the Trehalose Anomaly. *Journal of Physical Chemistry*, 93, 2880-2882.
161. Chen, T., Fowler, A. & Toner, M. (2000). Literature review: Supplemented phase diagram of the Trehalose-Water binary mixture. *Cryobiology*, 40, 277-282.
162. Suggert, A. & Clark, A.H. (1976). Molecular motion and Interactions in Aqueous Carbohydrate Solutions 1. Dielectric-Relaxation Studies. *Journal of Solution Chemistry*, 5, 1-15.
163. Koster, K.L., Webb, M.S., Bryant, G. & Lynch, D.V. (1994). Interactions between soluble sugars and POPC during dehydration: vitrification of sugars alters the phase behaviour of the phospholipid *Biochimica et Biophysica Acta,* 1193, 143-150.
164. Crowe, J.H., Carpenter, J.F. & Crowe, L.M. (1998). The role of vitrification in anhydrobiosis. *Annual Reviews of Physiology*, 60, 73-103.
165. Crowe, J.H., Carpenter, J.F. & Crowe, L.M. (1998). The role of vitrification in anhydrobiosis. *Annual Reviews of Physiology*, 60,73-103.
166. Angell, C.A. (2002). Liquid Fragility and the Glass Transition in Water and Aqueous Solutions. *Chemical Reviews*, 102, 2627- 2650.
167. Qin, Q. & McKenna, G.B. (2006) Correlation between dynamic fragility and glass transition temperature for different classes of glass forming liquids. *Journal of Non-crystalline Solids*, 352, 2977-2985.
168. Casalini, R. & Roland, C.M. (2005). Why liquids are fragile. *Physical Review E*, 72, 031503.
169. Magazu, S., Maisano, G., Migliardo, P., Musolino, A.M. & Villari, V. (1998). Fragile like behaviour and H-bond interactions of the glass forming water-trehalose system. *Philosophical Magazine B*, 77, 655-661.
170. Debenedetti, P.G. & Stillinger, F.H. (2001) Supercooled liquids and the glass transition. *Nature*, 410, 259-267.

171. Magazu, S., Maisano, G., Migliardo, F. & Mondelli, C. (2004). alpha-alpha(change to greek letter later)-Trehalose/Water Solutions. VII: An Elastic Incoherent Neutron Scattering Study on Fragility. *Journal Physical Chemistry B*, 108, 13580-13585.
172. Richert, R. & Angell, C.A. (1998). Dynamics of glass-forming liquids. V. On the link between molecular dynamics and configurational entropy. *Journal of Chemical Physics*, 108, 9016-9026.
173. Franks, F. Water- a matrix of life (2000) second ed. Oxford: Royal Society of Chemistry
174. Debenedetti, P.G. & Stanely, H.E. (2003). Supercooled and glassy water. *Physics Today*, June, 40-46.
175. Souda, R. (2007). Effects of methanol on crystallisation of water in the deeply supercooled region. *Physical Review B*, 75, 184116, 1 -7.
176. Netz, P.A., Starr, F., Barbosa, M.C. & Stanley, H.E. (2004). Computer Simulaiton of Dynamical Anomalies in strechted water. *Brazilian Journal of Physics*, 34, 24-31.
177. Poole, P.H., Sciortino, F., Essman, U. & Stanley, H.E. (1992). Phase behaviour of metastable water. *Nature*, 360, 324-328.
178. Stanley, H.E., Kumar, P., Xu, L., Yan, Z., Mazza, M.G., Buldyrev, S.V., Chen, S.H. & Mallamace, F. (2007). The puzzling unsolved mysteries of liquid water : Some recent progress. *Physica A*, 386, 729-743.
179. Bosio, L., Johari, G.P. & Teixeira, J. (1996) X-Ray Study of High-Density Amrophous Water. *Physical Review Letters*, 56, 460-464.
180. Head-Gordon, T. & Hura, G. (2002). Water Structure from Scattering Experiments and Simulation. *Chemical Reviews*, 102, 2651-2670.
181. Geiger, A. & Stanley, H.E. (1982). Low-Density "Patches" in the hydrogen bond Network of Liquid Water: Evidence from Molecular-Dynamics Computer Simulations. *Physical Review Letters*, 49, 1749-1751.
182. Starr, F.W., Bellisent-Funel, M. & Stanley, H.E.(1999). Structure of supercooled and glassy state water under pressure. *Physical Review E*, 60, 1084-1087.
183. Errington, J.R. & Debenedetti, P.G. (2000). Relationship between structural order and the anomalies of liquid water. *Nature,* 409, 318-321.
184. Errington, J.R. & Debenedetti, P.G. (2000) Relationship between structural order and the anomalies of liquid water. *Nature*, 409, 318-321.
185. Canpolat, M., Starr, F.W., Scala, A., Lahijany, S., Reza, M., Mishima, O., Havlin, S. & Stanley, H.E. (1998). Local structural heterogenities in Liquid water under pressure. *Chemical Physics Letters*, 294, 9-12.
186. Stanley, H.E., Kumar, P., Xu, L., Yan, Z., Mazza, M.G., Buldyrev, S.V., Chen, S.H. & Mallamace, F. (2008). Liquid Polymorphism: Possible relation to the anomalous bahaviour of water. *The European Physical Journal special topics*, 161, 1-17.
187. Mishima, O. & Stanley, H.E. (1998). The relationship between liquid, supercooled and glassy water. *Nature*, 396, 329-335.
188. Yamada, M., Mossa, S., Stanley, H.E. & Sciortino, F. (2002). Interplay between Time-Temperature Transofrmation and the Liquid- Liquid phase transition in Water. *Physical Review Letters*, 88, 195701, 1-4.
189. Harrington, S., Zhang, R., Poole, P.H., Sciortino, F. & Stanley, H.E. (1997). Liquid-Liquid Phase Transition: Evidence from Simulation. *Physical Review Letters*, 78, 2409-2412.

190. Van Gunsteren, W.F., Bakowies, D., Baron, R., Chandrasekhar, I., Christen, M., Daura, X., Gee, P., Geerke, D.P., Glattli, A., Huenenberger, P.H., Kastenholtz, M.A., Oostenbrink, C., Schenk, M., Trzesniak, D., Van der Vegt, N.F.A. & Yu, H.B. (2006). Biolmolecular modeling: Goals, Problems, Perspectives. *Angewandte Chemie International Journal*, 45, 4064-4092.
191. Van Der Spoel, D., Lindahl, E., Hess, B., Groenhof, G., Mark, A.E. & Berendsen, H.J. (2005). GROMACS: fast, flexible and free. *Journal of Computational Chemistry*, 26, 1701-1718.
192. Ryckaert, J-P, Ciccotti, G. & Berendsen, H.J.C. (1977). Numerical integration of the cartesian equations of motion of a system with constraints: Molecular dynamics of n-alkanes. *Journal of Computational Physics*, 23, 327-341.
193. Ewald, P.P. (1921). Die Berechnung optischer und elektrostasticher Gitterpotentiale. *Annals of Physics*, 64, 253-287.
194. Toukmaji, A.Y. & Board, J.A. (1996) Ewald summation techniques in perspective: A survey. .
195. Darden, T., York, D. & Pedersen, L. (1993). Particle mesh Ewald: An N log (N) method for Ewald sums in large systems. *Journal of Chemical Physics*, 98, 10089-10092.
196. Van der Spoel, D., Lindhal, E., Hess, B., Van Buuren, A.R., Apol, E., Meulenhoff, P.J., Tieleman, D.P., Sijbers, A.L.T.M., Feenstra, K.A., Van Drunen, R. & Berendsen, H.J.C. (2005) Gromacs User Manual version 3.3.3.
197. Giovambattista, N., Angell, C.A., Sciortino, F. & Stanley, H.E. (2004). Glass-transition temperature of water: A Simulation study. *Physical Review Letters*, 93, 047801.
198. Stillinger, F.H. (1980). Water Revisited, *Science*, 209, 451-457.
199. Guillot, B. (2002). A Reappraisal of what we have learnt during three decades of computer simulations on water. *Journal of Molecular Liquids*, 101, 219-260.
200. Stillinger, F.H. & Rahman, A. (1974). Molecular dynamics study of liquid water under high compression. *Journal of Chemical Physics*, 61, 4973-4980.
201. Guillot, B. & Guissani, Y. (2001). How to build a better pair potential for water. *Journal of Chemical Physics*, 114, 6720-6733.
202. Bernal, J.D. & Fowler, R.H. (1933). A theory of water and ionic solution, with particular reference to hydrogen and hydroxyl ions. *The Journal of Chemical Physics*, 1, 515-548.
203. Stillinger, F.H. & Rahman, A. (1974). Improved simulation of liquid water by molecular dynamics. *Journal of Chemical Physics*, 60, 1545-1557.
204. Head-Gordon, T. & Stillinger, F.H. (1992). An orientational perturbation theory for pure liquid water. *Journal of Chemical Physics*, 98, 3313-3327.
205. Lie, G.C., Clementi, E. & Yoshimine, M. (1975). Study of the structure of molecular complexes. Monte Carlo simulation of liquid water with a configuration interaction pair potential. *Journal of Chemical Physics*, 64, 2314-2323.
206. Berendsen, H.J.C., Postma, J.P.M., Van Gunsteren, W.F. & Hermans, J. (1981) Intermolecular forces. In: Pullman B, editor: Dordrecht.
207. Jorgensen, W.J., Chandrasekhar, J., Madura, J.D., Impey, R.W. & Klein, M.L. (1983). Comparison of simple potential functions for simulating liquid water. *Journal of Chemical Physics*, 79, 926-935.
208. Watanabe, K. & Klein, M.L. (1989) Effective pair potentials and the properties of water. *Chemical Physics*, 131, 157-167.

209. Errington, J.R. & Panagiotopoulos, A.Z. (1998). A fixed point charge model for water optimized to the vapor-liquid coexistence properties. *Journal of Physical Chemistry B*, 102, 7470-7475.
210. Mahoney, M.W. & Jorgensen, W.L. (2000). A five site model for liquid water and the reproduction of the density anomaly by rigid, non polarizable potential functions. *Journal of Chemical Physics*, 112, 8910-8922.
211. Grigera, J.R. (2001). An effective pair potential for heavy water. *Journal of Chemical Physics*, 114, 8064-8067.
212. Lemberg, H.W. & Stillinger, F.H. (1974). Central-force model for liquid water. *Journal of Chemical Physics*, 62, 1677-1690.
213. Rahman, A., Stillinger, F.H. & Lemberg, H.L. (1975). Study of a central force model for liquid water by molecular dynamics. *Journal of Chemical Physics*, 63, 5223-5230.
214. Duh, D.M., Perera, D.N. & Haymet, A.D.J. (1994). Structure and properties of the CF1 central force model of water: Integral equation theory. *Journal of Chemical Physics*, 102, 3737-3746.
215. Bopp, P., Jansco, G. & Heinzinger, K. (1983). An improved potential for non-rigid water molecules in the liquid phase. *Chemical Physics Letters,* 98,129-133.
216. Toukan, K. & Rahman, A. (1985). Molecular dynamics study of atomic motions in water. *Physical Review B*, 31, 2643-2648.
217. Lie, G.C. & Clementi, E. (1986). Molecular-dynamics simulation of liquid water with an ab initio flexible water-water interaction potential. *Physical Review A*, 33, 2679-2693.
218. Cieplak, P., Kollman, P. & Lybrand, T.A. (1990). A new water potential including polarization: Application to gas-phase, liquid, and crystal properties of water. *Journal of Chemical Physics*, 92, 6755-6760.
219. Zhu, S.B., Yao, S., Zhu, J.B., Singh, S. & Robinson, G.W. (1991). A flexible/polarizable simple point charge water model. *Journal of Physical Chemistry*, 95, 6211-6217.
220. Corongiu, G. (1992). Molecular dynamics simulation for liquid water using a polarizable and flexible potential. *International Journal of Quantum Chemistry*, 42, 1209-1235.
221. Saint-Martin, H., Medina, Llanos, C. & Ortega-Blake, I. (1990). Non additivity in an analytical intermolecular potential: the water-water interaction. *Journal of Chemical Physics*, 93, 6448-6452.
222. Nieser, U., Corongiu, G., Clementi, E., Kneller, G.R. & Bhattacharya, D.K. (1990). Molecular dynamics simulations of liquid water using the NCC ab initio potential. *Journal of Physical Chemistry*, 94, 7949-7956.
223. Wallqvist, A., Ahlstrom, P. & Karlstrom, G. (1990). A new intermolecular energy calculation scheme: Applications to potential surface and liquid properties of water. *Journal of Physical Chemistry,* 94, 1649-1656.
224. Sprik, M. (1991). Hydrogen bonding and the static dielectric constant in liquid water. *Journal of Chemical Physics*, 95, 6762-6769.
225. Kozack, R.E. & Jordan, P.C. (1992). Polarizability effects in a four-charge model for water. *Journal of Chemical Physics*, 96, 3120-3130.
226. Millot, C., Soetens, J.C., Costa, M.T.C., Hodges, M.P. & Stone, A.J. (1998). Revised anisotropic site potentials for the water dimer and calculated properties. *Journal of Physical Chemistry A*, 754-770.
227. Dang, L.X. (1992). The non additive intermolecular potential for water revisited. *Journal of Chemical Physics*, 97, 2659-2660.

228. Svishchev, I.M., Kusalik, P.G., Wang, J. & Boyd, R.J. (1996). Polarizable point-charge model for water: results under normal and extreme conditions. *Journal of Chemical Physics*, 105, 4742-4750.
229. Rick, S.W., Stuart, S.J. & Berne, B.J. (1994). Dynamical fluctuating charge force fields: application to liquid water. *Journal of Chemical Physics*, 101, 6141-6156.
230. Borgis, D. & Staib, A. (1995). A semi impirical quantum polarization model for water. *Chemical Physics Letters,* 238, 187-192.
231. Chialvo, A.A. & Cummings, P.T. (1996). Engineering a simple polarizable model for the molecular simulation of water applicable over wide range of state conditions. *Journal of Chemical Physics*, 105, 8274-8281.
232. Bursulaya, B.D. & Kim, H.J. (1998). Generalised molecular mechanics including quantum electronic structure variation of polar solvents. I. Theoretical formulation via a truncated adiabatic basis set description. *Journal of Chemical Physics*, 108, 3277-3285.
233. Horn, H.W., Swope, W.C., Pitera, J.W., Madura, J.D., Dick, T.J., Hura, G.L., & Head-Gordon, T. (2004). Development of an improved four-site water model for biomolecular simulations: TIP4P-Ew. *Journal of Chemical Physics*, 120, 9665-9678.
234. Abascal, J.L.F., Sanz, E., Fernandez, R.G. & Vega, C. A. (2005). A potential model for the study of ices and amorphous water: TIP4P/Ice. *Journal of Chemical Physics*, 122, 234511.
235. Abascal, J.L.F. & Vega, C. A. (2005). A general purpose model for the condensed phases of water: TIP4P/2005. *Journal of Chemical Physics,* 123, 234505.
236. Rick, S.W. (2004). A reoptimization of the five site water potential (TIP5P) for use with Ewald sums. *Journal of Chemical Physics*, 120, 6085-6093.
237. Berendsen, H.J.C., Grigera, J.R. & Straatsma, T.P. (1987). The missing term in effective pair potentials. *Journal of Chemical Physics*, 91, 6269-6271.
238. Nada, H. & Van der Eerden, J.P.M. (2003). An intermolecular potential model for the simulation of ice and water near the melting point: A six-site model for H_2O. *Journal of Chemical Physics*, 118, 7401-7413.
239. Dick, T.J. & Madura, J.D. (2005). A review of the TIP4P, TIP4P-Ew, TIP5P and TIP5P-Ew water models. *Annual Reports in Computational Chemistry*, 1, 59 - 73.
240. Martin-Conde, M., MacDowell, L.G. & Vega, C. (2006). Computer simulation of two new solid phases of water: Ice XIII and ice XIV. *Journal of Chemical Physics*, 125, 116101.
241. Vega, C. & Abascal, J.L.F. (2005). Relation between the melting temperature and the temperature of maximum density for the most common models of water. *Journal of Chemical Physics*, 123, 144504.
242. Sorenson, J.M., Hura, G., Glaeser, R.M. & Head-Gordon, T. (2000). What can x-ray scattering tell us about the radial distribution functions of water? *Journal of Chemical Physics*, 113, 9149-9161.
243. Ayala, R.B. & Tchijov, V. (2003). A molecular dynamics study of ices III and V using TIP4P and TIP5P water models. *Canadian Journal of Chemistry*, 81, 11-16.
244. Van Der Spoel, D. & Van Maaren, P.J. (2006). The Origin of Layer Structure Artifacts in Simulations of Liquid Water. *Journal of Chemical Theory and Computation*, 2, 1-11.

245. Mezei, M. & Beveridge, D.L. (1981). Theoretical studies of hydrogen bonding in liquid water and dilute aqueous solutions. *Journal of Chemical Physics*, 74, 622-632.
246. Luzar, A. & Chandler, D. (1996). Hydrogen bond kinetics in liquid water. *Nature*, 379, 55-57.
247. Luzar, A. & Chandler, D. (1993). Structure and hydrogen bond dynamics of water-dimethyl sulfoxide mixtures by computer simulations. *Journal of Chemical Physics*, 98, 8160-8173.
248. Van Der Spoel, D., Van Maaren, P.J. & Berendsen, H,J.C. (1998). A systematic study of water models for molecular simulation: Derivation of water models optimized for use with a reaction field. *Journal of Chemical Physics*, 108, 10220-10230.
249. Impey, R.W., Madden, P.A. & McDonald, I.R. (1982). Spectroscopic and transport properties of water model calculations and the interpretation of experimental results. *Molecular Physics*; 46, 513-539.
250. Noday, D.A., Steif, P.S. & Rabin, Y. (2009). Viscosity of Cryoprotective Agents near glass transition: a new device, technique, and data on DMSO, DP6, and VS55. *Experimental Mechanics* , 49, 663-672.
251. Anchordoguy, T.J., Cecchini, C.A., Crowe, J.H. & Crowe, L.M. (1991). Insights into the Cryoprotective mechanism of Dimethyl Sulfoxide for Phosholipid. *Cryobiology*, 28, 467-473.
252. Yu, Z. & Quinn, P.J. (1994). Dimethyl Sulphoxide: A review of its applications in Cell Biology. *Bioscience Reports*, 14, 259-281.
253. Baudot, A., Alger, L. & Boutron, P. (2000). Glass-forming Tendency in the system Water-Dimethyl Sulfoxide. *Cryobiology*, 40, 151-158.
254. Anchordoguy, T.J., Carpenter, J.F., Crowe, J.H. & Crowe, L.M. (1992). Temperature-dependent perturbation of phospholipid bilayers. *Biochimica et Biophysica Acta*, 1104, 117-122.
255. Chang, H.H. & Dea, P.K. (2001). Insights into the dynamics of DMSO in phosphatidylcholine bilayers. *Biophysical Chemistry*, 94, 33-40.
256. Kiyohara, O., Perron, G. & Desnoyers, J.E. (1975). Volumes and Heat capacities of Dimethylsulfoxide, Acetone, and Acetamide in Water and of some Electrolytes in these mixed Aqueous Solvents. *Canadian Journal of Chemistry*, 53, 3263-3268.
257. Cabral, J.T., Luzar, A., Teixeira, J. & Bellisent-Funel, M. (2000). Single-particle dynamics in dimethyl-sulfoxide/water eutectic mixture by neutron scattering. *Journal of Chemical Physics*, 113, 8736-8745.
258. Westh, P. (2004). Preferential interaction of dimethyl sulfoxide and phosphatidyl choline membranes. *Biochimica et Biophysica Acta*, 1664, 217-223.
259. Notman, R., Den Otter, W.K., Noro, M.G., Briels, W.J. & Anwar, J. (2007). The premeability Enhancing Mechanism of DMSO in Ceramide Bilayers Simulated by Molecular dynamics. *Biophysical Journal*, 93, 2056-2068.
260. Notman, R., Noro, M., O'Malley, B. & Anwar, J. (2006). Molecular basis for Dimethylsulfoxide (DMSO) Action on Lipid Membranes. *Journal of American Chemical Society*, 128, 13982-13983.
261. Jacob, S.W., Bischel, M. & Herschler, R.J. (1964). Dimethyl Sulfoxide: effects on the permeability of biologic membranes (preliminary report). *Current Therapeutic Research*, 6, 193-198.

262. Krishnan, C.V. & Friedman, H.L. (1969). Solvation enthalpies of Various Nonelectrolytes in Water, Propylene Carbonate, and Dimethyl Sulfoxide. *orunal of Physical Chemistry*, 73, 1572-1580.
263. Wiewoir, P.P., Shirota, H. & Castner Jr., E.W. (2002). Aqueous dimethyl sulfoxide solutions: Inter- and intra-molecular dynamics. *Journal of Chemical Physics*, 116, 4643-4654.
264. Brink, G. & Falk, M. (1970). The effect of Dimethyl Sulphoxide on the structure of Water. *Journal of Molecular Structure*, 5, 27-30.
265. Tokuhiro, T., Menafra, L. & Szmant, H.H. (1974). Contribution of relaxation and chemical shift results to the elucidation of the structure of the water-DMSO liquid system. *Journal of Chemical Physics*, 61, 2275-2282.
266. Safford, G.J., Shaffer, P.C., Leung, P.S., Doebbler, G.F., Brady, G.W. & Lyden, E.F.X. (1969). Neutron Inelastic Scattering and X-Ray Studies of Aqueous Solutions of Dimethylsulphoxide and Dimethylsulphone. *Journal of Chemical Physics*, 50, 2140-2159.
267. Soper, A.K. & Luzar, A. (1996). Orientation of Water Molecules around Small Polar and Nonpolar Groups in Solution: A Neutron Diffraction and Computer Simulation Study. *Jorunal of Physical Chemistry,*100,1357-1367.
268. McLain, S.E., Soper, A.K. & Luzar, A. (2007). Investigations on the structure of dimethyl sulfoxide and acetone in aqueous solution. *The Journal of Chemical Physics*, 127, 174515.
269. Catalan, J., Diaz, C. & Garcia-Blanco, F. (2001). Characterisation of Binary Solvent Mixtures of DMSO with Water and Other Cosolvents. *Journal of Organic Chemistry*, 66, 5846-5852.
270. Subrarangaiah, K., Murthy, N.M. & Subrahmanyam, S.V. (1981). Ultrasonic Investigation on the Structure of Aqueous Solutions of N,N-Dimethylformamide and Dimethyl Sulfoxide. *Bulletin of Chemical Society Japan*, 54, 2200-2204.
271. Bowen, D.E., Prelsand, M.A. & Eastman, M.P. (1974). Ultrasound Propagation in Binary Mixtures of Dimethyl Sulfoxide and Water. *Journal of Physical Chemistry,* 78, 2611-2615.
272. Tommila, E. & Pajunen, A. (1969). The dielectric constants and surface tensions of Dimethyl Sulphoxide-Water Mixtures. *Suomen Kemistilehti B*, 41,172-176.
273. Baker, E.S. & Jonas, J. (1985). Transport and Relaxation Properties of Dimethyl Sulfoxide-Water Mixtures at High Pressure. *Journal of Physical Chemistry*, 89, 1730-1735.
274. Fox, M.F. & Whittingham, K.P. (1973). Component Interactions in Aqueous Dimethyl Sulphoxide. *Journal of Chemical Society, Faraday Transactions*, 71, 1407-1412.
275. Skaf, M.S. (1999). Molecular Dynamics Study of Dielectric Properties of Water-Dimethyl Sulfoxide Mixtures. *Journal of Physical Chemistry A*, 103, 10719-10729.
276. Laria, D. & Skaf, M.S. (1999). Solvation repsonse of polar liquid mixtures: Water-dimethylsulfoxide. *Journal of Chemical Physics*, 111, 300-309.
277. Lei, Y., Li, H. & Han, S. (2003). An all atom simulation study on intermolecular interaction of DMSO-water system. *Chemical Physics Letters*, 380, 542-548.
278. Wulf, A. & Ludwig, R. (2006). Structure and Dynamics of Water Confined in Dimethyl Sulfoxide. *Chemical Physical Chem*istry, 7, 266-272.

279. Kirschner, B., Searles, D.J., Dyson, A.J., Vogt, P.S. & Huber, H. (2000). Disproving the iceberg effect? A Study of the Deuteron Quadrupole Coupling Constant of Water in a mixture with Dimethyl Sulfoxide via Computer Simulations. *Journal of American Chemical Society*, 122, 5379-5383.
280. Huber, H., Kirchner, B. & Searles, D.J. (2002). Is there an iceberg Effect in the Water/DMSO Mixture? Some information from Computational Chemistry. *Journal of Molecular Liquids*, 97-98, 71-77.
281. Mancera, R.L., Chalaris, M., Refson, K. & Samios, J. (2004). Molecular dynamics simulation of dilute aqueous DMSO solutions. A temperature-dependence study of the hydrophobic and hydrophilic behaviour around DMSO. *Physical Chemistry Chemical Physics*, 6, 94-102.
282. Chalaris, M. & Samios, J. (2002). Computer simulation studies of the liquid mixtures water-dimethylsulfoxide using different effective potential models: Thermodynamic and transport properties. *Journal of Molecular Liquids*, 98-99, 399-409.
283. Mancera, R., L., Chalaris, M. & Samios, J. (2004). The concentration effect on the 'hydrophobic' and 'hydrophilic' behaviour around DMSO in dilute aqueous DMSO solutions. A computer simulation study. *Journal of Molecular Liquids,* 110, 147-153.
284. Jitariu, L.,C., Wilson, C. & Hirst, D.M. (1997). An ab initio study of dimethyl sulfoxide and its adducts with H2O, HCl, and OH-. *Journal of Molecular Structure (Theochem),* 391, 111-116.
285. Van Der Vegt, N.F.A. & Van Gunsteren, W.F. (2004). Entropic Contributions in Cosolvent Binding to Hydrophobic Solutes in Water. *Journal of Physical Chemistry B,* 108, 1056-1064.
286. Blumberg, R.L., Stanley, H.E., Geiger, A. & Mausbach, P. (1984). Connectivity of hydrogen bonds in liquid water. *Journal of Chemical Physics*, 80, 5230-5241.
287. Macdonald, D.D., Smith, M.D. & Hyne, J.B. (1971). The influence of Sulfoxides and Sulfones on the Temperature of Maximum Density of Water. *Canadian Journal of Chemistry*, 49, 2817-2821.
288. Rallo, F., Rodante, & Silvestroni, P. (1970). Calorimetric Determination of Partial Molar Enthalpies of Solution of Water and Dimethylsulfoxide in their mixtures. *Thermochimica Acta*, 1, 311-316.
289. Vaisman, I.I. & Berkowitz, M.L. (1992). Local strucutral order and molecular associations in water-DMSO mixtures: Molecular dynamics study. *Journal of American Chemical Society*, 114, 7889-7896.
290. Vishnyakov, A., Lyubartsev A.P. & Laaksonen, A. (2001). Molecular dynamics simulations of Dimethyl sulfoxide and dimethyl sulfoxide- water mixture. *Journal of Physical chemistry A*, 105, 1702-1710.
291. Nieto-Draghi, C., Bonet Avalos, J. & Rousseau, B. (2003). Transport properties of dimethyl sulfoxide aqueous solutions. *Journal of Chemical Physics*, 119, 4782-4789.
292. Ferrario, M., Haughney, M., McDonald, I.R. & Klein, M.L. (1990). Molecular dynamics simulation of aqueous mixtures: Methanol, acetone, and ammonia. *Journal of Chemical Physics*, 93, 5156-5166.
293. Luzar, A. (1989). The contribution of hydrogen bonds to bulk and surface thermodynamic properties of dimethylsulfoxide-water mixtures. *Journal of Chemical Physics*, 91, 3603-3613.
294. Skaf, M.S. & Vechi, S.M. (2003). Polarizability anisotropy relaxation in pure and aqueous dimethylsulfoxide. *Journal of Chemical Physics*, 119, 2181-2187.

295. Koga, Y., Kasahara, Y., Yoshino, K. & Nishikawa, K. (2001). Mixing Schemes for Aqueous Dimethyl Sulfoxide Support by X-ray Diffraction Data. *Journal of Solution Chemistry*, 30, 885-893.
296. Bordallo, H.N., Herwig, K.W., Luther, B.M. & Levinger, N.E. (2004). Quasi-elastic neutron scattering study of dimethyl-sulfoxide-water mixtures:Probing molecular mobility in a nonideal solution. *Journal of Chemical Physics*, 121, 12457-12464.
297. Cowie, J.M.G. & Toporowski, P.M. (1961). Association in the binary liquid system Dimethylsulphoxide-Water. *Canadian Journal of Chemistry*, 39, 2240-2243.
298. Rasmussen, D.H. & Mackenzie, A.P. (1968). Phase diagram for the system water-dimethylsulphoxide. *Nature*, 220, 1315-1317.
299. Westh, P. (1994). Thermal expansivity, Molar volume, and Heat capacity of Liquid Dimethyl Sulfoxide-Water Mixtures at Subzero Temperatures. *Journal of Physical Chemistry*, 98, 3222-3225.
300. Murthy, S.S.N. (1997). Phase Behaviour of the Supercooled Aqueous Solutions of Dimethyl Sulfoxide, Ethylene Glycol, and Methanol As seen by Dielectric Spectroscopy. *Journal of Physical Chemistry B*, 101, 6043-6049.
301. Katayama, M. & Ozutsumi, K. (2008). The number of Water-Water Hydrogen Bonds in Water-Tetrahydrofuran and Water-Acetone Binary Mixtures Determined by Means of X-Ray Scattering. *Journal of Solution Chemistry*, 37, 841-856.
302. Venables, D.S. & Schmuttenmaer, C.A. (2000). Spectroscopy and dynamics of mixtures of water with acetone, acetonitrile, and methanol. *Journal of Chemical Physics*, 113, 11222-11236.
303. Max, J. & Chapados, C. (2004). Infrared spectroscopy of acetone-water liquid mixtures. *Journal of Chemical Physics*, 120, 6625-6641.
304. Max, J. & Chapados, C. (2003). Infrared spectroscopy of acetone-water liquid mixtures. I. Factor analysis. *Journal of Chemical Physics*, 119, 5632-5643.
305. Takebayashi, Y., Yoda, S., Sugeta, T., Otake, K., Sako, T. & Nakahara, M (2004). Acetone hydration in supercritical water: 13C-NMR spectroscopy and Monte Carlo simulation. *Journal of Chemical Physics*, 120, 6100-6110.
306. Garcia, A.H., Martin, J.A.S. & Arroyo, S.T. (2005). Theoretical-experimental study of the solvation enthalpy of acetone in dilute aqueous solution. *Chemical Physics*, 315, 76-80.
307. Mizuno, K., Ochi, T. & Shindo, Y. (1998). Hydrophobic hydration of acetone probed by nuclear magnetic resonance and infrared: Evidence for the interaction C-H...OH2. *Journal of Chemical Physics*, 109, 9502-9507.
308. Perera, A., Sokolic, F., Almasy, L., Westh, P. & Koga, Y. (2005). On the evaluation of the Kirkwood-Buff integrals of aqueous acetone mixtures. *Journal of Chemical Physics*, 123, 024503.
309. Arroyo, S.T., Martin, J.A. & Garcia, A.H. (2005). Theoretical-experimental study of the solvation enthalpy of acetone in dilute aqueous solution *Chemical Physics*, 315, 76-80.
310. Kamogawa, K. & Kitagawa, T. (1986). Raman Difference Spectroscopy of the C-H Streching Vibrations: Frequency Shifts and Excess Quantities for Acetone/Water and Acetonitrile/Water Solutions. *Journal of Physical Chemistry*, 90, 1077-1081.
311. Perera, A. & Sokolic, F. (2004). Modeling nonionic aqueous solutions: The acetone-water mixture. *Journal of Chemical Physics*, 121, 11272-11282.

312. Liang, W., Li, H., Lei, Y. & Han, S. (2004). Trasport properties of aqueous acetone solutions: molecular dynamics simulation and NMR studies. *Journal of Molecular Structure (Theochem)*. 686, 109-113.
313. Freitas, L.C.G., Codeiro, J.M.M. & Garbujo, F.L.L. (1999). Theoretical studies of liquids by computer simulations: The water-acetone mixture. *Journal of Molecular Liquids,* 79, 1-15.
314. Wheeler, D.R. & Rowley, R.L. (1998). Shear viscosity of polar liquid mixtures via non-equilibrium molecular dynamics: water, methanol, and acetone. *Molecular Physics*, 94, 555-564.
315. Brancato, G., Rega, N. & Barone, V. (2008). A discrete/continuum QM/MM MD study of the triplet state of acetone in aqueous solution. *Chemical Physics Letters*, 453, 202-206.
316. Canuto, S., Saavedra, N. & Coutinho, K. (1999). Theoretical analysis of the hydrogen bond interaction between acetone and water. *Journal of Molecular Structure (Theochem)*, 466, 69-75.
317. Jedlovszky, P., Idrissi, A. & Jancso, G. (2009). Can existing models qualitatively describe the mixing behavior of acetone with water? *The journal of Chemical Physics*, 130,124516.
318. Pavone, M., Crescenzi, O., Morelli, G., Rega, N. & Barone, V. (2006). Solvent effects on the UV (n-pi)* and NMR (17O) spectra of acetone in aqueous solution: development and validation of a modified AMBER forcefield for an integrated MD/DFT/PCM approach. *Theoretical Chemistry Accounts*,116, 456-461.
319. Weerasinghe, S. & Smith, P.E. (2003). Kirkwood-Buff derived force field for mixtures of acetone and water. *Journal of Chemical Physics,* 118, 10663.
320. Tom, D., Darrin, Y. & Lee, P. (1993). Particle mesh Ewald: An N.log(N) method for Ewald sums in large systems. *Journal of Chemical Physics*, 98, 10089-10092.
321. Jorgensen, W.L., Chandrasekhar, J., Madura, J.D., Impey, R.W. & Klein, M.L. (1983). Comparison of simple potential functions for simulating liquid water. *Journal of Chemical Physics*, 79, 926-936.
322. Jorgensen, W.J., Maxwell, D.S. & Tirado-Rives, J. (1996). Development and testing of the OPLS all-atom force field on conformational energetics and properties of organic liquids. *Journal of American Chemical Society*, 118, 11225-11236.
323. Lisal, M., Kolafa, J. & Nezbeda, I. (2002). An examination of the five-site potential (TIP5P) for water. *Journal of Chemical Physics*, 117, 8892-8897.
324. Sanz, E., Vega, C., Abascal, J.L.F. & MacDowell, L.G. (2004). Phase Diagram of Water from Computer Simulations. *Physical Review Letters*, 92, 255701.
325. Zielkiewicz, J. (2005). Structural properties of water: Comparison of the SPC, SPCE, TIP4P, and TIP5P models of water. *Journal of Chemical Physics*, 123, 104501.
326. Vega, C., Sanz, E. & Abascal, J.L.F. (2005). The melting temperature of the most common models of water. *The Journal of Chemical Physics*, 122, 114507.
327. Vega, C., Abascal, J.L.F., Sanz, E., MacDowell, L.G. & McBride, C. (2005) Can simple models describe the phase diagram of water. *Journal of Physics: Condensed Matter*, 17, S3283-3288.
328. Jorgensen, W.J. & Tirado-Rives, J. (1988). The OPLS Potential Functions for proteins. Energy Minimisations for Crystals of Cyclic peptides and Crambin. *Journal of American Chemical Society*, 110, 1657-1666.

329. Martinez, J.M. & Martinez, L. (2003). Packing Optimization for Automated Generation of Complex System's Initial Configurations for Molecular Dynamics and Docking. *Journal of Computational Chemistry*, 24, 819-825.
330. Berendsen, H.J.C., Postma, J.P.M., Van Gunsteren, W.F., DiNola, A. & Haak, J.R. (1984). Molecular dynamics with coupling to an external bath. *Journal of Chemical Physics*, 81, 3684-3690.
331. Svishchev, I.M. & Kusalik, P.G. (1994). Crystallisation of Liquid Water in a Molecular Dynamics Simulation. *Physical Review Letters*, 73, 975-978.
332. Ferrario, M. & Tani, A. (1985). A Molecular dynamics study of the TIP4P model of water. *Chemical Physics Letters*, 121, 182-186.
333. Cordeiro, J.M.M. (2007). Structure of acetone and dimethyl sulfoxide from Monte Carlo simulations and MM2 calculations. *Physics and Chemistry of Liquids*, 45, 31-39.
334. Kirchner, B. & Hutter, J. (2004). Solvent effects on electronic properties from Wannier functions in a dimethyl sulfoxide/water mixture. *Journal of Chemical Physics*, 121, 5133-5142.
335. Strader, M.L. & Feller, S.E. (2002) A flexible all atom model of Dimethyl Sulfoxide for Molecular Dynamics Simulations. *Journal of Physical Chemistry A,* 106, 1074-1080.
336. Caffarena, E. & Grigera, J.R. (1996). Crystal, melted and glassy states of glucose. *Journal of Chemical Society, Faraday Transactions*, 92, 2285-2289.
337. Liu, D., Zhang, Y., Chen, C., Mou, C., Poole, P.H. & Chen, S.H. (2007) Observation of the density minimum in deeply supercooled confined water. *Proceedings of National Academy of Sciences*, 104, 9570-9574.
338. Paschek, D. (2005). How liquid-liquid transition affects hydrophobic hydration in deeply supercooled water. *Physical Review Letters*, 94, 217802.
339. Tarjus, G., Kivelson, D., Mossa, S. & Alba-Simionesco, C. (2004). Disentangling density and temperature effects in the viscous slowing down of glassforming liquids. *Journal of Chemical Physics*, 120, 6135 - 6141.
340. Patra, M., Salonen, E., Terama, E., Vattulainen, I., Faller, R., Lee, B.W., Holopainen, J. & Karttunen, M. (2006). Under the Influence of Alcohol: The Effect of Ethanol and Methanol on Lipid Bilayers. *Biophysical Journal*, 90, 1121-1135.
341. Masella, M. & Flament, J.P. (1998). Relation between cooperative effects in cyclic water, methanol/water, and methanol trimers and hydrogen bonds in methanol/water, ethanol/water, and dimethylether/water heterodimers. *Journal of Chemical Physics*, 108, 7141-7151.
342. Hofer, K., Hallbrucker, A., Mayer, E. & Johari, G.P. (1989). Vitrified Dilute Aqueous Solutions. 3. Plasticization of water's H-Bonded Network and the Glass Transition Temperature's Minimum. *Journal of Physical Chemistry*, 93, 4674-4677.
343. Dougan, L., Bates, S.P., Hargreaves, R. & Fox, J.P. (2004). Methanol-water solutions: A bi-percolating liquid mixture. *Journal of Chemical Physics*, 121, 6456-6462.
344. Cheng, Y., Page, M. & Jolicoeur, C. (1993). Comparative Study of Hydrophobic Effects in Water/Alcohol and Water/Ethylene Glycol, Water/Ethylenediamine, and Water/2-Methoxyethanol Systems. *Journal of Physical Chemistry*, 97, 7359-7363.

345. Price, W.S., Ide, H. & Arata, Y. (2003). Solution Dynamics in Aqueous Monohydric Alcohol Systems. *Journal of Physical Chemistry A*, 107, 4784-4789.
346. Onori, G. & Santucci, A. (1996). Dynamical and structural properties of water/alcohol mixtures. *Journal of Molecular Liquids*, 69, 161-181.
347. Harvey, J.M., Jackson, S.E. & Symons, M.C.R. (1977). Interactions in Water-Alcohol mixtures studied by NMR Infrared spectroscopy. *Chemical Physics Letters*, 47, 440-441.
348. Soper, A.K., Dougan, L., Crain, J. & Finney, J.L. (2006). Excess Entropy in Alcohol-Water Solutions: A Simple Clustering Explanation. *Journal of American Chemical Society*, 110, 3472-3476.
349. Ma, G. & Allen, H.C. (2003). Surface Studies of Aqueous Methanol Solutions by Vibrational Broad Bandwidth Sum Frequency Generation Spectroscopy. *Journal of Physical Chemistry*, 107, 6343-6349.
350. Soper, A.K. & Finney, J.L. (1993). Hydration of Methanol in Aqueous Solution. *Physical Review Letters*, 71, 4346-4350.
351. Derlacki, Z.J., Easteal, A.J., Edge, A.V.J., Woolf, L.A. & Roksandic, Z. (1985). Diffusion Coefficients of Methanol and Water, and the Mutual Diffusion Coefficient in Methanol-Water Solutions at 278 and 298 K. *Journal of Physical Chemistry*, 89, 5318-5322.
352. Ludwig, R. (1995). NMR relaxation studies in water-alcohol mixtures: the water-rich region. *Chemical Physics*, 195, 329-337.
353. Onori, G. (1989). Structural properties of aqueous mixtures of monohydric alcohols from near-infrared absorption spectra. *Chemical Physics Letters,* 154, 212-216.
354. Noskov, S.Y., Kiselev, M.G., Kolker, A.M. & Rode, B.M. (2001). Structure of methanol-methanol associates in dilute methanol-water mixtures from molecular dynamics simulation. *Journal of Molecular Liquids*, 91, 157-165.
355. Yu, H., Geerke, D.P., Liu, H. & Van Gunsteren, W.F. (2006). Molecular Dynamics Simulations of Liquid Methanol and Methanol-Water Mixtures with Polarizable Models. *Journal of Computational Chemistry*, 27, 1494-1504.
356. Fidler, J. & Rodger, P.M. (1999) Solvation Structure around Aqueous Alcohols. *Journal of Physical Chemistry*, 103, 7695-7703.
357. Fleischman, S.H. & Brooks, C.L. III. (1987) Thermodynamics of aqueous solvation: Solution properties of alcohols and alkanes. *Journal of Chemical Physics*, 87, 3029-3037.
358. Palinkas, G., Hawlicka, E. & Heinzinger, K. (1991) Molecular dynamics simulations of water-methanol mixtures. *Chemical Physics*, 158, 65-76.
359. Bolis G, Corongiu, G. & Clementi, E. (1982). Methanol in water solution at 300K. *Chemical Physics Letters*, 86, 299-306.
360. Okazaki, S., Nakanishi, K. & Touhara, H. (1983). Computer experiments on aquoeus solution. I. Monte Carlo calculation on the hydration of methanol in an infinitely dilute aquoeus solution with a new water-methanol pair potential. *Journal of Chemical Physics*, 78, 454-469.
361. Gao, J., Habibollazadeh, D. & Shao, L. (1995). A Polarizable Intermolecular Potential Function for Simulation of Liquid Alcohols. *Journal of Physical Chemistry*, 99, 16460-16467.
362. Dixit, S., Soper, A.K., Finney, J.L. & Crain, J. (2002). Water structure and solute association in dilute aqueous methanol. *Euro Physics Letters*, 59, 377-383.

363. Richardi, J., Millot, C. & Fries, P.H. (1999). A molecular Ornstein-Zernike study of popular models for water and methanol. *Journal of Chemical Physics*, 110, 1138-1147.
364. Skaf, M.S. & Ladanyi, B.M. (1996). Molecular Dynamics Simulation of Solvation Dynamics in Methanol-Water Mixtures. *Journal of Physical Chemistry*, 100, 18258-18268.
365. Ladanyi, B.M. & Skaf, M.S. (1996). Wave Vector-Dependent Dielectric Relaxation of Methanol-Water Mixtures. *Journal of Physical Chemistry*, 100, 1368-1380.
366. Shah, P. & Roberts, C.J. (2007). Molecular solvation in water-methanol and water-sorbitol mixtures: The roles of preferential hydration, hydrophobicity, and the equation of state. *Journal of Physical Chemistry B*, 4467-4476.
367. Coccia, A., Indovina, P.L., Podo, F. & Viti, V. (1975). PMR studies on the structures of water- ethyl alcohol mixtures. *Chemical Physics*, 7, 30-40.
368. Egashira, K. & Nishi, N. (1998). Low-Frequency Raman Spectroscopy of Ethanol-Water Binary Solution: Evidence for Self-Association of Solute and Solvent Molecules. *Journal of Physical Chemistry B*, 102, 4054-4057.
369. Bosio, L., Teixeira, J. & Stanley, H.E. (1981). Enhanced Density Fluctuations in Supercooled H2O, D2O, and Ethanol-Water Solutions: Evidence from Small-Angle X-Ray Scattering. *Physical Review Letters*, 46, 597-600.
370. Nishikava, K. & Iijima, T. (1993). Small-Angle X-ray Scattering Study of Fluctuations in Ethanol and Water Mixtures. *Journal of Physical Chemistry*, 97, 10824-10828.
371. Petong, P., Pottel, R. & Kaatze, U. (2000). Water-Ethanol Mixtures at Different Compositions and Temperatures. A Dielectric Relaxation Study. *Journal of Physical Chemistry* 104, 7420-7428.
372. Bao, J.Z., Swicord, M.L. & Davis, C.C. (1995). Microwave dielectric characterisation of binary mixtures of water, methanol, and ethanol. *Journal of Chemical Physics*, 104, 4441-4450.
373. Sato, T., Chiba, A. & Nozaki, R. (1999). Dynamical aspects of mixing schemes in ethanol-water mixtures in terms of the excess partial molar activation free energy, enthalpy, and entropy of the dielectric relaxation process. *Journal of Chemical Physics*, 110, 2508-2521.
374. Van Erp, T.S. & Meijer, E.J. (2003). Ab initio molecular dynamics study of aqueous solvation of ethanol and ethylene. *Journal of chemical Physics*, 118, 8831-8840.
375. Chen, B., Siepman, J.I. & Klein, M.L. (2003). Simulating the nucleation of Water/Ethanol and Water/n-Nonane Mixtures: Mutual Enhancement and Two-Pathway Mechanism. *Journal of American Chemical Society*, 125, 3113-3118.
376. Yu, S., Lamoureux, G. & Roux, B. (2005). Molecular Dynamics Study of Hydration in Ethanol-Water Mixtures Using a Polarizable Forcefield. *Journal of Physical Chemistry B*, 109, 6705-6713.
377. Zhang, C. & Yang, X. (2005). Molecular dynamics simulation of ethanol/water mixtures for structure and diffusion properties. *Fluid Phase Equilibria*, 231,1-10.
378. Takaba, H., Koyama, A. & Nakao, S. (2000). Dual Ensemble Monte Carlo Simulation of Pervaporation of an Ethanol/Water Binary Mixture in Silicalite Membrane Based on a Lennard-Jones Interaction Model. *Journal of Physical Chemistry B*, 104, 6353-6359.

379. Onori, G. (1988). Adiabatic compressibility and structure of aqueous solutions of ethyl alcohol. *Journal of Chemical Physics*, 89, 4325-4332.
380. Sidhu, K.S., Goodfellow, J.M. & Turner, J.Z. (1999). Effect of molecular shape and electrostatic interactions on the water layer around polar and apolar groups in solution. *Journal of Chemical Physics*, 110, 7943-7950.
381. Levchuk, V.N., Sheykhet, I.I. & Simkin, B.Y. (1991). Calculation of the hydration energy of ethanol by the Monte Carlo method. *Chemical Physics Letters*, 185, 339-343.
382. Tarek, M., Tobias, D.J. & Klein, M.L.(1996). Molecular dynamics investigation of an ethanol-water solution. *Physica A*, 231, 117-122.
383. Zana, R. & Eljebari, M.J. (1993). Fluorescence Probing Investigation of the Self-Association of Alcohols in Aqueous Solution. *Journal of Physical Chemistry*, 97, 11134-11136.
384. Mashimo, S., Kuwabara, S., Yagihara, S. & Higasi, K. (1989). The dielectric relaxation of mixtures of water and primary alcohol. *Journal of Chemical Physics*, 90, 3292-3294.
385. Allison, S.K., Fox, J.P., Hargreaves, R. & Bates, S.P. (2005). Clustering and micro immiscibility in alcohol-water mixtures: Evidence from molecular-dynamics simulations. *Physical Review B*, 71, 024201.
386. Mashimo, S., Umehara, T. & Redlin, H. (1991). Structures of water and primary alcohol studied by microwave dielectric analysis. *Jounral of Chemical Physics*, 95, 6257-6260.
387. Laaksonen, A., Kusalik, P.G. & Svishchev, I.M. (1997). Three-Dimensional Structure in Water-Methanol Mixtures. *Journal of Physical Chemistry,* 101, 5910-5818.
388. Koga, Y., Nishikawa, K. & Westh, P. (2004). 'Icebergs" or No "Icebergs" in Aqueous Alcohols?: Composition-Dependent Mixing Schemes. *Journal of Physical Chemistry A*, 108:3873-3877.
389. Franks, F. & Ives, D.J.G. (1966). The structural properties of alcohol-water mixtures. *Quarterly Reviews* 20, 1-45.
390. Dixit, S., Crain, J., Poon, W.C.K., Finney, J.L. & Soper, A.K. (2002). Molecular segregation observed in a concentrated alcohol-water solution. *Nature* 2002;416:829-32.
391. Mizuno K, Miyashita, Y., Shindo, Y. & Ogawa, H. (1995). NMR and FT-IR Studies of Hydrogen Bonds in Ethanol-Water Mixtures. *Journal of Physical Chemistry*, 99, 3225-3228.
392. Noskov, S.Y., Lamoureux, G. & Roux, B. (2005). Molecular Dynamics Study of Hydration in Ethanol-Water Mixtures Using a Polarizable Forcefield. *Journal of Physical Chemistry B*, 109, 6705-6713.
393. Smith, R.L.J., Lee, S.B., Komori, H. & Arai, K. (1988). Relative permittivity and dielectric relaxtion in aqueous alcohol solutions. *Fluid Phase Equilibria,* 144, 315-322.
394. Miyata, K. & Kanno, H. (2005). Supercooling behaviour of aqueous solutions of alcohols and saccharides. *Journal of Molecular Liquids*, 119, 189-193.
395. Corsaro, C., Spooran, J., Branca, C., Leone, N., Broccio, M., Kim, C., Chen, S-H., Stanley, H.E. & Mallamace, F. (2008). Clustering Dynamics in Water/Methanol Mixtures: A Nuclear Magnetic Resonance Study at 205K< T< 295K. *Journal of Physical Chemistry B*, 112, 10449-10454.

396. Dougan, L., Hargreaves, R., Bates, S.P., Finney, J.L., Reat, V., Soper, A.K. & Crain, J. (2005). Segregation in aqueous methanol enhanced by cooling and compression. *Journal of Chemical Physics*, 122, 174514.
397. Bowron, D.T. & Finney, J.L. (2007) Association and dissociation of an aqueous amphiphile at elevated temperatures. *Journal of Physical Chemistry B*, 111, 9838-9852.
398. Zhang, Y., Yang, J., Yu, Y. & Li, Y. (2005). Structural and hydrogen bond analysis for supercritical ethanol: A molecular simulation study. *Journal of Supercritical fluids* , 36,145-153.
399. Wensink, E.J., Hoffman, A.C., Van Maaren, P.J. & Van der Spoel, D. (2003). Dynamic properties of water/alcohol mixtures studied by computer simulation. *Journal of Chemical Physics*, 119, 7308-7317.
400. Angell, C.A. (1983). Supercooled water. *Annual Review of Physical Chemistry*, 34, 593-630.
401. Velikov, V., Borick, S. & Angell, C.A. (2001). The glass transtion of water, based on hyperquenching experiments. *Science*, 294, 2335-2338.
402. Hallbrucker, A., Mayer, E., & Johari, G.P. (1989). Glass-Liquid Transition and the Enthalpy of Devitrification of Annealed Vapor-Deposited Amorphous Solid Water. A Comparison with Hyperquenched Glassy Water. *Journal of Physical Chemistry,* 93, 4986-4990.
403. Velikov, V., Borick, S. & Angell, C.A. (2001). The glass transition of water, based on hyperquenching experiments. *Science*, 294, 2335-2338.
404. Giovambattista, N., Angell, C.A., Sciortino, F. & Stanley, H.E. (2004). Glass-transition temperature of water: A Simulation study. *Physical Review Letters,* 93, 047801.
405. Brovchenko, I., Geiger, A. & Oleinikova, A. (2005). Liquid-liquid phase transitions in supercooled water studied by computer simulations of various water models. *Journal of Chemical Physics*, 123, 044515.
406. Baudot, A. & Boutron, P. (1998). Glass forming tendency and stability of aquoeus solutions of diethylformamide and dimethylformamide. *Cryobiology*, 37, 187-199.
407. Angell, C.A., Sare, J.M. & Sare, E.J. (1978). Glass transition temperatures for simple molecular liquids and their binary solutions. *Journal of Physical Chemistry*, 82, 2622 - 2629.
408. Lovelock, J.E. & Bishop, M.W.H. (1959). Prevention of freezing damage to living cells by dimethyl sulphoxide. *Nature*, 183, 1394-1395.
409. McGann, L.E. & Walterson M.L. (1987). Cryoprotection by dimethyl sulfoxide and dimethyl sulphone. *Cryobiology*, 24, 11-16.
410. Rall, W.F., & Fahy, G.M. (1985). Ice-free cryopreservation of mouse embryos at -196 oC by vitrification. *Nature*, 313, 573-575.
411. Angell, C.A. (2002). Liquid fragility and the glass transition in water and aqueous solutions. *Chemical Reviews,* 102, 2627-2650.
412. Angell, C.A. & Borick, S. (2002) Specific heats Cp, Cv, Cconf, and energy landscapes of glass forming liquids. *Journal of Non-crystalline Solids*, 307-310, 393-406.
413. Van Der Spoel, D., Lindahl, E., Hess, B., Groenhof, G.,Mark, A.E. & Berendsen, H.J. (2005). GROMACS: fast, flexible and free. *Journal of Computational Chemistry*, 26, 1701–1718.

414. Tom, D., Darrin, Y. & Lee, P. (1993). Particle Mesh Ewald: An N.log(N) method for Ewald sums in large systems. *Journal of Chemical Physics* 98, 10089-10092.
415. Angell, C.A. (2008). Glass formation and glass transition in supercooled liquids, with insights from study of related phenomena in crystals. *Journal of Non-Crystalline Solids*, 354, 4703-4712.
416. Liu, L, Faraone, A., Mou, C-Y, Yen, C-W & Chen, S-H. (2004). Slow dynamics of supercooled water confined in nanoporous silica materials. *Journal of Physics: Condensed matter*, 16, S5403.
417. Mandumpal, J.B., Kreck, C.A. & Mancera, R.L. (2011). A molecular mechanism of solvent cryoprotection in aqueous DMSO solutions. *Physical Chemistry and Chemical Physics*, 13, 3839-3842.
418. Faraone, A., Liu, L., Mou, C.Y., Yen, C.W. & Chen, S.H. (2004). Fragile-to-strong liquid transition in deeply supercooled confined water. *Journal of Chemical Physics*, 121, 10843-10846.
419. Angell, C.A. (2008). Insights into phases of liquid water from study of its unusual glass forming properties. *Science*, 319, 582-587.
420. Rasmussen, D.H. & Mackenzie, A.P. (1971). The glass transition in amorphous water. Application of the measurements to problems arising in cryobiology. *Journal of Physical Chemistry*, 75, 967-973.
421. Hall, R.W. & Wolynes, P.G. (2008). Intermolecukar forces and the glass transition. *Journal of Physical Chemistry B*, 112, 301-312.
422. Vilgis, T.A. (1993). Strong and fragile glasses: A powerful classification and its consequences. *Physical Review B* , 47, 2882 - 2885.
423. Sokolov, A.P., Roessler,E., Kisiliuk, A. & Quitmann, D. (1993). Dynamics of strong and fragile glass formers: differences and correlation with low-temperature properties. *Physical Review Letters*, 71, 2062-2065.
424. Murthy, S.S.N. (2000). Experimental study of the dynamics of water and the phase behaviour of the supercooled aqueous solutions of propylene glycol, glycerol, poly (ethylene glycol)s, and poly (vinylpyrrolidone). *Journal of Physical Chemistry B*, 104, 6955-6962.
425. Mancera, R.L, Chalaris, M. & Samios, J. (2004). The concentration effect on the „hydrophobic" and „hydrophilic" behaviour around DMSO in dilute aqueous DMSO solutions. A computer simulation study *Journal of Molecular Liquids*, 110, 147-153.
426. Soper, A.K. & Luzar, A. (1992). A neutron diffraction study of dimethyl sulphoxide-water mixtures. *Journal of Chemical Physics,* 97, 1320-1331.
427. Bowron, D.T., Finney, J.L. & Soper, A.K. (2006). Structural characteristics of a 0.23 mole fraction aqueous solution of Tetrahydrofuran at 2O^{o} C. *Journal of Physical Chemistry B*, 110, 20235-20245.

COPYRIGHT AGREEMENT

SPRINGER LICENSE
TERMS AND CONDITIONS

Jan 19, 2011

This is a License Agreement between Jestin Baby Mandumpal ("You") and Springer ("Springer") provided by Copyright Clearance Center ("CCC"). The license consists of your order details, the terms and conditions provided by Springer, and the payment terms and conditions.

All payments must be made in full to CCC. For payment instructions, please see information listed at the bottom of this form.

License Number 2592430215273

License date Jan 19, 2011

Licensed content publisher Springer

Licensed content publication Heart Failure Reviews

Licensed content title Principles of Low Temperature Cell Preservation

Licensed content author Boris Rubinsky

Licensed content date Jul 1, 2003

Volume number 8

Issue number 3

Type of Use Thesis/Dissertation

Portion Figures

Author of this Springer article No

Order reference number

Title of your thesis / dissertation Molecular Mechanism of solvent cryoprotection

Expected completion date Jan 2011

Estimated size (pages) 210

Total 0.00 USD

Terms and Conditions

Introduction

The publisher for this copyrighted material is Springer Science + Business Media. By clicking "accept" in connection with completing this licensing transaction, you agree that the following terms and conditions apply to this transaction (along with the Billing and Payment terms and conditions established by Copyright Clearance Center, Inc. ("CCC"), at the time that you opened your Rightslink account and that are available at any time at http://myaccount.copyright.com).

Limited License

With reference to your request to reprint in your thesis material on which Springer Science and Business Media control the copyright, permission is granted, free of charge, for the use indicated in your enquiry. Licenses are for one-time use only with a maximum distribution equal to the number that you identified in the licensing process.

This License includes use in an electronic form, provided it is password protected or on the university's intranet, destined to microfilming by UMI and University repository. For any other electronic use, please contact Springer at (permissions.dordrecht@springer.com or permissions.heidelberg@springer.com)

The material can only be used for the purpose of defending your thesis, and with a maximum of 100 extra copies in paper.

Although Springer holds copyright to the material and is entitled to negotiate on rights, this license is only valid, provided permission is also obtained from the (co) author (address is given with the article/chapter) and provided it concerns original material which does not carry references to other sources (if material in question appears with credit to another source, authorization from that source is required as well). Permission free of charge on this occasion does not prejudice any rights we might have to charge for reproduction of our copyrighted material in the future.

Altering/Modifying Material: Not Permitted

However figures and illustrations may be altered minimally to serve your work. Any other abbreviations, additions, deletions and/or any other alterations shall be made only with prior written authorization of the author(s) and/or Springer Science + Business Media. (Please contact Springer at permissions.dordrecht@springer.com or permissions.heidelberg@springer.com)

Reservation of Rights

Springer Science + Business Media reserves all rights not specifically granted in the combination of (i) the license details provided by you and accepted in the course of this licensing transaction, (ii) these terms and conditions and (iii) CCC's Billing and Payment terms and conditions.

Copyright Notice:

Please include the following copyright citation referencing the publication in which the material was originally published. Where wording is within brackets, please include verbatim.

"With kind permission from Springer Science+Business Media: <book/journal title, chapter/article title, volume, year of publication, page, name(s) of author(s), figure number(s), and any original (first) copyright notice displayed with material>."

Warranties: Springer Science + Business Media makes no representations or warranties with respect to the licensed material.

Indemnity

You hereby indemnify and agree to hold harmless Springer Science + Business Media and CCC, and their respective officers, directors, employees and agents, from and against any and all claims arising out of your use of the licensed material other than as specifically authorized pursuant to this license.

No Transfer of License

This license is personal to you and may not be sublicensed, assigned, or transferred by you to any other person without Springer Science + Business Media's written permission.

No Amendment Except in Writing

This license may not be amended except in a writing signed by both parties (or, in the case of Springer Science + Business Media, by CCC on Springer Science + Business Media's behalf).

Objection to Contrary Terms

Springer Science + Business Media hereby objects to any terms contained in any purchase order, acknowledgment, check endorsement or other writing prepared by you, which terms are inconsistent with these terms and conditions or CCC's Billing and Payment terms and conditions. These terms and conditions, together with CCC's Billing and Payment terms and conditions (which are incorporated herein), comprise the entire agreement between you and Springer Science + Business Media (and CCC) concerning this licensing transaction. In the event of any conflict between your obligations established by these terms and conditions and those established by CCC's Billing and Payment terms and conditions, these terms and conditions shall control.

Jurisdiction

All disputes that may arise in connection with this present License, or the breach thereof, shall be settled exclusively by the country's law in which the work was originally published.

Other terms and conditions:

v1.2

Gratis licenses (referencing $0 in the Total field) are free. Please retain this printable license for your reference. No payment is required.

If you would like to pay for this license now, please remit this license along with your payment made payable to "COPYRIGHT CLEARANCE CENTER" otherwise you will be invoiced within 48 hours of the license date. Payment should be in the form of a check or money order referencing your account number and this invoice number RLNK10916044.
Once you receive your invoice for this order, you may pay your invoice by credit card. Please follow instructions provided at that time.

Make Payment To:
Copyright Clearance Center
Dept 001
P.O. Box 843006
Boston, MA 02284-3006

If you find copyrighted material related to this license will not be used and wish to cancel, please contact us referencing this license number 2592430215273 and noting the reason for cancellation.

Questions? customercare@copyright.com or +1-877-622-5543 (toll free in the US) or +1-978-646-2777.

Dear Customer,

Thank you for your email.

- We hereby grant permission for the requested use expected that due credit is given to the original source.

If material appears within our work with credit to another source, authorisation from that source must be obtained.

Credit must include the following components:

- Books: Author(s)/ Editor(s) Name(s): Title of the Book. Page(s). Publication year. Copyright Wiley-VCH Verlag GmbH & Co. KGaA. Reproduced with permission.
- Journals: Author(s) Name(s): Title of the Article. Name of the Journal. Publication year. Volume. Page(s). Copyright Wiley-VCH Verlag GmbH & Co. KGaA. Reproduced with permission.

With kind regards

Heike Weller
****

Heike Weller
Copyright & Licensing Manager
Wiley-VCH Verlag GmbH & Co. KGaA
Boschstr. 12
69469 Weinheim
Germany

Phone: +49 (0) 62 01- 606 - 585
Fax: +49 (0) 62 01 - 606 - 332
Email: rights@wiley-vch.de

ELSEVIER LICENSE
TERMS AND CONDITIONS
Apr 10, 2011

This is a License Agreement between Jestin Baby Mandumpal ("You") and Elsevier ("Elsevier") provided by Copyright Clearance Center ("CCC"). The license consists of your order details, the terms and conditions provided by Elsevier, and the payment terms and conditions.
All payments must be made in full to CCC. For payment instructions, please see information listed at the bottom of this form.
Supplier
Elsevier Limited
The Boulevard,Langford Lane
Kidlington, Oxford,OX5 1GB,UK

Registered Company Number
1982084
Customer name
Jestin Baby Mandumpal
Customer address
Mandumpal house
Thrissur, other 680 503
License number
2645291296994
License date
Apr 10, 2011
Licensed content publisher
Elsevier
Licensed content publication
Cryobiology
Licensed content title
Extra- and intracellular ice formation in mouse oocytes
Licensed content author
Peter Mazur, Shinsuke Seki, Irina L. Pinn, F.W. Kleinhans, Keisuke Edashige
Licensed content date
ELSEVIER LICENSE
TERMS AND CONDITIONS
Apr 10, 2011
This is a License Agreement between Jestin Baby Mandumpal ("You") and Elsevier ("Elsevier") provided by Copyright Clearance Center ("CCC"). The license consists of your order details, the terms and conditions provided by Elsevier, and the payment terms and conditions.
All payments must be made in full to CCC. For payment instructions, please see information listed at the bottom of this form.
Supplier
Elsevier Limited
The Boulevard,Langford Lane
Kidlington,Oxford,OX5 1GB,UK
Registered Company Number
1982084
Customer name
Jestin Baby Mandumpal
Customer address
Mandumpal house
Thrissur, other 680 503
License number
2645291296994
License date
Apr 10, 2011
Licensed content publisher
Elsevier
Licensed content publication
Cryobiology
Licensed content title
Extra- and intracellular ice formation in mouse oocytes

Licensed content author
Peter Mazur, Shinsuke Seki, Irina L. Pinn, F.W. Kleinhans, Keisuke Edashige
Licensed content date
ELSEVIER LICENSE
TERMS AND CONDITIONS
Apr 10, 2011
This is a License Agreement between Jestin Baby Mandumpal ("You") and Elsevier ("Elsevier") provided by Copyright Clearance Center ("CCC"). The license consists of your order details, the terms and conditions provided by Elsevier, and the payment terms and conditions.
All payments must be made in full to CCC. For payment instructions, please see information listed at the bottom of this form.
Supplier
Elsevier Limited
The Boulevard,Langford Lane
Kidlington,Oxford,OX5 1GB,UK
Registered Company Number
1982084
Customer name
Jestin Baby Mandumpal
Customer address
Mandumpal house
Thrissur, other 680 503
License number
2645291296994
License date
Apr 10, 2011
Licensed content publisher
Elsevier
Licensed content publication
Cryobiology
Licensed content title
Extra- and intracellular ice formation in mouse oocytes
Licensed content author
Peter Mazur, Shinsuke Seki, Irina L. Pinn, F.W. Kleinhans, Keisuke Edashige
Licensed content date
ELSEVIER LICENSE
TERMS AND CONDITIONS
Apr 10, 2011
This is a License Agreement between Jestin Baby Mandumpal ("You") and Elsevier ("Elsevier") provided by Copyright Clearance Center ("CCC"). The license consists of your order details, the terms and conditions provided by Elsevier, and the payment terms and conditions.
All payments must be made in full to CCC. For payment instructions, please see information listed at the bottom of this form.
Supplier
Elsevier Limited
The Boulevard,Langford Lane
Kidlington, Oxford,OX5 1GB,UK
Registered Company Number

1982084
Customer name
Jestin Baby Mandumpal
Customer address
Mandumpal house
Thrissur, other 680 503
License number
2645291296994
License date
Apr 10, 2011
Licensed content publisher
Elsevier
Licensed content publication
Cryobiology
Licensed content title
Extra- and intracellular ice formation in mouse oocytes
Licensed content author
Peter Mazur, Shinsuke Seki, Irina L. Pinn, F.W. Kleinhans, Keisuke Edashige
Licensed content date
ELSEVIER LICENSE
TERMS AND CONDITIONS
Apr 10, 2011
This is a License Agreement between Jestin Baby Mandumpal ("You") and Elsevier ("Elsevier") provided by Copyright Clearance Center ("CCC"). The license consists of your order details, the terms and conditions provided by Elsevier, and the payment terms and conditions.
All payments must be made in full to CCC. For payment instructions, please see information listed at the bottom of this form.
Supplier
Elsevier Limited
The Boulevard, Langford Lane
Kidlington, Oxford, OX5 1GB,UK
Registered Company Number
1982084
Customer name
Jestin Baby Mandumpal
Customer address
Mandumpal house
Thrissur, other 680 503
License number
2645291296994
License date
Apr 10, 2011
Licensed content publisher
Elsevier
Licensed content publication
Cryobiology
Licensed content title
Extra- and intracellular ice formation in mouse oocytes
Licensed content author

Peter Mazur, Shinsuke Seki, Irina L. Pinn, F.W. Kleinhans, Keisuke Edashige
Licensed content date
ELSEVIER LICENSE
TERMS AND CONDITIONS
Apr 10, 2011
This is a License Agreement between Jestin Baby Mandumpal ("You") and Elsevier ("Elsevier") provided by Copyright Clearance Center ("CCC"). The license consists of your order details, the terms and conditions provided by Elsevier, and the payment terms and conditions.
All payments must be made in full to CCC. For payment instructions, please see information listed at the bottom of this form.
Supplier
Elsevier Limited
The Boulevard,Langford Lane
Kidlington, Oxford,OX5 1GB,UK
Registered Company Number
1982084
Customer name
Jestin Baby Mandumpal
Customer address
Mandumpal house
Thrissur, other 680 503
License number
2645291296994
License date
Apr 10, 2011
Licensed content publisher
Elsevier
Licensed content publication
Cryobiology
Licensed content title
Extra- and intracellular ice formation in mouse oocytes
Licensed content author
Peter Mazur, Shinsuke Seki, Irina L. Pinn, F.W. Kleinhans, Keisuke Edashige
Licensed content date

If you would like to pay for this license now, please remit this license along with your payment made payable to "COPYRIGHT CLEARANCE CENTER" otherwise you will be invoiced within 48 hours of the license date. Payment should be in the form of a check or money order referencing your account number and this invoice number RLNK10966604.
Once you receive your invoice for this order, you may pay your invoice by credit card. Please follow instructions provided at that time.
Make Payment To:
Copyright Clearance Center
Dept 001
P.O. Box 843006
Boston, MA 02284-3006
For suggestions or comments regarding this order, contact Rightslink Customer Support:

customercare@copyright.com or +1-877-622-5543 (toll free in the US) or +1-978-646-2777.

ELSEVIER LICENSE
TERMS AND CONDITIONS

Dec 21, 2010

This is a License Agreement between Jestin Baby Mandumpal ("You") and Elsevier ("Elsevier") provided by Copyright Clearance Center ("CCC"). The license consists of your order details, the terms and conditions provided by Elsevier, and the payment terms and conditions.

All payments must be made in full to CCC. For payment instructions, please see information listed at the bottom of this form.

Supplier

Elsevier Limited
The Boulevard, Langford Lane
Kidlington,Oxford,OX5 1GB,UK

Registered Company Number

1982084

Customer name

Jestin Baby Mandumpal

Customer address

Mandumpal house

Thrissur, other 680 503

License number

2573620842424

License date

Dec 21, 2010

Licensed content publisher

Elsevier

Licensed content publication

Cryobiology

Licensed content title

Cell–Cell Contact Affects Membrane Integrity after Intracellular Freezing

Licensed content author

Jason P. Acker, Locksley E. McGann

Licensed content date

February 2000

Licensed content volume number 40

Licensed content issue number 1

Number of pages 10

Start Page 54

End Page 63

Type of Use reuse in a thesis/dissertation

Intended publisher of new work other

Portion figures/tables/illustrations

Number of figures/tables/illustrations 1

Format electronic

Are you the author of this Elsevier article? No

Will you be translating? No

Order reference number

Title of your thesis/dissertation Molecular mechanism of solvent cryoprotection

Expected completion date Dec 2010

Estimated size (number of pages) 200

Elsevier VAT number GB 494 6272 12

Permissions price 0.00 USD

Value added tax 0.0% 0.0 USD / 0.0 GBP

Total 0.00 USD

Terms and Conditions

INTRODUCTION

1. The publisher for this copyrighted material is Elsevier. By clicking "accept" in connection with completing this licensing transaction, you agree that the following terms and conditions apply to this transaction (along with the Billing and Payment terms and conditions established by Copyright Clearance Center, Inc. ("CCC"), at the time that you opened your Rightslink account and that are available at any time at http://myaccount.copyright.com).

GENERAL TERMS

2. Elsevier hereby grants you permission to reproduce the aforementioned material subject to the terms and conditions indicated.

3. Acknowledgement: If any part of the material to be used (for example, figures) has appeared in our publication with credit or acknowledgement to another source, permission must also be sought from that source. If such permission is not obtained then that material may not be included in your publication/copies. Suitable acknowledgement to the source must be made, either as a footnote or in a reference list at the end of your publication, as follows:

"Reprinted from Publication title, Vol /edition number, Author(s), Title of article / title of chapter, Pages No., Copyright (Year), with permission from Elsevier [OR APPLICABLE SOCIETY COPYRIGHT OWNER]."Also Lancet special credit - "Reprinted from The Lancet, Vol. number, Author(s), Title of article, Pages No., Copyright (Year), with permission from Elsevier."

4. Reproduction of this material is confined to the purpose and/or media for which permission is hereby given.

5. Altering/Modifying Material: Not Permitted. However figures and illustrations may be altered/adapted minimally to serve your work. Any other abbreviations, additions, deletions and/or any other alterations shall be made only with prior written authorization of Elsevier Ltd. (Please contact Elsevier at permissions@elsevier.com)

6. If the permission fee for the requested use of our material is waived in this instance, please be advised that your future requests for Elsevier materials may attract a fee.

7. Reservation of Rights: Publisher reserves all rights not specifically granted in the combination of (i) the license details provided by you and accepted in the course of this licensing transaction, (ii) these terms and conditions and (iii) CCC's Billing and Payment terms and conditions.

8. License Contingent Upon Payment: While you may exercise the rights licensed immediately upon issuance of the license at the end of the licensing process for the transaction, provided that you have disclosed complete and accurate details of your proposed use, no license is finally effective unless and until full payment is received from you (either by publisher or by CCC) as provided in CCC's Billing and Payment terms and conditions. If full payment is not received on a timely basis, then any license preliminarily granted shall be deemed automatically revoked and shall be void as if never granted. Further, in the event that you breach any of these terms and conditions or any of CCC's Billing and Payment terms and conditions, the license is automatically revoked and shall be void as if never granted. Use of materials as described in a revoked license, as well as any use of the materials beyond the scope of an unrevoked license, may constitute copyright infringement and publisher reserves the right to take any and all action to protect its copyright in the materials.

9. Warranties: Publisher makes no representations or warranties with respect to the licensed material.

10. Indemnity: You hereby indemnify and agree to hold harmless publisher and CCC, and their respective officers, directors, employees and agents, from and against any and all claims arising out of your use of the licensed material other than as specifically authorized pursuant to this license.

11. No Transfer of License: This license is personal to you and may not be sublicensed, assigned, or transferred by you to any other person without publisher's written permission.

12. No Amendment Except in Writing: This license may not be amended except in a writing signed by both parties (or, in the case of publisher, by CCC on publisher's behalf).

13. Objection to Contrary Terms: Publisher hereby objects to any terms contained in any purchase order, acknowledgment, check endorsement or other writing prepared by you, which terms are inconsistent with these terms and conditions or CCC's Billing and Payment terms and conditions. These terms and conditions, together with CCC's Billing and Payment terms and conditions (which are incorporated herein), comprise the entire agreement between you and publisher (and CCC) concerning this licensing transaction. In the event of any conflict between your obligations established by these terms and conditions and those established by CCC's Billing and Payment terms and conditions, these terms and conditions shall control.

14. Revocation: Elsevier or Copyright Clearance Center may deny the permissions described in this License at their sole discretion, for any reason or no reason, with a full

refund payable to you. Notice of such denial will be made using the contact information provided by you. Failure to receive such notice will not alter or invalidate the denial. In no event will Elsevier or Copyright Clearance Center be responsible or liable for any costs, expenses or damage incurred by you as a result of a denial of your permission request, other than a refund of the amount(s) paid by you to Elsevier and/or Copyright Clearance Center for denied permissions.

LIMITED LICENSE

The following terms and conditions apply only to specific license types:

15. **Translation**: This permission is granted for non-exclusive world **English** rights only unless your license was granted for translation rights. If you licensed translation rights you may only translate this content into the languages you requested. A professional translator must perform all translations and reproduce the content word for word preserving the integrity of the article. If this license is to re-use 1 or 2 figures then permission is granted for non-exclusive world rights in all languages.

16. **Website**: The following terms and conditions apply to electronic reserve and author websites:
Electronic reserve: If licensed material is to be posted to website, the web site is to be password-protected and made available only to bona fide students registered on a relevant courseif: This license was made in connection with a course, This permission is granted for 1 year only. You may obtain a license for future website posting,
All content posted to the web site must maintain the copyright information line on the bottom of each image, A hyper-text must be included to the Homepage of the journal from which you are licensing at http://www.sciencedirect.com/science/journal/xxxxx or the Elsevier homepage for books at http://www.elsevier.com , and Central Storage: This license does not include permission for a scanned version of the material to be stored in a central repository such as that provided by Heron/XanEdu.

17. **Author website** for journals with the following additional clauses:

All content posted to the web site must maintain the copyright information line on the bottom of each image, and the permission granted is limited to the personal version of your paper. You are not allowed to download and post the published electronic version of your article (whether PDF or HTML, proof or final version), nor may you scan the printed edition to create an electronic version,
A hyper-text must be included to the Homepage of the journal from which you are licensing at http://www.sciencedirect.com/science/journal/xxxxx , As part of our normal production process, you will receive an e-mail notice when your article appears on Elsevier‟s online service ScienceDirect (www.sciencedirect.com). That e-mail will include the article‟s Digital Object Identifier (DOI). This number provides the electronic link to the published article and should be included in the posting of your personal version. We ask that you wait until you receive this e-mail and have the DOI to do any posting.
Central Storage: This license does not include permission for a scanned version of the material to be stored in a central repository such as that provided by Heron/XanEdu.

18. **Author website** for books with the following additional clauses: Authors are permitted to place a brief summary of their work online only. A hyper-text must be included to the Elsevier homepage at http://www.elsevier.com

All content posted to the web site must maintain the copyright information line on the bottom of each image. You are not allowed to download and post the published electronic version of your chapter, nor may you scan the printed edition to create an electronic version. Central Storage: This license does not include permission for a scanned version of the material to be stored in a central repository such as that provided by Heron/XanEdu.

19. **Website** (regular and for author): A hyper-text must be included to the Homepage of the journal from which you are licensing at http://www.sciencedirect.com/science/journal/xxxxx. or for books to the Elsevier homepage at http://www.elsevier.com

20. **Thesis/Dissertation**: If your license is for use in a thesis/dissertation your thesis may be submitted to your institution in either print or electronic form. Should your thesis be published commercially, please reapply for permission. These requirements include permission for the Library and Archives of Canada to supply single copies, on demand, of the complete thesis and include permission for UMI to supply single copies, on demand, of the complete thesis. Should your thesis be published commercially, please reapply for permission.

21. **Other Conditions**:

v1.6

Gratis licenses (referencing $0 in the Total field) are free. Please retain this printable license for your reference. No payment is required.

If you would like to pay for this license now, please remit this license along with your payment made payable to "COPYRIGHT CLEARANCE CENTER" otherwise you will be invoiced within 48 hours of the license date. Payment should be in the form of a check or money order referencing your account number and this invoice number RLNK10903239.Once you receive your invoice for this order, you may pay your invoice by credit card. Please follow instructions provided at that time.

Make Payment To:
Copyright Clearance Center
Dept 001
P.O. Box 843006
Boston, MA 02284-3006

If you find copyrighted material related to this license will not be used and wish to cancel, please contact us referencing this license number 2573620842424 and noting the reason for cancellation.

Dec 31, 2010

Licensed content publisher

Elsevier

Licensed content publication

Cryobiology

Licensed content title

Freezing, Drying, and/or Vitrification of Membrane– Solute–Water Systems

Licensed content author

Joe Wolfe, Gary Bryant

Licensed content date

September 1999

Licensed content volume number 39

Licensed content issue number 2

Number of pages 27

Start Page 103

End Page 129

Type of Use reuse in a thesis/dissertation

Intended publisher of new work other

Portion figures/tables/illustrations

Number of figures/tables/illustrations 2

Format both print and electronic

Are you the author of this Elsevier article? No

Will you be translating? No

Order reference number

Title of your thesis/dissertation Molecular mechanism of solvent cryoprotection

Expected completion date Dec 2010

Estimated size (number of pages) 200

Elsevier VAT number GB 494 6272 12

Permissions price 0.00 USD

Value added tax 0.0%

0.0 USD / 0.0 GBP

Total 0.00 USD

Terms and Conditions

INTRODUCTION

1. The publisher for this copyrighted material is Elsevier. By clicking "accept" in connection with completing this licensing transaction, you agree that the following terms and conditions apply to this transaction (along with the Billing and Payment terms and conditions established by Copyright Clearance Center, Inc. ("CCC"), at the time that you opened your Rightslink account and that are available at any time at http://myaccount.copyright.com).

GENERAL TERMS

2. Elsevier hereby grants you permission to reproduce the aforementioned material subject to the terms and conditions indicated.

3. Acknowledgement: If any part of the material to be used (for example, figures) has appeared in our publication with credit or acknowledgement to another source, permission must also be sought from that source. If such permission is not obtained then that material may not be included in your publication/copies. Suitable acknowledgement to the source must be made, either as a footnote or in a reference list at the end of your publication, as follows:

"Reprinted from Publication title, Vol /edition number, Author(s), Title of article / title of chapter, Pages No., Copyright (Year), with permission from Elsevier [OR APPLICABLE SOCIETY COPYRIGHT OWNER]." Also Lancet special credit - "Reprinted from The Lancet, Vol. number, Author(s), Title of article, Pages No., Copyright (Year), with permission from Elsevier."

4. Reproduction of this material is confined to the purpose and/or media for which permission is hereby given.

5. Altering/Modifying Material: Not Permitted. However figures and illustrations may be altered/adapted minimally to serve your work. Any other abbreviations, additions, deletions and/or any other alterations shall be made only with prior written authorization of Elsevier Ltd. (Please contact Elsevier at permissions@elsevier.com)

6. If the permission fee for the requested use of our material is waived in this instance, please be advised that your future requests for Elsevier materials may attract a fee.

7. Reservation of Rights: Publisher reserves all rights not specifically granted in the combination of (i) the license details provided by you and accepted in the course of this licensing transaction, (ii) these terms and conditions and (iii) CCC's Billing and Payment terms and conditions.

8. License Contingent Upon Payment: While you may exercise the rights licensed immediately upon issuance of the license at the end of the licensing process for the transaction, provided that you have disclosed complete and accurate details of your proposed use, no license is finally effective unless and until full payment is received from you (either by publisher or by CCC) as provided in CCC's Billing and Payment terms and conditions. If full payment is not received on a timely basis, then any license preliminarily granted shall be deemed automatically revoked and shall be void as if never granted. Further, in the event that you breach any of these terms and conditions or any of CCC's Billing and Payment terms and conditions, the license is automatically revoked and shall be void as if never granted. Use of materials as described in a revoked license, as well as any use of the materials beyond the scope of an unrevoked license, may constitute copyright infringement and publisher reserves the right to take any and all action to protect its copyright in the materials.

9. Warranties: Publisher makes no representations or warranties with respect to the licensed material.

10. Indemnity: You hereby indemnify and agree to hold harmless publisher and CCC, and their respective officers, directors, employees and agents, from and against any and all claims arising out of your use of the licensed material other than as specifically authorized pursuant to this license.

11. No Transfer of License: This license is personal to you and may not be sublicensed, assigned, or transferred by you to any other person without publisher's written permission.

12. No Amendment Except in Writing: This license may not be amended except in a writing signed by both parties (or, in the case of publisher, by CCC on publisher's behalf).

13. Objection to Contrary Terms: Publisher hereby objects to any terms contained in any purchase order, acknowledgment, check endorsement or other writing prepared by you, which terms are inconsistent with these terms and conditions or CCC's Billing and Payment terms and conditions. These terms and conditions, together with CCC's Billing and Payment terms and conditions (which are incorporated herein), comprise the entire agreement between you and publisher (and CCC) concerning this licensing transaction. In the event of any conflict between your obligations established by these terms and conditions and those established by CCC's Billing and Payment terms and conditions, these terms and conditions shall control.

14. Revocation: Elsevier or Copyright Clearance Center may deny the permissions described in this License at their sole discretion, for any reason or no reason, with a full

refund payable to you. Notice of such denial will be made using the contact information provided by you. Failure to receive such notice will not alter or invalidate the denial. In no event will Elsevier or Copyright Clearance Center be responsible or liable for any costs, expenses or damage incurred by you as a result of a denial of your permission request, other than a refund of the amount(s) paid by you to Elsevier and/or Copyright Clearance Center for denied permissions.

LIMITED LICENSE

The following terms and conditions apply only to specific license types:

15. **Translation**: This permission is granted for non-exclusive world **English** rights only unless your license was granted for translation rights. If you licensed translation rights you may only translate this content into the languages you requested. A professional translator must perform all translations and reproduce the content word for word preserving the integrity of the article. If this license is to re-use 1 or 2 figures then permission is granted for non-exclusive world rights in all languages.

16. **Website**: The following terms and conditions apply to electronic reserve and author websites:
Electronic reserve: If licensed material is to be posted to website, the web site is to be password-protected and made available only to bona fide students registered on a relevant course if:
This license was made in connection with a course,
This permission is granted for 1 year only. You may obtain a license for future website posting,
All content posted to the web site must maintain the copyright information line on the bottom of each image,
A hyper-text must be included to the Homepage of the journal from which you are licensing at http://www.sciencedirect.com/science/journal/xxxxx or the Elsevier homepage for books at http://www.elsevier.com , and
Central Storage: This license does not include permission for a scanned version of the material to be stored in a central repository such as that provided by Heron/XanEdu.

17. **Author website** for journals with the following additional clauses:

All content posted to the web site must maintain the copyright information line on the bottom of each image, and he permission granted is limited to the personal version of your paper. You are not allowed to download and post the published electronic version of your article (whether PDF or HTML, proof or final version), nor may you scan the printed edition to create an electronic version, A hyper-text must be included to the Homepage of the journal from which you are licensing at http://www.sciencedirect.com/science/journal/xxxxx , As part of our normal production process, you will receive an e-mail notice when your article appears on Elsevier‟s online service ScienceDirect (www.sciencedirect.com). That e-mail will include the article‟s Digital Object Identifier (DOI). This number provides the electronic link to the published article and should be included in the posting of your personal version. We ask that you wait until you receive this e-mail and have the DOI to do any posting.

Central Storage: This license does not include permission for a scanned version of the material to be stored in a central repository such as that provided by Heron/XanEdu.

18. **Author website** for books with the following additional clauses: Authors are permitted to place a brief summary of their work online only. A hyper-text must be included to the Elsevier homepage at http://www.elsevier.com

All content posted to the web site must maintain the copyright information line on the bottom of each image You are not allowed to download and post the published electronic version of your chapter, nor may you scan the printed edition to create an electronicversion.
Central Storage: This license does not include permission for a scanned version of the material to be stored in a central repository such as that provided by Heron/XanEdu.

19. **Website** (regular and for author): A hyper-text must be included to the Homepage of the journal from which you are licensing at http://www.sciencedirect.com/science/journal/xxxxx. or for books to the Elsevier homepage at http://www.elsevier.com

20. **Thesis/Dissertation**: If your license is for use in a thesis/dissertation your thesis may be submitted to your institution in either print or electronic form. Should your thesis be published commercially, please reapply for permission. These requirements include permission for the Library and Archives of Canada to supply single copies, on demand, of the complete thesis and include permission for UMI to supply single copies, on demand, of the complete thesis. Should your thesis be published commercially, please reapply for permission.

21. **Other Conditions**:

v1.6

Gratis licenses (referencing $0 in the Total field) are free. Please retain this printable license for your reference. No payment is required.

If you would like to pay for this license now, please remit this license along with your payment made payable to "COPYRIGHT CLEARANCE CENTER" otherwise you will be invoiced within 48 hours of the license date. Payment should be in the form of a check or money order referencing your account number and this **invoice number RLNK10906604.**
Once you receive your invoice for this order, you may pay your invoice by credit card. Please follow instructions provided at that time.

Make Payment To:
Copyright Clearance Center
Dept 001
P.O. Box 843006
Boston, MA 02284-3006

If you find copyrighted material related to this license will not be used and wish to cancel, please contact us referencing this license number 2579350384635 and

noting the reason for cancellation.

Questions? customercare@copyright.com or +1-877-622-5543 (toll free in the US) or +1-978-646-2777.

CAMBRIDGE
UNIVERSITY PRESS

The Edinburgh Building
Shaftesbury Road
Cambridge CB2 8RU, UK

www.cambridge.org

Telephone +44 (0)1223 312393
Fax +44 (0)1223 315052
Email information@cambridge.org

Jestin Mandumpal
Mandumpal House
Akathiyoor P.O.
Kunnamkulam
680 503
India

December 22, 2010

Dear Jestin Mandumpal

Figure 2 from Gary Bryant, Karen L. Koster and Joe Wolfe, "Membrane behaviour in seeds and other systems at low water content: the various effects of solutes", Seed Science Research, Volume 11(1), pp 17-25, (2001).

Thank you for your recent permission request to include the above extract(s) in:
your forthcoming doctoral/masters thesis, for non-commercial publication, in print and electronic format.

Non-exclusive permission is granted free of charge for this specific use on the understanding that you have checked that we do not acknowledge another source for this material.

Please ensure full acknowledgement (author, title, publication date, name of journal and Cambridge University Press).

Yours sincerely

C. Taylor

Claire Taylor
Publishing Assistant
email ctaylor@cambridge.org

ELSEVIER LICENSE
TERMS AND CONDITIONS

Jan 19, 2011

This is a License Agreement between Jestin Baby Mandumpal ("You") and Elsevier ("Elsevier") provided by Copyright Clearance Center ("CCC"). The license consists of your order details, the terms and conditions provided by Elsevier, and the payment terms and conditions.

All payments must be made in full to CCC. For payment instructions, please see information listed at the bottom of this form.

Supplier

Elsevier Limited
The Boulevard,Langford Lane
Kidlington,Oxford,OX5 1GB,UK

Registered Company Number

1982084

Customer name

Jestin Baby Mandumpal

Customer address

Mandumpal house

Thrissur, other 680 503

License number

2592430628277

License date

Jan 19, 2011

Licensed content publisher

Elsevier

Licensed content publication

Biophysical Journal

Licensed content title

The Effects of Solutes on the Freezing Properties of and Hydration Forces in Lipid Lamellar Phases

Licensed content author

Yong Hyeon Yoon, James M. Pope, Joe Wolfe

Licensed content date

April 1998

Licensed content volume number

74

Licensed content issue number

4

Number of pages

17

Start Page

1949

End Page

1965

Type of Use

reuse in a thesis/dissertation

Portion

figures/tables/illustrations

Number of figures/tables/illustrations

1

Format

both print and electronic

Are you the author of this Elsevier article?

No

Will you be translating?

No

Order reference number

Title of your thesis/dissertation

Molecular Mechanism of solvent cryoprotection

Expected completion date

Jan 2011

Estimated size (number of pages)

210

Elsevier VAT number

GB 494 6272 12

Permissions price

0.00 USD

Value added tax 0.0%

0.0 USD / 0.0 GBP

Total

0.00 USD

Terms and Conditions

INTRODUCTION

1. The publisher for this copyrighted material is Elsevier. By clicking "accept" in connection with completing this licensing transaction, you agree that the following terms and conditions apply to this transaction (along with the Billing and Payment terms and conditions established by Copyright Clearance Center, Inc. ("CCC"), at the time that you opened your Rightslink account and that are available at any time at http://myaccount.copyright.com).

GENERAL TERMS

2. Elsevier hereby grants you permission to reproduce the aforementioned material subject to the terms and conditions indicated.

3. Acknowledgement: If any part of the material to be used (for example, figures) has appeared in our publication with credit or acknowledgement to another source, permission must also be sought from that source. If such permission is not obtained then that material may not be included in your publication/copies. Suitable acknowledgement to the source must be made, either as a footnote or in a reference list at the end of your publication, as follows:

"Reprinted from Publication title, Vol /edition number, Author(s), Title of article / title of chapter, Pages No., Copyright (Year), with permission from Elsevier [OR APPLICABLE SOCIETY COPYRIGHT OWNER]." Also Lancet special credit - "Reprinted from The Lancet, Vol. number, Author(s), Title of article, Pages No., Copyright (Year), with permission from Elsevier."

4. Reproduction of this material is confined to the purpose and/or media for which permission is hereby given.

5. Altering/Modifying Material: Not Permitted. However figures and illustrations may be altered/adapted minimally to serve your work. Any other abbreviations, additions, deletions and/or any other alterations shall be made only with prior written authorization of Elsevier Ltd. (Please contact Elsevier at permissions@elsevier.com)

6. If the permission fee for the requested use of our material is waived in this instance, please be advised that your future requests for Elsevier materials may attract a fee.

7. Reservation of Rights: Publisher reserves all rights not specifically granted in the combination of (i) the license details provided by you and accepted in the course of this licensing transaction, (ii) these terms and conditions and (iii) CCC's Billing and Payment terms and conditions.

8. License Contingent Upon Payment: While you may exercise the rights licensed immediately upon issuance of the license at the end of the licensing process for the transaction, provided that you have disclosed complete and accurate details of your proposed use, no license is finally effective unless and until full payment is received from you (either by publisher or by CCC) as provided in CCC's Billing and Payment terms and conditions. If full payment is not received on a timely basis, then any license preliminarily granted shall be deemed automatically revoked and shall be void as if never granted. Further, in the event that you breach any of these terms and conditions or any of CCC's Billing and Payment terms and conditions, the license is automatically revoked and shall be void as if never granted. Use of materials as described in a revoked license, as well as any use of the materials beyond the scope of an unrevoked license, may constitute copyright infringement and publisher reserves the right to take any and all action to protect its copyright in the materials.

9. Warranties: Publisher makes no representations or warranties with respect to the licensed material.

10. Indemnity: You hereby indemnify and agree to hold harmless publisher and CCC, and their respective officers, directors, employees and agents, from and against any and all claims arising out of your use of the licensed material other than as specifically authorized pursuant to this license.

11. No Transfer of License: This license is personal to you and may not be sublicensed, assigned, or transferred by you to any other person without publisher's written permission.

12. No Amendment Except in Writing: This license may not be amended except in a writing signed by both parties (or, in the case of publisher, by CCC on publisher's behalf).

13. Objection to Contrary Terms: Publisher hereby objects to any terms contained in any purchase order, acknowledgment, check endorsement or other writing prepared by you, which terms are inconsistent with these terms and conditions or CCC's Billing and Payment terms and conditions. These terms and conditions, together with CCC's Billing and Payment terms and conditions (which are incorporated herein), comprise the entire agreement between you and publisher (and CCC) concerning this licensing transaction. In the event of any conflict between your obligations established by these terms and conditions and those established by CCC's Billing and Payment terms and conditions, these terms and conditions shall control.

14. Revocation: Elsevier or Copyright Clearance Center may deny the permissions described in this License at their sole discretion, for any reason or no reason, with a full refund payable to you. Notice of such denial will be made using the contact information provided by you. Failure to receive such notice will not alter or invalidate the denial. In no event will Elsevier or Copyright Clearance Center be responsible or liable for any costs, expenses or damage incurred by you as a result of a denial of your permission request, other than a refund of the amount(s) paid by you to Elsevier and/or Copyright Clearance Center for denied permissions.

LIMITED LICENSE

The following terms and conditions apply only to specific license types:

15. **Translation**: This permission is granted for non-exclusive world **English** rights only unless your license was granted for translation rights. If you licensed translation rights you may only translate this content into the languages you requested. A professional translator must perform all translations and reproduce the content word for word preserving the integrity of the article. If this license is to re-use 1 or 2 figures then permission is granted for non-exclusive world rights in all languages.

16. **Website**: The following terms and conditions apply to electronic reserve and author websites:
Electronic reserve: If licensed material is to be posted to website, the web site is to be password-protected and made available only to bona fide students registered on a relevant courseif:
This license was made in connection with a course,
This permission is granted for 1 year only. You may obtain a license for future website posting,
All content posted to the web site must maintain the copyright information line on the bottom of each image,
A hyper-text must be included to the Homepage of the journal from which you are licensing athttp://www.sciencedirect.com/science/journal/xxxxx or the Elsevier homepage for books athttp://www.elsevier.com , and
Central Storage: This license does not include permission for a scanned version of the material to be stored in a central repository such as that provided by Heron/XanEdu.

17. **Author website** for journals with the following additional clauses:

All content posted to the web site must maintain the copyright information line on the bottom of each image, and
he permission granted is limited to the personal version of your paper. You are not allowed to download and post the published electronic version of your article (whether PDF or HTML, proof or final version), nor may you scan the printed edition to create an electronic version,
A hyper-text must be included to the Homepage of the journal from which you are licensing athttp://www.sciencedirect.com/science/journal/xxxxx , As part of our normal production process, you will receive an e-mail notice when your article appears on Elsevier‟s online service ScienceDirect (www.sciencedirect.com). That e-mail will include the article‟s Digital Object Identifier (DOI). This number provides the electronic link to the published article and should be included in the posting of your personal version. We ask that you wait until you receive this e-mail and have the DOI to do any posting.
Central Storage: This license does not include permission for a scanned version of the material to be stored in a central repository such as that provided by Heron/XanEdu.

18. **Author website** for books with the following additional clauses: Authors are permitted to place a brief summary of their work online only. A hyper-text must be included to the Elsevier homepage at http://www.elsevier.com

All content posted to the web site must maintain the copyright information line on the bottom of each image. You are not allowed to download and post the published electronic version of your chapter, nor may you scan the printed edition to create an electronicversion.
Central Storage: This license does not include permission for a scanned version of the material to be stored in a central repository such as that provided by Heron/XanEdu.

19. **Website** (regular and for author): A hyper-text must be included to the Homepage of the journal from which you are licensing
at http://www.sciencedirect.com/science/journal/xxxxx. or for books to the Elsevier homepage at http://www.elsevier.com

20. **Thesis/Dissertation**: If your license is for use in a thesis/dissertation your thesis may be submitted to your institution in either print or electronic form. Should your thesis be published commercially, please reapply for permission. These requirements include permission for the Library and Archives of Canada to supply single copies, on demand, of the complete thesis and include permission for UMI to supply single copies, on demand, of the complete thesis. Should your thesis be published commercially, please reapply for permission.

21. **Other Conditions**:

v1.6

Gratis licenses (referencing $0 in the Total field) are free. Please retain this printable license for your reference. No payment is required.

If you would like to pay for this license now, please remit this license along with your payment made payable to "COPYRIGHT CLEARANCE CENTER" otherwise you will be invoiced within 48 hours of the license date. Payment should be in the form of a check or money order referencing your account number and this invoice number RLNK10916369.
Once you receive your invoice for this order, you may pay your invoice by credit card. Please follow instructions provided at that time.

Make Payment To:
Copyright Clearance Center
Dept 001
P.O. Box 843006
Boston, MA 02284-3006

If you find copyrighted material related to this license will not be used and wish to cancel, please contact us referencing this license number 2592430628277 and noting the reason for cancellation.

Questions? customercare@copyright.com or +1-877-622-5543 (toll free in the US) or +1-978-646-2777.

ELSEVIER LICENSE
TERMS AND CONDITIONS

Jan 03, 2011

This is a License Agreement between Jestin Baby Mandumpal ("You") and Elsevier ("Elsevier") provided by Copyright Clearance Center ("CCC"). The license consists of your order details, the terms and conditions provided by Elsevier, and the payment terms and conditions.

All payments must be made in full to CCC. For payment instructions, please see information listed at the bottom of this form.

Supplier

Elsevier Limited
The Boulevard,Langford Lane
Kidlington,Oxford,OX5 1GB,UK

Registered Company Number

1982084

Customer name

Jestin Baby Mandumpal

Customer address

Mandumpal house

Thrissur, other 680 503

License number

2581340892715

License date

Jan 03, 2011

Licensed content publisher

Elsevier

Licensed content publication

Cryobiology

Licensed content title

Vitrification as an approach to cryopreservation

Licensed content author

G. M. Fahy, D. R. MacFarlane, C. A. Angell, H. T. Meryman

Licensed content date

August 1984

Licensed content volume number

21

Licensed content issue number

4

Number of pages

20

Start Page

407

End Page

426

Type of Use

reuse in a thesis/dissertation

Portion

figures/tables/illustrations

Number of figures/tables/illustrations

1

Format

both print and electronic

Are you the author of this Elsevier article?

No

Will you be translating?

No

Order reference number

Title of your thesis/dissertation

Molecular Mechanism of solvent cryoprotection

Expected completion date

Jan 2011

Estimated size (number of pages)

210

Elsevier VAT number

GB 494 6272 12

Permissions price

0.00 USD

Value added tax 0.0%

0.0 USD / 0.0 GBP

Total

0.00 USD

Terms and Conditions

INTRODUCTION

1. The publisher for this copyrighted material is Elsevier. By clicking "accept" in connection with completing this licensing transaction, you agree that the following terms and conditions apply to this transaction (along with the Billing and Payment terms and conditions established by Copyright Clearance Center, Inc. ("CCC"), at the time that you opened your Rightslink account and that are available at any time at http://myaccount.copyright.com).

GENERAL TERMS

2. Elsevier hereby grants you permission to reproduce the aforementioned material subject to the terms and conditions indicated.

3. Acknowledgement: If any part of the material to be used (for example, figures) has appeared in our publication with credit or acknowledgement to another source, permission must also be sought from that source. If such permission is not obtained then that material may not be included in your publication/copies. Suitable acknowledgement to the source must be made, either as a footnote or in a reference list at the end of your publication, as follows:

"Reprinted from Publication title, Vol /edition number, Author(s), Title of article / title of chapter, Pages No., Copyright (Year), with permission from Elsevier [OR APPLICABLE SOCIETY COPYRIGHT OWNER]." Also Lancet special credit - "Reprinted from The Lancet, Vol. number, Author(s), Title of article, Pages No., Copyright (Year), with permission from Elsevier."

4. Reproduction of this material is confined to the purpose and/or media for which permission is hereby given.

5. Altering/Modifying Material: Not Permitted. However figures and illustrations may be altered/adapted minimally to serve your work. Any other abbreviations, additions, deletions and/or any other alterations shall be made only with prior written authorization of Elsevier Ltd. (Please contact Elsevier at permissions@elsevier.com)

6. If the permission fee for the requested use of our material is waived in this instance, please be advised that your future requests for Elsevier materials may attract a fee.

7. Reservation of Rights: Publisher reserves all rights not specifically granted in the combination of (i) the license details provided by you and accepted in the course of this licensing transaction, (ii) these terms and conditions and (iii) CCC's Billing and Payment terms and conditions.

8. License Contingent Upon Payment: While you may exercise the rights licensed immediately upon issuance of the license at the end of the licensing process for the transaction, provided that you have disclosed complete and accurate details of your proposed use, no license is finally effective unless and until full payment is received from you (either by publisher or by CCC) as provided in CCC's Billing and Payment terms and conditions. If full payment is not received on a timely basis, then any license preliminarily granted shall be deemed automatically revoked and shall be void as if never granted. Further, in the event that you breach any of these terms and conditions or any of CCC's Billing and Payment terms and conditions, the license is automatically revoked and shall be void as if never granted. Use of materials as described in a revoked license, as well as any use of the materials beyond the scope of an unrevoked license, may constitute copyright infringement and publisher reserves the right to take any and all action to protect its copyright in the materials.

9. Warranties: Publisher makes no representations or warranties with respect to the licensed material.

10. Indemnity: You hereby indemnify and agree to hold harmless publisher and CCC, and their respective officers, directors, employees and agents, from and against any and all claims arising out of your use of the licensed material other than as specifically authorized pursuant to this license.

11. No Transfer of License: This license is personal to you and may not be sublicensed, assigned, or transferred by you to any other person without publisher's written permission.

12. No Amendment Except in Writing: This license may not be amended except in a writing signed by both parties (or, in the case of publisher, by CCC on publisher's behalf).

13. Objection to Contrary Terms: Publisher hereby objects to any terms contained in any purchase order, acknowledgment, check endorsement or other writing prepared by you, which terms are inconsistent with these terms and conditions or CCC's Billing and Payment terms and conditions. These terms and conditions, together with CCC's Billing and Payment terms and conditions (which are incorporated herein), comprise the entire agreement between you and publisher (and CCC) concerning this licensing transaction. In the event of any conflict between your obligations established by these terms and conditions and those established by CCC's Billing and Payment terms and conditions, these terms and conditions shall control.

14. Revocation: Elsevier or Copyright Clearance Center may deny the permissions described in this License at their sole discretion, for any reason or no reason, with a full

refund payable to you. Notice of such denial will be made using the contact information provided by you. Failure to receive such notice will not alter or invalidate the denial. In no event will Elsevier or Copyright Clearance Center be responsible or liable for any costs, expenses or damage incurred by you as a result of a denial of your permission request, other than a refund of the amount(s) paid by you to Elsevier and/or Copyright Clearance Center for denied permissions.

LIMITED LICENSE

The following terms and conditions apply only to specific license types:

15. **Translation**: This permission is granted for non-exclusive world **English** rights only unless your license was granted for translation rights. If you licensed translation rights you may only translate this content into the languages you requested. A professional translator must perform all translations and reproduce the content word for word preserving the integrity of the article. If this license is to re-use 1 or 2 figures then permission is granted for non-exclusive world rights in all languages.

16. **Website**: The following terms and conditions apply to electronic reserve and author websites:
Electronic reserve: If licensed material is to be posted to website, the web site is to be password-protected and made available only to bona fide students registered on a relevant course if:
This license was made in connection with a course,This permission is granted for 1 year only. You may obtain a license for future website posting, All content posted to the web site must maintain the copyright information line on the bottom of each image, A hyper-text must be included to the Homepage of the journal from which you are licensing at http://www.sciencedirect.com/science/journal/xxxxx or the Elsevier homepage for books at http://www.elsevier.com , and
Central Storage: This license does not include permission for a scanned version of the material to be stored in a central repository such as that provided by Heron/XanEdu.

17. **Author website** for journals with the following additional clauses:

All content posted to the web site must maintain the copyright information line on the bottom of each image, and he permission granted is limited to the personal version of your paper. You are not allowed to download and post the published electronic version of your article (whether PDF or HTML, proof or final version), nor may you scan the printed edition to create an electronic version, A hyper-text must be included to the Homepage of the journal from which you are licensing at http://www.sciencedirect.com/science/journal/xxxxx , As part of our normal production process, you will receive an e-mail notice when your article appears on Elsevier‟s online service ScienceDirect (www.sciencedirect.com). That e-mail will include the article‟s Digital Object Identifier (DOI). This number provides the electronic link to the published article and should be included in the posting of your personal version. We ask that you wait until you receive this e-mail and have the DOI to do any posting.
Central Storage: This license does not include permission for a scanned version of the material to be stored in a central repository such as that provided by Heron/XanEdu.

18. **Author website** for books with the following additional clauses: Authors are permitted to place a brief summary of their work online only. A hyper-text must be included to the Elsevier homepage at http://www.elsevier.com All content posted to the web site must maintain the copyright information line on the bottom of each image. You are not allowed to download and post the published electronic version of your chapter, nor may you scan the printed edition to create an electronic version. Central Storage: This license does not include permission for a scanned version of the material to be stored in a central repository such as that provided by Heron/XanEdu.

19. **Website** (regular and for author): A hyper-text must be included to the Homepage of the journal from which you are licensing at http://www.sciencedirect.com/science/journal/xxxxx. or for books to the Elsevier homepage at http://www.elsevier.com

20. **Thesis/Dissertation**: If your license is for use in a thesis/dissertation your thesis may be submitted to your institution in either print or electronic form. Should your thesis be published commercially, please reapply for permission. These requirements include permission for the Library and Archives of Canada to supply single copies, on demand, of the complete thesis and include permission for UMI to supply single copies, on demand, of the complete thesis. Should your thesis be published commercially, please reapply for permission.

21. **Other Conditions**:

v1.6

Gratis licenses (referencing $0 in the Total field) are free. Please retain this printable license for your reference. No payment is required.

If you would like to pay for this license now, please remit this license along with your payment made payable to "COPYRIGHT CLEARANCE CENTER" otherwise you will be invoiced within 48 hours of the license date. Payment should be in the form of a check or money order referencing your account number and this invoice number RLNK10907084.
Once you receive your invoice for this order, you may pay your invoice by credit card. Please follow instructions provided at that time.

Make Payment To:
Copyright Clearance Center
Dept 001
P.O. Box 843006
Boston, MA 02284-3006
If you find copyrighted material related to this license will not be used and wish to cancel, please contact us referencing this license number 2581340892715 and noting the reason for cancellation.
Questions ? customercare@copyright.com or +1-877-622-5543 (toll free in the US) or +1-978-646-2777.